Construction of Optimal Cubature Algorithms with Applications to Econometrics and Uncertainty Quantification

vorgelegt von

Jens Oettershagen

aus

Bonn - Bad Godesberg

Bonn 2017

Angefertigt mit Genehmigung der Mathematisch-Naturwissenschaftlichen Fakultät der Rheinischen Friedrich-Wilhelms-Universität Bonn

Danksagung

An dieser Stelle möchte ich den zahlreichen Personen danken, die Anteil am Entstehen dieser Arbeit hatten. Großen Dank verdient mein Doktorvater Michael Griebel für die Überlassung des Themas, die Bereitstellung exzellenter Arbeitsbedingungen und dafür, dass er mich durch zahlreiche Diskussionen, Anregungen und Herausforderungen ausgebildet und gefördert hat. Außerdem möchte ich mich bei Jochen Garcke für die Übernahme des Zweitgutachtens bedanken. Zudem gilt mein Dank Babette Weißkopf für ihre Hilfsbereitschaft und Geduld in Verwaltungsangelegenheiten aller Art sowie den Systemadministratoren für den Betrieb der Parallelrechner.

Bei meinen (ehemaligen) Kollegen Bastian Bohn, Alexander Hullmann, Christopher Kacwin, Christian Kuske, Sebastian Mayer und Markus Siebenmorgen bedanke ich mich nicht nur für fachliche Diskussionen und das Korrekturlesen der Arbeit, sondern auch für die vielen interessanten und unterhaltsamen (Mittags-) Pausen. Des Weiteren danke ich Markus Bachmayr, Aicke Hinrichs, Mario Ullrich, Tino Ullrich und André Uschmajew, die durch Diskussionen, ihre Hilfsbereitschaft bei Fragen und viele Literaturhinweise zum Gelingen dieser Arbeit beigetragen haben.

Außerdem gebührt mein Dank der Deutschen Forschungsgesellschaft, welche im Rahmen des SFB 1060 *The mathematics of emergent effects* und des Projekts GR 1144/21-1 *Likelihood-Approximation für Discrete Choice Modelle mit Dünnen Gittern* meine Forschung finanziert hat. Zudem danke ich unseren Projektpartnern Florian Heiß und Constantin Weiser.

Zu guter Letzt verdient meine Familie, insbesondere meine Frau Viktoria, großen Dank für ihre Unterstützung.

Contents

Notation

Symbol	Definition
$\boldsymbol{a},\ldots,\boldsymbol{z}$	Vectors from $\mathbb{R}^m$ or $\mathbb{Z}^m$
$\boldsymbol{A},\ldots,\boldsymbol{Z}$	Matrices from $\mathbb{R}^{m \times m}$
$\boldsymbol{b}(X_n)$	Vector $(\ell_\Omega(\xi_1),\ldots,\ell_\Omega(\xi_n))$.
$\boldsymbol{e}_k$	k-th unit vector $(0,\ldots,0,1,0,\ldots,0)$
f,g	Real valued functions on Ω or $\Omega_{(d)}$
$K(x,y)$	Symmetric positive definite kernel function on $\Omega \subseteq \mathbb{R}$
$K(\boldsymbol{x},\boldsymbol{y})$	Symmetric positive definite kernel function on $\Omega \subseteq \mathbb{R}^d$ with $d \geq 2$
$K^{(l,j)}(x,y)$	Partial derivatives of the kernel, i.e. $\frac{\partial^l \partial^j}{\partial s^l t^j} K(s,t)_{\vert(s,t)=(x,y)}$
$K_{(d)}(\boldsymbol{x},\boldsymbol{y})$	Product kernel $\prod_{j=1}^d K_j(x_j,y_j)$ on product-domain $\Omega_{(d)}$
$\mathcal{H}_{K(\boldsymbol{X}_N)}$	N-dimensional subspace of $\mathcal{H}_K$, spanned by $K(\cdot,\boldsymbol{\xi}), \boldsymbol{\xi} \in \boldsymbol{X}_N$
$\mathbf{I}_d$	d-dimensional identity matrix
L_Ω	Integration functional defined by $L_\Omega(f) = \int_\Omega f(\boldsymbol{x})\, \omega(\boldsymbol{x})\, \mathrm{d}\boldsymbol{x}$
ℓ_Ω	Riesz-representer of L_Ω in $\mathcal{H}_K$.
$\boldsymbol{\Lambda}_N$	Set of N linear functionals $\Lambda_1,\ldots,\Lambda_N$
$\log$	Natural logarithm (base e)
$\boldsymbol{M}^\mathsf{T}$	The transpose of a matrix $\boldsymbol{M}$
$\boldsymbol{M}^*$	The conjugate transpose of a matrix $\boldsymbol{M}$, i.e. $\overline{\boldsymbol{M}}^\mathsf{T}$
N	Total number of points used by a general cubature rule
n	Number of points used by a univariate quadrature rule
$\mathbb{N}$	The set of natural numbers, i.e. $\{1,2,3,\ldots\}$
$\mathbb{N}_0$	The set of natural numbers including zero, i.e. $\{0,1,2,\ldots\}$
Ω	$\subset \mathbb{R}^d$
$\Omega_{(d)}$	$\Omega_{(d)} = \bigotimes_{j=1}^d \Omega_j$, where $\Omega_j \subset \mathbb{R}$
ω	Positive weight function on Ω
$\omega_{(d)}(\boldsymbol{x})$	$\omega_{(d)}(\boldsymbol{x}) = \prod_{j=1}^d \omega_j(x_j)$, where $\omega_j : \Omega_j \to \mathbb{R}_+$
$\check{Q}_{\boldsymbol{X}_N}$	Cubature rule using the N points $\boldsymbol{X}_N \subset \mathbb{R}^d$ with optimal weights
$\check{Q}_{X_n}$	Quadrature rule using the n points in $X_n \subset \mathbb{R}$ with optimal weights
$\check{R}_{X_n}$	Error functional $L_\Omega(f) - \check{Q}_{X_n}(f)$
$\check{r}_{X_n}$	Riesz-representer of $\check{R}_{X_n}$
$\check{\boldsymbol{w}}(X_n)$	Optimal weights for the points in X_n
$\check{\mathbf{ce}}(X_n)$	Worst-case error of the optimally weighted quadrature rule $\check{Q}_{X_n}$
X_n	Vector of n quadrature points $\xi_1,\ldots,\xi_n$ with $\xi_i \in \Omega \subset \mathbb{R}$
$\boldsymbol{X}_N$	Cubature points $\boldsymbol{\xi}^{(1)},\ldots,\boldsymbol{\xi}^{(N)}$ with $\boldsymbol{\xi}^{(i)} = (\xi_1^{(i)},\ldots,\xi_d^{(i)}) \in \Omega \subset \mathbb{R}^d$

Space	Definition
$\mathcal{G}_\gamma$	Gaussian space with shape parameter $\gamma > 0$
$\mathcal{H}$	Hilbert space
$\mathcal{H}^\star$	Dual space of a Hilbert space $\mathcal{H}$
$\mathcal{H}_K$	Reproducing kernel Hilbert space with kernel K
H^s	Sobolev space with smoothness $s \in \mathbb{N}$
$\tilde{H}^s$	Sobolev space of periodic functions with smoothness $s \in \mathbb{N}$
$\mathring{H}^s$	Sobolev space of functions f with $\mathrm{supp} f \subset (0,1)$ and smoothness $s \in \mathbb{N}$
H^s_{mix}	Sobolev space with dominating mixed smoothness on $[0,1]^d$
$\tilde{H}^s_{\mathrm{mix}}$	Periodic Sobolev space with dominating mixed smoothness on $\mathbb{T}^d \simeq [0,1)^d$
$\mathbb{H}_r$	Hardy space on disc with radius $r \geq 1$ equipped with L_2-norm on the boundary
$\mathcal{M}_\tau$	Mehler / Hermite space of functions whose Hermite coefficients decay like τ^{-r}
$\mathcal{T}_{\mathrm{Li}_2}$	Taylor space generated by the di-logarithm Li_2

Moreover, we will frequently make use of the notation $f(x) \preceq_{a,b} g(x)$, which is short for the existence of a constant $c(a,b) > 0$ such that it holds

$$f(x) \leq c(a,b)g(x) \quad \text{for all } x \geq 0.$$

Here, the constant $c(a,b) > 0$ can depend on numbers a and b but not on x. Consequently,

$$f(x) \asymp_{a,b} g(x)$$

means that it holds both, $f(x) \preceq_{a,b} g(x)$ and $g(x) \preceq_{a,b} f(x)$.

1 Introduction

The integration of multivariate functions plays a fundamental role in numerical mathematics with applications in all scientific fields where expectations and probabilities need to be computed. One example is engineering, where relevant parameters that describe a system are often not given as deterministic values, but due to measurement errors or even an intrinsic non-observability only as a probabilistic description. In such situations, it is important to quantify how the uncertainty of the input parameters relates to an uncertainty of the output, e.g. the solution of a differential equation. Further examples include physics [17], computational finance [73], machine learning [127] and also econometrics [75], where many relevant quantities are described as expectations of certain random variables. Unfortunately, these integrals can seldom be computed in closed-form, but rather require a numerical approximation based on evaluations of the integrand.

Classically, the integral

$$\int_\Omega f(x) \, \mathrm{d}x \tag{1.1}$$

of a function f over a domain $\Omega \subset \mathbb{R}$ represents the (signed) area that is enclosed between Ω on the x-axis and the graph $f(x)$. For two-dimensional $\Omega \subset \mathbb{R}^2$ the integral represents the volume between Ω in the (x_1, x_2)-plane and $f(x_1, x_2)$. In reference to these areas and volumes the numerical approximation of integrals is often called *quadrature* or *cubature*. To this end, one takes evaluations of f at N points and constructs algorithms that approximate (1.1) with as much accuracy as possible. The selection of proper quadrature points and the construction of efficient algorithms is the main topic of this thesis.

Numerical integration

Mathematically speaking, we deal with the approximation of the integral $L_\Omega(f)$ of some function $f : \Omega \to \mathbb{R}$ over a given d-dimensional domain $\Omega \subseteq \mathbb{R}^d$ with respect to a probability density function $\omega : \Omega \to \mathbb{R}_+$ by a cubature rule $Q_{\boldsymbol{X}_N, \boldsymbol{w}}$, i.e.

$$L_\Omega(f) \; := \; \int_\Omega f(\boldsymbol{x}) \, \omega(\boldsymbol{x}) \, \mathrm{d}\boldsymbol{x} \; \approx \; \sum_{i=1}^{N} w_i f(\boldsymbol{\xi}^{(i)}) \; =: \; Q_{\boldsymbol{X}_N, \boldsymbol{w}}(f). \tag{1.2}$$

Here, $Q_{\boldsymbol{X}_N, \boldsymbol{w}}$ uses N function values of f at the integration points $\boldsymbol{X}_N := (\boldsymbol{\xi}^{(1)}, \ldots, \boldsymbol{\xi}^{(N)}) \subset \mathbb{R}^d$ which are linearly combined with the vector of integration weights $\boldsymbol{w} = (w_1, \ldots, w_N)$. The choice of good integration points and weights depends on certain assumptions that can be imposed on the set of possible integrands f as well as on Ω and ω.

The fact that the left-hand-side of (1.2) represents the expectation of $f(\boldsymbol{x})$ motivates the so-called *Monte Carlo* (MC) approach. Here, for square-integrable functions, the average over

samples drawn identically and independently with respect to the distribution generated by ω converges to the expectation of $f(\boldsymbol{x})$ at a dimension-independent rate of $\mathcal{O}(N^{-1/2})$.

The assumption that the integrand f is in $L^2(\Omega, \omega)$ is rather weak because this includes even functions with infinitely many jumps. This makes MC-based approaches very robust in practical applications because parameters or models can be changed without giving much thought to regularity requirements or dimension dependence of the integration method. However, this robustness comes at the price of a rather slow convergence rate $\mathcal{O}(N^{-1/2})$, which is not only independent of the dimensionality but also independent of the smoothness of the integrand. Therefore, it is desirable to construct algorithms that can achieve higher convergence rates by exploiting additional structure or regularity of the integrand.

For example, in the univariate setting $d = 1$ one could consider integrands which have their first s derivatives bounded in L^2. Then, quadrature rules using equidistant points can be constructed that converge with the rate N^{-s}, cf. [46]. An example for $s = 2$ is the compound trapezoidal rule, which is related to a piecewise linear approximation of the integrand and achieves the convergence rate N^{-2}.

For a long time it was not clear how this can be generalized to multiple dimensions $d \geq 2$. If one assumes that $\partial^{\boldsymbol{k}} f \in L^2$ for $|\boldsymbol{k}|_1 \leq s$, the d-fold tensor product of suitable univariate quadrature rules can only achieve a rate of $N^{-s/d}$, which for $d > 2s$ is worse than Monte Carlo. This phenomenon of a convergence rate that deteriorates exponentially with the dimension d is often referred to as the *curse of dimensionality*, which was coined by Bellmann in 1961 [15].

If one aims to break the curse of dimensionality, it is necessary to impose further regularity assumptions on the integrand. In the 20th century it was discovered [98, 142] that it is possible to construct integration algorithms which achieve convergence of order $N^{-s} \log(N)^q$ with $q \geq \frac{d-1}{2}$ for integrands that fulfill $\|\partial^{\boldsymbol{k}} f\|_{L_2} < \infty$ for all $|\boldsymbol{k}|_\infty \leq s \in \mathbb{N}$. Functions that fulfill this condition belong to Sobolev spaces with *bounded mixed derivatives* denoted by H^s_{mix}.

Of course there are many other regularity assumptions that allow for quickly decaying integration errors, even in high dimensions. For example, if the integrand comes from a certain tensor product of analytic function spaces, it is possible to obtain convergence rates that decay even faster than any algebraic rate $N^{-s}, s \in \mathbb{R}_+$ independently of the dimension [80, Cor. 5.9].

Optimal cubature weights in reproducing kernel Hilbert spaces

A convenient way to impose regularity or structure onto the integrand $f : \Omega \to \mathbb{R}$ is the assumption that f belongs to a Hilbert space that has a reproducing kernel $K : \Omega \times \Omega \to \mathbb{R}$. These so-called *reproducing kernel Hilbert spaces* (RKHS) $\mathcal{H}_K$ are generated by their respective kernel $K : \Omega \times \Omega \to \mathbb{R}$ and many properties of K are inherited by the elements of $\mathcal{H}_K$. Moreover, in a RKHS it is possible to evaluate the worst-case error of $Q_{\boldsymbol{X}_N, \boldsymbol{w}}$

$$\mathbf{wce}(Q_{\boldsymbol{X}_N, \boldsymbol{w}}, \mathcal{H}_K) := \sup_{\|f\|_{\mathcal{H}_K} \leq 1} \left| L_\Omega(f) - \sum_{i=1}^N w_i f(\boldsymbol{\xi}^{(i)}) \right| \tag{1.3}$$

in closed-form. This is useful for comparing the performance of different cubature rules in $\mathcal{H}_K$. Another reason why the worst-case error (1.3) is an interesting object, is its relationship to Gaussian processes. If one assumes the prior knowledge that the integrand f is an instance of a

Gaussian process with covariance kernel K, the worst-case error $\mathbf{wce}(Q_{\boldsymbol{X}_N,\boldsymbol{w}}, \mathcal{H}_K)$ corresponds to the variance of the posterior distribution that is conditioned on the measurements of f at $\boldsymbol{X}_N$. This perspective on numerical integration is called *Bayesian integration* [29, 120, 128].

The explicit formula for (1.3) allows to determine optimal cubature weights $\check{\boldsymbol{w}}(\boldsymbol{X}_N)$ that still depend on a given set of cubature points $\boldsymbol{X}_N \subset \Omega$. These optimal weights yield an *optimal linear algorithm* $\check{Q}_{\boldsymbol{X}_N}(f) = \sum_{i=1}^{N} \check{w}_i(\boldsymbol{X}_N) f(\boldsymbol{\xi}^{(i)})$ that achieves the worst-case error

$$\mathbf{wce}(\check{Q}_{\boldsymbol{X}_N}, \mathcal{H}_K) = \inf_{\boldsymbol{w} \in \mathbb{R}^N} \mathbf{wce}(Q_{\boldsymbol{X}_N,\boldsymbol{w}}, \mathcal{H}_K), \tag{1.4}$$

which only depends on the point set $\boldsymbol{X}_N$.

The first major contribution of this thesis is the investigation to which extent optimal weights can improve the convergence rate of classical Monte Carlo points. To this end, we compute optimal cubature weights $\check{\boldsymbol{w}}(\boldsymbol{X}_N)$ for integration in H^s_{mix}, where $\boldsymbol{X}_N$ is a random set of uniformly distributed points in $[0,1]^d$. We observe that (1.4) decays with high probability like $N^{-s} \log(N)^q$, where $q > \frac{d-1}{2}$ seems to be dependent on the smoothness s. Here, the main rate of N^{-s} is known to be the best possible. On the theoretical side, we give upper bounds for (1.4) in H^s_{mix} for random $\boldsymbol{X}_N$. For this purpose, we use logarithmic oversampling to obtain a stable cubature rule with sufficiently high trigonometric degree of exactness to show that (1.4) is bounded with high probability by $N^{-s+1/2} \log(N)^{sd-1/2}$.

Even though these results are promising, one should note that the computation of the optimal weights in (1.4) requires the inversion of a dense $N \times N$-matrix. The resulting $\mathcal{O}(N^3)$-complexity is a problem especially in high-dimensions where a large number of integration points is often required. Moreover, it is questionable whether random points with optimal weights enjoy close-to-optimal convergence rates in other RKHS as well. At least for analytic functions this must be denied, because the Runge phenomenon requires either super-linear oversampling [39, 106], which would degrade an exponential convergence rate to sub-exponential, or a careful selection of the quadrature points.

In order to deal with both, good integration points and also the reduction of the computational cost for optimal integration weights, we will follow the sparse grid paradigm [32, 142, 161]. Here, the problem of constructing an algorithm for multivariate integration is reduced to the construction of a good univariate algorithm. To this end, we first consider the problem of univariate quadrature in more detail.

Optimal quadrature points for univariate integration

The problem of computing a set of n univariate quadrature points $X_n = \{\xi_1, \dots, \xi_n\}$ that minimizes the worst-case error can be rephrased as a nonlinear approximation problem, i.e.

$$\inf_{X_n \in \Omega^n} \inf_{\boldsymbol{w} \in \mathbb{R}^n} \left\| \ell_\Omega(\cdot) - \sum_{i=1}^{n} w_i K(\cdot, \xi_i) \right\|_{\mathcal{H}_K}, \tag{1.5}$$

where ℓ_Ω is the Riesz-representer of L_Ω. If all the points are allowed to vary, this is a best n-term approximation problem from the dictionary $\mathcal{D}_K(\Omega) = \{K(\cdot, x) : x \in \Omega\}$. In the univariate setting, (1.5) can be solved using results on total positivity. To this end, we characterize optimal quadrature rules and discuss their existence in Section 5.1. Moreover, we develop an efficient

and stable algorithm for the computation of optimal quadrature points in arbitrary RKHS whose kernel K is extended totally positive, cf. Def. 5.1.

However, for the aforementioned sparse grid paradigm it is advantageous if the quadrature points are nested, i.e. there exists a sequence $(n_j)_{j \in \mathbb{N}}$ such that $X_{n_j} \subset X_{n_{j+1}}$. Unfortunately, this is not the case for the optimal quadrature points. Therefore, instead of solving the best-n-term approximation problem (1.5), we follow [150] and use orthogonal matching pursuit (OMP) to construct a nested approximation to the best-n-term solution. By the Riesz-duality between the dictionary $\mathcal{D}_K(\Omega) = \{K(\cdot, x) : x \in \Omega\}$ and the set of quadrature points $x \in \Omega$ this greedy approach yields stable, efficient and maximally nested quadrature rules with $n_{j+1} - n_j = 1$. In order to deal with singular integrands or integration with respect to non-constant weight functions ω, we propose a *weighted OMP* approach that is inspired by results on Leja points. As it turns out, the resulting nested quadrature rules are not only very stable, but also exhibit a rate of convergence that is comparable to the one observed with optimal points. To be more precise, we observe that for algebraic decaying n-th minimal worst-case error, the error of the OMP greedy method decays at the same algebraic rate. Moreover, for the case of geometric decay of the nth-minimal worst-case error, say $e^{-\alpha n}$, the greedy method achieves half of the geometric decay rate, i.e. $e^{-(\alpha/2)n}$. Therefore, we are convinced that the OMP greedy approach is the right choice for the construction of optimally weighted nested quadrature rules. We remark that this approach is different from a direct greedy minimization of the worst-case error formula as it is proposed e.g. in [89, 136] which might yield coalescing quadrature points resulting in stability problems.

We validate the OMP greedy method for a broad range of function spaces in Chapter 6 by constructing quadrature rules in e.g. Sobolev-, Hardy-, Hermite and Gaussian spaces. Besides, we also investigate the distribution of both, optimal points and the points obtained by the OMP greedy procedure. Here, we observe a similarity between the relationship of optimal points to OMP greedy points on the one hand and Gaussian points to Leja points on the other.

Having the results for the univariate setting at hand, we are now in the position to construct efficient multivariate cubature rules at a reduced complexity using the idea of sparse grids.

Optimized tensor product methods for multivariate integrals

The sparse tensor product method [32, 142, 161] relies on a linear combination of tensor products of hierarchical quadrature rules, i.e.

$$Q_{\mathcal{A}}(f) := \sum_{\boldsymbol{k} \in \mathcal{A}} \bigotimes_{j=1}^{d} \left(\Delta_{k_j}^{(j)} \right)(f), \quad \text{where } \Delta_{k_j}^{(j)} = Q_{k_j+1}^{(j)} - Q_{k_j}^{(j)} \tag{1.6}$$

and the $Q_{k_j}^{(j)}$ are univariate quadrature rules. Here, $\mathcal{A} \subset \mathbb{N}_0^d$ denotes a downward-closed index set that can be tailored to the multivariate problem. If the univariate quadrature rules $Q_{k_j}^{(j)}$ use optimal weights for approximating $L_{\Omega_j}(f) = \int_{\Omega_j} f(x)\, \omega_j(x)\, \mathrm{d}x$ in the RKHS $\mathcal{H}_{K_j}$, the tensor product algorithm (1.6) also enjoys optimality with respect to the weights in the tensor product space $\mathcal{H}_{K_{(d)}} = \bigotimes_{j=1}^{d} \mathcal{H}_{K_j}$ for the approximation of $L_{\Omega_{(d)}}(f) = \bigotimes_{j=1}^{d} L_{\Omega_j}(f)$, i.e. the multivariate integral $\int_{\Omega_{(d)}} f(\boldsymbol{x}) \prod_{j=1}^{d} \omega_j(x_j)\, \mathrm{d}\boldsymbol{x}$. This holds independently of the index set $\mathcal{A}$ and allows for a simplified worst-case error representation. Then, using the ideas of [70], we

derive an algorithm that only requires the evaluation of the univariate kernels K_j and L_{Ω_j} to construct optimally weighted integration algorithms for $\mathcal{H}_{K_{(d)}}$ at cost $\mathcal{O}(N^2)$. Moreover, recalling that the OMP greedy algorithm for the construction of univariate nested optimal quadrature rules does not require any information beside the kernel K_j as well, we have obtained a true black-box algorithm for the construction of optimally weighted cubature rules in tensor product RKHS that are both stable and fast convergent.

If a priori information on the convergence rates of $Q_{k_j}^{(j)}$ is available, one can directly construct a quasi–optimal index set and derive error bounds for the associated quasi–optimal tensor product method (1.6). To this end, we investigate the setting of both, exponential and sub-exponential decay of the worst-case errors. While the case of exponentially decaying $\|\Delta_k^{(j)}\|_{\mathcal{H}_{K_j}}$ was already covered in [13, 80, 153], the case of sub-exponential convergence is novel. However, we will treat both settings in an unified way assuming that $\|\Delta_k^{(j)}\|_{\mathcal{H}_{K_j}} \asymp \exp(-a_j k^p)$, with $p \in (0, 1]$ and $1/p \in \mathbb{N}$. Then we show that the worst-case error of (1.6) with quasi–optimal index set satisfies

$$\|L_{\Omega_{(d)}}(f) - \check{Q}_{\mathcal{A}}(f)\|_{\mathcal{H}_{K_{(d)}}} \preceq_{\boldsymbol{a},d,p} \exp\Big(-\frac{\kappa(d/p)}{\kappa(1/p)} \mathrm{gm}(\boldsymbol{a}) N^{\frac{p}{d}}\Big) N^{\frac{1}{2}-\frac{p}{2d}}, \qquad (1.7)$$

where $\mathrm{gm}(\boldsymbol{a})$ denotes the geometric mean of $\boldsymbol{a} = (a_1, \ldots, a_d) \in \mathbb{R}_+^d$, $\kappa(n) = (n!)^{1/n}$ and N the total number of evaluations needed by (1.6). It is noteworthy that (1.7) represents the best error bound for the described setting that is known so far and improves on [13, 80, 153].

In order to validate both, our adaptive construction and the theoretical results we apply the method to various tensor product spaces in Section 7.5. Moreover, we consider standard model problems from numerical analysis to demonstrate the advantage that can be gained by resorting to our new approach.

Application to problems from econometrics and uncertainty quantification

We complete this thesis by applying our results to practical integration problems from econometrics and engineering. A notorious source for high-dimensional integration problems in many branches of science is the modelling of uncertainty. For example, within the *multinomial probit* model, that is used to model discrete choices, certain unobservable parameters have to be estimated by maximum-likelihood methods. In some situations, the evaluation of the likelihood function requires the solution of multivariate integrals, which are usually transformed to the unit-cube by means of the Genz-algorithm [66] and its generalizations. The transformed integrands are known to be bounded, but can have singular derivatives. Here, we employ sparse tensor products of the optimal quadrature rules in the Taylor space $\mathcal{T}_{\mathrm{Li}_2}$ which consists of bounded functions in the unit disc that have derivatives in the Hardy space. We compare the performance of the optimal algorithm with dimension-adaptive sparse grids based on Clenshaw-Curtis quadrature as well as (quasi-)Monte Carlo methods, which represent the current state-of-the-art.

Finally, we consider parametric differential equations. In engineering and mechanics, but also in other branches of science, there exist well-established models that produce reliable predictions of a given system's dynamics. These models, however, need to be initialized with correct parameters. To this end, measurements of real-world quantities have to be executed which usually involves a certain error or sometimes are not even observable at all. Therefore, it is

important to know how the output of the simulation depends on these uncertain parameters. Here, we consider a simple model problem that consists of an elliptic differential equations with parametric diffusion coefficient. Since regularity theory [40, 81, 153] implies that the solution with respect to the parametric variables is analytic in certain polydiscs within the complex plane, we use sparse tensor products of optimal quadrature rules tailored to the appropriate Hardy spaces. While our approach does not yield a real advantage over conventional approximation schemes for large domains of analyticity, it turns out that for small radii our optimal sparse tensor product method allows for a substantial reduction of computational cost. This can make the difference between using a laptop or needing an expensive parallel cluster.

Contributions of this thesis

This thesis is concerned with the construction of optimal integration methods for both, univariate and multivariate RKHS. The main contributions can be summarized as follows:

- Investigation of optimally weighted Monte Carlo integration in Sobolev spaces with dominating mixed smoothness resulting in close-to-optimal worst-case error convergence.

- Development of an efficient and stable algorithm for the computation of optimal quadrature points and weights in univariate RKHS.

- Employing (weighted) orthogonal matching pursuit for the construction of nested quadrature rules and comparing their performance, stability and distribution with optimal points in Sobolev spaces, Hardy spaces, Taylor spaces and Hermite spaces.

- Using sparse tensor products of optimal univariate quadrature rules to automatically construct optimally weighted cubature rules in tensor product spaces at cost $\mathcal{O}(N^2)$.

- Proving novel a priori error bounds for quasi-optimal tensor products of both, exponential and sub-exponential converging nested quadrature rules.

- Application of optimally weighted sparse tensor product integration to uncertainty quantification problems and the computation of multivariate normal probabilities with the Genz algorithm.

Outline

This thesis is organized as follows: In Chapter 2 we recall the basics about numerical integration. Chapter 3 deals with the theory on reproducing kernel Hilbert spaces and also contains a brief overview of the RKHS that will be discussed throughout this thesis. In Chapter 4 we put this theory into practice by computing optimal cubature weights at random points for integration of functions with dominating mixed smoothness. The choice of both, optimal and nested quadrature points is discussed in Chapter 5 and efficient and stable procedures to compute them are provided. In Chapter 6 we compare the aforementioned quadrature rules to different approaches common in the literature. These results are used in Chapter 7 as building blocks for optimally weighted tensor product methods that work almost automatically for any given tensor product RKHS. Chapter 8 is concerned with the practical application of our approach to problems from econometrics and and uncertainty quantification. Finally, Chapter 9 summarizes this thesis and discusses questions that have been left unanswered and gives an outlook to future research.

2 Numerical integration

In this chapter, we give a brief overview of cubature rules, their construction and the different notions of error and its normalization. We start with the discussion of abstract algorithms for the approximation of the linear functional

$$L_\Omega(f) := \int_\Omega f(\boldsymbol{x})\,\omega(\boldsymbol{x})\,\mathrm{d}\boldsymbol{x},$$

where $\Omega \subset \mathbb{R}^d$ is a d-dimensional domain and $\omega : \Omega \to \mathbb{R}_{\geq 0}$ is a non-negative weight function. Beside the knowledge that the integrand is from a given function space, i.e. $f \in \mathbf{F} \subset L_1(\Omega, \omega)$, an algorithm may use further information about f provided by a set of continuous functionals $\boldsymbol{\Lambda}_N = (\Lambda_1, \ldots, \Lambda_N) \subset \mathbf{F}^\star$, where $\mathbf{F}^\star$ denotes the dual of $\mathbf{F}$. If these functionals only consist of point or derivative evaluations of f, we are in the setting of *standard information*.

In order to compare the performance of different algorithms that use the same set of information one often uses the concept of worst-case error, cf. Section 2.1. In this setting, it is known that among all optimal algorithms there is also a linear algorithm. This allows the restriction to algorithms of the form

$$Q_{\boldsymbol{\Lambda}_N, \boldsymbol{w}}(f) = \sum_{i=1}^N w_i \Lambda_i(f) \quad \approx \quad L_\Omega(f)$$

for the approximation of L_Ω. Here, the most important special case is $\boldsymbol{\Lambda}_N = (\delta_{\boldsymbol{\xi}^{(1)}}, \ldots, \delta_{\boldsymbol{\xi}^{(N)}})$, where $\delta_{\boldsymbol{\xi}^{(i)}}(f) = f(\boldsymbol{\xi}^{(i)})$ denotes the point evaluation functional.

If the information is fixed it remains to choose the weights $\boldsymbol{w} \in \mathbb{R}^N$. This can be done such that certain quantities are minimized or exactness of $Q_{\boldsymbol{\Lambda}_N, \boldsymbol{w}}$ on a finite-dimensional subspace of $\mathbf{F}$ is achieved. Usually, this can be realized by solving systems of linear equations. The choice of good cubature points, however, is a much more difficult task and has been subject to intense research for many decades. In what follows we will give a brief overview on the most common approaches and strategies to obtain good cubature points and weights.

2.1 Algorithms and error notions

The goal of numerical integration is the approximation of

$$L_\Omega(f) = \int_\Omega f(\boldsymbol{x})\,\omega(\boldsymbol{x})\,\mathrm{d}\boldsymbol{x}$$

where $\Omega \subset \mathbb{R}^d$ is a d-dimensional domain and $\omega : \Omega \to \mathbb{R}_{\geq 0}$ is a non-negative weight function. Usually, one assumes that the integrand $f : \Omega \to \mathbb{R}$ comes from a given space of continuous

functions $\mathbf{F} \subset L_1(\Omega, \omega)$. At a later point in this thesis, we will specialize on $\mathbf{F}$ being a Hilbert space endowed with certain properties, but at this point we only assume that $\mathbf{F}$ is a separable Banach space of integrable functions on Ω. In this setting, $L_\Omega : \mathbf{F} \to \mathbb{R}$ is a linear functional that shall be approximated.

2.1.1 Information

In order to find an estimate of $L_\Omega(f)$, one needs certain *information* on the integrand $f \in \mathbf{F}$. Beside the information that f belongs to $\mathbf{F}$, further information is provided as a finite set of linear functionals that can can be evaluated on f, i.e.

$$\boldsymbol{\Lambda}_N = (\Lambda_1, \dots, \Lambda_N), \quad \Lambda_i \in \mathbf{F}^\star.$$

The most prominent example are of course function values. In this case, the information consists of

$$\boldsymbol{\Lambda}_N = \left(\delta_{\boldsymbol{\xi}^{(1)}}, \dots, \delta_{\boldsymbol{\xi}^{(N)}}\right), \quad \boldsymbol{\xi}^{(i)} \in \Omega$$

where $\delta_{\boldsymbol{x}}$ denotes the point evaluation functional at the point $\boldsymbol{x}$, i.e. $\delta_{\boldsymbol{x}}(f) = f(\boldsymbol{x})$. As another example one could assume that $\mathbf{F}$ consists of univariate analytic functions and choose

$$\boldsymbol{\Lambda}_N = \left(\delta_\xi, \delta_\xi^{(1)}, \dots, \delta_\xi^{(N-1)}\right),$$

where $\delta_x^{(j)}(f) = f^{(j)}(x)$ denotes the jth derivative of f evaluated at $x \in \Omega$. This is the kind of information that is used by the Taylor formula.

There are many more choices for the information $\boldsymbol{\Lambda}_N$, e.g. Fourier coefficients or integrals over smaller subdomains of Ω. However, in almost every practically relevant setting, one is restricted to so-called *standard information*, which consists of point- and derivative-evaluations only.

2.1.2 Linear algorithms and error criteria

After the information $\boldsymbol{\Lambda}_N \subset \mathbf{F}^\star$ has been fixed, one seeks to construct an algorithm that uses the available information to approximate $L_\Omega(f)$ as efficiently as possible. An algorithm is a mapping $\alpha_{\boldsymbol{\Lambda}_N} : \mathbf{F} \to \mathbb{R}$

$$\alpha_{\boldsymbol{\Lambda}_N}(f) = \phi(\Lambda_1(f), \dots, \Lambda_N(f)), \quad \phi : \mathbb{R}^N \to \mathbb{R}$$

such that $|L_\Omega(f) - \alpha_{\boldsymbol{\Lambda}_N}(f)|$ becomes small.

Throughout this thesis, we will concentrate on *linear algorithms* of the form

$$Q_{\boldsymbol{\Lambda}_N, \boldsymbol{w}}(f) = \sum_{i=1}^N w_i \Lambda_i(f), \tag{2.1}$$

which are completely determined by the information $\boldsymbol{\Lambda}_N \subset \mathbf{F}^\star$ and the choice of the weights $\boldsymbol{w} = (w_1, \dots, w_N) \in \mathbb{R}^N$.

Usually, an algorithm is not constructed for a single integrand, but rather should work on the whole class of functions $\mathbf{F}$. In order to compare the performance of different algorithms for approximating integrals L_Ω in $\mathbf{F}$, one has to define a meaningful error criterion. At this point, we mention two of them:

1. The *worst-case error* is defined as the error produced by the worst-possible function from the unit ball of $\mathbf{F}$, i.e.

$$\mathbf{wce}(Q_{\boldsymbol{\Lambda}_N, \boldsymbol{w}}, \mathbf{F}) := \sup_{\|f\|_{\mathbf{F}} \leq 1} |L_\Omega(f) - Q_{\boldsymbol{\Lambda}_N, \boldsymbol{w}}(f)|. \tag{2.2}$$

   Moreover, it is common to normalize the worst-case error with respect to the largest integral a function from the unit ball of $\mathbf{F}$ can attain, i.e.

$$\frac{\sup_{\|f\|_{\mathbf{F}} \leq 1} |L_\Omega(f) - Q_{\boldsymbol{\Lambda}_N, \boldsymbol{w}}(f)|}{\sup_{\|f\|_{\mathbf{F}} \leq 1} |L_\Omega(f)|}.$$

   The *normalized worst-case error* equals the worst-case error (2.2) up to a constant. Therefore, it does not affect asymptotic convergence rates but might have drastic impact on the constants that are usually neglected for asymptotic considerations. However, this works only for fixed dimensionality d. If d tends to infinity or the problem is foregone infinite-dimensional, the normalization has a huge impact on the difficulty and even the solvability of the problem.

2. The *average-case error* requires a probability distribution μ on $\mathbf{F}$ and then takes the average over all possible errors with respect to this distribution, i.e.

$$\mathbf{avg}(Q_{\boldsymbol{\Lambda}_N, \boldsymbol{w}}, \mathbf{F}) := \left(\int_{\mathbf{F}} |L_\Omega(f) - Q_{\boldsymbol{\Lambda}_N, \boldsymbol{w}}(f)|^2 \, \mathrm{d}\mu(f) \right)^{1/2}.$$

Throughout this thesis, we will concentrate on the *normalized worst-case error*. But we note in passing, cf. [118, 119, 154], that if the probability measure μ on $\mathbf{F}$ is Gaussian with zero mean and covariance kernel $K(\boldsymbol{x}, \boldsymbol{y}) = \int_{\mathbf{F}} f(\boldsymbol{x}) f(\boldsymbol{y}) \, \mathrm{d}\mu(f)$, the average case error of a linear algorithm equals the worst-case error in a reproducing kernel Hilbert space $\mathcal{H}_K$ with reproducing kernel K, cf. Chapter 3, i.e.

$$\mathbf{avg}(Q_{\boldsymbol{\Lambda}_N, \boldsymbol{w}}, \mathbf{F}) = \mathbf{wce}(Q_{\boldsymbol{\Lambda}_N, \boldsymbol{w}}, \mathcal{H}_K). \tag{2.3}$$

This is also well-known in statistics where (2.3) is the foundation of so-called Bayesian integration methods [120, 128, 29].

Another interesting property that linear integration algorithms enjoy in the worst-case setting is the following famous result from Smolyak and Bakhvalov, cf. [8] or [118, Thm 4.7].

Theorem 2.1. *Among all general algorithms α_{Λ_N} that use the information $\boldsymbol{\Lambda}_N$ and are optimal with respect to the worst-case error criterion in a function space $\mathbf{F}$, there is also an optimal linear algorithm $Q_{\boldsymbol{\Lambda}_N, \boldsymbol{w}}$.*

Theorem 2.1 justifies the restriction to approximations of the form (2.1) when constructing cubature rules for function spaces.

In the following, we will assume that the information $\mathbf{\Lambda}_N$ is given in terms of function values at a set $\boldsymbol{X}_N \subset \Omega$. In this setting, we define the following quantities.

The worst-case error of a linear integration algorithm $Q_{\boldsymbol{X}_N,\boldsymbol{w}}$ is denoted by

$$\mathbf{wce}(Q_{\boldsymbol{X}_N,\boldsymbol{w}}, \mathbf{F}) := \sup_{\|f\|_{\mathbf{F}} \leq 1} \left| \int_\Omega f(\boldsymbol{x})\,\omega(\boldsymbol{x})\,\mathrm{d}\boldsymbol{x} - \sum_{i=1}^N w_i f(\boldsymbol{\xi}^{(i)}) \right|.$$

Moreover, one can ask for an optimal algorithm, which uses an optimal vector of weights. The associated worst-case error is given by

$$\mathbf{w\check{c}e}(\boldsymbol{X}_N, \mathbf{F}) := \inf_{\boldsymbol{w}\in\mathbb{R}^N} \sup_{\|f\|_{\mathbf{F}} \leq 1} \left| \int_\Omega f(\boldsymbol{x})\,\omega(\boldsymbol{x})\,\mathrm{d}\boldsymbol{x} - \sum_{i=1}^N w_i f(\boldsymbol{\xi}^{(i)}) \right|. \tag{2.4}$$

The quantity $\mathbf{w\check{c}e}(\boldsymbol{X}_N, \mathbf{F})$ measures the information value of the specific point set $\boldsymbol{X}_N$. Therefore, it is often referred to as *radius of information.*

Sometimes the set of cubature points $\boldsymbol{X}_N$ is not fixed but can be chosen. This rises the question for optimal point sets. Therefore, we define the *N-th minimal worst-case error* as

$$\mathbf{w\check{c}e}_N(\mathbf{F}) := \inf_{\boldsymbol{X}_N\in\Omega^N} \inf_{\boldsymbol{w}\in\mathbb{R}^N} \sup_{\|f\|_{\mathbf{F}} \leq 1} \left| \int_\Omega f(\boldsymbol{x})\,\omega(\boldsymbol{x})\,\mathrm{d}\boldsymbol{x} - \sum_{i=1}^N w_i f(\boldsymbol{\xi}^{(i)}) \right|. \tag{2.5}$$

The $\mathbf{w\check{c}e}_N(\mathbf{F})$ measures the inherent difficulty of integration in $\mathbf{F}$ and therefore is used to measure the quality of other, non-optimal algorithms. Consider a class of algorithms $(Q_{\boldsymbol{X}_N,\boldsymbol{w}})_{N\in\mathbb{N}}$ that approximate L_Ω. If it holds that

$$\lim_{N\to\infty} \frac{\mathbf{wce}(Q_{\boldsymbol{X}_N,\boldsymbol{w}}, \mathbf{F})}{\mathbf{w\check{c}e}_N(\mathbf{F})} < \infty,$$

we say that $Q_{\boldsymbol{X}_N,\boldsymbol{w}}$ is an *order-optimal algorithm* in $\mathbf{F}$, i.e. its worst-case error decays at the same rate to zero as the best possible algorithm using the best possible point set.

2.1.3 Stability

The worst-case error of a cubature rule $Q_{\boldsymbol{X}_N,\boldsymbol{w}} : \mathbf{F} \to \mathbb{R}$ is one of the most important quantities studied in information based complexity. However, when it comes to practical applications, the stability of $Q_{\boldsymbol{X}_N,\boldsymbol{w}}$ is an important matter. To understand its importance, we recall that in a computer functions can usually only be evaluated up to a certain precision. Let us assume that the numeric evaluation $\tilde{f}(\boldsymbol{x})$ of f at all points $\boldsymbol{x} \in \Omega$ achieves a precision of $\varepsilon > 0$, i.e.

$$\left| \tilde{f}(\boldsymbol{x}) - f(\boldsymbol{x}) \right| \leq \varepsilon.$$

Therefore, the error of approximating $L_\Omega(f)$ with $Q_{\boldsymbol{X}_N,\boldsymbol{w}}(\tilde{f})$ can be bounded by

$$\left| L_\Omega(f) - Q_{\boldsymbol{X}_N,\boldsymbol{w}}(\tilde{f}) \right| = \left| L_\Omega(f) - Q_{\boldsymbol{X}_N,\boldsymbol{w}}(f) + Q_{\boldsymbol{X}_N,\boldsymbol{w}}(f) - Q_{\boldsymbol{X}_N,\boldsymbol{w}}(\tilde{f}) \right|$$

$$\leq |L_\Omega(f) - Q_{\boldsymbol{X}_N, \boldsymbol{w}}(f)| + \left|Q_{\boldsymbol{X}_N, \boldsymbol{w}}(f) - Q_{\boldsymbol{X}_N, \boldsymbol{w}}(\tilde{f})\right|$$

$$\leq \mathbf{wce}(Q_{\boldsymbol{X}_N, \boldsymbol{w}}, \mathbf{F})\|f\|_{\mathbf{F}} + \sum_{i=1}^{N} |w_i| \left|f(\boldsymbol{\xi}^{(i)}) - \tilde{f}(\boldsymbol{\xi}^{(i)})\right|$$

$$\leq \mathbf{wce}(Q_{\boldsymbol{X}_N, \boldsymbol{w}}, \mathbf{F})\|f\|_{\mathbf{F}} + \left(\sum_{i=1}^{N} |w_i|\right) \varepsilon.$$

Consequently, the quantity

$$|\boldsymbol{w}|_1 = \sum_{i=1}^{N} |w_i|$$

is an upper bound for the amplification of the numerical error ε by using the algorithm $Q_{\boldsymbol{X}_N, \boldsymbol{w}}$. The following theorem from [115, 116] ensures the existence of stable cubature rules for a broad range of spaces and integration problems.

Theorem 2.2. *Let $V_N \subset \mathbf{F}$ be an N-dimensional subspace of $\mathbf{F}$. Then, for every linear functional $L \in \mathbf{F}^\star$ and every $\varepsilon > 0$, there exist N points $\boldsymbol{X}_N$ and weights $\boldsymbol{w} \in \mathbb{R}^N$ such that it holds*

$$\sum_{i=1}^{N} w_i f(\boldsymbol{\xi}^{(i)}) = L(f) \quad \text{for all } f \in V_N$$

and

$$\|L\|_{\mathbf{F}^\star} \quad \leq \quad \sum_{i=1}^{N} |w_i| \quad \leq \quad \|L\|_{\mathbf{F}^\star} + \varepsilon.$$

Unfortunately, it can be quite difficult to construct these points and weights explicitly, cf. Section 2.3.4.

2.2 (Quasi–) Monte Carlo integration

In this section, we discuss cubature algorithms which use the same weight $w_i = 1/N$ for every function value. For random points this approach is referred to "Monte Carlo approach", while for deterministic point sets usually the term "Quasi–Monte Carlo" is used.

2.2.1 Monte Carlo integration

Assume that a probability measure μ on $\Omega \subseteq \mathbb{R}^d$ is absolutely continuous with respect to the Lebesgue measure. This implies the existence of a non-negative weight function $\omega : \Omega \to \mathbb{R}_{\geq 0}$ such that $\mathrm{d}\mu(\boldsymbol{x}) = \omega(\boldsymbol{x}) \, \mathrm{d}\boldsymbol{x}$.

The expected value of a function $f : \Omega \to \mathbb{R}$ is then given by its integral with respect to ω, i.e.

$$\mathbb{E}_\mu[f] = \int_\Omega f(\boldsymbol{x}) \, \omega(\boldsymbol{x}) \, \mathrm{d}\boldsymbol{x}.$$
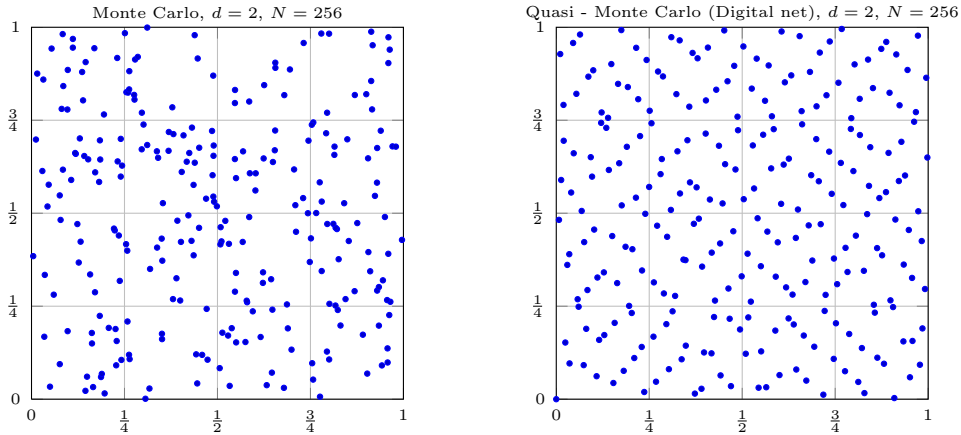
Figure 2.1: Scatter plot of $N = 256$ Monte Carlo points and quasi–Monte Carlo points in $[0,1]^2$.

For square-integrable f, the law of large numbers ensures that the average

$$\frac{1}{N} \sum_{i=1}^{N} f\left(\boldsymbol{\xi}^{(i)}\right), \qquad \text{where } \boldsymbol{\xi}^{(i)} \sim \omega \quad \text{i.i.d.} \tag{2.6}$$

converges to $\mathbb{E}_\mu[f]$ as N gets large. Moreover, the convergence of (2.6) both, in expectation and with high probability, is of order $\mathcal{O}(N^{-1/2})$, which is independent of the dimension. Here, the constant in the $\mathcal{O}$-notation depends on the variance of the integrand. Therefore, it is common to use variance reduction techniques, like e.g. control variates or importance sampling [73, 93].

2.2.2 Discrepancy and quasi–Monte Carlo integration

Similar to the Monte Carlo method is the class of so-called *quasi–Monte Carlo* methods which also relies on using the same weight $w_i = 1/N$ for every function value. However, the set of points $\boldsymbol{X}_N$ is not drawn randomly but chosen by a sophisticated strategy to be distributed as uniformly as possible within the domain of integration. This is even for the uniform weight function $\omega \equiv 1$ on $\Omega = [0,1]^d$ a difficult problem.

As can be seen in Figure 2.1, the quasi-random points are uniformly distributed over $[0,1]^2$ while the randomly distributed points have clusters, gaps and seem to be more irregular. The degree of irregularity of a given point set $\boldsymbol{X}_N$ is measured by its *discrepancy*, which comes in many different variations and has deep connections to harmonic analysis and number theory. The general idea behind discrepancy is the approximation of volumes by relative numbers of points. To be more precise, let

$$\operatorname{disc}(\boldsymbol{x}; \boldsymbol{X}_N) := \prod_{j=1}^{d} x_j - \frac{1}{N} \sum_{i=1}^{N} \chi_{[0,\boldsymbol{x})}(\boldsymbol{\xi}^{(i)}), \tag{2.7}$$

where $\chi_{[0,\boldsymbol{x})}$ is the indicator function of the box $[0,\boldsymbol{x}) := \bigotimes_{j=1}^{d}[0,x_j) \subset [0,1)^d$, which has the

volume $\prod_{j=1}^{d} x_j$. The local discrepancy $\text{disc}(\boldsymbol{x}; \boldsymbol{X}_N)$ measures how much the volume of $[0, \boldsymbol{x})$ deviates from the relative number of points from the set $\boldsymbol{X}_N = \{\boldsymbol{\xi}^{(1)}, \ldots, \boldsymbol{\xi}^{(N)}\}$ that fall into $[0, \boldsymbol{x})$.

The q-discrepancy of a point set $\boldsymbol{X}_N$ is now defined as the L_q-norm of (2.7), i.e.

$$\text{disc}_q(\boldsymbol{X}_N) := \left(\int_{[0,1]^d} |\text{disc}(\boldsymbol{x}; \boldsymbol{X}_N)|^q \, \mathrm{d}\boldsymbol{x} \right)^{1/q}.$$

This concept is useful because on the one hand the Koksma-Hlawka inequality for $q = 2$ states that

$$\left| \int_{[0,1]^d} f(\boldsymbol{x}) \, \mathrm{d}\boldsymbol{x} - \frac{1}{N} \sum_{i=1}^{N} f(\boldsymbol{\xi}^{(i)}) \right| \leq \text{disc}_2(\boldsymbol{X}_N) \|f\|_{H^1_{\text{mix}}}.$$

On the other hand it is known [52] that there exist point sets which fulfill

$$\text{disc}_2(\boldsymbol{X}_N) \preceq_d \frac{\log(N)^{(d-1)/2}}{N}.$$

This yields an error bound which is asymptotically smaller than the one of Monte Carlo. Examples for point sets with small discrepancy are digital nets, in particular the Sobol sequence [143], lattice rules [141] or the well-known Halton sequence [82].

Moreover, there exist so-called higher order quasi–Monte Carlo points which in theory allow an error bound of order $N^{-s} \log(N)^{\frac{d-1}{2}}$ if the integrand has bounded H^s_{mix} norm [74]. However, the construction, as well as the involved constants, are still a subject of intense research. For further details on point sets with small discrepancy and higher-order quasi-Monte Carlo we refer to [52].

Finally, there is a close relationship between generalized notions of discrepancy and worst-case errors in reproducing kernel Hilbert spaces, cf. Chapter 3. We also refer to [150] and Chapter 9 in [119] for a detailed discussion.

2.3 Quadrature with a degree of exactness

By the Stone-Weierstrass theorem every continuous function on a closed interval $[a, b] \subset \mathbb{R}$ can be approximated by polynomials. Therefore, it is a natural approach to construct quadrature rules that integrate polynomials exactly. Here, by cleverly choosing the n quadrature weights and the n quadrature points[1] the *Gaussian quadrature rules* achieves the maximal polynomial degree of exactness of $2n - 1$, i.e. all linear combinations of $\{1, x, x^2, \ldots, x^{2n-1}\}$ are integrated exactly.

However, sometimes non-polynomial sets of basis functions $\phi_m = \{\varphi_1, \ldots, \varphi_m\}$ are preferable to approximate certain classes of integrands, e.g. if singularities are present, cf. [79, 104]. If ϕ_m constitutes a so-called Tschebyscheff-system, cf. Def. 2.3, there exist n points $\xi_1, \ldots, \xi_n$ and

---

[1]Note at this point that we will denote the point numbers used by univariate quadrature rules by n instead of N, because we will use tensor products of univariate quadrature rules at a later point of this thesis.

positive weights $w_1, \ldots, w_n$ such that it holds, cf. [100]

$$\int_\Omega f(x)\,\omega(x)\,\mathrm{d}x = \sum_{i=1}^n w_i f(\xi_i) \quad \text{for all } f \in \operatorname{span} \phi_{2n}.$$

In this section, we first recall the basic properties of Tschebyscheff-systems and (generalized) Gaussian quadrature rules. Then, we discuss Leja points, which recently gained a lot of interest in the scientific computing community because they are maximally nested and still yield stable quadrature weights. Moreover, their distribution converges to the arc-sine distribution of the respective Gaussian set of quadrature points.

2.3.1 Tschebyscheff-systems

First, we recall so-called Tschebyscheff-systems (T-systems), cf. [96], which generalize the concept of univariate polynomials in the sense that linear combinations from an n-element T-system possess at most $(n-1)$ zeros and hence allow the construction of unique interpolants.

To this end, we define the generalized Vandermonde-matrix

$$\boldsymbol{V}(\varphi_1, \ldots, \varphi_m; t_1, \ldots, t_m) := \begin{pmatrix} \varphi_1(t_1) & \cdots & \varphi_1(t_m) \\ \vdots & \ddots & \vdots \\ \varphi_m(t_1) & \cdots & \varphi_m(t_m) \end{pmatrix} \tag{2.8}$$

for an arbitrary set of m real-valued functions $\varphi_1, \ldots, \varphi_m$ on $[a, b]$ and pairwise-distinct points $t_1 < t_2 < \ldots < t_m \in [a, b]$.

We can also remove the constraint that the points have to be pairwise distinct and write for the case $t_1 \le t_2 \le \ldots \le t_m$

$$\boldsymbol{V}(\varphi_1, \ldots, \varphi_m; t_1, \ldots, t_m) = \left(\varphi_i^{(l_j)}(t_j) \right)_{i,j=1}^m, \tag{2.9}$$

where now $l_j = \max\{l : t_{j-l} = t_j\}$. This means that repeated points correspond to higher order derivatives.

Definition 2.3. (Tschebyscheff-system)

A set of functions $\phi_m = \{\varphi_1, \ldots, \varphi_m\}, m \in \mathbb{N}$ is a *complete Tschebyscheff-system* (T-system) over a compact interval $[a, b] \subset \mathbb{R}$ iff the generalized Vandermonde-determinant

$$\det \boldsymbol{V}(\varphi_1, \ldots, \varphi_k; t_1, \ldots, t_k) \quad > \quad 0 \tag{2.10}$$

for all pairwise distinct $t_1, \ldots, t_k \in [a, b]$ and all $k = 1, \ldots, m$.

Moreover, if the interval $(a, b) \subseteq \mathbb{R}$ is not compact, we call ϕ_m a complete T-system on (a, b) if it is a complete T-system on every compact sub-interval $[\hat{a}, \hat{b}] \subset (a, b)$, cf. [104]. This of course extends to half-open intervals like $[a, b)$ or $(a, b]$.

Examples for sets of functions that form a T-system on their respective domains are given in [96] and include

- Polynomials $\{1, x, x^2, x^3, \ldots, x^{m-1}\}$.
- Fractional polynomials like $\{1, \sqrt{x}, x, x\sqrt{x}, x^2, x^2\sqrt{x}, \ldots, x^{(m-1)/2}\}$.
- Exponential translates $\{\exp(c_1 x), \ldots, \exp(c_m x)\}$ for pairwise distinct $c_i \in \mathbb{R}$.
- Radial basis functions like, e.g., $\{\exp(-\frac{(c_1-x)^2}{\sigma^2}), \ldots, \exp(-\frac{(c_m-x)^2}{\sigma^2})\}$ for pairwise distinct $c_i \in \mathbb{R}$ and $\sigma > 0$.

The property (2.10) is important because it ensures that $\boldsymbol{V}(\varphi_1, \ldots, \varphi_m; t_1, \ldots, t_m)$ is invertible for every given set of points $t_1 < t_2 < \ldots < t_m \in [a, b]$. Hence, for every given data vector $\boldsymbol{f} = (f_1, \ldots, f_m) \in \mathbb{R}^m$ there exists a unique function $f_m \in \operatorname{span} \phi_m$ which interpolates the data $\boldsymbol{f}$ at $(t_1, \ldots, t_m)$, i.e.

$$f_m(t_i) = \sum_{j=1}^{m} c_j \varphi(t_i) = f_i \quad \text{for all } i = 1, \ldots, m,$$

where $\boldsymbol{c} = \boldsymbol{V}^{-1}(\varphi_1, \ldots, \varphi_m; t_1, \ldots, t_m)\boldsymbol{f}$.

Definition 2.4. (Extended Tschebyscheff-system)

A set of functions $\phi_m = \{\varphi_1, \ldots, \varphi_m\}, m \in \mathbb{N}$ is an *extended complete Tschebyscheff-system* (ECT-system) of order p if the determinant of the matrix (2.9) is positive, i.e.

$$\det \boldsymbol{V}(\varphi_1, \ldots, \varphi_k; t_1, \ldots, t_k) > 0,$$

for all $t_1 \leq t_2 \leq \ldots, \leq t_k$, where at most p points may coincide, cf. (2.9). This shall hold for all $k = 1, \ldots, m$.

For an ECT-system it is known [96] that every function $u \in \operatorname{span} \phi_m$ has at most $m - 1$ zeros, including multiplicities up to order p.

2.3.2 (Generalized) Newton-Cotes quadrature

If ϕ_m constitutes a T-system on Ω and a set of n pairwise distinct points $X_n \subset \Omega$ is given, there is a straight-forward way to obtain quadrature weights $w_1, \ldots, w_n$ such that all functions from $\operatorname{span}\{\varphi_1, \ldots, \varphi_n\}$ are integrated exactly. This is equivalent to

$$\sum_{i=1}^{n} w_i \varphi_k(\xi_i) = \int_\Omega \varphi_k(x)\, \omega(x)\, \mathrm{d}x \quad \text{for all } k = 1, \ldots, n,$$

which can be rephrased as a linear system of equations

$$\boldsymbol{V}(\varphi_1, \ldots, \varphi_n; \xi_1, \ldots, \xi_n)\boldsymbol{w} = \boldsymbol{b}, \quad \text{where } b_k = \int_\Omega \varphi_k(x)\, \omega(x)\, \mathrm{d}x.$$

Since $\boldsymbol{V}(\varphi_1, \ldots, \varphi_n; \xi_1, \ldots, \xi_n)$ is invertible due to (2.10), the desired set of quadrature weights is given by $\boldsymbol{w} = \boldsymbol{V}^{-1}\boldsymbol{b}$.

In order to emphasize the dependence of $\boldsymbol{w}$ on the choice of the quadrature points X_n, we may also write $\boldsymbol{w}(X_n)$ to denote the set of quadrature weights that integrate polynomials up to degree $n - 1$ exactly by using function values at X_n.

Another example is related to Definition 2.4. Assume one seeks to approximate the integral of a function of which not only function values at a point set $X_n \subset \Omega$ are known, but also the value of the first derivatives at the points in X_n. Then, if $(\varphi_k)_{k=1}^{2n}$ is an ECT-system of order at least 2, it holds that

$$\sum_{i=1}^{n}\sum_{j=0}^{1} w_{i,j}\varphi_k^{(j)}(\xi_i) = \int_{\Omega}\varphi_k(x)\,\omega(x)\,\mathrm{d}x \quad \text{ for all } k = 1,\ldots,2n, \qquad (2.11)$$

where the weights $w_{i,j}, i = 1,\ldots,n$ and $j = 0,1$ are obtained by inverting the Vandermonde matrix $\boldsymbol{V}(\varphi_1,\ldots,\varphi_{2n};\xi_1,\xi_1,\xi_2,\xi_2,\ldots,\xi_n,\xi_n)$. To simplify the notation, we adopt the notation $X_n^{\boldsymbol{2}} := (\xi_1,\xi_1,\ldots,\xi_n,\xi_n)$ for the set of double integration points. The set of quadrature weights in (2.11) is then given by

$$\boldsymbol{w}(X_n^{\boldsymbol{2}}) = \boldsymbol{V}^{-1}(\varphi_1,\ldots,\varphi_{2n},X_n^{\boldsymbol{2}})\boldsymbol{b}, \quad \text{ where } b_k = \int_{\Omega}\varphi_k(x)\,\omega(x)\,\mathrm{d}x.$$

However, even though there always exists a vector of quadrature weights $\boldsymbol{w} \in \mathbb{R}^n$ which ensures exactness on span $\{\varphi_1,\ldots,\varphi_n\}$, one cannot be sure that the weights $\boldsymbol{w}$ are stable in the sense of Section 2.1.3. For example, if $\phi_j = x^{j-1}$ is the T-system of algebraic monomials and the prescribed points are equidistant in $[0,1]$, i.e. $\xi_j = j/n$, it is known [90] that already for moderate $n \geq 7$ the weights become highly unstable, which is related to Runge's phenomenon. On the other hand, if $(\varphi_k)_{k=1}^n$ is a set of compactly supported B-spline functions, equidistant points work well. Therefore, additional effort has sometimes to be made to find sets of quadrature points which guarantee the stability of the associated quadrature weights.

In fact, one can achieve even more. For extended Tschebyscheff-systems it is possible to find quadrature points which do not only result in stable quadrature weights, but are also exact on a space of $2n$ basis functions.

2.3.3 (Generalized) Gaussian quadrature

For given $n \in \mathbb{N}$ let ϕ_{2n} be a complete Tschebyscheff-system on an interval $(a,b) = \Omega \subseteq \mathbb{R}$. It was proven in [100], see also [96], that there exist pairwise distinct points $X_n = (\xi_1,\ldots,\xi_n)$ and positive weights $\boldsymbol{w} = (w_1,\ldots,w_n) \in \mathbb{R}_+$ such that it holds

$$\int_a^b \varphi_k(x)\,\omega(x)\,\mathrm{d}x = \sum_{i=1}^{n} w_i\varphi_k(\xi_i) \quad \text{ for all } k \in \{1,\ldots,2n\}. \qquad (2.12)$$

Hence, by the linearity of both sides in (2.12), all functions from span ϕ_{2n} are integrated exactly. The n points and weights are called *generalized Gaussian quadrature* points and weights, respectively.[2]

Moreover, one can also construct Gaussian quadrature rules that use not only function values but also higher order derivatives of the integrand. To this end, let $\boldsymbol{\mu} = (\mu_1,\ldots,\mu_n)$ be a

---

[2]In [72] it was shown that the points of a generalized Gaussian quadrature rule are unique.

given vector of multiplicities. In [12, 23] it was proven that there exists a unique set of points $\xi_1^*, \ldots, \xi_n^*$ such that

$$\int_a^b \varphi_k \, \omega(x) \, \mathrm{d}x = \sum_{i=1}^n \sum_{j=0}^{\mu_i-1} w_{i,j} \varphi^{(j)}(\xi_i^*) \quad \text{for all } k \in \{1, \ldots, 2N\}, \tag{2.13}$$

where $N := \sum_{i=1}^n \mu_i$ if each μ_i is odd. For arbitrary multiplicities $\boldsymbol{\mu}$, the exactness in (2.13) holds with $N = \sum_{i=1}^n \left\lfloor \frac{\mu_i+1}{2} \right\rfloor$.

2.3.4 Quadrature at Leja points

Leja points originate from polynomial interpolation where one is interested in point sets X_n with small Lebesgue constant, see [34, 36, 80, 92, 108, 149]. Of particular interest are nested sets, i.e. there exists a sequence $(n_j)_{j\in\mathbb{N}}$ such that $X_{n_j} \subset X_{n_{j+1}}$ for all $j \in \mathbb{N}$. Examples for such a set are the roots of Tschebyscheff polynomials, which, however, are only nested if the number of points is doubled on each level j, i.e. $X_{2^j} \subset X_{2^{j+1}}$. This implies an exponential growth of the nested point sets, i.e. $n_{j+1} - n_j \asymp 2^j$. An alternative are so-called *Leja-points* which are maximally nested, i.e. $n_{j+1} - n_j = 1$. This is an important property when using X_n as a building block for a tensor product method, cf. [37, 80, 138]. While it has not been proven yet, it is observed [36], that the Lebesgue constant of Leja points grows at most linearly in n. However, the theory only predicts a growth that is sub-exponential [92, 149].

In this section we will discuss using Leja points for quadrature as it was done in [80, 108, 138]. Here, despite several gaps in the existing theory, there is convincing numerical evidence, that Leja points allow for stable quadrature with polynomial degree of exactness in the spirit of Theorem 2.2.

For a given set $\Omega \subset \mathbb{C}$, a weight function $\omega : \Omega \to \mathbb{R}_{\geq 0}$ and a starting point $\xi_0 \in \Omega$, the associated Leja sequence $(\xi_i)_{i=0}^\infty \subset \Omega$ usually stems from a certain recursive optimization process. It is defined by

$$\xi_{m+1} = \arg\max_{z\in\Omega} \left| \prod_{i=0}^m (z - \xi_i) \right| \sqrt{\omega(z)}. \tag{2.14}$$

Defining $X_n := (\xi_0, \ldots, \xi_{n-1})$, it holds that

$$X_{n-1} \subset X_n \quad \text{for any } n \in \mathbb{N},$$

i.e. the hierarchy of sets $X_1, X_2, \ldots$ is *maximally nested*.

We note in passing that (2.14) is equivalent to a greedy maximization of the weighted Vandermonde matrix (2.8) for the Tschebyscheff-system of polynomials, i.e.

$$\xi_{m+1} := \arg\max_{z\in\Omega} |\det \boldsymbol{V}(\varphi_1, \ldots, \varphi_{m+2}; \xi_0, \ldots, \xi_m, z)| \; \sqrt{\omega(z)},$$

where $\varphi_j = x^{(j-1)}, j = 1, \ldots, m+2$.

In the following, we will discuss two kinds of specific Leja constructions. The first one is related
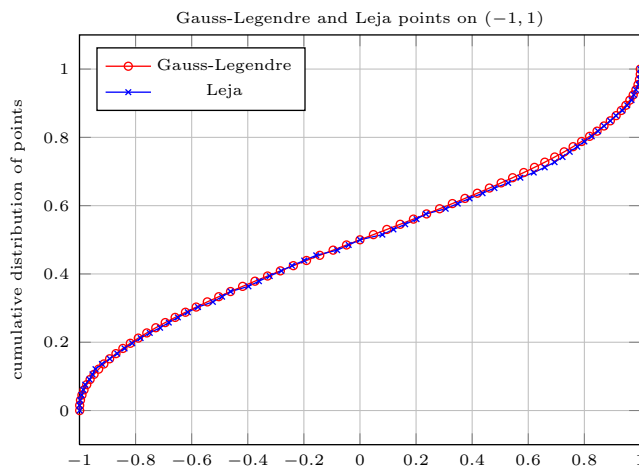
Figure 2.2: The distribution of Gauss-Legendre and Leja points on $(-1, 1)$ approaches the arcsine-distribution.

to integration on $[-1, 1]$ with respect to the uniform distribution, the other one to integration on $(-\infty, \infty)$ with respect to the Gaussian distribution.

Leja points on $[-1, 1]$

The Leja points on $\Omega = [-1, 1]$ are suited for integration with respect to the uniform measure $\frac{1}{2}\,\mathrm{d}x$ and are constructed by

$$\xi_{m+1} = \arg\max_{z \in \Omega} \left| \prod_{i=0}^{m} (z - \xi_i) \right|.$$

The starting point $\xi_0 \in [-1, 1]$ is arbitrary, but $\xi_0 = 1$ is an often proposed choice, see e.g. [37]. After a point set X_n is fixed, the vector of n quadrature weights $\boldsymbol{w}$ is determined such that it holds

$$\sum_{i=1}^{n} w_i \xi_i^k = \frac{1}{2} \int_{-1}^{1} x^k \,\mathrm{d}x \quad \text{for } k = 1, \dots, n.$$

Numerical experiments suggest that the resulting weights are stable, cf. Figure 2.3 and [108, 80]. However, this has not been proven yet. The only result regarding the stability of Leja points for polynomial interpolation can be found in [149], where it was proven that the Lebesgue constant does grow at most sub-exponentially.

An interesting property of the above definition of Leja points is that they asymptotically distribute like the Gauss-Legendre points, cf. Figure 2.2. To be more precise, let $\xi_{1,n}^*, \dots, \xi_{n,n}^*$ be the roots of the n-th Legendre polynomial. Then it holds (in the weak sense)

$$\lim_{n \to \infty} \frac{1}{n} \sum_{i=1}^{n} \delta_{\xi_i} \quad = \quad \lim_{n \to \infty} \frac{1}{n} \sum_{i=1}^{n} \delta_{\xi_{i,n}^*} \quad = \quad \tilde{v},$$
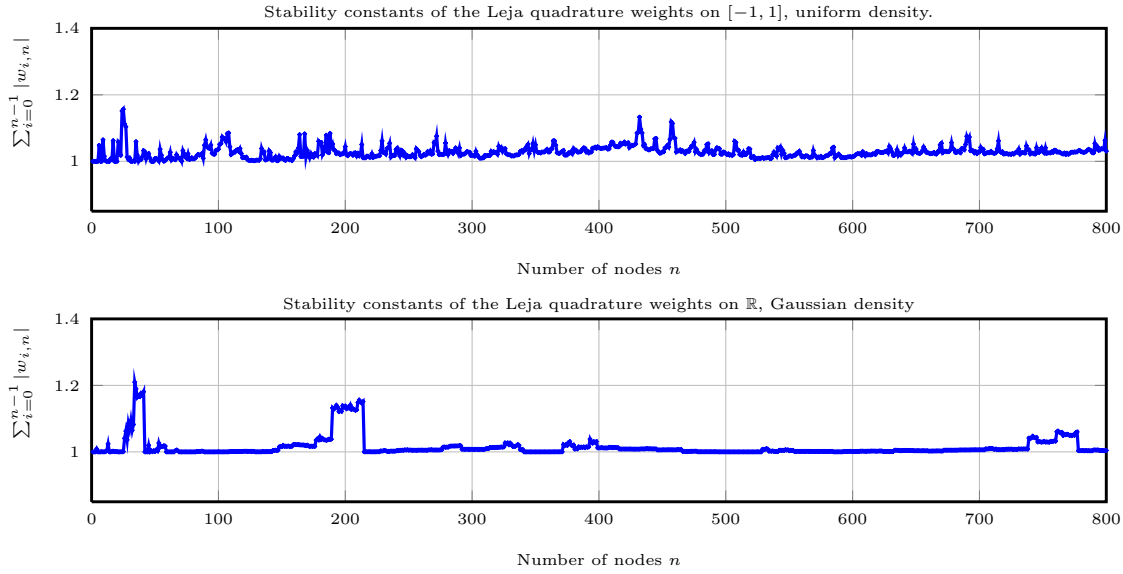
Figure 2.3: Stability of the Leja sequence on $[-1, 1]$ and $\mathbb{R}$.

where $\tilde{v}$ is the density of the logarithmic potential equilibrium measure of the domain Ω in the presence of a certain external field cf. [108, 132]. In this particular setting, $\tilde{v}$ is the so-called arcsin-distribution with cumulative distribution function $F(x) = \frac{1}{2} + \frac{1}{\pi} \arcsin(x)$.

Leja points on $(-\infty, \infty)$

The other important special case are Leja points on $\mathbb{R}$ with respect to the Gaussian density function $\omega(x) = \frac{1}{\sqrt{2\pi}} e^{-\frac{x^2}{2}}$. According to (2.14), the associated Leja points are computed by

$$\xi_{m+1} = \arg\max_{z \in \Omega} \left| \prod_{i=0}^{m} (z - \xi_i) \right| e^{-\frac{z^2}{4}},$$

where now ξ_0 is usually chosen to be $\xi_0 = 0$.

Then, the vector of n quadrature weights $\boldsymbol{w}$ for X_n is determined such that it holds

$$\sum_{i=1}^{n} w_i \xi_i^k = \frac{1}{\sqrt{2\pi}} \int_{-\infty}^{\infty} x^k e^{-\frac{x^2}{2}} \, \mathrm{d}x \quad \text{for } k = 1, \ldots, n.$$

Again, the only available results regarding the stability of this Leja sequence yield that the Lebesgue-constant is sub-exponential [92]. However, in numerical experiments, cf. Figure 2.3, the weights are obviously stable in the sense that $\sum_{i=1}^{n} |w_i| < 1.3$ for all $n \in \{1, 800\}$.

2.4 Tensor product based methods

The construction of efficient algorithms for multivariate integration is not a simple task. Most of the concepts that are available in the univariate setting do not generalize to multiple dimensions, e.g. because there are no T-systems in dimensions $d \geq 2$. This fact is known as the Mairhuber-Curtis theorem [163].

Therefore, it is natural to construct integration algorithms for multivariate problems by building onto the well-understood univariate methods.

2.4.1 Full tensor product cubature

The most straight-forward approach to apply univariate quadrature rules for multivariate problems is the *full tensor product*. Consider the integration problem

$$L_{\Omega_{(d)}}(f) := \int_{\Omega_{(d)}} f(\boldsymbol{x})\, \omega_{(d)}(\boldsymbol{x})\, \mathrm{d}\boldsymbol{x} = \int_{\Omega_1} \dots \int_{\Omega_d} f(\boldsymbol{x})\, \omega_1(x_1) \cdots \omega_d(x_d)\, \mathrm{d}\boldsymbol{x},$$

i.e. both, the integration domain $\Omega_{(d)} = \bigotimes_{j=1}^{d} \Omega_j$ and the density $\omega_{(d)}(\boldsymbol{x}) = \prod_{j=1}^{d} \omega_j(x_j)$ have product structure.

Assume that there exists a quadrature rule

$$Q_{n_j}^{(j)}(f) := \sum_{i=1}^{n_j} w_{i,j}^{(j)} f(\xi_{i,j}^{(j)}), \quad j \in \mathbb{N}$$

for each coordinate direction $j \in \{1, \dots, d\}$.

Defining $\mathbf{n} = (n_1, \dots, n_d) \in \mathbb{N}_0^d$, we can now discretize the j-th integral L_{Ω_j} with $Q_{n_j}^{(j)}$ and obtain

$$\begin{aligned}
Q_{\mathbf{n}}(f) &= Q_{n_1}^{(1)} \otimes \cdots \otimes Q_{n_d}^{(d)}(f) \\
&= \sum_{i_1=1}^{n_1} \cdots \sum_{i_d=1}^{n_d} \left(\prod_{j=1}^{d} w_{i_j,n_j}^{(j)} \right) f\left(\xi_{i_1,n_1}^{(1)}, \dots, \xi_{i_d,n_d}^{(d)} \right).
\end{aligned}$$

If $Q_{n_j}^{(j)}$ is exact on some m_j-dimensional space $V_{m_j}^{(j)} = \mathrm{span}\,\{\varphi_1^{(j)}, \dots, \varphi_{m_j}^{(j)}\}$, then $Q_{\mathbf{n}}$ is exact on

$$V_{\mathbf{m}} := V_{m_1}^{(1)} \otimes \dots \otimes V_{m_d}^{(d)} = \mathrm{span}\, \left\{ \prod_{j=1}^{d} \varphi_{k_j}^{(j)} : \mathbf{k} \leq \mathbf{m} \right\}.$$

Here, $\boldsymbol{k} \leq \mathbf{m}$ has to be understood component-wise.

With this construction, however, the number of points $N = \prod_{j=1}^{d} n_j$ grows exponentially with the dimensionality d.

2.4.2 Generalized sparse grid cubature

Sparse grids go back to ideas of Babenko [5], Smolyak [142] and Zenger [166]. They are based on a decomposition of the aforementioned tensor product method into a multi-indexed telescoping sum. Balancing cost and error, this sum is truncated in a way that substantially reduces the cost while maintaining almost the same error as the full tensor product.

Besides in numerical integration [69, 70, 117], sparse grids are nowadays also used for multivariate density estimation [76], uncertainty quantification [37, 113], the reconstruction of manifolds [60], time series prediction [19] or multivariate regression [64, 65].

However, in order to apply the sparse grid technique, the problem at hand has to fulfill certain prerequisites. To this end, define $\Omega_{(d)} := \Omega_1 \times \ldots \times \Omega_d$ and $\omega_{(d)}(\boldsymbol{x}) = \prod_{j=1}^{d} \omega_j(x_j)$ to be a product density function on a product domain. The multivariate integral then reads

$$L_{\Omega_{(d)}}(f) = \int_{\Omega_{(d)}} f(\boldsymbol{x})\, \omega_{(d)}(\boldsymbol{x})\, \mathrm{d}\boldsymbol{x}. \tag{2.15}$$

For an approximation of (2.15), we start from a sequence of univariate quadrature rules

$$Q_k^{(j)}(f) = \sum_{i=0}^{n_k-1} w_{i,k}^{(j)} f(\xi_{i,k}^{(j)}), \quad \text{for } k = 0, 1, 2, \ldots,$$

which shall be convergent in univariate function spaces $\mathbf{F}_j \subset L_1(\Omega_j, \omega_j)$, i.e.

$$\lim_{k \to \infty} Q_k^{(j)}(f) = L_{\Omega_j}(f), \quad \text{for all } f \in \mathbf{F}_j, j = 1, \ldots, d.$$

With the convention $Q_{-1}^{(j)}(f) = 0$, we define the hierarchical quadrature rules

$$\Delta_k^{(j)}(f) = Q_k^{(j)}(f) - Q_{k-1}^{(j)}(f), \quad k \in \mathbb{N}_0,$$

which clearly fulfill

$$L_{\Omega_j}(f) = \lim_{k \to \infty} Q_k^{(j)}(f) = \sum_{k=0}^{\infty} \Delta_k^{(j)}(f) \quad \text{for all } f \in \mathbf{F}_j.$$

Then, for every $f \in \mathbf{F}_{(d)} := \mathbf{F}_1 \otimes \ldots \otimes \mathbf{F}_d$ it holds

$$L_{\Omega_{(d)}}(f) = \sum_{k_1=0}^{\infty} \cdots \sum_{k_d=0}^{\infty} \Delta_{k_1}^{(1)} \otimes \cdots \otimes \Delta_{k_d}^{(d)} f =: \sum_{\boldsymbol{k} \in \mathbb{N}_0^d} \Delta_{\boldsymbol{k}}(f) \tag{2.16}$$

An approximation to $L_{\Omega_{(d)}}(f)$ is now given by a truncation of (2.16), i.e.

$$Q_{\mathcal{A}}(f) := \sum_{\boldsymbol{k} \in \mathcal{A}} \Delta_{\boldsymbol{k}}(f) \quad \approx \quad L_{\Omega_{(d)}}(f), \tag{2.17}$$

where $\mathcal{A} \subset \mathbb{N}_0^d$ is a downward-closed[3] index set. For example, $\mathcal{A} = \{\boldsymbol{k} \in \mathbb{N}_0^d : |\boldsymbol{k}|_\infty \leq L\}$ recovers the full tensor product method from the preceding section, i.e. $Q_{n_L}^{(1)} \otimes \cdots \otimes Q_{n_L}^{(d)}(f)$.

Before we proceed with the discussion on how the index set $\mathcal{A}$ can be chosen, we prove a result regarding the degree of exactness the sparse grid method can achieve.

To this end, let $\mathcal{A} \in \mathbb{N}_0^d$ be a downward-closed set, i.e.

$$\mathcal{A} \subset \mathbb{N}_0^d \text{ such that } \boldsymbol{k} \in \mathcal{A} \wedge \boldsymbol{l} \leq \boldsymbol{k} \text{ implies that } \boldsymbol{l} \in \mathcal{A}$$

and define

$$u_{\mathcal{A}} := \max\{k_1 \in \mathbb{N}_0 : (k_1, \ldots, k_d) \in \mathcal{A}\}$$

to be the largest element of the form $(k_1, 0, \ldots, 0) \in \mathbb{N}_0^d$ that is contained in $\mathcal{A}$. Moreover, let

$$\mathcal{A}_{d-1}(k_1) := \left\{(k_2, \ldots, k_d) \in \mathbb{N}_0^{d-1} : (k_1, \ldots, k_d) \in \mathcal{A}\right\}.$$

Clearly, it holds $\mathcal{A}_{d-1}(k_1) = \emptyset$ for $k_1 > u_{\mathcal{A}}$ and we can decompose every downward-closed set $\mathcal{A} \subset \mathbb{N}_0^d$ into

$$\bigcup_{k_1=0}^{u_{\mathcal{A}}} \bigcup_{(k_2,\ldots,k_d)\in\mathcal{A}_{d-1}(k_1)} \{(k_1, \ldots, k_d)\}. \tag{2.18}$$

Now, we are prepared to prove the following theorem, which relates the index set $\mathcal{A}$ to a finite-dimensional subspace on which $Q_{\mathcal{A}}$, defined in (2.17), is exact.

Theorem 2.5. *Let $Q_k^{(j)}(f), k \in \mathbb{N}_0$ be a sequence of univariate quadrature rules that are exact on a sequence of nested $m_k^{(j)}$-dimensional spaces $V_k^{(j)} = \mathrm{span}\{\varphi_1^{(j)}, \ldots, \varphi_{m_k}^{(j)}\}$, where $V_k^{(j)} \subset V_{k+1}^{(j)}$ for all $j = 1, \ldots, d$. Then, for every downward-closed index set $\mathcal{A} \subset \mathbb{N}_0^d$, the sparse tensor product algorithm*

$$Q_{\mathcal{A}}(f) = \sum_{\boldsymbol{k}\in\mathcal{A}} \left(\bigotimes_{j=1}^d \Delta_{k_j}^{(j)}\right)(f)$$

is exact on the space $V_{\mathcal{A}} = \bigoplus_{\boldsymbol{k}\in\mathcal{A}} \left(\bigotimes_{j=1}^d V_{k_j}^{(j)}\right)$ spanned by the basis functions

$$\bigcup_{\boldsymbol{k}\in\mathcal{A}} \left\{\prod_{j=1}^d \varphi_{i_j}^{(j)}(x_j) : \mathbf{i} \leq \boldsymbol{m_k}\right\}. \tag{2.19}$$

Proof. We generalize the proof for the special case of the classical Smolyak index set [117] to arbitrary downward-closed index sets $\mathcal{A} \subset \mathbb{N}_0^d$. We have to show that it holds for all $f \in V_{\mathcal{A}}$ that

$$L_{\Omega_{(d)}}f = Q_{\mathcal{A}}(f). \tag{2.20}$$

To this end, it is enough to show (2.20) for all elements of the basis (2.19), which have the form $f(\boldsymbol{x}) = \prod_{j=1}^d f_j(x_j)$ with $f_j \in V_{k_j}^{(j)}$ for some $\boldsymbol{k} \in \mathcal{A}$.

---

[3]Sometimes, this property is also referred to as *lower set*.

For $d = 1$ the claim holds true due to the exactness of the univariate quadrature rules. We assume that the claim holds for $d-1$ dimensions as well. Then, due to the decomposition (2.18) we can write $Q_{\mathcal{A}}(f)$ for a product function $f(\boldsymbol{x}) = \prod_{j=1}^{d} f_j(x_j)$ as

$$
\begin{aligned}
Q_{\mathcal{A}}(f) &= \sum_{k_1=0}^{u_{\mathcal{A}}} \sum_{(k_2,\dots,k_d)\in\mathcal{A}_{d-1}(k_1)} \left(\bigotimes_{j=1}^{d} \Delta_{k_j}^{(j)} \right)(f) = \sum_{k_1=0}^{u_{\mathcal{A}}} Q_{\mathcal{A}_{d-1}(k_1)}(f_2\cdot\ldots\cdot f_d)\cdot\Delta_{k_1}^{(1)}(f_1) \\
&= \sum_{k_1=0}^{u_{\mathcal{A}}} \left(\prod_{j=2}^{d} L_{\Omega_j}(f_j) \right)\cdot\Delta_{k_1}^{(1)}(f_1) = \left(\prod_{j=2}^{d} L_{\Omega_j}(f_j) \right) \sum_{k_1=0}^{u_{\mathcal{A}}} \cdot \left(Q_{k_1}^{(1)}(f_1) - Q_{k_1-1}^{(1)}(f_1) \right) \\
&= \left(\prod_{j=2}^{d} L_{\Omega_j}(f_j) \right)\cdot Q_{u_{\mathcal{A}}}^{(1)}(f_1) = \left(\prod_{j=2}^{d} L_{\Omega_j}(f_j) \right)\cdot L_{\Omega_1}(f_1) \\
&= L_{\Omega_{(d)}}(f).
\end{aligned}
$$

$\square$

In order to derive error bounds one can simply use the triangle inequality and a scaling of the unit ball to obtain

$$
\begin{aligned}
|L_{\Omega_{(d)}}(f) - Q_{\mathcal{A}}(f)| &\leq \sum_{\boldsymbol{k}\in\mathbb{N}_0^d\setminus\mathcal{A}} |\Delta_{\boldsymbol{k}}(f)|, \\
&\leq \sum_{\boldsymbol{k}\in\mathbb{N}_0^d\setminus\mathcal{A}} \|\Delta_{\boldsymbol{k}}\|_{\mathbf{F}^\star}\|f\|_{\mathbf{F}}.
\end{aligned} \tag{2.21}
$$

The choice of a good index set now depends on the magnitude of the norms of $\|\Delta_{\boldsymbol{k}}\|_{\mathbf{F}^\star}$ and on the cost $c(\boldsymbol{k})$ which is the number of additional function evaluations required by $\Delta_{\boldsymbol{k}}$. Then, cf. [32], an optimal index set for f consists of the elements with largest benefit-cost ratio, i.e. $|\Delta_{\boldsymbol{k}}(f)|/c(\boldsymbol{k})$. An index set that is optimal with respect to the upper bound (2.21) for the whole class $\mathbf{F}$ is then given by

$$
\mathcal{A}(\varepsilon) = \{ \boldsymbol{k}\in\mathbb{N}_0^d : \frac{\|\Delta_{\boldsymbol{k}}\|_{\mathbf{F}^\star}}{c(\boldsymbol{k})} \geq \varepsilon \}.
$$

We refer to [31, 78] for the details.

However, bounds for $\|\Delta_{\boldsymbol{k}}\|_{\mathbf{F}^\star}$ are not always available or difficult to obtain. Moreover, in practical applications when dealing with a specific function f, it is not clear which space is suited best since often f belongs to a whole scale of function spaces. In such a setting it is advantageous to tailor the index set $\mathcal{A}$ specifically to f instead of fixing it a priorily.

2.4.3 Dimension-adaptive sparse grids

In practice, algorithms are required which can construct appropriate index sets $\mathcal{A}$ automatically during the actual computation. Such algorithms were presented in [70, 84], where the index sets are found in a dimension-adaptive way by the use of suitable error indicators.

Algorithm 1: Dimension-adaptive construction of the index set $\mathcal{A}$.

Input:

- Desired accuracy $\varepsilon > 0$.

- Lookahead $p \in \{1, 2, \ldots\}$.

Initialize:

- Set of active indices: $\mathcal{A} = \{(0, \ldots, 0)\}$.

- $S = \Delta_{(0,\ldots,0)} f$.

repeat

    1. Determine neighbourhood indices $\mathcal{B} = \{\mathcal{A} + \alpha \boldsymbol{e}_j : j = 1, \ldots, d \text{ and } \alpha = 1, \ldots, p\}$.

    2. For all $\boldsymbol{k} \in \mathcal{B}$ compute $\Delta_{\boldsymbol{k}} f$ and associated cost $c(\boldsymbol{k})$.

    3. Determine (some) $\boldsymbol{k}^* = \arg\max_{\boldsymbol{k} \in \mathcal{B}} |\Delta_{\boldsymbol{k}} f| / c(\boldsymbol{k})$.

        foreach $\boldsymbol{k} \leq \boldsymbol{k}^* : \boldsymbol{k} \notin \mathcal{A}$ **do**

            a) Add the index $\boldsymbol{k}$ to $\mathcal{A}$.

            b) Update the sum $S = S + \Delta_{\boldsymbol{k}} f$.

        end

until $|\Delta_{\boldsymbol{k}^*} f| < \varepsilon$;

Output: $\mathrm{Q}_{\mathcal{A}} f = S$.

The adaptive method that is outlined in Algorithm 1 starts with the smallest index set $\mathcal{A} = \{(0, \ldots, 0)\}$. Then, step-by-step the index $\boldsymbol{k}^*$ which has the largest value $|\Delta_{\boldsymbol{k}} f| / c(\boldsymbol{k})$ from the set of all neighbouring admissible indices $\boldsymbol{k} \in \mathcal{B}$ is added. This index is expected to provide the largest error reduction, see [68, 70, 77, 107] for details. The lookahead parameter p determines the size of the neighbourhood that is taken into account. In most cases a lookahead of $p = 1$ or $p = 2$ will be sufficient.

The downward-closedness of the index set $\mathcal{A}$ is ensured at all times by adding the required parent indices of $\boldsymbol{k}^*$ in every step to $\mathcal{A}$ as well.

Altogether, Algorithm 1 provides an adaptive detection of the important coordinate directions and constructs $\mathcal{A}$ by a greedy approach that leads to quasi-optimal index sets in the sense of [31, 78].

3 Reproducing kernel Hilbert spaces

Reproducing kernel Hilbert spaces (RKHS) are Hilbert spaces of functions in which point evaluation is a bounded linear functional. The eponymous property of RKHS is the existence of a unique kernel function K that represents all point evaluation functionals and therefore encodes the structure of the space.

RKHS are used in many branches of applied mathematics, e.g. in statistics where there are relationships to Gaussian processes or in machine learning where they are used within support vector machines [16, 139], but also for the solution of partial differential equations [59].

In this chapter, we recall the definition and the most important properties of RKHS that we need in the sequel of this thesis with the goal of constructing efficient cubature rules. To this end, we discuss the approximation of linear functionals by linear combinations of other linear functionals in Section 3.2. Of particular importance is the choice of weights that minimize the worst-case error. These are derived directly from their normal equations, but there is an important relationship to the more general theory of spline algorithms, which is discussed in Section 3.3. Since we have to use quadrature rules that do not only rely on function values but on more general classes of information in several proofs in Chapter 5, we will treat the subject on an abstract level with general *linear information*. The case of function values then follows as a special case.

Moreover, we quote some composition formulas to construct kernels of subspaces or tensor product spaces in Section 3.5. A brief overview on kernels that will be important in the remainder of this thesis complements this chapter in Section 3.6.

3.1 Basics

In the following we recall the basic definitions of reproducing kernel Hilbert spaces (RKHS) as well as their most important properties that will be useful in the remainder of this thesis. Herein, we mostly follow [4, 16, 59, 135].

Definition 3.1. (Symmetric positive definite kernel)

A function $K : \Omega \times \Omega \to \mathbb{R}$, where $\Omega \subseteq \mathbb{R}^d$, is called *symmetric positive definite kernel* if

1. $K(\boldsymbol{x}, \boldsymbol{y}) = K(\boldsymbol{y}, \boldsymbol{x})$ for all $\boldsymbol{x}, \boldsymbol{y} \in \Omega$.

2. For every $N \in \mathbb{N}$ and all sets of N pairwise distinct points $\boldsymbol{X}_N = \{\boldsymbol{\xi}^{(1)}, \ldots, \boldsymbol{\xi}^{(N)}\} \subset \Omega$, the *kernel matrix* $\boldsymbol{G}(\boldsymbol{X}_N) \in \mathbb{R}^{N \times N}$ with

$$G_{i,j}(\boldsymbol{X}_N) = K\left(\boldsymbol{\xi}^{(i)}, \boldsymbol{\xi}^{(j)}\right)$$

is positive definite, i.e. $\boldsymbol{c}^\intercal \boldsymbol{G}(\boldsymbol{X}_N)\boldsymbol{c} > 0$ for all $\boldsymbol{0} \neq \boldsymbol{c} \in \mathbb{R}^N$.

The following theorem describes the relationship between symmetric positive definite kernels and certain Hilbert spaces. It is proven in e.g. [4, 16, 59].

Theorem 3.2.

(i) *Let $\mathcal{H}$ be a Hilbert space of real-valued functions on $\Omega \subseteq \mathbb{R}^d$, where $\langle \cdot, \cdot \rangle_{\mathcal{H}}$ denotes the inner-product of $\mathcal{H}$. Assume that the point-evaluation functional $\delta_{\boldsymbol{x}}(f) = f(\boldsymbol{x})$ is continuous in $\mathcal{H}$ for all $\boldsymbol{x} \in \Omega$. Then, there exists a* unique *symmetric positive definite kernel function $K : \Omega \times \Omega \to \mathbb{R}$ such that*

   (a) *The Riesz-representer of the point evaluation functional $\delta_{\boldsymbol{x}}$ in $\mathcal{H}$ is $K(\cdot, \boldsymbol{x})$, i.e.*

   $$f(\boldsymbol{x}) = \delta_{\boldsymbol{x}}(f) = \langle f, K(\cdot, \boldsymbol{x}) \rangle_{\mathcal{H}} \text{ for all } f \in \mathcal{H} \text{ and all } \boldsymbol{x} \in \Omega. \tag{3.1}$$

   We say that the kernel K reproduces point evaluation in $\mathcal{H}$.

   (b) *The closure of the span of all point evaluation representers $K(\cdot, \boldsymbol{x})$ equals $\mathcal{H}$, i.e.*

   $$\mathcal{H} = \overline{\text{span} \{K(\cdot, \boldsymbol{x}) | \boldsymbol{x} \in \Omega\}}.$$

(ii) *The converse is also true: For every symmetric positive definite kernel $K : \Omega \times \Omega$ there exists a unique Hilbert space for which the properties (a) and (b) hold true.*

From now on we only consider separable Hilbert spaces that fulfill the assumptions of Theorem 3.2, i.e. point evaluation is a continuous linear functional and $\mathcal{H}$ contains a countable subset that is dense in $\mathcal{H}$. Because of the one-to-one correspondence between such Hilbert spaces and symmetric positive definite kernel functions, we will write $\mathcal{H}_K$ to denote the Hilbert space in which the kernel K is reproducing. Hence, $\mathcal{H}_K$ is called a *reproducing kernel Hilbert space*, which usually is abbreviated as *RKHS*.

First, we note that convergence in $\mathcal{H}_K$ always implies uniform convergence.

Proposition 3.3. *If a sequence of functions $(f_n)_{n \in \mathbb{N}}$ converges to a function f with respect to the $\| \cdot \|_{\mathcal{H}_K}$-norm, then $f_n \to f$ uniformly on every compact subset $S \subset \Omega$.*

Proof.

$$|f(x) - f_n(x)| = |\langle f(\cdot) - f_n(\cdot), K(\cdot, \boldsymbol{x}) \rangle_{\mathcal{H}_K}| \leq \|f - f_n\|_{\mathcal{H}_K} \|K(\cdot, \boldsymbol{x})\|_{\mathcal{H}_K} = \|f - f_n\|_{\mathcal{H}_K} \sqrt{K(\boldsymbol{x}, \boldsymbol{x})}.$$

$\square$

The next proposition discusses the role of orthonormal bases in separable RKHS. Its proof can be found e.g. in [16, Sec. 1.5].

Proposition 3.4. *Let $\mathcal{H}_K$ be a RKHS with associated kernel $K : \Omega \times \Omega \to \mathbb{R}$. Let $(\psi_k)_{k=0}^{\infty}$ be an orthonormal basis of $\mathcal{H}_K$, i.e. $\langle \psi_i, \psi_j \rangle_{\mathcal{H}_K} = \delta_{i,j}$ for all $i, j \in \mathbb{N}_0$. Then the kernel can be expressed as*

$$K(\boldsymbol{x}, \boldsymbol{y}) = \sum_{k=0}^{\infty} \psi_k(\boldsymbol{x}) \psi_k(\boldsymbol{y}).$$

The following result allows to explicitly compute the Riesz-representer and operator norm of arbitrary bounded functionals in $\mathcal{H}_K^\star$, which is isomorphic to $\mathcal{H}_K$. To this end, we use the notation $L^{(\boldsymbol{y})}K(\boldsymbol{x}, \boldsymbol{y})$ to denote the application of the functional L to the variable $\boldsymbol{y}$, e.g. $\delta_{\boldsymbol{\xi}}^{(\boldsymbol{y})}K(\boldsymbol{x}, \boldsymbol{y}) = K(\boldsymbol{x}, \boldsymbol{\xi})$.

Proposition 3.5. *Let* $L : \mathcal{H}_K \to \mathbb{R}$ *be a bounded linear functional on* $\mathcal{H}_K$, *i.e.* $L \in \mathcal{H}_K^\star$. *Then, there exists a function* $\ell \in \mathcal{H}_K$ *such that*

$$L(f) = \langle \ell, f \rangle_{\mathcal{H}_K} \text{ holds for all } f \in \mathcal{H}_K.$$

The Riesz-representer $\ell \in \mathcal{H}_K$ *of* L *is explicitly given by*

$$\ell(\boldsymbol{x}) = L^{(\boldsymbol{y})}K(\boldsymbol{x}, \boldsymbol{y}) = L\left(K(\boldsymbol{x}, \cdot)\right). \tag{3.2}$$

Moreover, the norm of L *is given by*

$$\|L\|_{\mathcal{H}_K^\star} = \sup_{\|f\|_{\mathcal{H}_K} \leq 1} |L(f)| = \sqrt{L^{(\boldsymbol{x})}L^{(\boldsymbol{y})}K(\boldsymbol{x}, \boldsymbol{y})}. \tag{3.3}$$

Proof. By the Riesz-representation theorem there exists a unique function $\ell \in \mathcal{H}_K$ such that $L(f) = \langle \ell, f \rangle_{\mathcal{H}_K}$ for all $f \in \mathcal{H}_K$. To see that ℓ is given by (3.2), we use the reproduction formula (3.1) to obtain

$$\ell(\boldsymbol{x}) = \langle \ell, K(\cdot, \boldsymbol{x}) \rangle_{\mathcal{H}_K} = L(K(\cdot, \boldsymbol{x})) = L^{(\boldsymbol{y})}K(\boldsymbol{x}, \boldsymbol{y}).$$

Regarding (3.3) we use (3.2) and compute

$$\|L\|_{\mathcal{H}_K^\star}^2 = \|\ell\|_{\mathcal{H}_K}^2 = \langle \ell, \ell \rangle_{\mathcal{H}_K} = L(\ell) = L(L^{(\boldsymbol{y})}K(\cdot, \boldsymbol{y})) = L^{(\boldsymbol{x})}L^{(\boldsymbol{y})}K(\boldsymbol{x}, \boldsymbol{y}).$$

$\square$

Using Proposition 3.4, the norm of L can also be written as an infinite series, i.e.

$$\|L\|_{\mathcal{H}_K^\star}^2 = L^{(\boldsymbol{x})}L^{(\boldsymbol{y})}K(\boldsymbol{x}, \boldsymbol{y}) = \sum_{k=0}^{\infty} L^{(\boldsymbol{x})}L^{(\boldsymbol{y})}\psi_k(\boldsymbol{x})\psi_k(\boldsymbol{y}) = \sum_{k=0}^{\infty} |L(\psi_k)|^2, \tag{3.4}$$

where $(\psi_k)_{k=0}^{\infty}$ is an orthonormal basis in $\mathcal{H}_K$.

3.2 Approximation of linear functionals

Since numerical integration seeks to approximate a given linear functional by linear combinations of different functionals (mostly point evaluations), we now consider the approximation of bounded linear functionals in reproducing kernel Hilbert spaces. To this end, we stay in a rather abstract setting during this section, but turn to more concrete examples in Section 3.4 of this Chapter.

We are now interested in approximating a continuous linear functional $L : \mathcal{H}_K \to \mathbb{R}$ using the *information* (c.f. Section 2.1) that is given by a finite set of linearly independent functionals

$$\boldsymbol{\Lambda}_N := \{\Lambda_1, \ldots, \Lambda_N\}, \quad \Lambda_i \in \mathcal{H}_K^{\star}.$$

In the following we assume that $L \notin \operatorname{span} \boldsymbol{\Lambda}_N$.

From Proposition 3.5 we know that the Riesz-representers of L and $\Lambda_1, \ldots, \Lambda_N$ are given by $\ell(\boldsymbol{x}) = L^{(\boldsymbol{y})} K(\boldsymbol{x}, \boldsymbol{y})$ and $\lambda_i(\boldsymbol{x}) = \Lambda_i^{(\boldsymbol{y})} K(\boldsymbol{x}, \boldsymbol{y}), i = 1, \ldots, N$, respectively.

Motivated by Theorem 2.1, we restrict ourselves to linear approximation algorithms, i.e.

$$Q_{\boldsymbol{\Lambda}_N, \boldsymbol{w}}(f) = \sum_{i=1}^{N} w_i \cdot \Lambda_i(f) \approx L(f). \tag{3.5}$$

The choice of the weights $\boldsymbol{w} = (w_1, \ldots, w_N) \in \mathbb{R}^N$ will be discussed later.

The approximation error

$$R_{\boldsymbol{\Lambda}_N, \boldsymbol{w}}(f) := L(f) - Q_{\boldsymbol{\Lambda}_N, \boldsymbol{w}}(f)$$

is a bounded linear functional itself which has a representer $r_{\boldsymbol{\Lambda}_N, \boldsymbol{w}} \in \mathcal{H}_K$ given by

$$r_{\boldsymbol{\Lambda}_N, \boldsymbol{w}}(\boldsymbol{x}) = R_{\boldsymbol{\Lambda}_N, \boldsymbol{w}}^{(\boldsymbol{y})} K(\boldsymbol{x}, \boldsymbol{y}) = L^{(\boldsymbol{y})} K(\boldsymbol{x}, \boldsymbol{y}) - \sum_{i=1}^{n} w_i \, \Lambda_i^{(\boldsymbol{y})} K(\boldsymbol{x}, \boldsymbol{y}).$$

Its norm

$$\|R_{\boldsymbol{\Lambda}_N, \boldsymbol{w}}\|_{\mathcal{H}_K^{\star}} = \sup_{\|f\|_{\mathcal{H}_K} \leq 1} |R_{\boldsymbol{\Lambda}_N, \boldsymbol{w}}|$$

can be computed by

$$
\begin{aligned}
\|R_{\boldsymbol{\Lambda}_N, \boldsymbol{w}}\|_{\mathcal{H}_K^{\star}}^2 =& R_{\boldsymbol{\Lambda}_N, \boldsymbol{w}}(r_{\boldsymbol{\Lambda}_N, \boldsymbol{w}}) = R_{\boldsymbol{\Lambda}_N, \boldsymbol{w}}^{(\boldsymbol{x})} R_{\boldsymbol{\Lambda}_N, \boldsymbol{w}}^{(\boldsymbol{y})} K(\boldsymbol{x}, \boldsymbol{y}) \\
=& R_{\boldsymbol{\Lambda}_N, \boldsymbol{w}}^{(\boldsymbol{x})} \left(L^{(\boldsymbol{y})} K(\boldsymbol{x}, \boldsymbol{y}) - Q_{\boldsymbol{\Lambda}_N, \boldsymbol{w}}^{(\boldsymbol{y})} K(\boldsymbol{x}, \boldsymbol{y}) \right) \\
=& L^{(\boldsymbol{x})} L^{(\boldsymbol{y})} K(\boldsymbol{x}, \boldsymbol{y}) - 2 Q_{\boldsymbol{\Lambda}_N, \boldsymbol{w}}^{(\boldsymbol{x})} L^{(\boldsymbol{y})} K(\boldsymbol{x}, \boldsymbol{y}) + Q_{\boldsymbol{\Lambda}_N, \boldsymbol{w}}^{(\boldsymbol{x})} Q_{\boldsymbol{\Lambda}_N, \boldsymbol{w}}^{(\boldsymbol{y})} K(\boldsymbol{x}, \boldsymbol{y}) \\
=& L^{(\boldsymbol{x})} L^{(\boldsymbol{y})} K(\boldsymbol{x}, \boldsymbol{y}) - 2 \sum_{j=1}^{N} w_j L^{(\boldsymbol{x})} \Lambda_j^{(\boldsymbol{y})} K(\boldsymbol{x}, \boldsymbol{y}) \\
& + \sum_{i=1}^{N} \sum_{j=1}^{N} w_i w_j \Lambda_i^{(\boldsymbol{x})} \Lambda_j^{(\boldsymbol{y})} K(\boldsymbol{x}, \boldsymbol{y}) \\
=& \|L\|_{\mathcal{H}_K} - 2 \sum_{j=1}^{N} w_j \Lambda_j(\ell) + \sum_{i=1}^{N} \sum_{j=1}^{N} w_i w_j \Lambda_i^{(\boldsymbol{x})} \Lambda_j^{(\boldsymbol{y})} K(\boldsymbol{x}, \boldsymbol{y}),
\end{aligned}
\tag{3.6}
$$

which is known as the squared *worst-case error formula* (see e.g. [119, 154]) or the *power function* of the functional L (see e.g. [59, 135]).

Moreover, having in mind Proposition 3.4, according to (3.4) the worst-case error can also be

written as

$$\|R_{\boldsymbol{\Lambda}_N, \boldsymbol{w}}\|_{\mathcal{H}_K^\star}^2 = \sum_{k=0}^\infty |R_{\boldsymbol{\Lambda}_N, \boldsymbol{w}}(\psi_k)|^2 = \sum_{k=0}^\infty \left| L(\psi_k) - \sum_{j=1}^N w_j \Lambda_j(\psi_k) \right|^2, \tag{3.7}$$

where $(\psi_k)_{k=0}^\infty$ is an orthonormal basis of $\mathcal{H}_K$.

For a given set of information $\boldsymbol{\Lambda}_N \subset \mathcal{H}_K^\star$, the optimal linear algorithm is defined by the vector of optimal weights $\check{\boldsymbol{w}}(\boldsymbol{\Lambda}_N) = (\check{w}_1(\boldsymbol{\Lambda}_N), \ldots, \check{w}_n(\boldsymbol{\Lambda}_N))$, i.e.

$$\check{\boldsymbol{w}}(\boldsymbol{\Lambda}_N) := \arg\min_{\boldsymbol{w} \in \mathbb{R}^N} \|R_{\boldsymbol{\Lambda}_N, \boldsymbol{w}}\|_{\mathcal{H}_K^\star}. \tag{3.8}$$

It can be seen from (3.6) that $\|R_{\boldsymbol{\Lambda}_N, \boldsymbol{w}}\|_{\mathcal{H}_K^\star}^2$ is a quadratic form in $\boldsymbol{w}$ whose partial derivatives are given by

$$\frac{\partial}{\partial w_k} \|R_{\boldsymbol{\Lambda}_N, \boldsymbol{w}}\|_{\mathcal{H}_K^\star}^2 = -2 \left(L^{(\boldsymbol{x})} \Lambda_k^{(\boldsymbol{y})} K(\boldsymbol{x}, \boldsymbol{y}) - \sum_{i=1}^N w_i \Lambda_i^{(\boldsymbol{x})} \Lambda_k^{(\boldsymbol{y})} K(\boldsymbol{x}, \boldsymbol{y}) \right),$$

such that the first-order conditions for optimality $\frac{\partial}{\partial w_k} \|R_{\boldsymbol{\Lambda}_N, \boldsymbol{w}}\|_{\mathcal{H}_K^\star}^2 = 0$ for $k = 1, \ldots, N$ imply

$$L^{(\boldsymbol{x})} \Lambda_k^{(\boldsymbol{y})} K(\boldsymbol{x}, \boldsymbol{y}) = \sum_{i=1}^N w_i \Lambda_i^{(\boldsymbol{x})} \Lambda_k^{(\boldsymbol{y})} K(\boldsymbol{x}, \boldsymbol{y}) \quad \text{for } k = 1, \ldots, N. \tag{3.9}$$

This leads to a linear system of equations, i.e. the vector of optimal weights is *uniquely* determined by

$$\check{\boldsymbol{w}}(\boldsymbol{\Lambda}_N) = \check{\boldsymbol{w}}(\boldsymbol{\Lambda}_N, K) = \arg\min_{\boldsymbol{w} \in \mathbb{R}^n} \|R_{\boldsymbol{\Lambda}_N, \boldsymbol{w}}\| = \boldsymbol{G}_{\boldsymbol{\Lambda}_N}^{-1} \cdot \boldsymbol{b}(\boldsymbol{\Lambda}_N). \tag{3.10}$$

Here, the matrix $\boldsymbol{G}(\boldsymbol{\Lambda}_N) \in \mathbb{R}^{N \times N}$ is the Gramian of the representers λ_i of the functionals Λ_i that act on $\mathcal{H}_K$, i.e.

$$\boldsymbol{G}(\boldsymbol{\Lambda}_N) = \boldsymbol{G}(\boldsymbol{\Lambda}_N, K) = (\langle \lambda_i, \lambda_j \rangle_{\mathcal{H}_K})_{i,j=1}^N = \left(\Lambda_i^{(\boldsymbol{x})} \Lambda_j^{(\boldsymbol{y})} K(\boldsymbol{x}, \boldsymbol{y}) \right)_{i,j=1}^N \tag{3.11}$$

and the right-hand side vector $\boldsymbol{b}(\boldsymbol{\Lambda}_N) \in \mathbb{R}^N$ is given by

$$\boldsymbol{b}(\boldsymbol{\Lambda}_N) := \boldsymbol{b}(\boldsymbol{\Lambda}_N, K) := (\Lambda_i(\ell))_{i=1}^N = \left(L^{(\boldsymbol{x})} \Lambda_i^{(\boldsymbol{y})} K(\boldsymbol{x}, \boldsymbol{y}) \right)_{i=1}^N. \tag{3.12}$$

If it is clear from the context, we will drop the dependence of $\boldsymbol{G}$, $\boldsymbol{b}$ and $\check{\boldsymbol{w}}$ on K to keep the notation more simple.

In the following we will denote the linear approximation (3.5) that uses optimal weights $\check{\boldsymbol{w}}(\boldsymbol{\Lambda}_N)$ defined in (3.10) by $\check{Q}_{\boldsymbol{\Lambda}_N}$. The associated error functional will be denoted by $\check{R}_{\boldsymbol{\Lambda}_N}$ and its Riesz-representer as $\check{r}_{\boldsymbol{\Lambda}_N}$.

Moreover, it will be helpful to express the worst-case error $\|\check{R}_{\boldsymbol{\Lambda}_N}\|_{\mathcal{H}_K^\star}$ in a more convenient form. To this end, we note that by (3.9) the choice of optimal weights $\check{\boldsymbol{w}}(\boldsymbol{\Lambda}_N)$ is equivalent to

$$\check{R}_{\boldsymbol{\Lambda}_N}(\lambda_k) = \Lambda_k(\check{r}_{\boldsymbol{\Lambda}_N}) = 0 \quad \text{for } k =, 1 \ldots, N.$$

Therefore, the worst-case error formula (3.6) takes the simpler form

$$
\begin{aligned}
\|\check{R}_{\boldsymbol{\Lambda}_N}\|_{\mathcal{H}_K^\star}^2 &= \check{R}_{\boldsymbol{\Lambda}_N}(\check{r}_{\boldsymbol{\Lambda}_N}) = L(\check{r}_{\boldsymbol{\Lambda}_N}) - \check{Q}_{\boldsymbol{\Lambda}_N}(\check{r}_{\boldsymbol{\Lambda}_N}) \\
&= L(\check{r}_{\boldsymbol{\Lambda}_N}) = L^{(\boldsymbol{x})}L^{(\boldsymbol{y})}K(\boldsymbol{x},\boldsymbol{y}) - \sum_{j=1}^N \check{w}_j(\boldsymbol{\Lambda}_N) L^{(\boldsymbol{x})}\Lambda_j^{(\boldsymbol{y})}K(\boldsymbol{x},\boldsymbol{y}) \\
&= \|L\|_{\mathcal{H}_K^\star}^2 - \sum_{j=1}^N \check{w}_j(\boldsymbol{\Lambda}_N)\Lambda_j(\ell) \\
&= \|L\|_{\mathcal{H}_K^\star}^2 - \boldsymbol{b}^\mathsf{T}(\boldsymbol{\Lambda}_N)\boldsymbol{G}^{-1}(\boldsymbol{\Lambda}_N)\boldsymbol{b}(\boldsymbol{\Lambda}_N).
\end{aligned}
\tag{3.13}
$$

Before we proceed, we note the following property of the optimally weighted worst-case error $\|\check{R}_{\boldsymbol{\Lambda}_N}\|_{\mathcal{H}_K^\star}$. Let $\tilde{\Lambda}_N \subset \mathcal{H}_K^\star$ be a set of linear functionals such that $\operatorname{span}\tilde{\boldsymbol{\Lambda}}_N = \operatorname{span}\boldsymbol{\Lambda}_N$, i.e. there exists a matrix $\boldsymbol{A} \in \mathrm{GL}(n)$ such that $\tilde{\Lambda}_i = \sum_{k=1}^N a_{i,k}\Lambda_k$. Then, it holds

$$
\|\check{R}_{\boldsymbol{\Lambda}_N}\|_{\mathcal{H}_K^\star} = \|\check{R}_{\tilde{\boldsymbol{\Lambda}}_N}\|_{\mathcal{H}_K^\star},
$$

i.e. the worst-case error of an optimal algorithm is independent of any (invertible) linear transformation of the underlying information. This follows from (3.13) because

$$
\begin{aligned}
\|\check{R}_{\tilde{\boldsymbol{\Lambda}}_N}\|_{\mathcal{H}_K^\star}^2 &= \|L\|_{\mathcal{H}_K^\star}^2 - \boldsymbol{b}^\mathsf{T}(\tilde{\boldsymbol{\Lambda}}_N)\boldsymbol{G}^{-1}(\tilde{\boldsymbol{\Lambda}}_N)\boldsymbol{b}(\tilde{\boldsymbol{\Lambda}}_N) \\
&= \|L\|_{\mathcal{H}_K^\star}^2 - (\boldsymbol{A}\cdot\boldsymbol{b}(\boldsymbol{\Lambda}_N))^\mathsf{T}(\boldsymbol{A}\cdot\boldsymbol{G}(\boldsymbol{\Lambda}_N)\cdot\boldsymbol{A}^\mathsf{T})^{-1}\boldsymbol{A}\cdot\boldsymbol{b}(\boldsymbol{\Lambda}_N) \\
&= \|L\|_{\mathcal{H}_K^\star}^2 - \boldsymbol{b}^\mathsf{T}(\boldsymbol{\Lambda}_N)\boldsymbol{G}^{-1}(\boldsymbol{\Lambda}_N)\boldsymbol{b}(\boldsymbol{\Lambda}_N).
\end{aligned}
$$

The following corollary summarizes the most important properties of optimally weighted approximations to bounded linear functionals in reproducing kernel Hilbert spaces.

Corollary 3.6. *Let $L \in \mathcal{H}_K^\star$ be a bounded linear functional with representer $\ell \in \mathcal{H}_K$. Moreover, $\boldsymbol{\Lambda}_N = (\Lambda_1,\ldots,\Lambda_N) \subset \mathcal{H}_K^\star$ denotes N different linear functionals as information. Then, it holds*

(i) For an arbitrary linear approximation

$$
Q_{\boldsymbol{\Lambda},\boldsymbol{w}}(f) = \sum_{i=1}^N w_i \Lambda_i(f)
$$

the worst-case error is given by

$$
\begin{aligned}
\|L - Q_{\boldsymbol{\Lambda},\boldsymbol{w}}\|_{\mathcal{H}_K^\star}^2 &= L^{(\boldsymbol{x})}L^{(\boldsymbol{y})}K(\boldsymbol{x},\boldsymbol{y}) - 2Q_{\boldsymbol{\Lambda},\boldsymbol{w}}^{(\boldsymbol{x})}L^{(\boldsymbol{y})}K(\boldsymbol{x},\boldsymbol{y}) + Q_{\boldsymbol{\Lambda},\boldsymbol{w}}^{(\boldsymbol{x})}Q_{\boldsymbol{\Lambda},\boldsymbol{w}}^{(\boldsymbol{y})}K(\boldsymbol{x},\boldsymbol{y}) \\
&= \|L\|_{\mathcal{H}_K^\star}^2 - 2Q_{\boldsymbol{\Lambda},\boldsymbol{w}}(\ell) + \|Q_{\boldsymbol{\Lambda},\boldsymbol{w}}\|_{\mathcal{H}_K^\star}^2.
\end{aligned}
\tag{3.14}
$$

(ii) For an orthonormal basis $(\psi_k)_{k=0}^\infty$ of $\mathcal{H}_K$ the worst-case error can be computed by

$$
\|L - Q_{\boldsymbol{\Lambda},\boldsymbol{w}}\|_{\mathcal{H}_K^\star}^2 = \sum_{k=0}^\infty |L(\psi_k) - Q_{\boldsymbol{\Lambda},\boldsymbol{w}}(\psi_k)|^2
$$

(iii) The vector of weights that minimizes the worst-case error (3.14) is given by

$$\check{\boldsymbol{w}}(\boldsymbol{\Lambda}_N) = \boldsymbol{G}^{-1}(\boldsymbol{\Lambda}_N)\,\boldsymbol{b}(\boldsymbol{\Lambda}_N).$$

The resulting linear approximation to L

$$\check{Q}_{\boldsymbol{\Lambda}_N}(f) = \sum_{i=1}^{N} \check{w}_i(\boldsymbol{\Lambda}_N)\Lambda_i(f)$$

achieves the smallest worst-case error among all (possibly nonlinear) algorithms that use the information $\boldsymbol{\Lambda}_N$.

(iv) The representer of the error functional $\check{R}_{\boldsymbol{\Lambda}_N} = L - \check{Q}_{\boldsymbol{\Lambda}_N}$ vanishes at Λ_k, i.e.

$$\Lambda_k(\check{r}_{\boldsymbol{\Lambda}_N}) = 0, \quad \text{ for all } k = 1, \dots, N$$

and the vector of optimal weights $\check{\boldsymbol{w}}_{\boldsymbol{\Lambda}_N}$ is uniquely determined by these conditions. Equivalently, the optimal algorithm $\check{Q}_{\boldsymbol{\Lambda}_N}$ treats exactly all functions from the span of the representers $\{\lambda_i, i = 1, \dots, N\}$, where $\lambda_i(\boldsymbol{x}) = \Lambda_i^{(\boldsymbol{y})} K(\boldsymbol{x}, \boldsymbol{y})$, i.e.

$$\check{Q}_{\boldsymbol{\Lambda}_N}(\lambda_i) = L(\lambda_i) \text{ for all } i = 1, \dots, N.$$

(v) The worst case error of $\check{Q}_{\boldsymbol{\Lambda}_N}$ takes the simpler form

$$\|\check{R}_{\boldsymbol{\Lambda}_N}\|_{\mathcal{H}_K^\star}^2 = \check{R}_{\boldsymbol{\Lambda}_N}(\ell) = \|L\|_{\mathcal{H}_K^\star}^2 - \check{Q}_{\boldsymbol{\Lambda}_N}(\ell)$$

$$= \|L\|_{\mathcal{H}_K^\star}^2 - \sum_{i=1}^{N} \check{w}_i(\boldsymbol{\Lambda}_N)\Lambda_i(\ell)$$

$$= \|L\|_{\mathcal{H}_K^\star}^2 - \boldsymbol{b}^\mathsf{T}(\boldsymbol{\Lambda}_N)\boldsymbol{G}^{-1}(\boldsymbol{\Lambda}_N)\boldsymbol{b}(\boldsymbol{\Lambda}_N).$$

(vi) The worst-case error $\|\check{R}_{\boldsymbol{\Lambda}_N}\|_{\mathcal{H}_K^\star}$ of an optimal algorithm that uses the information given by $\boldsymbol{\Lambda}_N \subset \mathcal{H}_K^\star$ is independent of any (non-singular) linear transformation of $\boldsymbol{\Lambda}_N$.

Finally, the following proposition states that the error of an optimal approximation algorithm can always be reduced by adding a further information functional.

Lemma 3.7. *If $L \notin \operatorname{span} \boldsymbol{\Lambda}_N$, the error of any optimal linear approximation $\check{Q}_{\boldsymbol{\Lambda}_N}$ to L can be reduced by adding a functional $\Lambda_{N+1} \in \mathcal{H}_K^\star$ with $\Lambda_{N+1}(\check{r}_{\boldsymbol{\Lambda}_N}) \neq 0$ to the information.*

Proof. We choose Λ_{N+1}, such that $\Lambda_{N+1}(\check{r}_{\boldsymbol{\Lambda}_N}) \neq 0$ and define the linear algorithm

$$Q_{N+1}(f) := Q_{\boldsymbol{\Lambda}_N}(f) + \tilde{w}_{N+1}\Lambda_{N+1}(f),$$

whose error representer is $r_{N+1}(\boldsymbol{x}) := \check{r}_{\boldsymbol{\Lambda}_N}(\boldsymbol{x}) - \tilde{w}_{N+1}\Lambda_{N+1}^{(\boldsymbol{x})} K(\boldsymbol{x}, \boldsymbol{y})$.

Choosing $\tilde{w}_{N+1} = \Lambda_{N+1}(\check{r}_{\boldsymbol{\Lambda}_N}) \cdot \left(\Lambda_{N+1}^{(\boldsymbol{x})} \Lambda_{N+1}^{(\boldsymbol{y})} K(\boldsymbol{x}, \boldsymbol{y}) \right)^{-1}$, we obtain $\Lambda_{N+1}(\check{r}_{\boldsymbol{\Lambda}_N}) = 0$. Then, we

can compute

$$\begin{aligned}
\|R_{N+1}\|^2 = R_{N+1}(r_{N+1}) &= R_{\mathbf{\Lambda}_N}(r_{N+1}) - \tilde{w}_{N+1}\Lambda_{N+1}(r_{N+1}) \\
&= R_{\mathbf{\Lambda}_N}(r_{N+1}) = R_{\mathbf{\Lambda}_N}(\check{r}_{\mathbf{\Lambda}_N}) - \tilde{w}_{N+1}\Lambda_{N+1}(\check{r}_{\mathbf{\Lambda}_N}) \\
&= \|\check{r}_{\mathbf{\Lambda}_N}\|^2 - \tilde{w}_{N+1}^2\left(\Lambda_{N+1}^{(\boldsymbol{x})}\Lambda_{N+1}^{(\boldsymbol{y})}K(\boldsymbol{x},\boldsymbol{y})\right).
\end{aligned}$$

As $\|\check{R}_{\mathbf{\Lambda}_{N+1}}\| \leq \|R_{N+1}\| < \|\check{R}_{\mathbf{\Lambda}_N}\|$, the claim is proven.

$\square$

Corollary 3.8. *If K is normalized such that $\|L\|_{\mathcal{H}_K} = 1$, then $\|\check{r}_{\mathbf{\Lambda}_N}\|_{\mathcal{H}_K} < 1$ for all $N \geq 1$.*

3.3 Relationship to spline algorithms

In the following we will discuss the relation of optimal cubature rules to so-called spline algorithms, which are treated in a much more general setting in [154]. In what follows, we will keep the level of abstraction as low as possible.

Definition 3.9. (Spline interpolation)
For a given set of linear functionals $\mathbf{\Lambda}_N = (\Lambda_1, \ldots, \Lambda_N) \subset \mathcal{H}_K^\star$ and a data vector $\boldsymbol{f} = (\Lambda_i(f))_{i=1}^N$ generated by a function $f \in \mathcal{H}_K$, the associated interpolatory spline $S_f \in \mathcal{H}_K$ is defined by

(i) $\Lambda_i(S_f) = f_i$ for $i = 1, \ldots, N$, i.e. S_f interpolates the data $\boldsymbol{f}$ at $\mathbf{\Lambda}_N$.

(ii) $\|S_f\|_{\mathcal{H}_K} = \min\{\|g\| : g \in \mathcal{H}_K \text{ and } \Lambda_i(g) = f_i, i = 1, \ldots, N\}$, i.e. among all functions that interpolate $\boldsymbol{f}$, the spline S_f has minimal $\mathcal{H}_K$-norm.

We can construct the interpolatory spline algorithm explicitly since it is the orthogonal projection of f onto $\mathcal{H}_{K(\mathbf{\Lambda}_N)}$. To this end, we define

$$\begin{aligned}
S_f(\boldsymbol{x}) := \sum_{k=1}^N c_k(f)\lambda_k(\boldsymbol{x}), \quad \text{where } \boldsymbol{c}(f) := \boldsymbol{G}^{-1}(\mathbf{\Lambda}_N)\boldsymbol{f} \\
= \sum_{k=1}^N \sum_{l=1}^N G_{k,l}^{-1}(\mathbf{\Lambda}_N)f_l\Lambda_l^{(\boldsymbol{y})}K(\boldsymbol{x},\boldsymbol{y}),
\end{aligned} \quad (3.15)$$

where the matrix $\boldsymbol{G}(\mathbf{\Lambda}_N)$ was defined in (3.11). The property (i) in Definition 3.9 now follows from $\Lambda_i(\lambda_k) = G_{i,k}(\mathbf{\Lambda}_N)$ and hence

$$\Lambda_i(S_f) = \sum_{k=1}^N c_k(f)\Lambda_i(\lambda_k) = \boldsymbol{c}^\mathsf{T}(f)\boldsymbol{G}(\mathbf{\Lambda}_N)\boldsymbol{e}_i = \boldsymbol{f}^\mathsf{T}\boldsymbol{G}^{-1}(\mathbf{\Lambda}_N)\boldsymbol{G}(\mathbf{\Lambda}_N)\boldsymbol{e}_i = f_i.$$

To see (ii), we first show that $f - S_f$ is orthogonal to S_f in $\mathcal{H}_K$, i.e.

$$\langle f - S_f, S_f\rangle_{\mathcal{H}_K} = 0 \quad \text{for all } f \in \mathcal{H}_K. \quad (3.16)$$

This follows by

$$\langle f - S_f, S_f \rangle_{\mathcal{H}_K} = \sum_{k=1}^{N} c_k(f) \langle f - S_f, \lambda_k \rangle_{\mathcal{H}_K} = \sum_{k=1}^{N} c_k(f) \underbrace{\Lambda_k(f - S_f)}_{=0} = 0.$$

Then, we can conclude from (3.16) that

$$\|f - S_f\|_{\mathcal{H}_K}^2 = \|f\|_{\mathcal{H}_K}^2 - \|S_f\|_{\mathcal{H}_K}^2,$$

which implies $\|S_f\|_{\mathcal{H}_K}^2 \leq \|f\|_{\mathcal{H}_K}^2$. In other words, the norm of S_f never exceeds the norm of f and therefore is the desired minimum norm interpolant.

Next, we construct a *cardinal representation* of the spline (3.15) which consists of functions $H_1, \ldots, H_N \in \text{span}\{\lambda_1, \ldots, \lambda_N\}$ such that $\Lambda_i(H_j) = \delta_{i,j}$. In the context of polynomial interpolation such functions are sometimes called *Lagrange basis*.

The functions $H_1, \ldots, H_N$ can be constructed by finding a matrix of coefficients $\boldsymbol{C} \in \mathbb{R}^{N \times N}$ which fulfills

$$\sum_{k=1}^{N} C_{j,k} \Lambda_i(\lambda_k) = \delta_{i,j} \quad \text{for all } i, j = 1, \ldots, N.$$

Because it holds $\Lambda_i(\lambda_k) = \langle \lambda_i, \lambda_k \rangle_{\mathcal{H}_K} = \Lambda_i^{(\boldsymbol{x})} \Lambda_j^{(\boldsymbol{y})} K(\boldsymbol{x}, \boldsymbol{y}) = G_{i,k}(\boldsymbol{\Lambda}_N)$, we conclude that the coefficient matrix is given by $\boldsymbol{C} = \boldsymbol{G}^{-1}(\boldsymbol{\Lambda}_N)$, i.e.

$$H_j(\boldsymbol{x}) = \sum_{k=1}^{N} G_{j,k}^{-1}(\boldsymbol{\Lambda}_N) \lambda_k(\boldsymbol{x}).$$

Now, the spline interpolant (3.15) can be written as

$$S_f(\boldsymbol{x}) = \sum_{i=1}^{N} f_i H_i(\boldsymbol{x}).$$

It is interesting to note that the optimal weights $\breve{w}_1(\boldsymbol{\Lambda}_N), \ldots, \breve{w}_N(\boldsymbol{\Lambda}_N)$ for the approximation of a linear functional $L \in \mathcal{H}_K^\star$ from (3.8) can also be obtained from the cardinal functions $H_1, \ldots, H_N$ via $\breve{w}_i(\boldsymbol{\Lambda}_N) = L(H_i)$. To see this, we compute

$$L(H_i) = \sum_{k=1}^{N} G_{i,k}^{-1} L(\lambda_k) = \sum_{k=1}^{N} G_{i,k}^{-1} \Lambda_k(\ell) = \left(\boldsymbol{G}^{-1}(\boldsymbol{\Lambda}_N) \boldsymbol{b}(\boldsymbol{\Lambda}_N) \right)_i = \breve{w}_i(\boldsymbol{\Lambda}_N). \tag{3.17}$$

3.4 Application to numerical integration

Until now we kept everything rather abstract by considering only general linear information in form of $\boldsymbol{\Lambda}_N \subset \mathcal{H}_K^\star$ to approximate $L \in \mathcal{H}_K^\star$. In order to get more concrete, we now consider

the setting where L is an integration functional of the form

$$L_\Omega(f) := \int_\Omega f(\boldsymbol{x})\,\omega(\boldsymbol{x})\,\mathrm{d}\boldsymbol{x}.$$

Here, $\Omega \subseteq \mathbb{R}^d$ and $\omega : \Omega \to \mathbb{R}_{\geq 0}$ is a non-negative weight function. We have to assume that $L_\Omega \in \mathcal{H}_K^\star$, which is the case if the kernel K is integrable, i.e. $L_\Omega^{(\boldsymbol{x})} L_\Omega^{(\boldsymbol{y})} K(\boldsymbol{x}, \boldsymbol{y}) < \infty$. We will discuss two scenarios that are important in the remainder of this thesis.

3.4.1 Integration using function values

The most classical choice of the set of information $\boldsymbol{\Lambda}_N$ would be point evaluations at a set of N points $\boldsymbol{X}_N = (\boldsymbol{\xi}^{(1)}, \ldots, \boldsymbol{\xi}^{(N)})$. In what follows, the information provided by the functionals $\Lambda_N = (\delta_{\boldsymbol{\xi}^{(1)}}, \ldots, \delta_{\boldsymbol{\xi}^{(N)}})$ will be denoted by $\boldsymbol{X}_N$ as well.

For an arbitrary vector of cubature weights $\boldsymbol{w} \in \mathbb{R}^N$ the error functional is

$$R_{\boldsymbol{X}_N, \boldsymbol{w}}(f) = \int_\Omega f(\boldsymbol{x})\,\omega(\boldsymbol{x})\,\mathrm{d}\boldsymbol{x} - \sum_{i=1}^N w_i f\left(\boldsymbol{\xi}^{(i)}\right).$$

The associated worst-case error formula, c.f. (3.6) now reads

$$\begin{aligned}
\|R_{\boldsymbol{X}_N, \boldsymbol{w}}\|_{\mathcal{H}_K^\star}^2 = &\int_\Omega \int_\Omega K(\boldsymbol{x}, \boldsymbol{y})\,\omega(\boldsymbol{x})\omega(\boldsymbol{y})\,\mathrm{d}\boldsymbol{x}\,\mathrm{d}\boldsymbol{y} - 2\sum_{i=1}^N w_i \int_\Omega K(\boldsymbol{\xi}^{(i)}, \boldsymbol{y})\,\omega(\boldsymbol{y})\,\mathrm{d}\boldsymbol{y} \\
&+ \sum_{i=1}^N \sum_{j=1}^N w_i w_j K(\boldsymbol{\xi}^{(i)}, \boldsymbol{\xi}^{(j)}).
\end{aligned} \tag{3.18}$$

If optimal weights

$$\check{\boldsymbol{w}}(\boldsymbol{X}_N) = \boldsymbol{G}^{-1}(\boldsymbol{X}_N)\boldsymbol{b}(\boldsymbol{X}_N)$$

are chosen, the resulting cubature rule

$$L_\Omega(f) \approx \sum_{i=1}^N \check{w}_i(\boldsymbol{X}_N) f\left(\boldsymbol{\xi}^{(i)}\right)$$

has the simplified worst-case error representation, c.f. Corollary 3.6, given by

$$\begin{aligned}
\|\check{R}_{\boldsymbol{X}_N}\|_{\mathcal{H}_K^\star}^2 &= \int_\Omega \int_\Omega K(\boldsymbol{x}, \boldsymbol{y})\,\omega(\boldsymbol{x})\omega(\boldsymbol{y})\,\mathrm{d}\boldsymbol{x}\,\mathrm{d}\boldsymbol{y} - \sum_{i=1}^N w_i \int_\Omega K(\boldsymbol{\xi}^{(i)}, \boldsymbol{y})\,\omega(\boldsymbol{y})\,\mathrm{d}\boldsymbol{y} \\
&= \int_\Omega \int_\Omega K(\boldsymbol{x}, \boldsymbol{y})\,\omega(\boldsymbol{x})\omega(\boldsymbol{y})\,\mathrm{d}\boldsymbol{x}\,\mathrm{d}\boldsymbol{y} - \boldsymbol{b}^\mathsf{T}(\boldsymbol{X}_N)\boldsymbol{G}^{-1}(\boldsymbol{X}_N)\boldsymbol{b}(\boldsymbol{X}_N).
\end{aligned}$$

According to (3.11) and (3.12), we have the Gramian $\boldsymbol{G}(\boldsymbol{X}_N) = (K(\boldsymbol{\xi}^{(i)}, \boldsymbol{\xi}^{(j)}))_{i,j=1}^N$ and the right-hand side vector $\boldsymbol{b}(\boldsymbol{X}_N) = (\ell_\Omega(\boldsymbol{\xi}^{(i)}))_{i=1}^N$ in this setting.

3.4.2 Integration using higher order derivatives

A different setting that will be important in Chapter 5 is univariate integration where not only function values but also values of the derivative of the integrand can be used. To this end, let $\Omega \subseteq \mathbb{R}$ and a set of n points $X_n = (\xi_1, \ldots, \xi_n) \in \Omega^n$ be given. For a vector of multiplicities $\boldsymbol{\mu} = (\mu_1, \ldots, \mu_n) \in \mathbb{N}^n$ with $N = \sum_{i=1}^n \mu_i$ we write

$$X_n^{\boldsymbol{\mu}} = \begin{pmatrix} \xi_1 & \xi_2 & \cdots & \xi_n \\ \mu_1 & \mu_2 & \cdots & \mu_n \end{pmatrix}, \quad \mu_i > 0,$$

which is short for the information given by

$$\boldsymbol{\Lambda}_N = X_n^{\boldsymbol{\mu}} = (\delta_{\xi_1}, \delta_{\xi_1}^1, \ldots, \delta_{\xi_1}^{\mu_1-1}, \ldots, \delta_{\xi_n}, \ldots, \delta_{\xi_n}^{\mu_n-1}).$$

Here, $\delta_x^j(f) = f^{(j)}(x)$ denotes the evaluation of the j-th derivative of f at the point $x \in \Omega$. We assume that δ_x^j is a bounded linear functional in $\mathcal{H}_K$, i.e. $(\delta_x^j)^{(s)}(\delta_x^j)^{(t)} K(s,t) = K^{(j,j)}(x,x) < \infty$. The resulting optimal quadrature rule then reads

$$L_\Omega(f) \approx \sum_{i=1}^n \sum_{j=0}^{\mu_i-1} \check{w}_{i,j}(X_n^{\boldsymbol{\mu}}) f^{(j)}(\xi_i).$$

Again, due to (3.11) and (3.12) the vector of optimal weights $\check{\boldsymbol{w}}(X_n^{\boldsymbol{\mu}})$, which is now indexed by i and j, can be computed by $\check{\boldsymbol{w}}(X_n^{\boldsymbol{\mu}}) = \boldsymbol{G}^{-1}(X_n^{\boldsymbol{\mu}})\boldsymbol{b}(X_n^{\boldsymbol{\mu}})$.

Consequently, the Gramian matrix $\boldsymbol{G}(X_n^{\boldsymbol{\mu}}) \in \mathbb{R}^{N \times N}$ is given by

$$\begin{pmatrix} K(\xi_1,\xi_1) & \cdots & K^{(0,\mu_1-1)}(\xi_1,\xi_1) & \cdots & K(\xi_1,\xi_n) & \cdots & K^{(0,\mu_n-1)}(\xi_1,\xi_n) \\ \vdots & \ddots & \vdots & & \vdots & \ddots & \vdots \\ K^{(\mu_1-1,0)}(\xi_1,\xi_1) & \cdots & K^{(\mu_1-1,\mu_1-1)}(\xi_1,\xi_1) & \cdots & K^{(\mu_1-1,0)}(\xi_1,\xi_n) & \cdots & K^{(\mu_1-1,\mu_n-1)}(\xi_1,\xi_n) \\ & & \vdots & & & \vdots & \\ K(\xi_n,\xi_1) & \cdots & K^{(0,\mu_1-1)}(\xi_n,\xi_1) & \cdots & K(\xi_n,\xi_n) & \cdots & K^{(0,\mu_n-1)}(\xi_n,\xi_n) \\ \vdots & \ddots & \vdots & & \vdots & \ddots & \vdots \\ K^{(\mu_n-1,0)}(\xi_n,\xi_1) & \cdots & K^{(\mu_n-1,\mu_1-1)}(\xi_n,\xi_1) & \cdots & K^{(\mu_n-1,0)}(\xi_n,\xi_n) & \cdots & K^{(\mu_n-1,\mu_n-1)}(\xi_n) \end{pmatrix}$$

and the right-hand-side vector $\boldsymbol{b}(X_n^{\boldsymbol{\mu}}) \in \mathbb{R}^N$ is

$$\boldsymbol{b}(X_n^{\boldsymbol{\mu}}) = \left(\ell_\Omega(\xi_1), \ldots, \ell_\Omega^{(\mu_1-1)}(\xi_1), \cdots, \ell_\Omega(\xi_n), \ldots, \ell_\Omega^{(\mu_n-1)}(\xi_n) \right)^\top.$$

3.5 Construction and composition of reproducing kernels

We have seen that the theory on reproducing kernels is very useful to tackle approximation and interpolation in certain Hilbert spaces. In this section we will summarize some composition formulas for kernels.

3.5.1 Product of reproducing kernels

Let $K_1 : \Omega_1 \times \Omega_1 \to \mathbb{R}$ and $K_2 : \Omega_2 \times \Omega_2 \to \mathbb{R}$ be reproducing kernels of $\mathcal{H}_{K_1}$ and $\mathcal{H}_{K_2}$ on domains $\Omega_1, \Omega_2 \subseteq \mathbb{R}$. Then, for $\Omega_{(2)} := \Omega_1 \times \Omega_2$ the kernel

$$K_{(2)}(\boldsymbol{x}, \boldsymbol{y}) := K_1(x_1, y_1) K_2(x_2, y_2)$$

is reproducing in the tensor product space

$$\mathcal{H}_{K_{(2)}} = \mathcal{H}_{K_1} \otimes \mathcal{H}_{K_2}.$$

More generally, it holds that for d symmetric positive definite kernel functions $K_j : \Omega_j \times \Omega_j \to \mathbb{R}$, $j = 1, \ldots, d$ the kernel

$$K_{(d)}(\boldsymbol{x}, \boldsymbol{y}) := \prod_{j=1}^{d} K_j(x_j, y_j)$$

is the reproducing kernel of the tensor product space

$$\mathcal{H}_{K_{(d)}} := \bigotimes_{j=1}^{d} \mathcal{H}_{K_j}.$$

See [16, Sec 4.6] and the references therein for more details.

3.5.2 Sum and differences of reproducing kernels

Let K_1 and K_2 be reproducing kernels on $\Omega \times \Omega$ with associated RKHSs $\mathcal{H}_{K_1}$ and $\mathcal{H}_{K_2}$. Then, $K_1(\boldsymbol{x}, \boldsymbol{y}) + K_2(\boldsymbol{x}, \boldsymbol{y})$ is the reproducing kernel of

$$\mathcal{H}_{K_1+K_2} = \mathcal{H}_{K_1} \oplus \mathcal{H}_{K_2} = \{ f_1 + f_2 : f_1 \in \mathcal{H}_{K_1} \text{ and } f_2 \in \mathcal{H}_{K_2} \}.$$

If $\mathcal{H}_{K_1} \cap \mathcal{H}_{K_2} = \{0\}$, then $\mathcal{H}_K$ is a direct sum, i.e. $\mathcal{H}_{K_2}$ is the orthogonal complement of $\mathcal{H}_{K_1}$ in $\mathcal{H}$, c.f. [16].

The norm in $\mathcal{H}_{K_1+K_2}$ is given by

$$\|f\|_{\mathcal{H}_{K_1+K_2}}^2 = \min\{\|f_1\|_{\mathcal{H}_{K_1}}^2 + \|f_2\|_{\mathcal{H}_{K_2}}^2 : f_1 \in \mathcal{H}_{K_1} \text{ and } f_2 \in \mathcal{H}_{K_2}\}.$$

Now, assume that $\mathcal{H}_{K_1}$ is a closed subspace of $\mathcal{H}_K$. Then, the orthogonal complement of $\mathcal{H}_{K_1}$ in $\mathcal{H}_K$, i.e. $\mathcal{H}_{K_1}^{\perp}$ has the reproducing kernel

$$K_1^{\perp}(\boldsymbol{x}, \boldsymbol{y}) = K(\boldsymbol{x}, \boldsymbol{y}) - K_1(\boldsymbol{x}, \boldsymbol{y}).$$

3.5.3 Restriction of reproducing kernels

Let $K : \Omega \times \Omega \to \mathbb{R}$ be the reproducing kernel of $\mathcal{H}_K$ and $\tilde{\Omega} \subset \Omega$. Then the restriction $\tilde{K} = K_{|\tilde{\Omega}}$ of K to $\tilde{\Omega}$ is the reproducing kernel of the space $\{f_{|\tilde{\Omega}} : f \in \mathcal{H}_K\} =: \mathcal{H}_{\tilde{K}}$. The norm of $\mathcal{H}_{\tilde{K}}$ is

given by [16]

$$\|\tilde{f}\|_{\mathcal{H}_{\tilde{K}}} = \min_{f \in \mathcal{H}_K : f_{|\tilde{\Omega}} = f} \|f\|_{\mathcal{H}_K}.$$

This result is important when considering spaces of holomorphic functions that are real valued for real argument.

3.5.4 Kernels of finite dimensional spaces

If $\psi_1, \ldots, \psi_n$ is an orthonormal basis of an n-dimensional space $\mathcal{H}_K$, the kernel K is due to Proposition 3.4 simply given by

$$K(\boldsymbol{x}, \boldsymbol{y}) = \sum_{k=1}^{n} \psi_k(\boldsymbol{x}) \psi_k(\boldsymbol{y}).$$

However, if only a non-orthonormal basis $\phi_1, \ldots, \phi_n$ of $\mathcal{H}_K$ is available one can compute the Gramian matrix $\boldsymbol{G} \in \mathbb{R}^{n \times n}$ with

$$G_{i,j} = \langle \phi_i, \phi_j \rangle_{\mathcal{H}_K}, \quad i, j = 1, \ldots, n$$

and the reproducing kernel of $\mathcal{H}_K$ is given by [16, Sec. 6.1]

$$K(\boldsymbol{x}, \boldsymbol{y}) = \sum_{i=1}^{n} \sum_{j=1}^{n} G_{i,j}^{-1} \phi_i(\boldsymbol{x}) \phi_j(\boldsymbol{y}). \tag{3.19}$$

If $\boldsymbol{\Lambda}_N = (\Lambda_1, \ldots, \Lambda_N) \subset \mathcal{H}_K^\star$ we can project on the subspace spanned by the Riesz-representers of $\boldsymbol{\Lambda}_N$, i.e.

$$\mathcal{H}_{K_{\boldsymbol{\Lambda}_N}} := \operatorname{span}\{\lambda_1, \ldots, \lambda_N\}$$

whose reproducing kernel is according to (3.19) given by

$$K_{\boldsymbol{\Lambda}_N}(\boldsymbol{x}, \boldsymbol{y}) = \sum_{i=1}^{n} \sum_{j=1}^{n} G_{i,j}^{-1}(\boldsymbol{\Lambda}_N) \Lambda_i^{(\boldsymbol{y})} K(\boldsymbol{x}, \boldsymbol{y}) \, \Lambda_j^{(\boldsymbol{x})} K(\boldsymbol{x}, \boldsymbol{y}). \tag{3.20}$$

3.5.5 Kernels of a certain subspace

Sometimes one is interested in the subspace of a RKHS which is defined by the property that its elements vanish at a finite set of certain linear functionals, i.e.

$$\{f \in \mathcal{H}_K : \Lambda_i(f) = 0 \quad \text{for } i = 1, \ldots, N\}.$$

Examples are subspaces with prescribed zeros or zeros of derivatives. But one could also construct subspaces of functions with vanishing moments.

The following proposition gives an explicit formula for the kernel of such subspaces.

Proposition 3.10. *For a given set of N linear functionals $\mathbf{\Lambda}_N = (\Lambda_1, \ldots, \Lambda_N) \subset \mathcal{H}_K^\star$ let*

$$K_{\mathbf{\Lambda}_N}^\perp(\boldsymbol{x}, \boldsymbol{y}) := K(\boldsymbol{x}, \boldsymbol{y}) - K_{\mathbf{\Lambda}_N}(\boldsymbol{x}, \boldsymbol{y}),$$

where $K_{\mathbf{\Lambda}_N}(\boldsymbol{x}, \boldsymbol{y})$ was given in (3.20). The unique Hilbert space in which $K_{\mathbf{\Lambda}_N}^\perp$ is reproducing is given by

$$\mathcal{H}_{K_{\mathbf{\Lambda}_N}^\perp} = \{f \in \mathcal{H}_K : \Lambda_i(f) = 0 \quad \text{for } i = 1, \ldots, N\}.$$

Proof. First, we note that the Riesz-representer of $\Lambda_k \in \mathcal{H}_K^\star$ in $\mathcal{H}_{K_{\mathbf{\Lambda}_N}}^\perp$ is given by

$$\tilde{\lambda}_k(\boldsymbol{x}) = \Lambda_k^{(\boldsymbol{y})} K_{\mathbf{\Lambda}_N}^\perp(\boldsymbol{x}, \boldsymbol{y}).$$

Since $\Lambda_k(f) = \langle \tilde{\lambda}_k, f \rangle_{\mathcal{H}_{K_{\mathbf{\Lambda}_N}}^\perp}$, it suffices to show that $\tilde{\lambda}_k \equiv 0$. To this end, we compute

$$\tilde{\lambda}_k(\boldsymbol{x}) = \Lambda_k^{(\boldsymbol{y})} \left(K_{\mathbf{\Lambda}_N}^\perp(\boldsymbol{x}, \boldsymbol{y}) = \Lambda_k^{(\boldsymbol{y})} K(\boldsymbol{x}, \boldsymbol{y}) - K_{\mathbf{\Lambda}_N}(\boldsymbol{x}, \boldsymbol{y}) \right)$$

$$= \Lambda_k^{(\boldsymbol{y})} K(\boldsymbol{x}, \boldsymbol{y}) - \sum_{i=1}^n \sum_{j=1}^n \boldsymbol{G}_{i,j}^{-1}(\mathbf{\Lambda}_N) \Lambda_i^{(\boldsymbol{y})} K(\boldsymbol{x}, \boldsymbol{y}) \, \Lambda_j^{(\boldsymbol{x})} \Lambda_k^{(\boldsymbol{y})} K(\boldsymbol{x}, \boldsymbol{y})$$

$$= \Lambda_k^{(\boldsymbol{y})} K(\boldsymbol{x}, \boldsymbol{y}) - \sum_{i=1}^n \sum_{j=1}^n G_{i,j}^{-1}(\mathbf{\Lambda}_N) \Lambda_i^{(\boldsymbol{y})} K(\boldsymbol{x}, \boldsymbol{y}) \, G_{j,k}(\mathbf{\Lambda}_N)$$

$$= \Lambda_k^{(\boldsymbol{y})} K(\boldsymbol{x}, \boldsymbol{y}) - \sum_{i=1}^n \Lambda_i^{(\boldsymbol{y})} K(\boldsymbol{x}, \boldsymbol{y}) \sum_{j=1}^n G_{i,j}^{-1}(\mathbf{\Lambda}_N) G_{j,k}(\mathbf{\Lambda}_N)$$

$$= \Lambda_k^{(\boldsymbol{y})} K(\boldsymbol{x}, \boldsymbol{y}) - \sum_{i=1}^n \Lambda_i^{(\boldsymbol{y})} K(\boldsymbol{x}, \boldsymbol{y}) \, \delta_{i,k}$$

$$= \Lambda_k^{(\boldsymbol{y})} K(\boldsymbol{x}, \boldsymbol{y}) - \Lambda_k^{(\boldsymbol{y})} K(\boldsymbol{x}, \boldsymbol{y})$$

$$= 0.$$

$\square$

3.5.6 Kernels of L_2 subspaces

Let $L_2(\Omega, \omega)$ denote the space of functions that are square-integrable on $\Omega \subseteq \mathbb{R}^d$ with respect to the weight function ω. The inner product is given by

$$\langle f, g \rangle_{L_2(\Omega, \omega)} = \int_\Omega f(\boldsymbol{x}) g(\boldsymbol{x}) \, \omega(\boldsymbol{x}) \, \mathrm{d}\boldsymbol{x}.$$

Let $(\phi_k)_{k=0}^\infty$ be an orthonormal basis of $L_2(\Omega, \omega)$. Then, every $f \in L_2(\Omega, \omega)$ can be written as

$$f(\boldsymbol{x}) = \sum_{k=0}^\infty \langle f, \phi_k \rangle_{L_2(\Omega, \omega)} \phi_k(\boldsymbol{x})$$

where we will abbreviate $\hat{f}_k := \langle f, \phi_k \rangle_{L_2(\Omega, \omega)}$. By Parseval's identity, it holds

$$\|f\|^2_{L_2(\Omega, \omega)} = \sum_{k=0}^{\infty} \left| \hat{f}_k \right|^2 < \infty$$

for all $f \in L_2(\Omega, \omega)$.

Now consider a subspace of $L_2(\Omega, \omega)$ defined by some weight function $\rho : \mathbb{N}_0 \to \mathbb{R}_+$, which fulfills

$$\rho(0) = 1 \quad \text{and} \quad \rho(k+1) \geq \rho(k).$$

We can define the norm

$$\|f\|^2_{H_\rho} := \sum_{k=0}^{\infty} \rho(k) \left| \hat{f}_k \right|^2$$

and the space generated by ρ is then the subset of L_2 with finite $\|f\|_{H_\rho}$-norm, i.e.

$$H_\rho := \left\{ f \in L_2(\Omega, \omega) : \|f\|_{H_\rho} < \infty \right\}.$$

The inner product in this space is

$$\langle f, g \rangle_{H_\rho} = \sum_{k=0}^{\infty} \rho(k) \hat{f}_k \, \hat{g}_k$$

and the set of functions

$$\psi_k(\boldsymbol{x}) := \frac{1}{\sqrt{\rho(k)}} \phi_k(\boldsymbol{x})$$

is orthonormal in H_ρ. Consequently, according to Proposition 3.4, the reproducing kernel of H_ρ is given by

$$K(\boldsymbol{x}, \boldsymbol{y}) = \sum_{k=0}^{\infty} \psi_k(\boldsymbol{x}) \psi_k(\boldsymbol{y}) = \sum_{k=0}^{\infty} \rho(k)^{-1} \phi_k(\boldsymbol{x}) \phi_k(\boldsymbol{y}).$$

3.5.7 Kernels from Taylor spaces

A similar approach consists in so-called Taylor spaces. The idea goes back at least to [33] and more recently was studied in [51, 168]. The basic principle is to replace the Fourier series expansion in the preceding subsection by the power series expansion

$$f(z) = \sum_{k=0}^{\infty} f_k z^k \tag{3.21}$$

of functions that are analytic in open discs of radius $r \in (0, \infty]$, i.e. $\mathbb{D}_r = \{z \in \mathbb{C} : |z| < r\}$. Because $f_k = f^{(k)}(0)/k!$ is also the k-th Taylor coefficient, (3.21) is the Taylor series of f.

Following [33] let the function

$$\theta(z) := \sum_{k=0}^{\infty} \theta_k z^k$$

be analytic in $\mathbb{D}_r$ and real-valued for $z \in \mathbb{R}$. We define the space

$$\mathcal{T}_\theta := \left\{ f \in \mathrm{Hol}(\mathbb{D}_r) : \sum_{k=0}^{\infty} \frac{|f_k|^2}{\theta_k} < \infty \right\}$$

with the inner product between $f(z) = \sum_{k=0}^{\infty} f_k z^k$ and $g(z) = \sum_{k=0}^{\infty} g_k z^k$ given by

$$\langle f, g \rangle_{\mathcal{T}_\theta} = \sum_{k=0}^{\infty} \theta_k^{-1} f_k \, \overline{g_k}$$

and norm

$$\|f\|_{\mathcal{T}_\theta}^2 = \langle f, f \rangle_{\mathcal{T}_\theta} = \sum_{k=0}^{\infty} \theta_k^{-1} |f_k|^2.$$

The reproducing kernel $K : \mathbb{D}_r \times \mathbb{D}_r \to \mathbb{C}$ is then given by

$$K(x, y) = \sum_{k=0}^{\infty} \theta_k x^k \overline{y}^k = \theta(x \, \overline{y}).$$

Indeed, it holds for real $x \in (-r, r)$ that

$$\langle f, K(\cdot, x) \rangle_{\mathcal{T}_\theta} = \sum_{k=0}^{\infty} \theta_k^{-1} f_k \, \theta_k x^k = \sum_{k=0}^{\infty} f_k x^k = f(x).$$

Many well-known function spaces fit into this framework, c.f. [168], and the examples given in the sequel.

3.6 Examples of relevant RKHS

In the following we will give several examples for univariate reproducing kernel Hilbert spaces, whose tensor products are relevant in numerical analysis, scientific computing, machine learning and engineering.

3.6.1 Sobolev spaces

The scale of Sobolev spaces $H^s(\Omega)$, $\Omega \subset \mathbb{R}$, $s \in \mathbb{N}$ consists of square-integrable functions on Ω, whose first s weak derivatives are bounded in L^2 as well, i.e.

$$H^s(\Omega) = \left\{ f \in L_2(\Omega) : \int_\Omega \left| f^{(k)}(x) \right|^2 \, \mathrm{d}x < \infty \text{ for } k = 0, 1, \ldots, s \right\}. \qquad (3.22)$$

There are several ways to choose a norm for $H^s(\Omega)$ c.f. [101]. In what follows we will concentrate on a particular class of norms which result in an easy closed-form expression of the associated reproducing kernel.

Periodic Sobolev space

We will start with the Sobolev space on the torus $\mathbb{T} = [0,1)$ which consists of periodic functions that fulfill (3.22) and whose first $s-1$ derivatives are periodic.
A possible norm for the periodic Sobolev space

$$\tilde{H}^s = H^s(\mathbb{T}) = \left\{ f \in H^s(\Omega) \quad \text{and } f^{(k)}(0) = f^{(k)}(1) \text{ for } k = 0, \ldots, s-1 \right\}.$$

is given by

$$\|f\|_{\tilde{H}^s}^2 := \left(\int_0^1 f(x) \, \mathrm{d}x \right)^2 + \int_0^1 \left| f^{(s)}(x) \right|^2 \, \mathrm{d}x, \tag{3.23}$$

because the integrals of the derivatives $k \in \{1, \ldots, s-1\}$ vanish due to the periodic boundary conditions.
Having in mind the construction from Section 3.5.6, we define the weight

$$\rho(k) := \max(1, 2\pi|k|).$$

Inserting the Fourier expansion

$$f(x) = \sum_{k \in \mathbb{Z}} \hat{f} e^{2\pi \mathrm{i}kx},$$

where $\hat{f}_k = \int_0^1 f(x) e^{-2\pi \mathrm{i}kx} \, \mathrm{d}x$ denotes the k-th Fourier coefficient, we note that (3.23) equals

$$\|f\|_{\tilde{H}^s}^2 = \sum_{k \in \mathbb{Z}} \rho(k)^{2s} |\hat{f}_k|^2.$$

Consequently, the reproducing kernel of $\tilde{H}^s$ is given by

$$\tilde{K}_s(x,y) = \sum_{k \in \mathbb{Z}} \rho(k)^{-2s} \exp(2\pi \mathrm{i}k\, x)\overline{\exp(2\pi \mathrm{i}k\, y)} = \sum_{k \in \mathbb{Z}} \rho(k)^{-2s} \exp\left(2\pi \mathrm{i}k(x-y)\right).$$

For $s \in \mathbb{N}$, this infinite series can be written as [157]

$$\tilde{K}_s(x,y) = 1 + \frac{(-1)^{s+1}}{(2s)!} B_{2s}(|x-y|),$$

where $B_{2s} : [0,1] \to \mathbb{R}$ denotes the Bernoulli polynomial of degree $2s$.
We will also briefly comment on the space $\tilde{H}_{\mathrm{mix}}^s = \tilde{H}^s \otimes \ldots \otimes \tilde{H}^s$, which is the d-fold tensor product of univariate periodic Sobolev spaces. Due to the tensor product structure its norm is given by

$$\|f\|_{\tilde{H}^s}^2 = \sum_{\boldsymbol{k} \in \mathbb{Z}^d} \prod_{j=1}^d \rho(k_j)^{2s} |\hat{f}_{\boldsymbol{k}}|^2, \quad \hat{f}_{\boldsymbol{k}} = \int_{[0,1]^d} f(x) e^{-2\pi \mathrm{i}\boldsymbol{k}\cdot\boldsymbol{x}} \, \mathrm{d}\boldsymbol{x} \tag{3.24}$$

and according to Section 3.5.1 the reproducing kernel of $\tilde{H}_{\text{mix}}^s$ is

$$\prod_{j=1}^{d} \tilde{K}_s(x_j, y_j) = \sum_{\boldsymbol{k} \in \mathbb{Z}^d} \prod_{j=1}^{d} \rho(k_j)^{-2s} \exp\left(2\pi \mathrm{i} \boldsymbol{k} \cdot (\boldsymbol{x} - \boldsymbol{y})\right).$$

Nonperiodic Sobolev space

The so-called *unanchored Sobolev space* on $[0,1]$ is constructed from $\tilde{H}^s$ by adding those functions that reproduce the boundary values of $f^{(k)}$ for $k = 0, \ldots, s-1$. To this end, we note that the Bernoulli polynomials $B_1, \ldots, B_s$ have the property $\int_0^1 B_j(x)\,\mathrm{d}x = 0$ and they reproduce the values of functions on the boundary of $[0,1]$, c.f. [158]. Therefore, by the additive composition formula in Section 3.5.2, the kernel

$$K_s(x, y) = 1 + \frac{(-1)^{s+1}}{(2s)!} B_{2s}(|x - y|) + \sum_{j=1}^{s} \frac{B_j(x)B_j(y)}{(j!)^2}$$

reproduces point evaluation in $H^s([0,1])$ with respect to the inner product

$$\langle f, g \rangle_{H^s} = \sum_{j=0}^{s-1} \left(\int_0^1 f^{(j)}(x)\,\mathrm{d}x \right) \left(\int_0^1 g^{(j)}(x)\,\mathrm{d}x \right) + \int_0^1 f^{(s)}(x)g^{(s)}(x)\,\mathrm{d}x.$$

We refer to [52, 158] for details.

Zero boundary condition

More restrictive is the class of functions, whose support is strictly contained in the open interval $(0,1)$, i.e. $f \in H^s$ and $\mathrm{supp} f \subset (0,1)$. These functions play a role in the construction of Frolov cubature methods, cf. [63, 156]. An equivalent definition is

$$\mathring{H}^s(\Omega) = \left\{ f \in H^s(\Omega) \quad \text{and } f^{(k)}(0) = f^{(k)}(1) = 0 \text{ for } k = 0, \ldots, s-1 \right\}.$$

Obviously, we have

$$\mathring{H}^s(\Omega) \quad \subset \quad \tilde{H}^s(\Omega) \quad \subset \quad H^s(\Omega).$$

Since $\mathring{H}^s$ is a subspace of $\tilde{H}^s$, we can invoke the results from Section 3.5.5 to construct the reproducing kernel of $\mathring{H}^s$.

To this end, we first note that it holds for $f \in \tilde{H}^s$ that $f^{(j)}(0) = f^{(j)}(1)$ for $j = 0, \ldots, s-1$. In order to determine the subspace where

$$f^{(j)}(0) = f^{(j)}(1) = 0,$$

we first define the set $X_1 := \{0\}$ and $\boldsymbol{\mu} = (s-1)$. Then, in the notation of Section 3.5.5 the

space $\mathcal{H}_{K(X_1^{\boldsymbol{\mu}})}$ is the orthogonal complement of $\mathring{H}^s$. Consequently, the kernel of $\mathring{H}^s$ is given by

$$\mathring{K}_s(x,y) = \tilde{K}_s(x,y) - \sum_{i=1}^{s} \sum_{j=1}^{s} G_{i,j}^{-1}(X_1^{\boldsymbol{\mu}}) \tilde{K}_s^{(0,i-1)}(x,0) \tilde{K}_s^{(j-1,0)}(0,y),$$

where $K^{(p,q)}(x,y) = \frac{\partial^p \partial^q}{x^p y^q} K(x,y)$ and the Gramian $\boldsymbol{G}(X_1^{\boldsymbol{\mu}}) \in \mathbb{R}^{s \times s}$ is defined by

$$G_{i,j}(X_1^{\boldsymbol{\mu}}) = \tilde{K}_s^{(i-1,j-1)}(0,0) \quad \text{for } i,j = 1, \ldots, s.$$

3.6.2 Hardy spaces on open discs

Classically, c.f. [54], the scale of univariate Hardy spaces $\mathbb{H}_r^p$ with $r \in (1,\infty)$ and $p \in [1,\infty]$ is defined as the set of functions that are holomorphic on the open disc $\mathbb{D}_r = \{z \in \mathbb{C} : |z| < r\}$ and have bounded L^p-norms on all circles of radius $t < r$, i.e. $(\frac{1}{2\pi} \int_0^{2\pi} |f(te^{i\varphi})|^p \, \mathrm{d}\varphi)^{1/p} < \infty$ for all $0 \leq t < r$. Then, functions $f \in \mathbb{H}_r^p$ can be extended point-wise to the boundary of $\mathbb{D}_r$ almost everywhere and their norm[1] is given by

$$\|f\|_{\mathbb{H}_r^p} = \left(\frac{1}{2\pi r} \int_{\partial \mathbb{D}_r} |f(z)|^p d|z| \right)^{\frac{1}{p}} = \left(\frac{1}{2\pi} \int_0^{2\pi} |f(re^{i\varphi})|^p d\varphi \right)^{\frac{1}{p}},$$

i.e. by the L^p-norm on the circle bounding $\mathbb{D}_r$ or equivalently on the torus $\mathbb{T} = [0,2\pi)$. Therefore, analogously to the scale of $L^p(\mathbb{T})$-spaces, $\mathbb{H}_r^1$ are Banach spaces and we have the inclusion $\mathbb{H}_r^q \subset \mathbb{H}_r^p$ for $1 \leq p < q \leq \infty$, see e.g. [54]. Moreover, for $1 \leq t < r$ it holds $\mathbb{H}_r^p \subset \mathbb{H}_t^p$.

In the context of approximation theory, functions of this class have been studied for quite some time, e.g. the case $r > 1$ and $p = 2$ in [103, 133], $r \geq 1$ and $p = \infty$ in [99] or $r = 1$ and $p \in (1,\infty]$ in [3, 145].

In the following we will be interested in the case $p = 2$ when $\mathbb{H}_r := \mathbb{H}_r^2$ becomes a Hilbert space with inner product

$$\langle f, g \rangle_{\mathbb{H}_r} = \left(\frac{1}{2\pi} \int_0^{2\pi} f(re^{i\varphi}) \overline{g(re^{i\varphi})} \, \mathrm{d}\varphi \right)^{1/2}. \tag{3.25}$$

Using that $f, g \in \mathbb{H}_r$ can be represented as absolutely convergent power series on $\mathbb{D}_r$, i.e.

$$f(z) = \sum_{k \in \mathbb{N}_0} f_k z^k \quad \text{and} \quad g(z) = \sum_{k \in \mathbb{N}_0} g_k z^k,$$

together with the orthogonality of the monomial basis with respect to (3.25) we obtain an alternative representation of the inner product, i.e.

$$\begin{aligned}
\langle f, g \rangle_{\mathbb{H}_r}^2 &= \frac{1}{2\pi} \int_0^{2\pi} f(re^{i\varphi}) \overline{g(re^{i\varphi})} \, \mathrm{d}\varphi \\
&= \sum_{k_1 \in \mathbb{N}_0} \sum_{k_2 \in \mathbb{N}_0} f_{k_1} \overline{g_{k_2}} \frac{1}{2\pi} \int_0^{2\pi} (re^{i\varphi})^{k_1} \overline{(re^{i\varphi})^{k_2}} \, \mathrm{d}\varphi
\end{aligned}$$

---

[1] In the case $p = \infty$ we have the obvious modification $\|f\|_{\mathbb{H}_r^\infty} = \operatorname{ess\,sup}_{z \in \partial \mathbb{D}_r} |f(z)|$.

$$= \sum_{k_1 \in \mathbb{N}_0} \sum_{k_2 \in \mathbb{N}_0} f_{k_1} \overline{g_{k_2}} \frac{1}{2\pi} \int_0^{2\pi} r^{k_1+k_2} e^{i\varphi k_1} e^{-i\varphi k_2} \, d\varphi$$

$$= \sum_{k \in \mathbb{N}_0} r^{2k} f_k \overline{g_k}.$$

Therefore, the $\mathbb{H}_r$-norm can also be realized in terms of the weighted ℓ_2-norm of the power series coefficients, i.e.

$$\|f\|_{\mathbb{H}_r} = \Big(\sum_{k \in \mathbb{N}_0} r^{2k} |f_k|^2 \Big)^{1/2},$$

which fits into the setting of Section 3.5.7, by choosing

$$\theta(z) := \sum_{k=0}^{\infty} r^{-2k} z^k = \frac{r^2}{r^2 - z}.$$

Consequently, for $x, y \in \mathbb{R}$ the reproducing kernel of $\mathbb{H}_r^2$ is given by

$$K_r(x, y) = \frac{r^2}{r^2 - xy}.$$

3.6.3 Taylor space generated by the di-logarithm

Our next example consists of functions that are analytic on the open disc of radius $r = 1$, i.e. $\mathbb{D}_1 = \{z \in \mathbb{C} : |z| < 1\}$, and have derivatives in the Hardy space $\mathbb{H}_r$ with $r = 1$. This property is important for certain integrands that appear in econometrics, cf. Section 8.3 of Chapter 8.

We will denote this space by $\mathcal{T}_{\mathrm{Li}_2}$ which refers to the *di-logarithm*

$$\mathrm{Li}_2(x) = \sum_{k=1}^{\infty} \frac{x^k}{k^2}.$$

In the notation of Section 3.5.7 we set

$$\theta(x) = 1 + \sum_{k=1}^{\infty} k^{-2} x^k = 1 + \mathrm{Li}_2(x).$$

Consequently, the norm of $f(z) = \sum_{k=0}^{\infty} f_k z^k$ in $\mathcal{T}_{\mathrm{Li}_2}$ is

$$\|f\|_{\mathcal{T}_{\mathrm{Li}_2}}^2 := \left(|f_0|^2 + \sum_{k=1}^{\infty} k^2 |f_k|^2 \right)^{1/2}$$

and the associated inner product is

$$\langle f, g \rangle_{\mathcal{T}_{\mathrm{Li}_2}} = f_0 \overline{g_0} + \sum_{k=1}^{\infty} k^2 f_k \overline{g_k}.$$

Moreover, the reproducing kernel K of $\mathcal{T}_{\mathrm{Li}_2}$ for real arguments is given by

$$K(x, y) = 1 + \mathrm{Li}_2(xy).$$

Finally, we note that the first derivative of functions from $\mathcal{T}_{\mathrm{Li}_2}$ belongs to the Hardy space $\mathbb{H}_r$ with radius $r = 1$.

Proposition 3.11. *For every $f \in \mathcal{T}_{\mathrm{Li}_2}$ it holds that*

$$f' \in \mathbb{H}_1,$$

i.e. the first derivative is in the Hardy space of functions analytic on the open unit disc.

Proof. For a given $f \in \mathcal{T}_{\mathrm{Li}_2}$ it holds

$$f'(z) = \sum_{k=1}^{\infty} k f_k z^{k-1} = \sum_{k=0}^{\infty} (k+1) f_{k+1} z^k,$$

i.e. the power series coefficients of f' are given by $((k+1)f_{k+1})_{k=0}^{\infty}$. The $\|\cdot\|_{\mathbb{H}_1}$-norm of f' is therefore

$$\|f'\|_{\mathbb{H}_1}^2 = \sum_{k=0}^{\infty} |(k+1)f_{k+1}|^2 = \sum_{k=1}^{\infty} |k f_k|^2 = \sum_{k=1}^{\infty} k^2 |f_k|^2 \leq \|f\|_{\mathcal{T}_{\mathrm{Li}_2}}^2 < \infty.$$

$$\square$$

3.6.4 Hermite spaces

The scale of Hermite spaces $\mathcal{M}_\tau$ was introduced in [91] and consists of functions whose Hermite-coefficients fulfill certain decay conditions in the spirit of Section 3.5.6. To this end, let the k-th degree Hermite polynomial be denoted by

$$H_k(x) = \frac{(-1)^k}{\sqrt{k!}} e^{\frac{x^2}{2}} \frac{\mathrm{d}^k}{\mathrm{d}x^k} e^{\frac{-x^2}{2}}.$$

For $\Omega = \mathbb{R}$ and $\omega(x) = \frac{1}{\sqrt{2\pi}} e^{-x^2/2}$ it holds

$$\langle H_i, H_j \rangle_{L_2(\Omega, \omega)} = \delta_{i,j}.$$

Let

$$\hat{f}_k = \langle f, H_k \rangle_{L^2(\Omega, \omega)}$$

denote the k-th Hermite coefficient of a function $f \in L_2(\Omega, \omega)$. In the following we will consider the class of functions whose Hermite coefficients decay exponentially. To this end, for a parameter $\tau \in (0, 1)$ we define the norm

$$\|f\|_{\mathcal{M}_\tau}^2 := \sum_{k=0}^{\infty} \tau^{-k} \hat{f}_k^2$$

and the function space

$$\mathcal{M}_\tau := \{f \in L_2(\Omega, \omega) : \|f\|_{\mathcal{M}_\tau} < \infty\}.$$

Consequently, the reproducing kernel of $\mathcal{M}_\tau$ is given by

$$K(x, y) = \sum_{k=0}^{\infty} \tau^k H_k(x) H_k(y). \tag{3.26}$$

By Mehler's formula, c.f. [91, 148], (3.26) can be written as

$$K(x, y) = \frac{1}{\sqrt{1 - \tau^2}} \exp\left(\frac{1}{\tau^{-1} + 1} xy - \frac{1}{2(\tau^{-2} - 1)}(x - y)^2\right).$$

Moreover, it was shown in [91] that $f \in \mathcal{M}_\tau$ is analytic in a strip of width $\tau^{-1} - 1$, i.e.

$$f \in \text{Hol}(S_{\tau-1}), \quad \text{with } S_{\tau-1} = \left\{z \in \mathbb{C} : z = x + \mathrm{i}t \text{ for } t \in (-(\tau^{-1} - 1), \tau^{-1} - 1)\right\}.$$

3.6.5 Gaußian spaces

Our final example consists of most famous kernel, namely the Gaussian kernel

$$K(x, y) = \exp\left(-\gamma^2(x - y)^2\right),$$

which is frequently used within support vector machines for machine learning problems [139].

Due to a general theorem by Bochner, c.f. [163], the space in which the Gaußian kernel is reproducing consists of entire functions, i.e. $f \in \text{Hol}(\mathbb{C})$, whose Fourier transform $\mathcal{F}(f)(\omega) = \frac{1}{2\pi} \int_{\mathbb{R}} f(t) e^{\mathrm{i}\omega t} \, \mathrm{d}t$ decays exponentially, i.e.

$$\|f\|_{\mathcal{H}_K}^2 = \frac{1}{2\pi} \int_{\mathbb{R}} |\mathcal{F}(f)(\omega)|^2 \exp\left(\frac{\omega^2}{2\gamma^2}\right) \, \mathrm{d}\omega < \infty.$$

Further details on $\mathcal{H}_K$ can be found in [144] or [102], where the space is characterized in terms of an L^2 eigenfunction basis.

4 Optimal cubature using random point sets

In this chapter we investigate to which extent optimal cubature weights can improve the convergence rate of plain Monte Carlo and classical quasi–Monte Carlo in Sobolev spaces with dominating mixed smoothness on the d-dimensional torus $\mathbb{T} = [0,1)^d$ and the d-dimensional unit cube $[0,1]^d$. In other words, as information, cf. Section 2.1, we use function values at uniformly distributed points or low-discrepancy point sets $\boldsymbol{X}_N = (\boldsymbol{\xi}^{(1)}, \ldots, \boldsymbol{\xi}^{(N)}) \subset [0,1)^d$. Classical (quasi–)Monte Carlo methods, abbreviated by (q)MC, like e.g. the Halton sequence [82], use uniform weights $w_i = 1/N$, i.e.

$$Q_{\boldsymbol{X}_N}^{(q)MC}(f) = \frac{1}{N} \sum_{i=1}^{N} f\left(\boldsymbol{\xi}^{(i)}\right).$$

They can achieve a convergence rate of $N^{-1/2}$ or $N^{-1} \log(N)^{(d-1)/2}$, respectively, in H_{mix}^s for $s \geq 1$. There are also so-called *higher order quasi–Monte Carlo* methods [52] as well as lattice rules [141]. They can achieve higher order convergence for $s > 1$ but are not studied at this point because the former are difficult to construct already for moderate $d \geq 6$ and the latter only work for periodic functions.

For a given $s \in \mathbb{N}$ we will consider the cubature rule

$$\check{Q}_{\boldsymbol{X}_N}(f) := \sum_{i=1}^{N} \check{w}_i(\boldsymbol{X}_N, H_{\mathrm{mix}}^s) f\left(\boldsymbol{\xi}^{(i)}\right)$$

that uses the optimal vector of weights $\check{\boldsymbol{w}}_i(\boldsymbol{X}_N)$ which minimize the worst-case error in H_{mix}^s among all linear algorithms that use the point set $\boldsymbol{X}_N$ as information. Hence, the radius of information of the point set $\boldsymbol{X}_N$ in H_{mix}^s equals the worst-case error of this optimally weighted cubature rule, i.e.

$$\check{\mathbf{wce}}(\boldsymbol{X}_N, H_{\mathrm{mix}}^s) = \mathbf{wce}(\check{Q}_{\boldsymbol{X}_N}, H_{\mathrm{mix}}^s).$$

In order to compute $\check{\boldsymbol{w}}_i(\boldsymbol{X}_N)$, we will make use of the reproducing kernel Hilbert space based computation of the worst-case error, cf. Chapter 3, which can rather easily be implemented in a computer. Therefore, it is a natural approach to conduct numerical experiments, analyze the resulting data, and put forward a theory which then hopefully can be proven.

The numerical experiments can be found in Section 1 of this chapter. Here, we compare the worst-case errors of classical (quasi–) Monte Carlo point sets with uniform $1/N$ weights to their optimally weighted counterparts as well as to the sparse grid construction. As it turns out, the choice of optimal cubature weights can improve the convergence rate from $\mathcal{O}(N^{-1/2})$ for conventional uniformly weighted Monte Carlo or $\mathcal{O}(N^{-1} \log(N)^{(d-1)/2})$ for quasi–Monte Carlo cubature to $\mathcal{O}(N^{-s} \log(N)^q)$. Here, q seems to be substantially smaller than $(d-1)(s+1/2)$, as

would be the case for sparse grids. However, even though the worst-case error formula is exact, we can only compute it numerically for rather small $N \in \{1, \dots, 2^{15}\}$. Therefore, in Section 4.2 we will deal with the derivation of sound asymptotic results on the radius of information of random points. Here, we obtain an upper bound which is of order $N^{-s+1/2} \log(N)^{ds-1/2}$. Unfortunately, this leaves a gap to the previously observed optimal main rate N^{-s}.

Finally, in Section 3 we will comment on the reasons why the promising results of Section 1 and 2 can not be expected to be carried over to analytic function spaces.

4.1 Numerical experiments

In the first part of this section we consider integration in $\Omega = [0,1]^d$ with respect to the uniform density function $\omega(\boldsymbol{x}) \equiv 1$. We will investigate the radius of information, cf. (2.4), of both random and quasi–random point sets for the approximation of

$$L_\Omega(f) := \int_{[0,1]^d} f(\boldsymbol{x}) \, \mathrm{d}\boldsymbol{x},$$

in periodic and non-periodic Sobolev spaces with bounded mixed derivatives numerically. We will see that they achieve an optimal main rate of $N^{-s} \log(N)^{q(s,d)}$, where the best possible log-exponent is $q(s,d) = (d-1)/2$ and hence independent of the smoothness s, cf. [43, 150]. However, the numerical experiments suggest that for optimally weighted random points the exponent $q(s,d)$ in fact is depending on s.

4.1.1 Setup

Recalling Section 3.6.1 the reproducing kernel $\tilde{K}$ of the periodic Sobolev space with bounded mixed derivatives $\tilde{H}^s_{\mathrm{mix}} := H^s_{\mathrm{mix}}(\mathbb{T}^d)$ can be written as

$$\tilde{K}(x,y) = \sum_{k \in \mathbb{Z}} \rho(k)^{-2s} \exp\left(2\pi \mathrm{i} k(x-y)\right) = 1 + \frac{(-1)^{s+1}}{(2s)!} B_{2s}(|x-y|), \tag{4.1}$$

where $s \in \mathbb{N}$ and B_j denotes the j-th Bernoulli polynomial.

Moreover, the kernel of the non-periodic Sobolev space $H^s_{\mathrm{mix}} := H^s_{\mathrm{mix}}([0,1]^d)$ is given by, cf. Section 3.6.1,

$$K(x,y) = \tilde{K}(x,y) + \sum_{j=1}^{s} \frac{B_j(x)B_j(y)}{(j!)^2}. \tag{4.2}$$

Consequently, according to the results in Section 3.5.1, the kernel of the tensor product spaces $\tilde{H}^s_{\mathrm{mix}}$ and H^s_{mix} are given by the product of the univariate kernels, i.e.

$$\tilde{K}(\boldsymbol{x}, \boldsymbol{y}) = \prod_{j=1}^{d} \tilde{K}_j(x_{j,j}) \quad \text{and} \quad K(\boldsymbol{x}, \boldsymbol{y}) = \prod_{j=1}^{d} K_j(x_{j,j}),$$

respectively.

Moreover, we can directly obtain from (4.1) and the zero mean property of the Bernoulli polynomials that the Riesz-representer of $L_\Omega(f) = \int_{[0,1]^d} f(\boldsymbol{x}) \, \mathrm{d}\boldsymbol{x}$ is constant in both, $\tilde{H}^s_{\mathrm{mix}}$ and H^s_{mix}, i.e.

$$\ell_\Omega(\boldsymbol{x}) = \int_{[0,1]^d} K(\boldsymbol{x}, \boldsymbol{y}) \, \mathrm{d}\boldsymbol{y} = \int_{[0,1]^d} \tilde{K}(\boldsymbol{x}, \boldsymbol{y}) \, \mathrm{d}\boldsymbol{y} = 1.$$

Therefore, we also have

$$\|L_\Omega\|_{(H^s_{\mathrm{mix}})^\star} = \|L_\Omega\|_{(\tilde{H}^s_{\mathrm{mix}})^\star} = 1.$$

Since we will put an emphasis on the periodic Sobolev space in the following, we will from now on explain our approach for $\tilde{H}^s_{\mathrm{mix}}$. However, by replacing $\tilde{K}$ by K every formula holds for the non-periodic setting as well.

Before we proceed, we recall (3.10), i.e. the vector of optimal weights for a given set $\boldsymbol{X}_N \subset [0,1)^d$ of N cubature points is given by

$$\check{\boldsymbol{w}}(\boldsymbol{X}_N) := \boldsymbol{G}^{-1}(\boldsymbol{X}_N) \cdot \boldsymbol{b}(\boldsymbol{X}_N), \tag{4.3}$$

where $\boldsymbol{b}(\boldsymbol{X}_N) = (\ell_\Omega(\boldsymbol{\xi}^{(i)}))_{i=1}^N = \boldsymbol{1} \in \mathbb{R}^N$ and $\boldsymbol{G}(\boldsymbol{X}_N) = \left(\tilde{K}(\boldsymbol{\xi}^{(i)}, \boldsymbol{\xi}^{(j)}) \right)_{i,j=1}^N \in \mathbb{R}^{N \times N}$.

Moreover, recalling (3.18), the worst-case error of a cubature-rule

$$Q_N(f) := \sum_{i=1}^N w_i f(\boldsymbol{\xi}^{(i)})$$

is given by

$$\mathbf{wce}(Q_N, \tilde{H}^s_{\mathrm{mix}}) = \sqrt{1 - 2 \sum_{i=1}^N w_i + \sum_{i=1}^N \sum_{j=1}^N w_i w_j \tilde{K}(\boldsymbol{\xi}^{(i)}, \boldsymbol{\xi}^{(j)})}. \tag{4.4}$$

The expression on the right-hand side of (4.4) has to be computed with a precision of ε^2 to guarantee an accuracy of ε for $\mathbf{wce}(Q_N, \tilde{H}^s_{\mathrm{mix}})$ on the left-hand side. Depending on the magnitude of $\mathbf{wce}(Q_N, \tilde{H}^s_{\mathrm{mix}})$, we thus have to use data types with a precision beyond 10^{-16}, as is the standard double floating point arithmetic.

4.1.2 Numerical results

We compute the optimal weights $\check{\boldsymbol{w}}(\boldsymbol{X}_N)$ in (4.3) using a Cholesky decomposition of $\boldsymbol{G}(\boldsymbol{X}_N)$. This involves costs of approximately N^3 floating point operations. For the numerical experiments with $s \geq 2$ we use the *GNU Multiple-precision library* MPFR [62] with a fixed precision of 96 binary digits. This equals a decimal precision of about 10^{-27} and hence is sufficient to compute worst-case errors up to 10^{-13} accurately.

The set of uniformly distributed random cubature points $\boldsymbol{X}_N$ is drawn with the Mersenne twister implementation of C++11, using the number 2016 as seed. For the generation of the Halton and Sobol quasi–random point sets we used the *GNU Scientific Library* (GSL) [58].
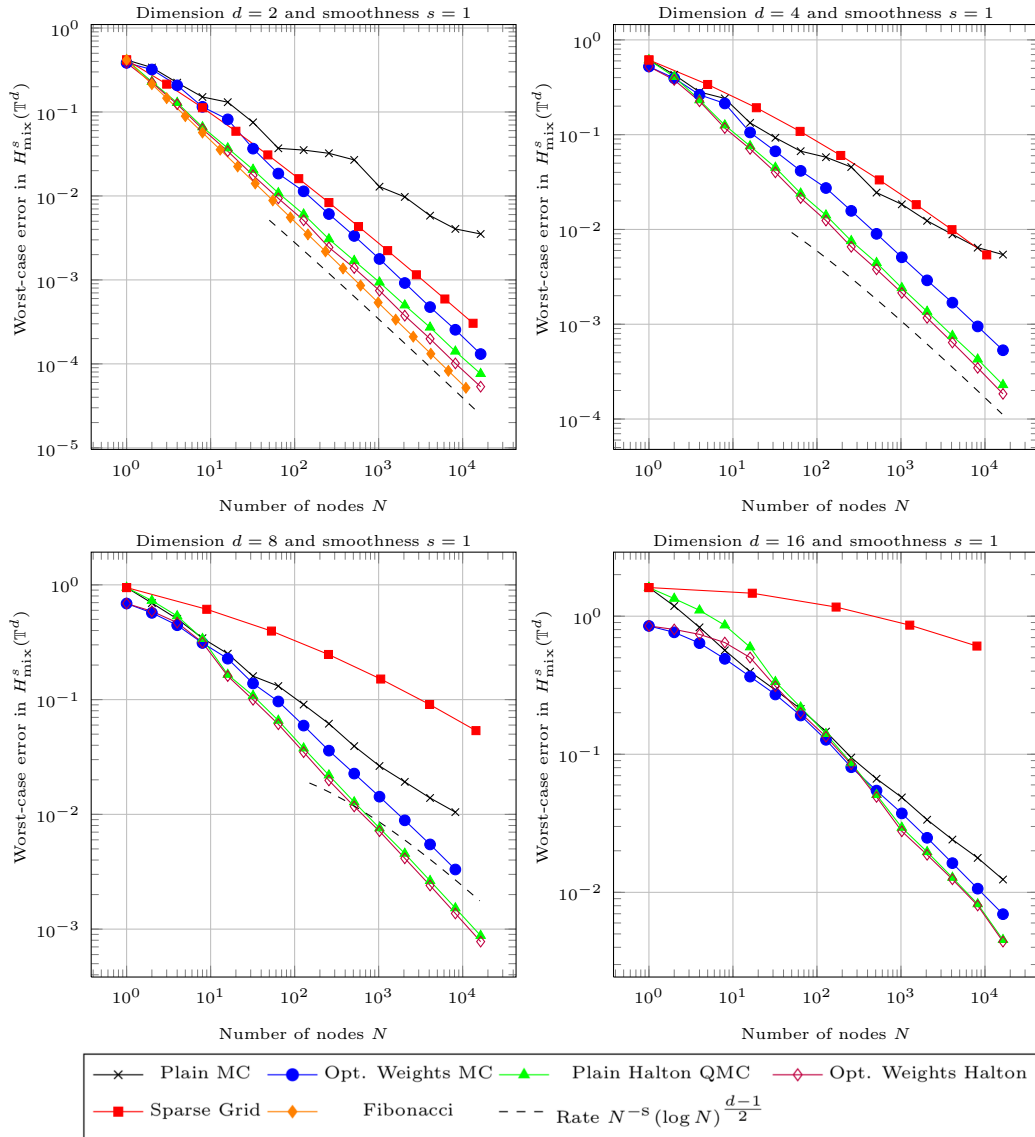
Figure 4.1: Numerical results for the mixed-Sobolev space $H_{\mathrm{mix}}^s(\mathbb{T}^d)$ with smoothness parameter $s = 1$ on the torus.

4.1.3 Worst-case error in the periodic setting

We will start with the detailed numerical investigation of the periodic setting, i.e. the space $\tilde{H}_{\mathrm{mix}}^s = H_{\mathrm{mix}}^s(\mathbb{T}^d)$. Here, we compare optimally weighted random and Halton points to their unweighted counterparts as well as to sparse grids based on the rectangle rule, which is known to be optimal for integration in univariate Sobolev spaces of periodic functions, cf. [22, 30]. In Section 4.1.4 we will demonstrate that similar results hold for the non-periodic Sobolev space $H_{\mathrm{mix}}^s([0,1]^d)$ as well.

For the smoothness parameter $s = 1$, we give the results of the worst-case error computation

(4.4) in dimensions $d \in \{2, 4, 8, 16\}$ in Figure 4.1. In $d = 2$ it is known that the Fibonacci lattice gives the optimal order of the convergence rate $N^{-1} \log(N)^{1/2}$. Moreover, in [88] we gave a computer-based proof by exhaustion that for N up to 16 the Fibonacci lattice represents the true global minimum of the worst-case error function with respect to the location of the points. Here, we can see that Halton points with and without optimal weights also attain this optimal rate of convergence. Random points with uniform weight $1/N$ achieve the rate of $N^{-1/2}$, which improves to N^{-1} with optimal weights. It is not clear whether an additional log-factor comes into play here. Finally, sparse grids also attain the main rate N^{-1}, but an additional log factor is clearly present.

In higher dimensions $d \in \{4, 8, 16\}$ the picture is basically the same: For $s = 1$, Halton points with and without optimal weights seem to achieve the best possible rate

$$N^{-s} \log(N)^{(d-1)/2}. \tag{4.5}$$

Unfortunately, the Fibonacci lattice does not have a canonical counterpart in higher dimensions. Therefore, it appears in the plots for $d = 2$ only.

It is noteworthy that the rate (4.5) only holds asymptotically. For small $N \leq e^{\frac{d-1}{2s}}$, the rate (4.5) is not even meaningful at all because it is not decreasing. Therefore, the Halton sequence with and without optimal weights, as well as the optimally weighted Monte Carlo method, achieve a pre-asymptotic rate that is better than (4.5) in $d = 8$ and $d = 16$, where (4.5) was not even plotted at all.

Another observation for $s = 1$ is that sparse grids, as well as uniformly weighted Halton and random points, yield the same worst-case error if $N = 1$. This is due to the periodicity in $H_{\mathrm{mix}}^s(\mathbb{T}^d)$ – it simply does not matter where the first point is placed, as long as the weight is 1. However, with non-uniform weights one can improve the worst-case error, as it is the case for the optimally weighted (quasi–) Monte Carlo rules. We will see that this effect becomes less influential in higher smoothness.

For smoothness parameter $s = 2$, the results of the worst-case error computation (4.4) in dimensions $d \in \{2, 4, 8, 16\}$ are given in Figure 4.2. Again, the Fibonacci lattice attains the best possible rate (4.5) in $d = 2$. As opposed to $s = 1$, now the Halton sequence with uniform weights still has a main rate of N^{-1}. This can be improved by computing optimal weights: The optimally weighted Halton sequence achieves a main rate of N^{-2}, where a log-factor seems to be involved. The same holds for Monte Carlo points which have order $N^{-1/2}$ convergence for uniform weights and a main rate of N^{-2} when optimal weights are used. Additional log-factors seem to be involved here as well. However, as the dimensionality becomes larger, i.e. $d = 8$ or $d = 16$, one can clearly see that the optimally weighted random and quasi–random point sets converge much faster than the sparse grid method, which has a log-factor with exponent $(d-1)(s+1/2)$, cf. [44]. Therefore, we believe that the dimension and smoothness dependence of the log-factors for the optimally weighted (q)MC methods is much weaker than with sparse grids.

Another effect that becomes visible in $d = 16$ is that the optimally weighted random points have a smaller worst-case error than optimally weighted Halton points for small N. However, the Halton sequence becomes more efficient than random points as N gets larger. We explain this behaviour by the fact that most quasi–random constructions in high dimensions attain their
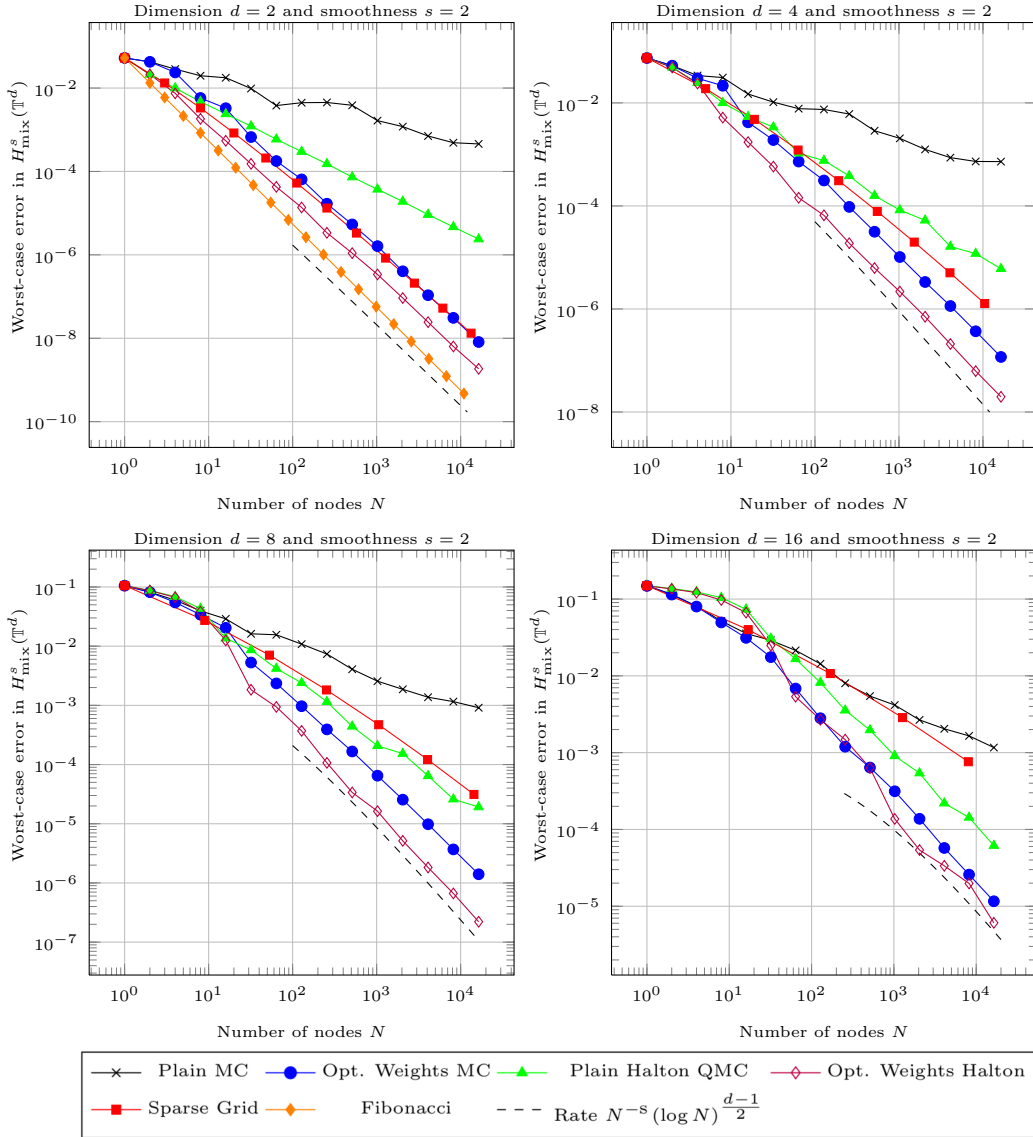
Figure 4.2: Numerical results for the mixed-Sobolev space $H^s_{\mathrm{mix}}(\mathbb{T}^d)$ with smoothness parameter $s = 2$ on the torus.

small discrepancy bounds only for large N, i.e. large constants are involved. The discrepancy of random points, however, can be bounded by $\sqrt{d/N}$, cf. [85], which is only mildly dependent on d.

In Figure 4.3 the plots for the case $s = 3$ are given. Here, the gap between the optimal Fibonacci lattice and optimally weighted Halton and Monte Carlo points for $d = 2$ is even more prominent than in the case $s = 2$. Therefore, we conclude that there is an s-dependency in the log-term of optimally weighted (quasi–) random sequences, even though it might be possible that just the constant gets worse.
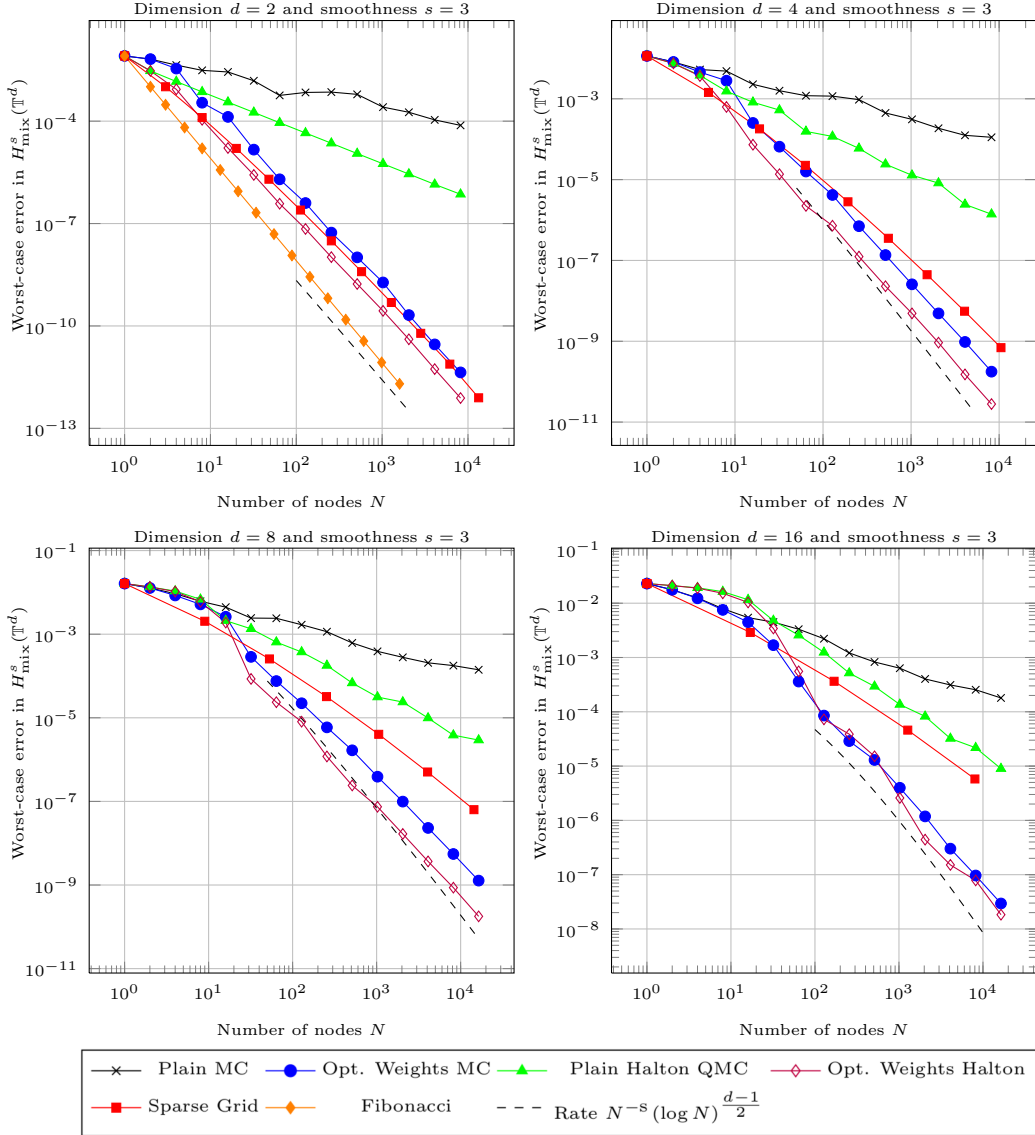
Figure 4.3: Numerical results for the mixed-Sobolev space $H_{\mathrm{mix}}^s(\mathbb{T}^d)$ with smoothness parameter $s = 3$ on the torus.

Looking at the higher dimensional settings $d \in \{4, 8, 16\}$, we get a similar picture as in the cases before: For small point sets optimally weighted random points are the best choice, but, as N increases, the optimally weighted Halton becomes superior. In all cases we observe that optimally weighted (quasi–) random points achieve the best possible main rate N^{-3} and even outperform sparse grids, especially if d gets large.

In order to investigate whether the log-exponent of optimally weighted random and Halton points is s-dependent at all, we multiplied the respective worst-case errors $\mathbf{w\check{c}e}(\boldsymbol{X}_N, \tilde{H}_{\mathrm{mix}}^s)$ with N^s and plotted the resulting data against the logarithmically scaled point numbers N. As
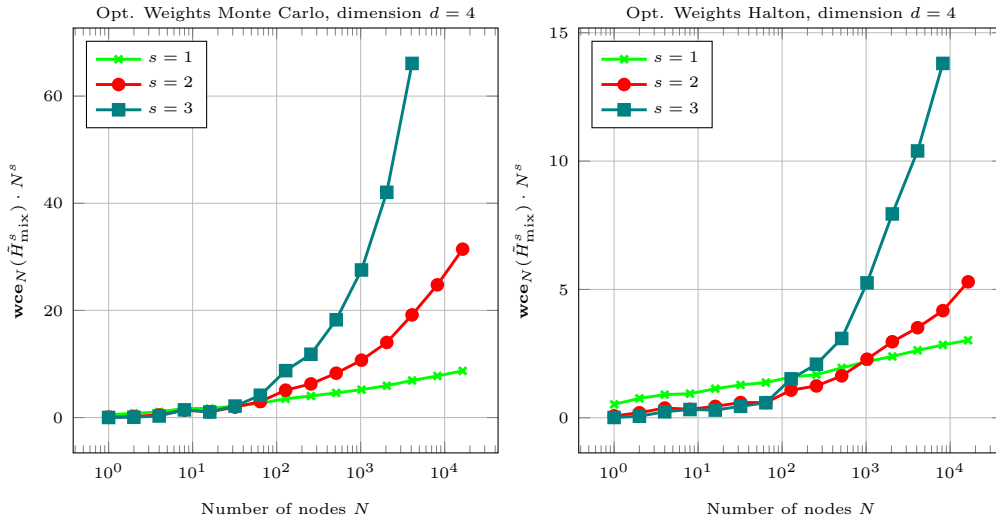
Figure 4.4: Dependency of the log-term on the smoothness $s \in \{1, 2, 3\}$.

can be observed in Figure 4.4, the depicted curves clearly depend on the smoothness parameter $s \in \{1, 2, 3\}$. Therefore, it can be ruled out that optimally weighted random points do achieve the best possible rate $N^{-s} \log(N)^{(d-1)/2}$, whose log-term is independent of the smoothness s.

Stability

Finally, we comment on the stability of the optimal weights $\check{\boldsymbol{w}}(\boldsymbol{X}_N)$. We recall that a cubature rule is called stable if $|\check{\boldsymbol{w}}(\boldsymbol{X}_N)|_1$ is uniformly bounded by some constant for all N or at least does not grow faster than a power of $\log(N)$.

In Figure 4.5 the values of $|\check{\boldsymbol{w}}(\boldsymbol{X}_N)|_1$ are given for different smoothness parameters $s \in \{1, 2, 3\}$ and $N = 2^k$. The point set $\boldsymbol{X}_N$ is either the Halton sequence or the random sequence used in the worst-case error experiments before. Clearly, the optimally weighted cubature rules are stable for large N. However, between $N = 10$ and $N = 100$ the random points and for $s = 3$ also the Halton sequence get less stable. Still, $|\check{\boldsymbol{w}}(\boldsymbol{X}_N)|_1$ is bounded by 4 for all the considered combinations of the number of points N, the dimensionality d and the smoothness s.

4.1.4 Extension to the non-periodic setting

It is a natural question whether the results of the preceding section are related to the periodicity of the considered function spaces. To this end, we compute the worst-case error in H^s_{mix} on $[0, 1]^d$ with the very same approach as before. As mentioned in Section 4.1.1, all the formulas apply in the non-periodic setting as well, albeit replacing the kernel $\tilde{K}$ with the kernel K given in (4.2). The associated reproducing kernel Hilbert space $H^s_{\mathrm{mix}}([0, 1])$ contains all functions from its periodic counterpart $\tilde{H}^s_{\mathrm{mix}}$ as well as all of its products with multivariate polynomials of the form

$$p(\boldsymbol{x}) = \sum_{|\boldsymbol{k}|_\infty \leq s} c_{\boldsymbol{k}} \prod_{j=1}^{d} x_j^{k_j}.$$
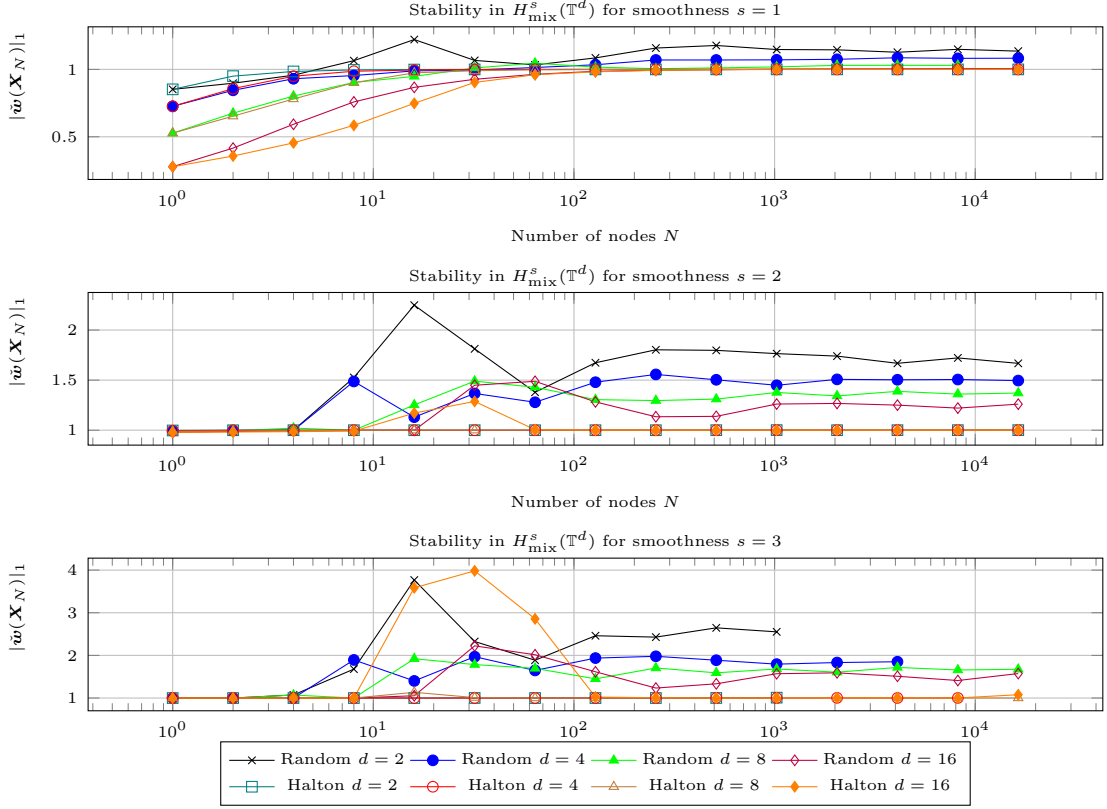
Figure 4.5: Stability of optimal cubature in the mixed-Sobolev space $H_{\mathrm{mix}}^s(\mathbb{T}^d)$ for smoothness parameters $s \in \{1, 2, 3\}$.

Therefore, $H_{\mathrm{mix}}^s([0,1])$ is substantially larger than $\tilde{H}_{\mathrm{mix}}^s$. Yet, it is known [150] that there exist cubature algorithms which can achieve the same optimal asymptotic rate of convergence as in the periodic setting, i.e. $\mathcal{O}(N^{-s} \log(N)^{(d-1)/2})$. However, not much is known about the constant that is involved in the $\mathcal{O}$-notation.

Again, we compute the optimal weights $\breve{\boldsymbol{w}}(\boldsymbol{X}_N)$ in (4.3) using a Cholesky decomposition of $\boldsymbol{G}(\boldsymbol{X}_N)$, where $\boldsymbol{X}_N$ are either Halton points or uniformly distributed random points generated with the Mersenne twister.

These optimally weighted random and Halton points are compared to their unweighted counterparts. In Figure 4.6 we give the results for $s = 2$. We observe that using optimal weights improves the convergence rate to the best possible main rate N^{-s}. Moreover, the Halton sequence with equal weights has a worst-case error that is larger than 1. We explain this by the fact that the first Halton point is $\boldsymbol{0} \in \mathbb{R}^d$ which is a corner of the domain of integration. This is no problem for periodic functions, but in the non-periodic setting, where boundary effect are present, it is usually advantageous to avoid placing points too close to the boundary [122].
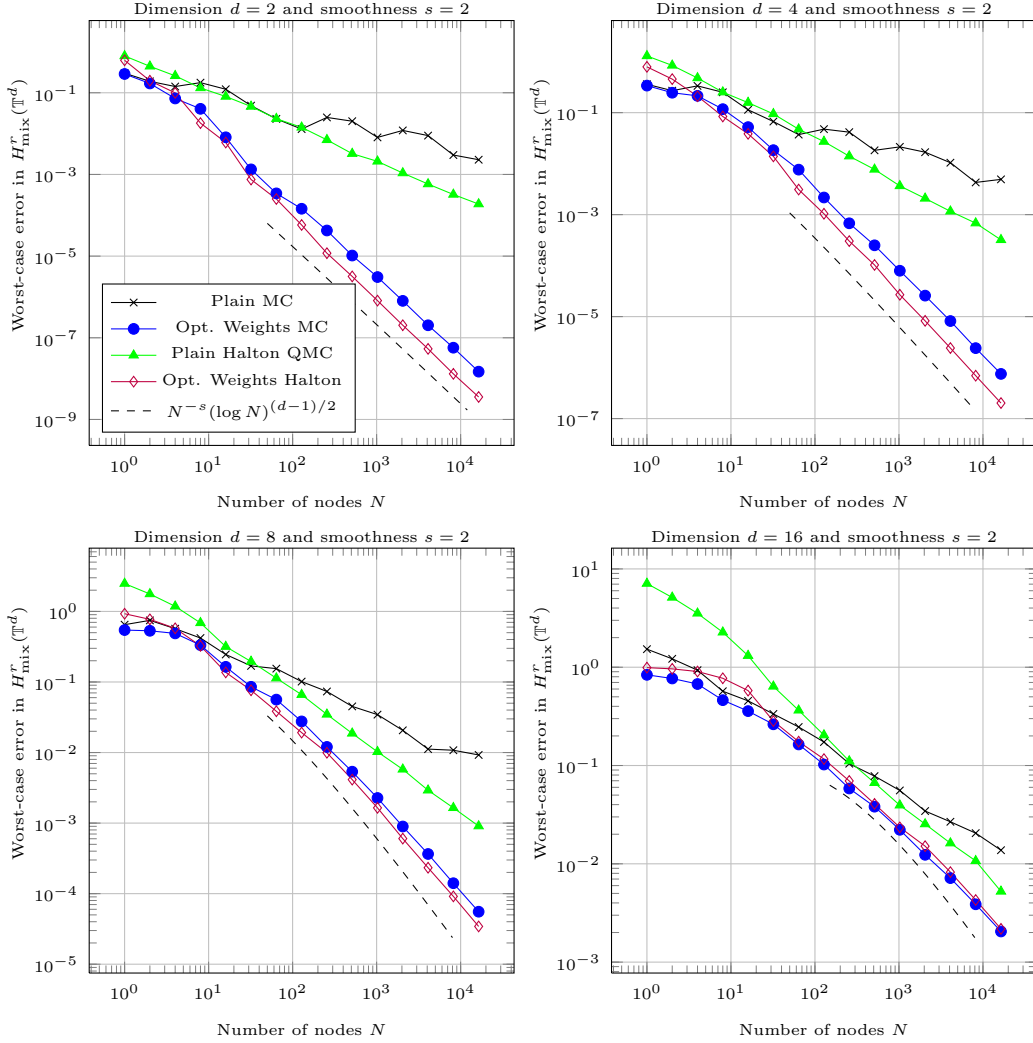
Figure 4.6: Worst-case errors for the non-periodic Sobolev space H^s_{mix} on $[0,1]^d$ with $s = 2$.

4.2 Upper bounds

In this section, we will prove bounds for the worst-case error in $\tilde{H}^s_{\mathrm{mix}}$ for optimally weighted Monte Carlo cubature rules of the form

$$\check{Q}_{\boldsymbol{X}_N}(f) := \sum_{i=1}^{N} \check{w}_i(\boldsymbol{X}_N) f(\boldsymbol{\xi}^{(i)}), \quad \boldsymbol{X}_N = \{\boldsymbol{\xi}^{(1)}, \dots, \boldsymbol{\xi}^{(N)}\} \sim \mathcal{U}([0,1]^{dN}), \tag{4.6}$$

i.e. we draw a set of N uniformly distributed random points in $[0,1]^d$ and compute the associated optimal cubature weights. Related results for isotropic Sobolev spaces on the cube and the sphere are discussed in [29]. The numerical results in Section 1 of this Chapter suggested that optimally weighted random points do not only achieve the optimal main rate of N^{-s} in $\tilde{H}^s_{\mathrm{mix}}$,

but also have a fairly good log-exponent that is close to the optimal $\frac{d-1}{2}$.

However, it is very difficult to analyze the properties of the aforementioned optimally weighted cubature rule $\check{Q}_{\boldsymbol{X}_N}(f)$ directly. Therefore, we will use the following approach:

1. Construct a stable cubature rule

$$Q_N^+(f) := \sum_{i=1}^N w_i^+(\boldsymbol{X}_N) f(\boldsymbol{\xi}^{(i)})$$

   that is exact on a finite-dimensional subspace of trigonometric polynomials and uses the same random point set $\boldsymbol{X}_N$ as information, but certain non-optimal weights $w_i^+(\boldsymbol{X}_N)$.

2. Prove upper bounds for the worst-case error of $Q_N^+(f)$ in $\tilde{H}_{\mathrm{mix}}^s$.

3. Finally, by the optimality of the cubature weights in (4.6), it follows that $\check{Q}_{\boldsymbol{X}_N}$ has at least the convergence rate of $Q_N^+(f)$.

Unfortunately, this will not lead to the desired optimal main rate N^{-s} that we saw numerically. Nevertheless, we will obtain a main rate $N^{-s+1/2}$ which still is a substantial improvement over $N^{-1/2}$ for $s > 1$.

To get started, we first recall (3.24), i.e. the $\tilde{H}_{\mathrm{mix}}^s$-norm can be realized as

$$\|f\|_{\tilde{H}_{\mathrm{mix}}^s}^2 = \sum_{\boldsymbol{k} \in \mathbb{Z}^d} \rho(\boldsymbol{k})^{2s} |\hat{f}_{\boldsymbol{k}}|^2,$$

where $\hat{f}_{\boldsymbol{k}}$ denotes the $\boldsymbol{k}$-th Fourier coefficient and

$$\rho(\boldsymbol{k}) = \prod_{j=1}^d \max(1, 2\pi |k_j|).$$

Hence, the reproducing kernel of $\tilde{H}_{\mathrm{mix}}^s$ is given by

$$\tilde{K}(\boldsymbol{x}, \boldsymbol{y}) = \sum_{\boldsymbol{k} \in \mathbb{Z}^d} \rho(\boldsymbol{k})^{-2s} \psi_{\boldsymbol{k}}(\boldsymbol{x}) \overline{\psi_{\boldsymbol{k}}(\boldsymbol{y})},$$

where we denote

$$\psi_{\boldsymbol{k}}(\boldsymbol{x}) := \exp(2\pi \mathrm{i} \boldsymbol{k} \cdot \boldsymbol{x}) = \prod_{j=1}^d e^{2\pi \mathrm{i} k_j x_j}.$$

Therefore, by (3.7), it holds for an arbitrary cubature rule $Q_N(f) = \sum_{i=1}^N w_i f(\boldsymbol{\xi}^{(i)})$ that

$$\mathbf{wce}(Q_N, \tilde{H}_{\mathrm{mix}}^s)^2 = \sum_{\boldsymbol{k} \in \mathbb{Z}^d} \rho(\boldsymbol{k})^{-2s} \left| \int_{[0,1]^d} \psi_{\boldsymbol{k}}(\boldsymbol{x}) \, \mathrm{d}\boldsymbol{x} - \sum_{i=1}^N w_i \psi_{\boldsymbol{k}}\left(\boldsymbol{\xi}^{(i)}\right) \right|^2.$$

Now we can bound the error of cubature rules that are exact on a certain set of trigonometric monomials.

Proposition 4.1. *Let a cubature rule Q_N be exact on a hyperbolic cross of radius $T > 0$, i.e. on $\{\psi_{\boldsymbol{k}}, \boldsymbol{k} \in \mathcal{HC}(T))\}$ with*

$$\mathcal{HC}(T) := \left\{ \boldsymbol{k} \in \mathbb{Z}^d : \prod_{j=1}^{d} \max(1, |k_j|) \leq T \right\}.$$

In addition, assume that Q_N is stable in the sense that there exists a constant $C > 0$ such that $\sum_{i=1}^{N} |w_i| < C$ for all $N \in \mathbb{N}$. Then it holds that

$$\mathbf{wce}(Q_N, \tilde{H}_{\mathrm{mix}}^s) \preceq_{s,d} T^{-s+1/2} \log(T)^{\frac{d-1}{2}}. \tag{4.7}$$

Moreover, (4.7) can be rephrased in terms of the cardinality $m := |\mathcal{HC}(T)|$ as

$$\mathbf{wce}(Q_N, \tilde{H}_{\mathrm{mix}}^s) \preceq_{s,d} m^{-s+1/2} \log(m)^{s(d-1)}. \tag{4.8}$$

Proof. For $\boldsymbol{k} \neq \boldsymbol{0}$ it holds $\int_{[0,1]^d} \psi_{\boldsymbol{k}}(\boldsymbol{x})\, \mathrm{d}\boldsymbol{x} = 0$. We use the stability of Q_N to obtain

$$
\begin{aligned}
\left| \int_{[0,1]^d} \psi_{\boldsymbol{k}}(\boldsymbol{x})\, \mathrm{d}\boldsymbol{x} - \sum_{i=1}^{N} w_i \psi_{\boldsymbol{k}}\left(\boldsymbol{\xi}^{(i)}\right) \right|^2 &= \left| -\sum_{i=1}^{N} w_i \psi_{\boldsymbol{k}}\left(\boldsymbol{\xi}^{(i)}\right) \right|^2 \\
&\leq \left(\sum_{i=1}^{N} |w_i| \underbrace{\left| \psi_{\boldsymbol{k}}\left(\boldsymbol{\xi}^{(i)}\right) \right|}_{=1} \right)^2 \\
&\leq \left(\sum_{i=1}^{N} |w_i| \right)^2 \\
&\leq C^2.
\end{aligned}
\tag{4.9}
$$

Therefore, it follows from the exactness of Q_N on $\mathcal{HC}(T)$ for $T > 0$ that

$$
\begin{aligned}
\mathbf{wce}(Q_N, \tilde{H}_{\mathrm{mix}}^s)^2 &= \sum_{\boldsymbol{k} \in \mathbb{Z}^d} \rho(\boldsymbol{k})^{-2s} \left| \int_{[0,1]^d} \psi_{\boldsymbol{k}}(\boldsymbol{x})\, \mathrm{d}\boldsymbol{x} - \sum_{i=1}^{N} w_i \psi_{\boldsymbol{k}}\left(\boldsymbol{\xi}^{(i)}\right) \right|^2 \\
&= \sum_{\boldsymbol{k} \in \mathbb{Z}^d \setminus \mathcal{HC}(T)} \rho(\boldsymbol{k})^{-2s} \left| \int_{[0,1]^d} \psi_{\boldsymbol{k}}(\boldsymbol{x})\, \mathrm{d}\boldsymbol{x} - \sum_{i=1}^{N} w_i \psi_{\boldsymbol{k}}\left(\boldsymbol{\xi}^{(i)}\right) \right|^2 \\
&\leq \sum_{\boldsymbol{k} \in \mathbb{Z}^d \setminus \mathcal{HC}(T)} \rho(\boldsymbol{k})^{-2s} C^2 \\
&\preceq_{d,s} T^{-2s+1} \log(T)^{d-1},
\end{aligned}
$$

where the last inequality can be found e.g. in [43, Sec. 2.3].

Regarding (4.8), we also know from [43, Sec. 2.3] that the cardinality $m := |\mathcal{HC}(T)|$ of a hyperbolic cross with radius T behaves like $m \asymp_{d,s} T \log(T)^{d-1}$. Hence, we can conclude that
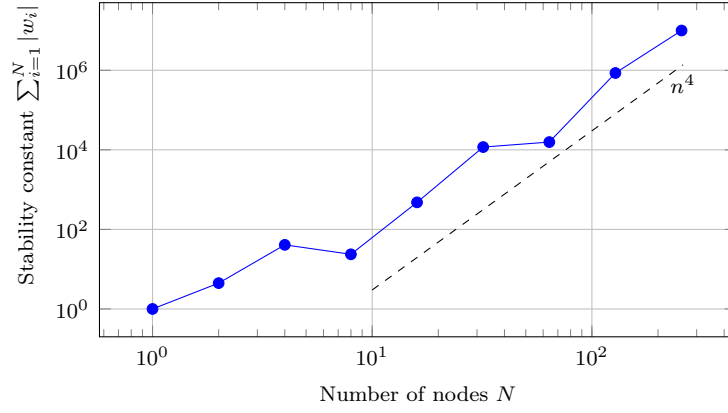
Figure 4.7: Without oversampling, i.e. $m = N$ the quadrature weights in (4.12) get unstable already for $d = 1$.

$m^{-2s+1} \asymp T^{-2s+1} \log(T)^{(-2s+1)(d-1)}$, which implies

$$
\begin{aligned}
\mathbf{wce}(Q_N, \tilde{H}_{\mathrm{mix}}^s)^2 &\preceq_{d,s} T^{-2s+1} \log(T)^{d-1} \\
&\asymp_{d,s} m^{-2s+1} \log(T)^{(2s-1)(d-1)} \log(T)^{d-1} \\
&= m^{-2s+1} \log(T)^{2s(d-1)} \\
&\leq m^{-2s+1} \log(m)^{2s(d-1)}.
\end{aligned}
$$

$\square$

Let us discuss the assumptions of Proposition 4.1 in more detail. First, let $m := |\mathcal{HC}(T)|$ denote the cardinality of $\mathcal{HC}(T)$ and define the non-decreasing re-arrangement of the multi-indices $\boldsymbol{k} \in \mathcal{HC}(T)$ by a function $\boldsymbol{h} : \mathbb{N} \to \mathbb{Z}^d$, which fulfills $\boldsymbol{h}(1) = \boldsymbol{0}$ and

$$
k \leq l \quad \Leftrightarrow \quad \rho(\boldsymbol{h}(k)) \leq \rho(\boldsymbol{h}(l)).
$$

Basically, this means that the countable set $\mathbb{Z}^d$ is ordered with respect to the magnitude of ρ. This translates also to our basis functions $\psi_{\boldsymbol{h}}$ which we will write as

$$
\psi_k(\boldsymbol{x}) := \psi_{\boldsymbol{h}(k)}(\boldsymbol{x}) = \exp\left(2\pi \mathrm{i} \boldsymbol{h}(k) \cdot \boldsymbol{x}\right).
$$

Now, we can define the Vandermonde-type matrix $\boldsymbol{V} \in \mathbb{R}^{m \times N}$ by

$$
V_{k,i} = \psi_k\left(\boldsymbol{\xi}^{(i)}\right), \quad k = 1, \dots, m \text{ and } i = 1, \dots, N. \tag{4.10}
$$

as well as the vector $\boldsymbol{b} \in \mathbb{R}^m$ by

$$
b_k = \int_{[0,1]^d} \psi_k(\boldsymbol{x}) \, \mathrm{d}\boldsymbol{x}, \quad k = 1, \dots, m. \tag{4.11}
$$

Clearly, it holds that $\boldsymbol{b} = (1, 0, \ldots, 0)$.

If $m = N$ and $\boldsymbol{V} \in \mathrm{GL}(m)$, which holds with probability 1, the cubature rule

$$Q_N(f) = \sum_{i=1}^{N} w_i f(\boldsymbol{\xi}^{(i)}), \quad \text{where } \boldsymbol{w} = \boldsymbol{V}^{-1}\boldsymbol{b} \tag{4.12}$$

is exact for all basis functions with index $\boldsymbol{k} \in \mathcal{HC}(T)$. Still, we have to ensure the stability of Q_N, i.e. $\sum_{i=1}^{N} |w_i| \leq C$ for all $N \in \mathbb{N}$ to fulfill the assumptions of Proposition 4.1. Unfortunately, numerical experiments suggest that for $m = N$ the $|\cdot|_1$-norm of $\boldsymbol{w}$ grows super-linearly in N, cf. Figure 4.7. Therefore, we will follow an oversampling approach to ensure stability. This means that we choose $m < N$ and use the $(N - m)$ remaining degrees of freedom not to achieve the maximal degree of exactness but instead for stabilizing the weights. In particular, we will aim for the solution with minimal ℓ_2-norm, i.e.

$$\boldsymbol{w}^+ := \arg\min\{\|\boldsymbol{w}\|_2 : \boldsymbol{w} \in \mathbb{R}^N \text{ and } \boldsymbol{V}\boldsymbol{w} = \boldsymbol{b}\}.$$

Using results from [39] it will turn out that for logarithmic oversampling one can ensure the stability of $\boldsymbol{w}^+$.

To simplify the notation we define the matrix $\boldsymbol{G} \in \mathbb{R}^{m \times m}$ by

$$\boldsymbol{G} := \boldsymbol{V}\boldsymbol{V}^*,$$

which means that $G_{k,l} = \sum_{i=1}^{N} \psi_k(\boldsymbol{\xi}^{(i)})\overline{\psi_l(\boldsymbol{\xi}^{(i)})}, k, l = 1, \ldots, m$. We note that $\boldsymbol{G}$ is Hermitian and positive semi-definite. The expectation of $\frac{1}{N}\boldsymbol{G}$ with respect to all possible uniformly distributed point sets $\boldsymbol{X}_N \subset [0,1]^d$ is the m-dimensional identity matrix $\mathbf{I}_m \in \mathbb{R}^{m \times m}$.

We will need the following concentration inequality, which is basically proven in [39] and quantifies the deviation of $\frac{1}{N}\boldsymbol{G}$ from $\mathbf{I}_m$ with respect to the spectral norm

$$\|\boldsymbol{A}\| = \max_{\|\boldsymbol{v}\|_2=1} \|\boldsymbol{A}\boldsymbol{v}\|_2.$$

Theorem 4.2. *For $s > 0$ assume*

$$S(m) := \sup_{\boldsymbol{x} \in [0,1]^d} \sum_{k=1}^{m} |\psi_k(\boldsymbol{x})|^2 \quad \leq \quad \frac{1 - \log 2}{2 + 2s} \frac{N}{\log N}.$$

Then, it holds that

$$\mathbb{P}\left\{ \left\| \frac{1}{N}\boldsymbol{G} - \mathbf{I}_m \right\| \geq \frac{1}{2} \right\} \quad \leq \quad 2N^{-s}. \tag{4.13}$$

In our situation we have $S(m) = m$ because

$$\sum_{k=1}^{m} |\psi_k(\boldsymbol{x})|^2 = \sum_{k=1}^{m} |\exp(\boldsymbol{h}(k) \cdot \boldsymbol{x})|^2 = \sum_{k=1}^{m} 1 = m.$$

Hence, in order to fulfill (4.13), one has to choose m such that

$$m \leq c_s \frac{N}{\log N}, \quad \text{with } c_s := \frac{1 - \log 2}{2 + 2s}. \tag{4.14}$$

Now we are ready to pose conditions on the interplay between m and N such that stable weights can be constructed.

Theorem 4.3. *Let $\boldsymbol{X}_N = \{\boldsymbol{\xi}^{(1)}, \ldots, \boldsymbol{\xi}^{(N)}\}$ be a set of N uniformly distributed points in $[0,1]^d$ and $\mathcal{HC}(T)$ a hyperbolic cross with cardinality $|\mathcal{HC}(T)| = m$. Moreover, assume that N and m fulfill (4.14). Then, for $\boldsymbol{V} \in \mathbb{R}^{m \times N}$ and $\boldsymbol{b} \in \mathbb{R}^m$ defined in (4.10) and (4.11), respectively we define the cubature rule $Q_N^+(f) = \sum_{i=1}^N w_i^+ f(\boldsymbol{\xi}^{(i)})$ with*

$$\boldsymbol{w}^+ := \boldsymbol{V}^* (\boldsymbol{V}\boldsymbol{V}^*)^{-1} \boldsymbol{b}.$$

It holds that

  (i) *The cubature rule Q_N^+ is exact on $V_m = \{\psi_1, \ldots, \psi_m\}$.*

  (ii) *Among all possible weights that ensure the exactness of Q_N^+ on V_m, $\boldsymbol{w}^+$ is the one with minimal ℓ_2-norm, i.e.*

$$\boldsymbol{w}^+ = \arg\min\{\|\boldsymbol{w}\|_2 : \boldsymbol{w} \in \mathbb{R}^N \text{ and } \boldsymbol{V}\boldsymbol{w} = \boldsymbol{b}\}.$$

  (iii) *$\boldsymbol{w}^+$ is stable with high probability, i.e.*

$$\mathbb{P}\left\{ \|\boldsymbol{w}^+\|_1 \leq \sqrt{6} \right\} \geq 1 - N^{-2s}.$$

Proof. The exactness of Q_N^+ on V_m holds true because

$$\boldsymbol{V}\boldsymbol{w}^+ = \boldsymbol{V}\boldsymbol{V}^*(\boldsymbol{V}\boldsymbol{V}^*)^{-1}\boldsymbol{b} = \mathbf{I}_m\boldsymbol{b} = \boldsymbol{b}.$$

Next, we show that $\boldsymbol{w}^+$ is the minimum norm solution of $\boldsymbol{V}\boldsymbol{w} = \boldsymbol{b}$ by elementary linear algebra. To this end, take another $\boldsymbol{w} \in \mathbb{R}^N$ that fulfills $\boldsymbol{V}\boldsymbol{w} = \boldsymbol{b}$. We show that $\|\boldsymbol{w}\|_2 \geq \|\boldsymbol{w}^+\|$. First, we note that it holds $(\boldsymbol{w} - \boldsymbol{w}^+)^*\boldsymbol{w}^+ = 0$ because

$$(\boldsymbol{w} - \boldsymbol{w}^+)^*\boldsymbol{w}^+ = (\boldsymbol{w} - \boldsymbol{w}^+)^*\boldsymbol{V}^*\boldsymbol{G}^{-1}\boldsymbol{b} = (\boldsymbol{V}\boldsymbol{w} - \boldsymbol{V}\boldsymbol{w}^+)^*\boldsymbol{G}^{-1}\boldsymbol{b} = 0.$$

Therefore,

$$\begin{aligned}
\|\boldsymbol{w}\|_2^2 &= \|\boldsymbol{w} - \boldsymbol{w}^+ - \boldsymbol{w}^+\|_2^2 \\
&= \|\boldsymbol{w} - \boldsymbol{w}^+\|_2^2 - 2(\boldsymbol{w} - \boldsymbol{w}^+)^*\boldsymbol{w}^+ + \|\boldsymbol{w}^+\|_2^2 = \|\boldsymbol{w} - \boldsymbol{w}^+\|_2^2 + \|\boldsymbol{w}^+\|_2^2 \geq \|\boldsymbol{w}^+\|_2^2.
\end{aligned}$$

Finally, following [39], we observe that $\|\frac{1}{N}\boldsymbol{G} - \mathbf{I}_m\| \leq \frac{1}{2}$ implies

$$\frac{1}{2}N \quad \leq \quad \|\boldsymbol{G}\| \quad \leq \quad \frac{3}{2}N$$

and hence

$$\|\boldsymbol{G}^{-1}\| \leq 2N^{-1}. \tag{4.15}$$

Moreover, because of $\boldsymbol{G} = \boldsymbol{G}^*$ we have

$$\|\boldsymbol{G}\| = \lambda_{\max}(\boldsymbol{G}) = \max_{\|\boldsymbol{x}\|_2=1} \boldsymbol{x}^*\boldsymbol{G}\boldsymbol{x} = \max_{\|\boldsymbol{x}\|_2=1} \boldsymbol{x}^*\boldsymbol{V}^*\boldsymbol{V}\boldsymbol{x} = \max_{\|\boldsymbol{x}\|_2=1} \|\boldsymbol{V}\boldsymbol{x}\|_2^2 = \|\boldsymbol{V}\|^2,$$

which implies

$$\|\boldsymbol{V}^*\| = \|\boldsymbol{V}\| = \sqrt{\|\boldsymbol{G}\|} \leq \sqrt{3/2}\sqrt{N}. \tag{4.16}$$

Now, combining (4.15) and (4.16), we arrive at

$$\|\boldsymbol{w}^+\|_2 = \left\|\boldsymbol{V}^* \left(\boldsymbol{V}\boldsymbol{V}^*\right)^{-1} \boldsymbol{b}\right\|_2 \leq \|\boldsymbol{V}\|\|\boldsymbol{G}^{-1}\|\|\boldsymbol{b}\|_2 \leq \sqrt{3/2}\sqrt{N}2N^{-1}\|\boldsymbol{b}\|_2 = \sqrt{6}N^{-1/2}.$$

Finally, by Hoelder's inequality we obtain the desired result:

$$\|\boldsymbol{w}^+\|_1 \leq \sqrt{N}\|\boldsymbol{w}^+\|_2 \leq \sqrt{6}.$$

$$\square$$

Remark 4.4. $\boldsymbol{w}^+ = \boldsymbol{V}^* \left(\boldsymbol{V}\boldsymbol{V}^*\right)^{-1} \boldsymbol{b} = \boldsymbol{V}^+\boldsymbol{b}$, where $\boldsymbol{V}^+$ denotes the Moore-Penrose pseudo inverse of the fat matrix $\boldsymbol{V} \in \mathbb{R}^{m \times N}$.

Now we are in the position to determine a final error estimate for the cubature-rule Q_N^+ in terms of the number of function evaluations N.

Theorem 4.5. *Let* $\boldsymbol{X}_N = \{\boldsymbol{\xi}^{(1)}, \ldots, \boldsymbol{\xi}^{(N)}\}$ *be a set of N uniformly distributed points in $[0,1]^d$ and $\mathcal{HC}(T)$ a hyperbolic cross with cardinality $|\mathcal{HC}(T)| = m$. Choose m as large as possible such that (4.14) is still fulfilled. Then, the worst-case error of $Q_N^+(f) = \sum_{i=1}^{N} w_i^+ f(\boldsymbol{\xi}^{(i)})$ in $\tilde{H}_{\mathrm{mix}}^s$ can be bounded from above by*

$$\mathbf{wce}(Q_N^+, \tilde{H}_{\mathrm{mix}}^s) \quad \preceq_{d,s} \quad N^{-s+1/2} \log{(N)}^{sd-1/2}$$

Proof. Let $m = m(T) = |\mathcal{HC}(T)|$, where T is chosen as large as possible to fulfill (4.14), i.e. $m(T) \leq c_s N/\log(N)$. It follows that $m(T+1) > c_s N/\log(N)$. Moreover, there exists a dimension-dependent constant α such that $m(T+1) \leq \alpha m(T)$ for all $T \in \mathbb{R}_+$. This implies $m(T) \geq \frac{c_s}{\alpha} N/\log(N)$. Then, using (4.8), we can conclude that it holds

$$\begin{aligned}
\mathbf{wce}(Q_N, \tilde{H}_{\mathrm{mix}}^s) &\preceq_{d,s} m^{-s+1/2} \log(m)^{s(d-1)} \\
&\preceq_{d,s} \left(\frac{N}{\log N}\right)^{-s+1/2} \log\left(\frac{N}{\log N}\right)^{s(d-1)} \\
&\leq N^{-s+1/2} \log(N)^{s-1/2} \log{(N)}^{s(d-1)} \\
&= N^{-s+1/2} \log{(N)}^{sd-1/2}.
\end{aligned}$$

$$\square$$

In the following remark we comment on possible alterations of our result to obtain the best possible main rate of N^{-s}, which we saw in the numerical experiments of Section 1.

Remark 4.6. In fact, numerical experiments suggest that Q_N^+ decays with a main rate of N^{-s} instead of $N^{-s+1/2}$. We are convinced that the missing $N^{-1/2}$ gets lost in (4.9), where the bound

$$\left| \sum_{i=1}^N w_i \psi_{\boldsymbol{k}} \left(\boldsymbol{\xi}^{(i)} \right) \right| \leq \sum_{i=1}^N |w_i| \left| \psi_{\boldsymbol{k}} \left(\boldsymbol{\xi}^{(i)} \right) \right| \quad \text{for all } \boldsymbol{k} \in \mathbb{Z}^d$$

seems to be too rough for our choice of $\boldsymbol{w}^+$. Due to extensive numerical simulations, we believe that it actually holds

$$\left| \sum_{i=1}^N w_i^+ \psi_{\boldsymbol{k}} \left(\boldsymbol{\xi}^{(i)} \right) \right| \leq C N^{-1/2} \tag{4.17}$$

for sufficiently many $\boldsymbol{k} \in \mathbb{Z}^d$.

For example, in the univariate setting $d = 1$, assume that (4.17) holds for all but a fixed number of elements in every dyadic block $D_j = \{\pm 2^j, \pm(2^j + 1), \ldots, \pm(2^j + 2^j - 1)\}, j \in \mathbb{N}$. Then, the desired main rate N^{-s} could be obtained with a simple modification of Proposition 4.1.

However, the validity of (4.17) seems to be difficult to prove and is ongoing joint work with Aicke Hinrichs and Mario Ullrich (JKU Linz).

The following remark gives an outlook to possible extensions of the proof-technique used here.

Remark 4.7. In Theorem 4.3 we constructed the set of auxiliary cubature weights to be of minimal $\|\cdot\|_2$-norm among all weights that ensure a certain degree of exactness on trigonometric polynomials. Of course it is also reasonable to follow the same approach, but replace the $\|\cdot\|_2$ with the $\|\cdot\|_1$- norm, i.e.

$$\boldsymbol{w} = \arg\min\{\|\boldsymbol{w}\|_1 : \boldsymbol{w} \in \mathbb{R}^N \text{ and } \boldsymbol{V}\boldsymbol{w} = \boldsymbol{b}\},$$

which is closely related to compressed-sensing, see e.g. [61].

Beside proving upper bounds for the periodic Sobolev spaces with dominating mixed smoothness, one could consider non-periodic setting as well.

Remark 4.8. The concentration inequality from [39] only holds for orthonormal bases. In [18] this was generalized to Riesz-bases, in particular to the hierarchical Faber basis. Therefore, it is possible to obtain a similar result as for the periodic Sobolev space for its non-periodic counterpart as well.

4.3 Random information in analytic function spaces

At first glance, it seems to be a natural approach to extend the results from this chapter to function spaces of infinite or analytic smoothness. However, it is known that in this case the precise location of points is much more important than it seems to be the case for integration of functions with finite smoothness. A well-known example is the so-called *Runge phenomenon*, originally observed for polynomial interpolation and hence also for Newton-Cotes quadrature.
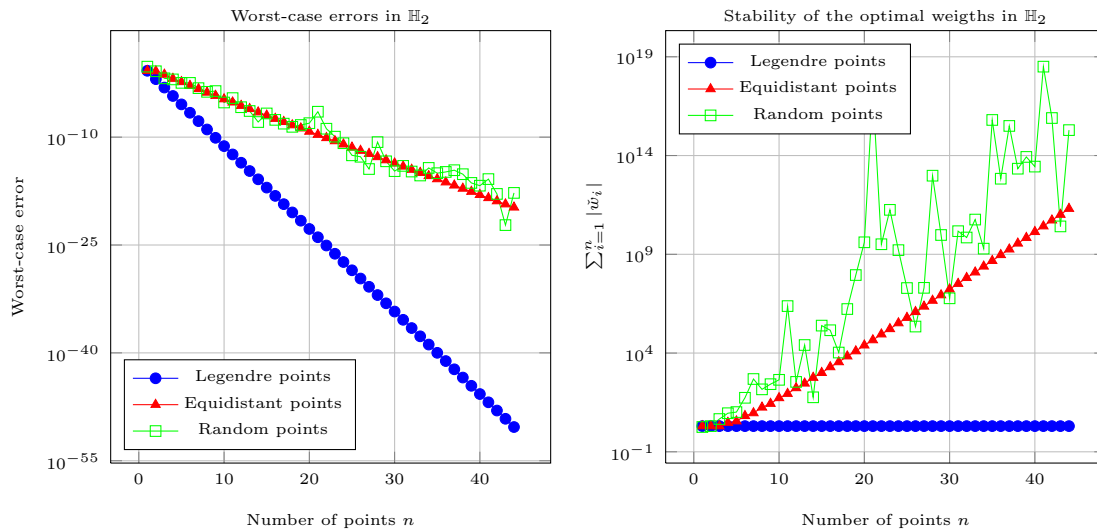
Figure 4.8: Worst-case error and stability of optimally weighted point sets in the analytic Hardy space $\mathbb{H}_2$.

Basically, it says that polynomial interpolation becomes extremely unstable for equidistant points. In [125] it was proven that the Runge-phenomenon is present also for arbitrary interpolation operators when applied to analytic functions.

In Figure 4.8, we computed optimal weights for integration in the Hardy space $\mathbb{H}_2$ which consists of functions that are analytic in a disc of radius $r = 2$. It is known that in this space one can achieve convergence rates of order 2^{-2n}, cf. [80]. This rate is approximately achieved by optimally weighted Gauss-Legendre points. However, for optimally weighted equidistant or random points the rate is substantially smaller. Moreover, looking at the right-hand side of Figure 4.8, the optimal weights are highly unstable, which is consistent with the results in [125]. Since the instability of the optimal quadrature weights grows exponentially with n, the resulting quadrature rules have no practical value at all.

A possible workaround is using quadratic oversampling, cf. [90], which, however, reduces the rate exponential convergence rates of order $\mathcal{O}(e^{-\alpha n})$ to a sub-exponential rate of order $\mathcal{O}(e^{-\alpha\sqrt{n}})$. Moreover, even if logarithmic oversampling, like in the finite smoothness setting, would be sufficient, still an exponential rate of convergence deteriorates to the order of

$$\exp\left(-\alpha\frac{N}{\log N}\right),$$

which is also sub-exponential.

Therefore, we believe that for integrands with infinite or even analytic regularity the precise location of the points plays an important role, which is our motivation for the next chapter.

5 Computation of optimal and nested quadrature points

In Chapter 4 we studied the radius of information of uniformly distributed random and low-discrepancy point sets. It turned out that they provide almost optimal information in the sense that they allow convergence of order $N^{-s+\varepsilon}$, where the $\varepsilon > 0$ neglects possible log-terms. Even with optimal cubature points one cannot beat the $N^{-s+\varepsilon}$-asymptotic of the worst-case error in H^s_{mix}, cf. [43]. However, as discussed in Section 4.3 the situation is quite different in the setting of analytic regularity. Now, the precise choice of the cubature points is much more important, but also more delicate because of the nonlinear structure of the worst-case error with respect to the points.

This chapter deals with the problem of choosing good or even optimal point sets for numerical integration in a given RKHS $\mathcal{H}_K$. Here, our main focus is the treatment of infinitely differentiable functions, but most results are applicable to spaces with finite smoothness as well, albeit with additional effort to deal with certain technicalities.

First, we note that the best possible linear integration algorithm consisting of N points $\check{\boldsymbol{X}}_N$ and weights $\check{\boldsymbol{w}}$ for integration in $\mathcal{H}_K$ is represented by

$$
(\check{\boldsymbol{X}}_N, \check{\boldsymbol{w}}) := \underset{\substack{\boldsymbol{X}_N \in \Omega \\ \boldsymbol{w} \in \mathbb{R}^N}}{\arg\min} \ \sup_{\|f\|_{\mathcal{H}_K} \leq 1} \left| \int_\Omega f(\boldsymbol{x})\, \omega(\boldsymbol{x})\, \mathrm{d}\boldsymbol{x} - \sum_{i=1}^N w_i f(\boldsymbol{\xi}^{(i)}) \right| \tag{5.1}
$$

$$
= \underset{\substack{\boldsymbol{X}_N \in \Omega \\ \boldsymbol{w} \in \mathbb{R}^N}}{\arg\min} \left\| \ell_\Omega(\cdot) - \sum_{i=1}^N w_i K(\cdot, \boldsymbol{\xi}^{(i)}) \right\|_{\mathcal{H}_K}.
$$

We see that by the Riesz-duality in $\mathcal{H}_K$ the problem of finding a set of N points $\check{\boldsymbol{X}}_N \subset \Omega \subseteq \mathbb{R}^d$ that minimize the worst-case error is equivalent to finding the *best N-term approximation* of $\ell_\Omega \in \mathcal{H}_K$ by elements from the set $\{K(\cdot, \boldsymbol{x}) : \boldsymbol{x} \in \Omega\}$, cf. [49, 151].

As a first step, we decouple the problem of finding the optimal point set $\check{\boldsymbol{X}}_N$ from the problem of finding the optimal weights $\check{\boldsymbol{w}} \in \mathbb{R}^N$. To this end, we recall Corollary 3.6, which states that for a given set of points $\boldsymbol{X}_N$, the optimal weights can be computed by solving the linear system

$$
\check{\boldsymbol{w}}(\boldsymbol{X}_N) := \boldsymbol{G}^{-1}(\boldsymbol{X}_N)\boldsymbol{b}(\boldsymbol{X}_N),
$$

where $\boldsymbol{G}(\boldsymbol{X}_N) = K(\boldsymbol{\xi}^{(i)}, \boldsymbol{\xi}^{(j)})_{i,j=1}^N \in \mathbb{R}^{N \times N}$ and $\boldsymbol{b}(X_N) = (\ell_\Omega(\boldsymbol{\xi}^{(i)}))_{i=1}^N \in \mathbb{R}^N$.

Then, the worst-case error can be written as (cf. Corollary 3.6)

$$\sup_{\|f\|_{\mathcal{H}_K} \leq 1} \left| \int_\Omega f(\boldsymbol{x})\,\omega(\boldsymbol{x})\,\mathrm{d}\boldsymbol{x} - \sum_{i=1} \breve{w}_i(\boldsymbol{X}_N) f(\boldsymbol{\xi}^{(i)}) \right| = \|L_\Omega\|^2_{\mathcal{H}_K^\star} - \boldsymbol{b}^\intercal(\boldsymbol{X}_N) \boldsymbol{G}^{-1}(\boldsymbol{X}_N) \boldsymbol{b}(\boldsymbol{X}_N), \quad (5.2)$$

which is a nonlinear function of $\boldsymbol{X}_N$. Unfortunately, direct minimization of (5.2) in multiple dimensions has three main drawbacks:

1. For analytic kernels the problem is very ill-conditioned, cf. the discussion in Section 5.2.

2. For $d \geq 2$ there exist many local minima. In fact, there exist approximately $N!$ local minima already for $d = 2$, see the discussion in [88].

3. Every single evaluation of (5.2) for a set of points $\boldsymbol{X}_N$ requires the inversion of a dense $N \times N$ matrix with high precision, cf. the discussion at the beginning of Section 4.1.2. Therefore, the computation of an amount of points that is sufficient for multivariate integration problems is not tractable, even with parallel computers.

We deal with the ill-conditionedness by a reformulation of the best-approximation problem (5.2) as a nonlinear, but stable system of equations that can be solved efficiently with Newton's method. However, this approach only works for $d = 1$ because it relies on the properties of extended Tschebyscheff-systems, which only exist for $d = 1$, cf. Section 2.3.1. Therefore, we postpone the second and third problem to future work and treat the problem of finding optimal points throughout this thesis in the univariate quadrature setting only.

To this end, we use the concept of *total positivity*, which relates the theory of interpolation with extended Tschebyscheff systems, cf. Definition 2.4, to approximation with kernel functions. Then, the zeros and hence the behaviour of the error representer can be controlled to derive several important properties of optimal quadrature rules in the univariate setting. This leads to an efficient method for the computation of optimal quadrature points, which can be further improved by exploiting certain symmetry properties of the kernel.

Because we will tackle the problem of multivariate integration with optimal weights by a sparse tensor product approach in Chapter 7, we also need good quadrature rules with nested points. To this end, we rely on the best-N-term approximation perspective (5.1) again and use *orthogonal matching pursuit* to construct a greedy approximation to ℓ_Ω from the dictionary $\mathcal{D}_\Omega(K)$. By Riesz-duality this corresponds to nested quadrature rules. Moreover, for non-uniform integration, i.e. $\omega \neq 1$, we propose a weighted variant of the matching pursuit approach that is inspired by Leja points, cf. Section 2.3.4.

The algorithms that are developed throughout this chapter will be validated in Chapter 6, where we compare the performance of the greedy approach to optimal quadrature points as well as to classical quadrature rules like e.g. Gaussian quadrature.

5.1 Optimal quadrature points and their properties

In this section, we discuss optimal quadrature rules, i.e. numerical integration in the univariate setting, where both the weights $\boldsymbol{w} = (w_1, \ldots, w_n)$ and the points $X_n = (\xi_1, \ldots, \xi_n)$ are chosen

to minimize the worst-case error, i.e.

$$
\begin{aligned}
(\check{X}_n, \check{\boldsymbol{w}}) &:= \arg\min_{\substack{\boldsymbol{w}\in\mathbb{R}^m \\ X_n\in\Omega^n}} \mathbf{wce}(X_n, \boldsymbol{w}, K) = \arg\min_{\substack{\boldsymbol{w}\in\mathbb{R}^m \\ X_n\subset\Omega^n}} \sup_{\|f\|_{\mathcal{H}_K}\leq 1} \left| L_\Omega(f) - \sum_{i=1}^n w_i f(\xi_i) \right| \\
&= \arg\min_{\substack{\boldsymbol{w}\in\mathbb{R}^m \\ X_n\subset\Omega^n}} \left\| \ell_\Omega - \sum_{i=1}^n w_i K(\cdot,\xi_i) \right\|_{\mathcal{H}_K}.
\end{aligned}
\tag{5.3}
$$

Apparently, by Riesz-duality, this problem is closely related to the approximation of

$$
\ell_\Omega(x) = L_\Omega^{(y)} K(x,y) = \int_\Omega K(x,y)\,\omega(y)\,\mathrm{d}y
$$

by functions from the set $\{K(\cdot,x)|x\in\Omega\}$.

The residual of such an approximation

$$
\ell_\Omega(x) - \sum_{i=1}^n w_i K(x,\xi_i)
$$

is called an *extended monospline* if K is extended totally positive, cf. Definition 5.1. Given a norm $\|\cdot\|_*$ and $n\in\mathbb{N}$, one can ask for

$$
\inf_{\substack{\boldsymbol{w}\in\mathbb{R}^m \\ X_n\subset\Omega^n}} \left\| \ell_\Omega(\cdot) - \sum_{i=1}^n w_i K(\cdot,\xi_i) \right\|_*,
\tag{5.4}
$$

i.e. a *monospline of least deviation* with respect to the $\|\cdot\|_*$-norm. If $\|\cdot\|_* = \|\cdot\|_{\mathcal{H}_K}$, the problem (5.4) becomes (5.3). Moreover, we will show that the points that minimize the error for the $\mathcal{H}_K$-norm are the same that minimize the $L_1(\Omega,\omega)$-norm.

This problem has been extensively studied in the 1970's and 1980's, e.g. in [9, 10, 11, 20, 27, 30, 56, 95, 103, 129, 130, 167] after it was considered for the first time in [164]. Therefore, this first Section does not offer new insights, however we give some new proofs that are specifically tailored to the RKHS setting we are dealing with.

Before we proceed, we recall some results from Chapter 3, especially Section 3.4: For a vector of n given quadrature points $X_n := (\xi_1,\ldots,\xi_n)$ the vector of optimal quadrature weights in a RKHS $\mathcal{H}_K$ with kernel $K:\Omega\times\Omega\to\mathbb{R}$ is defined by

$$
\check{\boldsymbol{w}}(X_n, K) := \boldsymbol{G}^{-1}(X_n, K)\boldsymbol{b}(X_n, K).
$$

Here, the positive definite matrix $\boldsymbol{G}(X_n, K)\in\mathbb{R}^{n\times n}$ denotes the Gramian of point-evaluation functionals and is given by

$$
G_{k,l}(X_n, K) = K(\xi_j, \xi_l) \quad j,l = 1,\ldots,n.
$$

Moreover, the vector $\boldsymbol{b}(X_n, K) \in \mathbb{R}^n$ is defined by

$$b_k(X_n, K) = \ell_\Omega(\xi_k) = L_\Omega^{(y)} K(x, y) = \int_\Omega K(\xi_k, y)\, \omega(y)\, \mathrm{d}y.$$

In the following, we will assume that the kernel K is fixed and hence omit the dependence on K, writing

$$\check{\boldsymbol{w}}(X_n) = \boldsymbol{G}^{-1}(X_n)\boldsymbol{b}(X_n)$$

for the vector of optimal quadrature weights associated to X_n for approximation of L_Ω in $\mathcal{H}_K$. As stated in Corollary 3.6, the optimally weighted quadrature rule

$$\check{Q}_{X_n}(f) := \sum_{i=1}^{n} \check{w}_i(X_n) f(\xi_i)$$

is exact on the n-dimensional space

$$\mathcal{H}_{K_{X_n}} = \mathrm{span}\,\{K(\cdot, \xi_i) : i = 1, \ldots, n\}.$$

For the error functional $\check{R}_{X_n} \in \mathcal{H}_K^\star$ given by

$$\check{R}_{X_n}(f) := L_\Omega(f) - \check{Q}_{X_n}(f) = L_\Omega(f) - \sum_{i=1}^{n} \check{w}_i(X_n) f(\xi_i)$$

this exactness property implies

$$\check{R}_{X_n}(K(\cdot, \xi_k)) = 0 \quad \text{for } k = 1, \ldots, n.$$

This is equivalent to

$$\check{r}_{X_n}(\xi_k) = 0,$$

where $\check{r}_{X_n} \in \mathcal{H}_K$ is the Riesz-representer of $\check{R}_{X_n}$ given by

$$\check{r}_{X_n}(t) := \ell_\Omega(t) - \sum_{i=1}^{n} \check{w}_i(X_n) K(\xi_i, t).$$

Therefore, the squared worst-case error formula simplifies to

$$\mathbf{w\check{c}e}^2(X_n) = \|\check{R}_{X_n}\|_{\mathcal{H}_K^\star}^2 = L_\Omega\left(\ell_\Omega(\cdot) - \sum_{i=1}^{n} \check{w}_i(X_n) K(\cdot, \xi_i)\right) = \|L_\Omega\|_{\mathcal{H}_K^\star}^2 - \sum_{i=1}^{n} \check{w}_i(X_n)\ell_\Omega(\xi_i).$$

Hence, by $\check{\boldsymbol{w}}(X_n) = \boldsymbol{G}^{-1}(X_n)\boldsymbol{b}(X_n)$ we can define the function $\mathbf{w\check{c}e}^2 : \Omega^n \to \mathbb{R}_+$ via

$$\mathbf{w\check{c}e}^2(X_n) = \|L_\Omega\|_{\mathcal{H}_K^\star}^2 - \sum_{i=1}^{n} \check{w}_i(X_n)\ell_\Omega(\xi_i) = \|L_\Omega\|_{\mathcal{H}_K^\star}^2 - \boldsymbol{b}^\intercal(X_n) \cdot \boldsymbol{G}^{-1}(X_n) \cdot \boldsymbol{b}(X_n), \qquad (5.5)$$

whose minimization with respect to $X_n = (\xi_1, \ldots, \xi_n) \in \Omega^n$ yields a set of (locally) optimal quadrature points. Since quadrature points are indistinguishable, we will assume in the following that the points are ordered, i.e. $\xi_1 \leq \xi_2 \leq \ldots \leq \xi_n$. This means that we restrict the set X_n to come from the simplex defined by

$$\mathbb{S}^n(\Omega) := \{(\xi_1, \ldots, \xi_n) \in \Omega^n : \xi_1 \leq \xi_2 \leq \ldots \leq \xi_n\}.$$

At this point, the function $\mathbf{w\check{c}e}^2 : \mathbb{S}^n(\Omega) \to \mathbb{R}$ is only defined on the inside of $\mathbb{S}^n(\Omega)$, i.e.

$$\mathring{\mathbb{S}} = \{X_n \in \mathbb{S}^n(\Omega) : \xi_1 < \xi_2 < \ldots < \xi_n\},$$

because for $\xi_i = \xi_k$ with $i \neq k$ the matrix $\boldsymbol{G}(X_n)$ is singular. Unfortunately, the inside of $\mathbb{S}^n(\Omega)$ is open. It would be desirable to establish the continuity of the function $\mathbf{w\check{c}e}^2$ on the whole $\mathbb{S}^n(\Omega)$ since by the extreme value theorem continuous functions on a compact set attain their minima. Therefore, we will now discuss the continuous extension of $\mathbf{w\check{c}e}^2$ to the boundary of $\mathbb{S}^n(\Omega)$, i.e the case when two or more points coincide.

Before we proceed with the continuous extension of $\mathbf{w\check{c}e}^2$ to the boundary of $\mathbb{S}^n(\Omega)$, we need to impose additional assumptions on the kernel K.

5.1.1 Extended totally positive kernels

In this subsection, we deal with a variant of positive definite kernels, where not only the kernel function K is evaluated at a given set of points, but also the kernel function's partial derivatives play a certain role. To this end, we recall the notation $K^{(l,j)}(x,y) = \frac{\partial^l \partial^j}{\partial x^l \partial y^j} K(x,y)$ and the definition of an *extended totally positive kernel* from [94].

Definition 5.1. (Extended total positivity)
For $\Omega \subset \mathbb{R}$, a symmetric positive definite kernel $K \in C^\infty(\Omega \times \Omega)$ is called *extended totally positive* (e.t.p.) if the sets

$$\left\{ K^{(0,j)}(\cdot, x_i) : i = 1, \ldots, n \text{ and } j = 0, \ldots, \mu_i - 1 \right\}$$

are extended Tschebyscheff-systems for all $n \in \mathbb{N}$ and all choices of n points $x_1, \ldots, x_n \in \Omega$ with associated multiplicites $\mu_1, \ldots, \mu_n \in \mathbb{N}_0$.

Remark 5.2. By the symmetry of K, also the sets

$$\left\{ K^{(j,0)}(x_i, \cdot) : i = 1, \ldots, n \text{ and } j = 0, \ldots, \mu_i - 1 \right\}$$

form extended T-systems on Ω.

Hence, the condition in Definition 5.1 can be re-phrased into

$$\det \left(K^{(\nu_i, \mu_j)}(s_i, t_j) \right)_{i,j=1}^{N} > 0$$

for all $s_1 \leq \cdots \leq s_N, t_1 \leq \cdots \leq t_N \subset \Omega$, where $\nu_i = \max\{k : s_{i-k} = s_i, k \geq 0\}$ and $\mu_i = \max\{k : t_{i-k} = t_i, k \geq 0\}$.

The following theorem from [33] will help us to identify kernels that are extended totally positive.

Theorem 5.3. *For $\Omega \subset \mathbb{R}$ let $u \in C^{\infty}(\Omega)$ be positive and increasing. Then, if the sum*

$$K(x,y) = \sum_{k=0}^{\infty} \lambda_k u(x)^k u(y)^k, \quad \lambda_k > 0$$

converges for all $(x,y) \in \Omega^2$, the kernel K is e.t.p. on Ω.

Another useful characterization of e.t.p. kernels can be found in [94].

Theorem 5.4. *Let $\tilde{K} : \Omega \to \Omega$ be e.t.p. and the function $v : \Omega \to \mathbb{R}_+$ positive. Then, the kernel*

$$K(x,y) := \tilde{K}(x,y)v(x)v(y)$$

is e.t.p. on $\Omega \times \Omega$ as well.

Throughout the remainder of this chapter, we will assume that the kernel K is extended totally positive.

5.1.2 Continuity of the worst-case error

Even though the worst-case error for optimal weights of the form (5.5) is not defined for identical points, the limit of coalescing points exists and the resulting quadrature rule is of the form

$$Q_{X_n^{\boldsymbol{\mu}}}(f) := \sum_{i=1}^{n} \sum_{j=0}^{\mu_i - 1} \breve{w}_{i,j}(X_n^{\boldsymbol{\mu}}) f^{(j)}(\xi_i). \tag{5.6}$$

Here, cf. also Section 3.4, the notation

$$X_n^{\boldsymbol{\mu}} = \begin{pmatrix} \xi_1 & \xi_2 & \cdots & \xi_n \\ \mu_1 & \mu_2 & \cdots & \mu_n \end{pmatrix}, \quad \mu_i > 0$$

is short for the vector

$$X_N = \underbrace{\xi_1, \ldots, \xi_1}_{\mu_1 \text{ times}}, \underbrace{\xi_2, \ldots, \xi_2}_{\mu_2 \text{ times}}, \ldots, \underbrace{\xi_n, \ldots, \xi_n}_{\mu_n \text{ times}}),$$

where $N = \sum_{i=1}^{n} \mu_i$. Note that $X_n^{\boldsymbol{\mu}}$ means that each point ξ_i appears *at least* $\mu_i - 1$ times. Still, two or more ξ_i may coincide such that there exists $X_m^{\boldsymbol{\nu}} = X_n^{\boldsymbol{\mu}}$ with $m < n$ and $\boldsymbol{\nu} \geq \boldsymbol{\mu}$.

Never the less, we will see that $X_n^{\boldsymbol{\mu}}$ represents the information given by function values at $\xi_1, \ldots, \xi_n$ and in addition also the values of derivatives up to order $\mu_i - 1$ at the points ξ_i. This is well-known for polynomial interpolation, where Lagrange basis functions converge to the respective Hermite-Birkhoff cardinal functions, when the interpolation points coalesce. In the context of radial basis functions, this was observed e.g. in [134].

In this setting, cf. Section 3.4.2, the optimal weights $\breve{\boldsymbol{w}}(X_n^{\boldsymbol{\mu}})$ are

$$\breve{\boldsymbol{w}}(X_n^{\boldsymbol{\mu}}) := \boldsymbol{G}^{-1}(X_n^{\boldsymbol{\mu}})\boldsymbol{b}(X_n^{\boldsymbol{\mu}}).$$

Recalling the notation $K^{(l,j)}(x,y) = \frac{\partial^l}{\partial x^l}\frac{\partial^j}{\partial y^j}K(x,y)$, the matrix $\boldsymbol{G}(X_n^{\boldsymbol{\mu}}) = \boldsymbol{G}(X_n^{\boldsymbol{\mu}}, K)$ is

$$\begin{pmatrix} K(\xi_1,\xi_1) & \cdots & K^{(0,\mu_1-1)}(\xi_1,\xi_1) & \cdots & K(\xi_1,\xi_n) & \cdots & K^{(0,\mu_n-1)}(\xi_1,\xi_n) \\ \vdots & \ddots & \vdots & & \vdots & \ddots & \vdots \\ K^{(\mu_1-1,0)}(\xi_1,\xi_1) & \cdots & K^{(\mu_1-1,\mu_1-1)}(\xi_1,\xi_1) & \cdots & K^{(\mu_1-1,0)}(\xi_1,\xi_n) & \cdots & K^{(\mu_1-1,\mu_n-1)}(\xi_1,\xi_n) \\ & \vdots & & & & \vdots & \\ K(\xi_n,\xi_1) & \cdots & K^{(0,\mu_1-1)}(\xi_n,\xi_1) & \cdots & K(\xi_n,\xi_n) & \cdots & K^{(0,\mu_n-1)}(\xi_n,\xi_n) \\ \vdots & \ddots & \vdots & & \vdots & \ddots & \vdots \\ K^{(\mu_n-1,0)}(\xi_n,\xi_1) & \cdots & K^{(\mu_n-1,\mu_1-1)}(\xi_n,\xi_1) & \cdots & K^{(\mu_n-1,0)}(\xi_n,\xi_n) & \cdots & K^{(\mu_n-1,\mu_n-1)}(\xi_n) \end{pmatrix}$$

and the right-hand-side vector $\boldsymbol{b}(X_n^{\boldsymbol{\mu}}) = \boldsymbol{b}(X_n^{\boldsymbol{\mu}}, K)$ is given by

$$\boldsymbol{b}(X_n^{\boldsymbol{\mu}}) = \left(\ell_\Omega(\xi_1),\ldots,\ell_\Omega^{(\mu_1-1)}(\xi_1),\cdots,\ell_\Omega(\xi_n),\ldots,\ell_\Omega^{(\mu_n-1)}(\xi_n)\right)^\mathsf{T}.$$

Since derivative evaluation is assumed to be a continuous linear functional in $\mathcal{H}_K$, the Gramian matrix $\boldsymbol{G}(X_n^{\boldsymbol{\mu}}) \in \mathbb{R}^{N\times N}$ is invertible and its dimensionality $N = \sum_{i=1}^n \mu_i$ is the total number of (derivative) evaluations that are used by $Q_{X_n^{\boldsymbol{\mu}}}$.

Consequently, the associated error functional will be denoted by $\check{R}_{X_n^{\boldsymbol{\mu}}}(f) = L_\Omega(f) - \check{Q}_{X_n^{\boldsymbol{\mu}}}(f)$. Its Riesz-representer

$$\check{r}_{X_n^{\boldsymbol{\mu}}}(t) = \ell_\Omega(t) - \sum_{i=1}^n \sum_{j=0}^{\mu_i-1} \check{w}_{i,j}(X_n^{\boldsymbol{\mu}})K^{(0,j)}(t,\xi_i),$$

has zeros of multiplicity $\mu_1,\ldots,\mu_n$ at the points $\xi_1,\ldots,\xi_n$, i.e.

$$\check{r}_{X_n^{\boldsymbol{\mu}}}^{(j)}(\xi_k) = 0 \quad \text{for all } k = 1,\ldots,n \text{ and } j = 0,\ldots,\mu_k - 1.$$

Moreover, the squared worst-case error of the higher-order quadrature rule (5.6) is

$$\mathbf{\check{w}ce}^2(X_n^{\boldsymbol{\mu}}) = \|\check{r}_{X_n^{\boldsymbol{\mu}}}\|_{\mathcal{H}_K}^2 = \|\ell_\Omega\|_{\mathcal{H}_K}^2 - \sum_{i=1}^n \sum_{j=0}^{\mu_i-1} \check{w}_{i,j}(X_n^{\boldsymbol{\mu}})\ell_\Omega^{(j)}(\xi_i). \tag{5.7}$$

Proposition 5.5. *The function* $\mathbf{\check{w}ce}^2(X_N) = \|\check{R}_{X_N}\|_{\mathcal{H}_K}^2$ *is continuous on* $\mathbb{S}^N(\Omega)$.

Proof. First we note that $\|\check{R}_{X_N}\|_{\mathcal{H}_K^\star}^2 = \|\check{r}_{X_N}\|_{\mathcal{H}_K}^2 = \|L_\Omega\|_{\mathcal{H}_K^\star}^2 - \boldsymbol{b}^\mathsf{T}(X_N) \cdot \boldsymbol{G}^{-1}(X_N) \cdot \boldsymbol{b}(X_N)$ is continuous in the inside of $\mathbb{S}^N(\Omega)$ because $\boldsymbol{G}$ and $\boldsymbol{b}$, as well as matrix-inversion, are continuous functions of X_N. We have to take care of the case where two or more points coalesce, which happens on the boundary of $\mathbb{S}^N(\Omega)$. To this end, we follow [20]. Let $(X^{(q)})_{q=1}^\infty$ be a sequence of points $X^{(q)} \in \mathbb{S}^N(\Omega)$. Each $X^{(q)}$ can be written as

$$X^{(q)} = X_n^{\boldsymbol{\mu}},$$

such that $N = \sum_{i=1}^n \mu_i$ and $X_n \in \mathring{\mathbb{S}}^n(\Omega)$, i.e. $\xi_1 < \ldots < \xi_n$. Assume that $\lim_{q\to\infty} X^{(q)} = X_m^{\boldsymbol{\nu}}$

with $X_m \in \mathbb{S}^m(\Omega)$. We have to prove that

$$\lim_{q \to \infty} \|\check{r}_{X^{(q)}}\|^2 = \|\check{r}_{X_m^{\boldsymbol{\nu}}}\|^2.$$

To this end, we recall the recursive definition of divided differences

$$D_{[\xi_k,\dots,\xi_{k+l}]}f = \frac{D_{[\xi_{k+1},\dots,\xi_{k+l}]}f - D_{[\xi_k,\dots,\xi_{k+l-1}]}f}{\xi_{k+l} - \xi_k},$$

which are linear combinations of the function values at X_N. In order to deal with confluent points, we need the Hermite-Genocci formulation of the divided-differences [48], i.e.

$$D_{[\xi_k,\dots,\xi_{k+l}]}f = \int_0^1 \int_0^{\tau_1} \cdots \int_0^{\tau_{l-1}} f^{(k)}\left(\xi_k + \sum_{i=1}^l \tau_i(\xi_{k+i} - \xi_k)\right) \, \mathrm{d}\tau_l \dots \mathrm{d}\tau_1,$$

which is well-defined for confluent points $\xi_k = \xi_{k+1} = \dots = \xi_{k+l}$ and equals $\frac{f^{(l)}(\xi_k)}{l!}$ in this case. The information provided by $X^{(q)} = (\xi_1^{(q)}, \dots, \xi_N^{(q)}) \in \Omega^N$ can therefore be expressed as a linear combination of the information given by

$$\Lambda_N^{(q)} := (D[\xi_1^{(q)}]f, D[\xi_1^{(q)}, \xi_1^{(q)}]f, \dots, D[\xi_1^{(q)}, \dots, \xi_N^{(q)}]f)$$

and by Corollary 3.6 it holds

$$\mathbf{\check{w}\check{c}e}^2(X^{(q)}) = \mathbf{\check{w}\check{c}e}^2(\Lambda_N^{(q)}).$$

Now, for confluent points the divided differences converge uniformly to the respective derivative value and it holds that

$$\lim_{q \to \infty} \boldsymbol{G}(X^{(q)}) = \boldsymbol{G}(X_m^{\boldsymbol{\nu}}) \quad \text{and} \quad \boldsymbol{b}(X^{(q)}) = \boldsymbol{b}(X_m^{\boldsymbol{\nu}}),$$

which implies $\lim_{q \to \infty} \boldsymbol{G}^{-1}(X^{(q)}) = \boldsymbol{G}^{-1}(X_m^{\boldsymbol{\nu}})$ and hence $\lim_{q \to \infty} \check{\boldsymbol{w}}(X^{(q)}) = \check{\boldsymbol{w}}(X_m^{\boldsymbol{\nu}})$, which proves the claim. $\qquad\square$

Now we know that the optimally weighted worst-case error depends continuously on the quadrature points in $\mathbb{S}^n(\Omega)$ and therefore attains its minimum. However, it is not clear whether this minimum consists of n different points or whether all the points coalesce to one single point yielding a Taylor-style quadrature rule that uses derivative values of increasing order at one single point.

In order to address this question, we will study the behaviour of the error representer $\check{r}_{X_n^{\boldsymbol{\mu}}}$ in more detail.

5.1.3 Properties of optimal quadrature points

In the following, we discuss the properties of optimal quadrature weights $\check{\boldsymbol{w}}(\check{X}_n)$ associated to a local minimizer $\check{X}_n$ of the $\mathbf{\check{w}\check{c}e}^2$ function.

Proposition 5.6. *For $X_n^{\boldsymbol{\mu}}$, where $\boldsymbol{\mu} = (\mu_1, \ldots, \mu_n)$ with all μ_i even, it holds for the error representer $\check{r}_{X_n^{\boldsymbol{\mu}}}$ that*

(i) $\check{r}_{X_n^{\boldsymbol{\mu}}}$ has exactly n zeros $\xi_1, \ldots, \xi_n$, each with multiplicity $\mu_1, \ldots, \mu_n$, respectively.

(ii) $\check{r}_{X_n^{\boldsymbol{\mu}}}(t) \geq 0$ for all $t \in \Omega$.

(iii) $\check{r}_{X_n^{\boldsymbol{\mu}}}^{(\mu_i)}(\xi_i) > 0$ for $i = 1, \ldots, n$.

Proof. Let $N := \sum_{i=1}^n \mu_i$. We recall that $\check{Q}_{X_n^{\boldsymbol{\mu}}}$ is exact on the N-dimensional space

$$\mathcal{H}_{K(X_n^{\boldsymbol{\mu}})} = \text{span}\left\{K^{(0,j)}(\cdot, \xi_i), i = 1, \ldots, n \text{ and } j = 0, \ldots, \mu_i - 1\right\}$$

which implies that

$$\check{r}_{X_n^{\boldsymbol{\mu}}}(x) = \ell_\Omega(x) - \sum_{i=1}^n \sum_{j=0}^{\mu_i - 1} \check{w}_{i,j}(X_n^{\boldsymbol{\mu}}) K^{(0,j)}(x, \xi_i)$$

has vanishing derivatives up to order $\mu_k - 1$ at ξ_k, i.e. $\check{r}_{X_n^{\boldsymbol{\mu}}}^{(j)}(\xi_k) = 0$ for $k = 1, \ldots, n$ and $j = 0, \ldots, \mu_k - 1$. For (i), we have to prove that there are no additional zeros. To this end, we assume that $\check{r}_{X_n^{\boldsymbol{\mu}}}(x)$ has an additional zero, which can either be a new simple zero at a point $z \in \Omega \setminus \{\xi_1, \ldots, \xi_n\}$, or an existing zero with then increased multiplicity. Without loss of generality we assume the first case, i.e. $\check{r}_{X_n^{\boldsymbol{\mu}}}(z) = 0$. This implies that $\check{Q}_{X_N^{\boldsymbol{\mu}}}$ is exact on the span of

$$\mathcal{H}_{K(X_n^{\boldsymbol{\mu}})} \cup \{K(\cdot, z)\},$$

which is an extended Tschebyscheff-system of $N+1$ functions. Therefore, we can find a function $g \in \mathcal{H}_{K(X_n^{\boldsymbol{\mu}})} \oplus \{K(\cdot, z)\}$ which fulfills the interpolation conditions

$$g^{(j)}(\xi_i) = 0 \text{ for } i = 1, \ldots, n \text{ and } j = 0, \ldots, \mu_i - 1 \quad \text{and} \quad g(z) = 1.$$

The function g cannot have more than N zeros (counting multiplicities) and all zeros are of even multiplicity. Therefore, g cannot cross the x-axis and has to be positive because of $g(z) = 1$. This implies $L_\Omega(g) > 0$. But $\check{Q}_{X_N^{\boldsymbol{\mu}}}(g) = 0$, which is a contradiction to the exactness of $\check{Q}_{X_n^{\boldsymbol{\mu}}}$ on $\mathcal{H}_{K(X_n^{\boldsymbol{\mu}})} \cup \{K(\cdot, z)\}$.

Next, (ii) is a direct consequence of (i) and $\int_\Omega \check{r}_{X_n^{\boldsymbol{\mu}}}(x)\,\omega(x)\,\mathrm{d}x = \|\check{r}_{X_n^{\boldsymbol{\mu}}}\|_{\mathcal{H}_K}^2 \geq 0$ because it has to be positive at least at one point and cannot cross the x-axis since all zeros are of even multiplicity. Because of $\check{r}_{X_n^{\boldsymbol{\mu}}}(\xi_k) = 0$, the points $\xi_1, \ldots, \xi_n$ have to be local minima of $\check{r}_{X_n^{\boldsymbol{\mu}}}$, which implies (iii). $\qquad\square$

Proposition 5.7. *Let $X_n \in \mathring{\mathbb{S}}^n(\Omega)$, i.e. the points are pairwise distinct. Then, the partial derivative of $\mathbf{w\check{c}e}^2(X_n^{\boldsymbol{\mu}})$ given by (5.7) with respect to a quadrature points ξ_k is*

$$\frac{\partial}{\partial \xi_k} \mathbf{w\check{c}e}^2(X_n^{\boldsymbol{\mu}}) = -2\check{w}_{k,\mu_k-1}(X_n^{\boldsymbol{\mu}})\, \check{r}_{X_n^{\boldsymbol{\mu}}}^{(\mu_k)}(\xi_k). \tag{5.8}$$

Proof. In order to differentiate $\mathbf{w\check{c}e}^2(X_n^{\boldsymbol{\mu}}) = \|\check{r}_{X_n^{\boldsymbol{\mu}}}\|_{\mathcal{H}_K}^2$ with respect to the point ξ_k we use the

(inner) product rule and $\check{r}^{(j)}_{X^{\boldsymbol{\mu}}_n}(\xi_i) = 0$ for $i = 1, \ldots, n$ and $j = 0, \ldots, \mu_i - 1$ to obtain

$$
\begin{aligned}
\frac{\partial}{\partial \xi_k} \|\check{r}_{X^{\boldsymbol{\mu}}_n}\|^2_{\mathcal{H}_K} &= \frac{\partial}{\partial \xi_k} \langle \check{r}_{X^{\boldsymbol{\mu}}_n}, \check{r}_{X^{\boldsymbol{\mu}}_n} \rangle_{\mathcal{H}_K} \\
&= 2 \Big\langle \frac{\partial}{\partial \xi_k} \check{r}_{X^{\boldsymbol{\mu}}_n}, \check{r}_{X^{\boldsymbol{\mu}}_n} \Big\rangle_{\mathcal{H}_K} \\
&= -2 \Big\langle \sum_{i=1}^{n} \sum_{j=0}^{\mu_i-1} \frac{\partial}{\partial \xi_k} \{\check{w}_{i,j}(X^{\boldsymbol{\mu}}_n)\} K^{(j,0)}(\xi_i, \cdot) + \sum_{j=0}^{\mu_k-1} \check{w}_{k,j}(X^{\boldsymbol{\mu}}_n) K^{(j+1,0)}(\xi_k, \cdot), \check{r}_{X^{\boldsymbol{\mu}}_n} \Big\rangle_{\mathcal{H}_K} \\
&= -2 \Big(\sum_{i=1}^{n} \sum_{j=0}^{\mu_i-1} \frac{\partial}{\partial \xi_k} \{\check{w}_{i,j}(X^{\boldsymbol{\mu}}_n)\} \langle K^{(j,0)}(\xi_i, \cdot), \check{r}_{X^{\boldsymbol{\mu}}_n} \rangle_{\mathcal{H}_K} \\
&\qquad\qquad + \sum_{j=0}^{\mu_k-1} \check{w}_{k,j}(X^{\boldsymbol{\mu}}_n) \langle K^{(j+1,0)}(\xi_k, \cdot), \check{r}_{X^{\boldsymbol{\mu}}_n} \rangle_{\mathcal{H}_K} \Big) \\
&= -2 \Big(\sum_{i=1}^{n} \sum_{j=0}^{\mu_i-1} \frac{\partial}{\partial \xi_k} \{\check{w}_{i,j}(X^{\boldsymbol{\mu}}_n)\} \check{r}^{(j)}_{X^{\boldsymbol{\mu}}_n}(\xi_i) + \sum_{j=0}^{\mu_k-1} \check{w}_{k,j}(X^{\boldsymbol{\mu}}_n) \check{r}^{(j+1)}_{X^{\boldsymbol{\mu}}_n}(\xi_k) \Big) \\
&= -2 \check{w}_{k,\mu_k-1}(X^{\boldsymbol{\mu}}_n) \, \check{r}^{(\mu_k)}_{X^{\boldsymbol{\mu}}_n}(\xi_k).
\end{aligned}
$$

$\square$

From now on, we will call a set of points $\check{X}^{\boldsymbol{\mu}}_n$ *optimal* of type $\boldsymbol{\mu}$ if

$$
\frac{\partial}{\partial \xi_k} \mathbf{w\check{c}e}^2(\check{X}^{\boldsymbol{\mu}}_n) = -2\check{w}_{k,\mu_k-1}(X^{\boldsymbol{\mu}}_n) \, \check{r}^{(\mu_k)}_{X^{\boldsymbol{\mu}}_n}(\xi_k) = 0 \tag{5.9}
$$

holds true for all $k = 1, \ldots, n$.

Next, we discuss the properties of optimal quadrature weights associated to optimal quadrature points. To this end, we need the following lemma which is standard in analysis text books, see e.g. [2].

Lemma 5.8. *Let $k \in \mathbb{N}$ be even and $f \in C^{k+1}(a, b)$. Assume it holds for some $x \in (a, b)$ that*
1. *$f^{(j)}(x) = 0$ for $j = 0, \ldots, k-1$ and $f^{(k)}(x) > 0$. Then x is a local minimum of f.*
2. *$f^{(j)}(x) = 0$ for $j = 0, \ldots, k$ and $f^{(k+1)}(x) > 0$. Then f is strictly increasing at x.*

Theorem 5.9. *For even $\boldsymbol{\mu} \in \mathbb{N}^n_+$ it holds for the optimal weights $\check{\boldsymbol{w}}(\check{X}^{\boldsymbol{\mu}}_n)$ at optimal points $\check{X}_n$ that*

$$
\check{w}_{k,\mu_k-1}(\check{X}^{\boldsymbol{\mu}}_n) = 0 \quad \text{and} \quad \check{w}_{k,\mu_k-2}(\check{X}^{\boldsymbol{\mu}}_n) > 0 \quad \text{for all } k = 1, \ldots, n.
$$

Proof. According to Proposition 5.6 (iii), it holds $\check{r}^{(\mu_i)}_{X^{\boldsymbol{\mu}}_n}(\xi_k) > 0$ for $k = 1, \ldots, n$. The first-order optimality condition (5.9) requires for optimal $\check{X}^{\boldsymbol{\mu}}$ that

$$
-2\check{w}_{k,\mu_k-1}(\check{X}^{\boldsymbol{\mu}}_n) \, \check{r}^{(\mu_k)}_{\check{X}^{\boldsymbol{\mu}}_n}(\check{\xi}_k) = 0.
$$

This implies $\check{w}_{k,\mu_k-1}(\check{X}^{\boldsymbol{\mu}}_n) = 0$, i.e. the first equality.
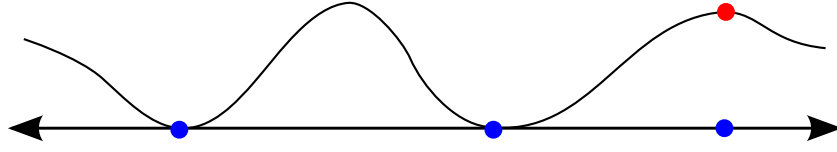
Figure 5.1: The function $f \in V_{N-1}$ for $n = 3$ and $\boldsymbol{\mu} = (2, 2, 2)$ from the proof of Theorem 5.9.

Regarding the second inequality consider the unique function

$$f \in V_{N-1} := \mathrm{span}\,\{K^{(0,j)}(\cdot, \check{\xi}_i) : i = 1, \ldots, n,\ j = 0, \ldots, \mu_i - 1\} \setminus \{K^{(0,\mu_k-1)}(\cdot, \check{\xi}_k)\},$$

that fulfills

$$\begin{aligned}
f^{(j)}(\check{\xi}_i) &= 0 \text{ for } k \neq i = 1, \ldots, n \text{ and } j = 0, \ldots, \mu_i - 1 \\
f^{(j)}(\check{\xi}_k) &= 0 \text{ for } j = 0, \ldots, \mu_k - 3 \quad \text{if } \mu_k \geq 3 \\
f^{(\mu_k-2)}(\check{\xi}_k) &= 1.
\end{aligned} \tag{5.10}$$

We will show that f is non-negative and we consider the more complicated case $\mu_k \geq 3$ first. We note that functions from V_{N-1} can have at most $N - 2$ zeros (counting multiplicities). Therefore, all possible zeros of f are already fixed by (5.10). Moreover, by Lemma 5.8 (i) f has a local minimum at $\check{\xi}_n$. Therefore, $f(x) > 0$ for all $x \in \Omega \setminus \check{X}_n$, which implies $L_\Omega(f) > 0$.

Then we apply $\check{Q}_{\check{X}_n}$, which is exact on $V_{N-1} \subset \mathcal{H}_{K(\check{X}_n^{\boldsymbol{\mu}})}$, to f and use $\check{w}_{k,\mu_k-1}(\check{X}_n^{\boldsymbol{\mu}}) = 0$ to obtain

$$\begin{aligned}
L_\Omega(f) = \check{Q}_{\check{X}_n}(f) &= \sum_{i=1}^{n} \sum_{j=0}^{\mu_i-1} \check{w}_{i,j}(\check{X}_n) f^{(j)}(\check{\xi}_n) \\
&= \check{w}_{k,\mu_k-2}(\check{X}_n^{\boldsymbol{\mu}}) f^{(\mu_n-2)}(\check{\xi}_n) = \check{w}_{k,\mu_k-2}(\check{X}_n^{\boldsymbol{\mu}}).
\end{aligned}$$

The case $\mu_k = 2$ follows similarly with $f(\check{\xi}_k) = 1$, cf. Figure 5.1. Again, $L_\Omega f$ is positive and by the exactness of $\check{Q}_{\check{X}_n}$ on V_{N-1} the weight $\check{w}_{k,0}(\check{X}_n^{\boldsymbol{\mu}})$ is positive. $\qquad\square$

Proposition 5.10. *For even* $\boldsymbol{\mu} \in \mathbb{N}^n$ *the optimality of* $\check{X}_n^{\boldsymbol{\mu}}$ *implies the optimality of* $\check{X}_n^{\boldsymbol{\mu}-1}$.

Proof. By Theorem 5.9 it holds $\check{w}_{i,\mu_i-1}(\check{X}_n^{\boldsymbol{\mu}}) = 0$ for $i = 1, \ldots, n$. This implies

$$\check{r}_{\check{X}_n^{\boldsymbol{\mu}}}(x) = \check{r}_{\check{X}_n^{\boldsymbol{\mu}-1}}(x).$$

Moreover, by Proposition 5.6 (i) it holds $\check{r}^{(\mu_i-1)}_{\check{X}_n^{\boldsymbol{\mu}}}(\check{\xi}_i) = 0$ and therefore also $\check{r}^{(\mu_i-1)}_{\check{X}_n^{\boldsymbol{\mu}-1}}(\check{\xi}_i) = 0$. This implies the optimality of $\check{X}_n^{\boldsymbol{\mu}-1}$.

$\qquad\square$

Next, we deal with the location of optimal quadrature nodes. We show that under certain conditions the optimal points are located in the interior of the domain of integration.
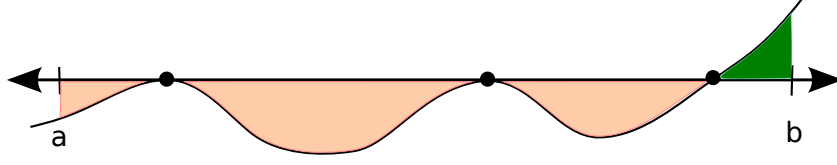
Figure 5.2: Visualization of the cardinal function $H_{n,\mu_n-1}(x)$ from the proof of Proposition 5.11.

Proposition 5.11. *Let K be extended totally positive on $\tilde{\Omega} \supsetneq \Omega =: (a,b)$. Then, for even $\boldsymbol{\mu} \in \mathbb{N}^n$, the nodes of an optimal quadrature formula are all located within (a,b), i.e. there exists $a < \alpha < \beta < b$ such that it holds for all optimal points $\check{\xi}_i^{\boldsymbol{\mu}}, i = 1, \ldots, n$ that*

$$\alpha \le \check{\xi}_1 \le \check{\xi}_2 \le \ldots \le \check{\xi}_n \le \beta.$$

Proof. We will prove that for all n there exists $\beta < b$, such that for $\xi_n \ge \beta$ it holds

$$\frac{\partial}{\partial \xi_n} \mathbf{w\check{c}e}^2(X_n^{\boldsymbol{\mu}}) > 0.$$

This implies that if the largest node gets to close to the right border b, then $\mathbf{w\check{c}e}^2(X_n^{\boldsymbol{\mu}})$ is strictly increasing. The same argument yields $\frac{\partial}{\partial \xi_1} \mathbf{w\check{c}e}^2(X_n^{\boldsymbol{\mu}}) < 0$.

By (5.8) we have to show that $\check{w}_{n,\mu_n-1}(X_n^{\boldsymbol{\mu}}) < 0$ for $\xi_n \in (\beta, b)$. To this end, we use that the weights can be written as

$$\check{w}_{i,j}(X_n^{\boldsymbol{\mu}}) = L_\Omega(H_{i,j}) = \int_a^b H_{i,j}(x)\,\omega(x)\,\mathrm{d}x \quad \text{for all } i = 1, \ldots, n \text{ and } j = 0, \ldots, \mu_i - 1, \quad (5.11)$$

where $H_{i,j}$ denotes the elements of the cardinal basis of $\mathcal{H}_{K(X_n^{\boldsymbol{\mu}})}$, cf. (3.17) in Section 3.3. Because of the cardinal property it holds $H_{n,\mu_n-1}^{(j)}(\xi_k) = \delta_{n,k}\delta_{j,\mu_n-1}$. Besides those prescribed $\sum_{i=1}^{n-1} \mu_i + \mu_n - 1$ zeros, H_{n,μ_n-1} cannot have additional zeros. Moreover, because μ_n is even, so is $\mu_n - 2$. Therefore, $H_{n,\mu_n-1}^{(j)}(\xi_n) = 0, j = 0, \ldots, \mu_n - 2$ and $H_{n,\mu_n-1}^{(\mu_n-1)}(\xi_n) = 1$ imply by Lemma 5.8 (ii) that H_{n,μ_n-1} is strictly increasing at ξ_n. Since all other zeros have even multiplicities, we conclude that H_{n,μ_n-1} has only this one sign-change from negative to positive at ξ_n, i.e.

$$H_{n,\mu_n-1}(x) \begin{cases} < 0 & \text{for } x < \xi_n \\ > 0 & \text{for } x > \xi_n. \end{cases}$$

Therefore, (5.11) can be decomposed into

$$\check{w}_{n,\mu_n-1}(X_n^{\boldsymbol{\mu}}) = \int_a^{\xi_n} H_{n,\mu_n-1}(x)\,\omega(x)\,\mathrm{d}x \quad + \quad \int_{\xi_n}^b H_{n,\mu_n-1}(x)\,\omega(x)\,\mathrm{d}x,$$

where the first summand is strictly negative and the second one strictly positive if $a < \xi_n < b$, cf. Figure 5.2. We conclude that for $\xi_n = b$ it holds $\check{w}_{n,\mu_n-1}(X_n^{\boldsymbol{\mu}}) < 0$, which by continuity also holds for $\xi_n = \beta < b$ sufficiently close. $\qquad\square$

Now we are prepared to deal with the existence of optimal quadrature formulas. To this end, we recall Proposition 5.5 and note that the function $\mathbf{w\check{c}e}^2 : \mathbb{S}^n(\Omega) \to \mathbb{R}$ attains its minimum $X_n^{\boldsymbol{\mu}}$ within $\mathbb{S}^n(\Omega)$. It remains to show that this minimum consists of n different points.

This result has been established in many contexts before, e.g. [11, 20, 55, 95, 124], mostly using abstract results on monosplines of least deviation or specific properties of certain kernels. In the following, we sketch an elementary proof from [21].

Theorem 5.12. *Let* $n \in \mathbb{N}$, $\boldsymbol{\mu} \in \mathbb{N}^n$, $N = \sum_{i=1}^n \mu_i$, $\Omega \subset \tilde{\Omega} \subset \mathbb{R}$ *and* $K \in C^\infty(\tilde{\Omega} \times \tilde{\Omega})$ *be e.t.p. Assume that*

$$X_m^{\boldsymbol{\nu}} := \operatorname*{arg\,min}_{X_n^{\boldsymbol{\mu}} \in \mathbb{S}^n(\Omega)} \left\| \ell_\Omega(\cdot) - \sum_{i=1}^n \sum_{j=0}^{\mu_i-1} \check{w}_{i,j}(X_n^{\boldsymbol{\mu}}) K^{(0,j)}(\cdot, \xi_i) \right\|_{\mathcal{H}_K}. \tag{5.12}$$

Then it holds $m = n$ *and* $\boldsymbol{\mu} = \boldsymbol{\nu}$, *i.e. the* n *points minimizing the right-hand-side of* (5.12) *are pairwise distinct.*

Proof. Before we proceed, we define the $C^\infty(\Omega)$ function

$$F_{X_n^{\boldsymbol{\mu}}}(x) = \frac{\check{r}_{X_n^{\boldsymbol{\mu}}}(x)}{\|\check{r}_{X_n^{\boldsymbol{\mu}}}\|_{\mathcal{H}_K}},$$

which belongs to the unit ball of $\mathcal{H}_K$. Then it holds

$$\int_a^b F_{X_n^{\boldsymbol{\mu}}}(x)\,\omega(x)\,\mathrm{d}x = \|\check{r}_{X_n^{\boldsymbol{\mu}}}\|_{\mathcal{H}_K} = \mathbf{w\check{c}e}(X_n^{\boldsymbol{\mu}})$$

and $F_{X_n^{\boldsymbol{\mu}}}^{(j)}(\xi_k) = 0$ for $k = 1, \dots, n$ and $j = 0, \dots, \mu_i - 1$.

For now, let $\boldsymbol{\mu}$ be even. We have to show that for

$$X_m^{\boldsymbol{\nu}} := \operatorname*{arg\,min}_{\xi_1, \dots, \xi_n} \mathbf{w\check{c}e}(X_n^{\boldsymbol{\mu}}),$$

it holds $m = n$ and hence $\boldsymbol{\nu} = \boldsymbol{\mu}$. Assume to the contrary that $m < n$ and hence at least one $\nu_k > \mu_k$. We will produce a contradiction by showing that there exists

$$\tilde{X}(h) := \begin{pmatrix} \xi_1 & \cdots & \xi_{k-1} & \tau - h & \tau + h & \xi_{k+1} & \cdots & \xi_m \\ \nu_1 & \cdots & \nu_{k-1} & \mu_k & \nu_k - \mu_k & \nu_{k+1} & \cdots & \nu_m \end{pmatrix}$$

such that $\mathbf{w\check{c}e}(\tilde{X}(h)) < \mathbf{w\check{c}e}(X_m^{\boldsymbol{\nu}})$ for sufficiently small $h > 0$. The parameter $\tau \in [\xi_k - h, \xi_k + h]$ is chosen such that it holds $F_{\tilde{X}(h)}^{(\nu_k - 1)}(\xi_k) = 0$. Then it holds by the argumentation in [21] that

$$F_{\tilde{X}(h)}^{(\nu_k - 2)}(\xi_k) < 0 \quad \text{and} \quad |F_{\tilde{X}(h)}^{(\nu_k - 2)}(\xi_k)| > A_2 h^2, \text{ with } A_2 > 0.$$

Moreover, there exists $A_1 > 0$ such that

$$|F_{\tilde{X}(h)}^{(l)}(\xi_k)| \leq A_1 h^{\nu_k - l} \quad \text{for } l = 0, \dots, \nu_k - 1.$$

Next, we will use $\check{Q}_{X_m^\nu}$ to integrate $F_{\tilde{X}(h)}$. But first we note that

$$\check{R}_{X_m^\nu}(F_{\tilde{X}(h)}) \leq \sup_{\|f\|_{\mathcal{H}_K \leq 1}} |\check{R}_{X_m^\nu}(f)| = \check{R}_{X_m^\nu}(F_{X_m^\nu}) = \|\check{R}_{X_m^\nu}\|_{\mathcal{H}_K^\star}.$$

Now we can compute

$$\begin{aligned}
\|\check{R}_{X_m^\nu}\|_{\mathcal{H}_K^\star} &\geq \check{R}_{X_m^\nu}(F_{\tilde{X}(h)}) = L_\Omega\left(F_{\tilde{X}(h)}\right) - \check{Q}_{X_m^\nu}\left(F_{\tilde{X}(h)}\right) \\
&= \|\check{R}_{\tilde{X}(h)}\|_{\mathcal{H}_K^\star} - \check{Q}_{X_m^\nu}\left(F_{\tilde{X}(h)}\right) = \|\check{R}_{\tilde{X}(h)}\|_{\mathcal{H}_K^\star} - \sum_{i=1}^m \sum_{j=1}^{\nu_i-1} \check{w}_{i,j}(X_m^\nu) F_{\tilde{X}(h)}^{(j)}(\xi_k) \\
&= \|\check{R}_{\tilde{X}(h)}\|_{\mathcal{H}_K^\star} - \sum_{j=1}^{\nu_k-2} \check{w}_{k,j}(X_m^\nu) F_{\tilde{X}(h)}^{(j)}(\xi_k) \\
&\geq \|\check{R}_{\tilde{X}(h)}\|_{\mathcal{H}_K^\star} - \left(-\check{w}_{k,\mu_k-2}(X_m^\nu) A_2 h^2\right) - \sum_{j=1}^{\nu_k-3} \check{w}_{k,j}(X_m^\nu) F_{\tilde{X}(h)}^{(j)}(\xi_k) \\
&\geq \|\check{R}_{\tilde{X}(h)}\|_{\mathcal{H}_K^\star} + \check{w}_{k,\nu_k-2}(X_m^\nu) A_2 h^2 - \sum_{j=1}^{\nu_k-3} \left|\check{w}_{k,j}(X_m^\nu) F_{\tilde{X}(h)}^{(j)}(\xi_k)\right| \\
&\geq \|\check{R}_{\tilde{X}(h)}\|_{\mathcal{H}_K^\star} + \check{w}_{k,\nu_k-2}(X_m^\nu) A_2 h^2 - \sum_{j=1}^{\nu_k-3} \left|\check{w}_{k,j}(X_m^\nu)\right| A_1 h^{\nu_k-j} \\
&\geq \|\check{R}_{\tilde{X}(h)}\|_{\mathcal{H}_K^\star} + \check{w}_{k,\nu_k-2} h^2 - \mathcal{O}(h^3).
\end{aligned}$$

For sufficiently small h we obtain $\|\check{R}_{\tilde{X}(h)}\|_{\mathcal{H}_K^\star} < \|\check{R}_{X_m^\nu}\|_{\mathcal{H}_K^\star}$, which contradicts the optimality of X_m^ν. We can conclude that it holds $m = n$ and $\nu = \mu$. The case of non-even μ follows by Proposition 5.10. $\qquad\square$

We sum up the most important properties of optimal quadrature points, now specializing on the practically most relevant case $\mu = 1$.

Corollary 5.13. *Let $\check{X}_n = (\check{\xi}_1, \ldots, \check{\xi}_n)$ be optimal in $\mathcal{H}_K$, i.e. local minimizers of the squared worst-case error $\check{\mathbf{wce}}^2$. Let K be e.t.p. on $\tilde{\Omega} \supset \Omega = (a,b)$. Then it holds*

(i) *Optimal points are pairwise distinct and located within the domain of integration, i.e.*

$$a < \check{\xi}_1 < \check{\xi}_2 < \ldots < \check{\xi}_n < b.$$

(ii) *The optimal weights $\check{\mathbf{w}}(\check{X}_n)$ that are associated to an optimal point set $\check{X}_n$ are all positive, i.e. $\check{w}_i(\check{X}_n) > 0$.*

(iii) *Optimal n points quadrature rules $\check{Q}_{\check{X}_n}$ are exact on the $2n$-dimensional space spanned by*

$$\{K^{(0,j)}(\cdot, \xi_i) : i = 1, \ldots, n \text{ and } j \in \{0,1\}\}.$$

Therefore, they are a generalized Gaussian quadrature rule for a kernel dependent ETC.

(iv) *The Riesz-representer of the error functional of $\check{Q}_{\check{X}_n}$ is non-negative, i.e.*

$$\check{r}_{\check{X}_n}(t) \geq 0 \quad \text{for all } t \in \Omega.$$

   and equality only holds for $t \in \{\check{\xi}_1, \ldots, \check{\xi}_n\}$.

(v) *It holds that*

$$\mathbf{w\check{c}e}^2(\check{X}_n) = \|\check{r}_{\check{X}_n}\|_{\mathcal{H}_K}^2 = \int_{\Omega} \check{r}_{\check{X}_n}(t)\,\omega(t)\,\mathrm{d}t = \int_{\Omega} |\check{r}_{\check{X}_n}(t)|\,\omega(t)\,\mathrm{d}t = \|\check{r}_{\check{X}_n}\|_{L_1(\Omega,\omega)},$$

   i.e. the monospline of least deviation with respect to the $\mathcal{H}_K$-norm is the same as the one with smallest $L_1(\Omega, \omega)$-norm.

(vi) *The optimality of $\check{X}_n$ is implied by $\check{w}_{i,1}(\check{X}_n^2) = 0, i = 1, \ldots, n.$*

5.2 Efficient computation of optimal quadrature points

In this section we discuss the computational aspects of optimal quadrature rules in RKHS. To this end, we will reformulate the minimization problem as a nonlinear system of equations that is much more stable and allows for the first time to compute optimal quadrature points with a sufficient amount of points in RKHS of smooth functions. Moreover, we will make use of certain symmetry properties of the reproducing kernel that allow to reduce the number of points that have to be considered by a factor of about one half. We will concentrate on the simple node case, i.e. the setting $X_n = X_n^\mathbf{1}$.

5.2.1 Direct minimization

The most straight-forward approach to the computation of optimal quadrature points $\check{X}_n$ is of course the direct minimization of the squared worst-case error formula for optimal weights

$$\begin{aligned}
\check{X}_n &:= \operatorname*{arg\,min}_{X_n \in \mathbb{S}^n(\Omega)} \mathbf{w\check{c}e}^2(X_n) = \operatorname*{arg\,min}_{X_n \in \mathbb{S}^n(\Omega)} \|\check{R}_{X_n}\|_{\mathcal{H}_K^\star}^2 \\
&= \operatorname*{arg\,min}_{X_n \in \mathbb{S}^n(\Omega)} \{\|L_\Omega\|_{\mathcal{H}_K^\star}^2 - \boldsymbol{b}^\mathsf{T}(X_n) \cdot \boldsymbol{G}^{-1}(X_n) \cdot \boldsymbol{b}(X_n)\}.
\end{aligned} \tag{5.13}$$

This is a nonlinear problem because both, $\boldsymbol{b}(X_n)$ and $\boldsymbol{G}(X_n)$ depend in a nonlinear way on the points $X_n = (\xi_1, \ldots, \xi_n)$.

From Proposition 5.7 we recall the partial derivatives of $\mathbf{w\check{c}e}^2$ with respect to the points, i.e.

$$\frac{\partial}{\partial \xi_k} \mathbf{w\check{c}e}^2(X_n) = -2\check{w}_k(X_n)\, \check{r}'_{X_n^\mu}(\xi_k).$$

Hence, we can utilize classic optimization approaches, like e.g. nonlinear conjugate gradient or (quasi-)Newton methods [114].

In each step of an iterative optimization procedure it is necessary for the evaluation of both, the objective function $\mathbf{w\check{c}e}^2$ and its derivative, to compute the optimal weights $\check{\boldsymbol{w}}(X_n) \in \mathbb{R}^n$.

We recall that

$$\check{w}(X_n) = \boldsymbol{G}^{-1}(X_n)\boldsymbol{b}(X_n), \tag{5.14}$$

where

$$\boldsymbol{G}(X_n) = (K(\xi_i, \xi_j))_{i,j=1}^n \in \mathbb{R}^{n \times n} \quad \text{and} \quad \boldsymbol{b}(X_n) = (\ell_\Omega(\xi_i))_{i=1}^n \in \mathbb{R}^n.$$

Since $\boldsymbol{G}(X_n)$ is a dense positive definite matrix, the Cholesky decomposition is the canonical method to compute (5.14), which comes at costs of approximately $\frac{n^3}{3}$ floating point operations [48]. Therefore, it is the main bottle-neck in the minimization of (5.13).

This naive approach seems to work fine for Sobolev spaces with finite smoothness, e.g. $H^s([0,1])$ or $H^s(\mathbb{T})$, cf. the left-hand side plot in Figure 5.3. Here, the Fletcher-Reeves nonlinear conjugate gradient method [114] as well as Newton's method for optimization are used to compute $n = 10$ optimal quadrature points. Clearly, Newton's method outperforms the CG-approach, yet both methods converge reasonably well.

However, the situation changes dramatically when considering analytic function spaces in the right-hand side plot of Figure 5.3. Again, $n = 10$ points for optimal quadrature in the Gaussian space shall be computed. Now, it takes much longer for the Newton minimization to converge and the CG method does not seem to work at all. We conclude that in smooth function spaces already for moderate point numbers n the optimization problem becomes very ill-conditioned. Therefore, we will aim for a different approach.

5.2.2 Reformulation as stable nonlinear system

We will make use of Proposition 5.10 and instead of solving (5.13) consider the equivalent problem of computing optimal points of order $\boldsymbol{\mu} = \boldsymbol{2}$, i.e.

$$\check{X}_n := \underset{X_n \in \mathbb{S}^n(\Omega)}{\arg\min} \; \mathbf{w\check{c}e}^2(X_n^{\boldsymbol{2}}) = \underset{X_n \in \mathbb{S}^n(\Omega)}{\arg\min} \; \|\check{R}_{X_n^{\boldsymbol{2}}}\|_{\mathcal{H}_K^\star}^2$$

$$= \underset{X_n \in \mathbb{S}^n(\Omega)}{\arg\min} \; \{\|L_\Omega\|_{\mathcal{H}_K^\star}^2 - \boldsymbol{b}^\intercal(X_n^{\boldsymbol{2}}) \cdot \boldsymbol{G}^{-1}(X_n^{\boldsymbol{2}}) \cdot \boldsymbol{b}(X_n^{\boldsymbol{2}})\}.$$

We use that every point set $\check{X}_n$ that is optimal for $\boldsymbol{\mu} = \boldsymbol{2}$ is also optimal for $\boldsymbol{\mu} = \boldsymbol{1}$.

Now, the vector of optimal weights is given by

$$\check{w}(X_n^{\boldsymbol{2}}) = \boldsymbol{G}^{-1}(X_n^{\boldsymbol{2}})\boldsymbol{b}(X_n^{\boldsymbol{2}}),$$

where

$$\boldsymbol{G}(X_n^{\boldsymbol{2}}) = \begin{pmatrix} (K(\xi_i, \xi_j))_{i,j=1}^n & \left(K^{(0,1)}(\xi_i, \xi_j)\right)_{i,j=1}^n \\ \left(K^{(1,0)}(\xi_i, \xi_j)\right)_{i,j=1}^n & \left(K^{(1,1)}(\xi_i, \xi_j)\right)_{i,j=1}^n \end{pmatrix} \in \mathbb{R}^{2n \times 2n}$$

and

$$\boldsymbol{b}(X_n^{\boldsymbol{2}}) = \begin{pmatrix} (\ell_\Omega(\xi_i))_{i=1}^n \\ (\ell_\Omega'(\xi_i))_{i=1}^n \end{pmatrix} \in \mathbb{R}^{2n}.$$

On first glance, this does not make much sense because the computation of optimal weights $\check{w}(X_n^{\boldsymbol{2}})$ now requires solving a $2n \times 2n$ system. Using the Cholesky decomposition this involves costs of approximately $\frac{(2n)^3}{3} = \frac{8}{3}n^3$ floating point operations, which is about 8 times more costly than the direct approach.
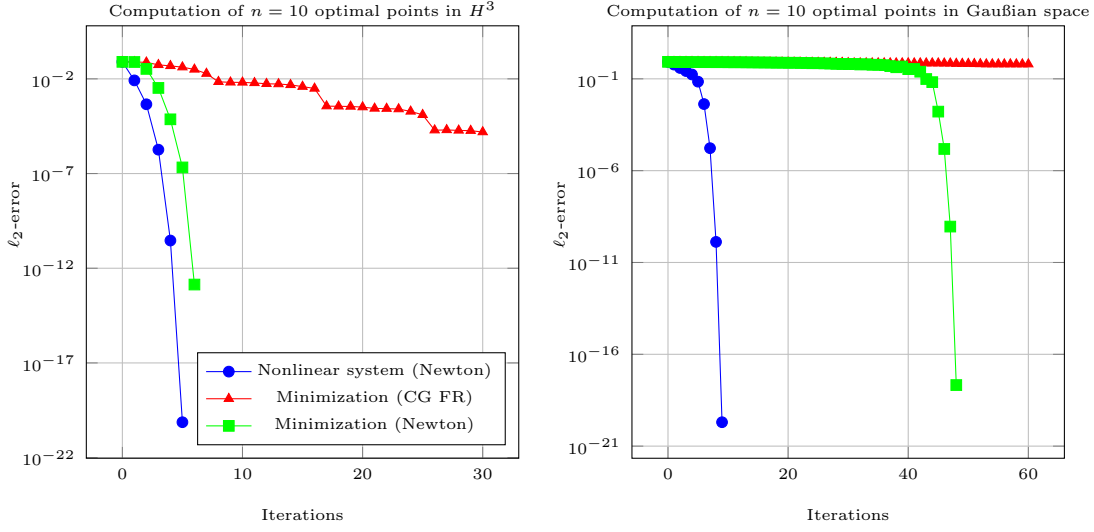
Figure 5.3: Convergence for different approaches to compute $n = 10$ optimal points in the Sobolev space of finite smoothness $H^3([0,1])$ and the analytic Gaußian space with shape parameter $\gamma = 1$.

However, we can make use of Theorem 5.9, which states that the quadrature points $\check{X}_n$ are optimal if it holds

$$\Psi(\check{X}_n) := \big(\check{w}_{1,1}(\check{X}_n^{\boldsymbol{2}}), \ldots, \check{w}_{n,1}(\check{X}_n^{\boldsymbol{2}})\big) = \boldsymbol{0} \in \mathbb{R}^n. \tag{5.15}$$

This is a nonlinear system of n equations which is much better conditioned than the original minimization problem and can easily be solved by Newton's method. This was already observed in [57, 105] for the Hardy and Bergman spaces, but their approach relied heavily on the special structure of these spaces. We will demonstrate that the aforementioned reformulation is beneficial in a much wider setting, namely for all RKHS of sufficiently smooth functions. To this end, we refer to Figure 5.3 where the superiority of this reformulation as nonlinear system of equations over the naive minimization of the worst-case error from Section 5.2.1 can be observed.

For an efficient implementation of Newton's method a closed formula for the Jacobian of the objective function $\Psi : \Omega^n \to \mathbb{R}^n$ is beneficial. To this end, we need the following lemma regarding the derivative of parameterized linear systems.

Lemma 5.14. *Let a matrix $\boldsymbol{A}(\theta) \in \mathrm{GL}(n) \subset \mathbb{R}^{n \times n}$ and a vector $\boldsymbol{b}(\theta) \in \mathbb{R}^n$ be parameterized with parameter $\theta \in \mathbb{R}$. Then, with $\boldsymbol{x}(\theta) = \boldsymbol{A}^{-1}(\theta)\boldsymbol{b}(\theta)$ it holds*

$$\frac{\mathrm{d}}{\mathrm{d}\theta}\boldsymbol{x}(\theta) = \boldsymbol{A}^{-1}(\theta)\left(\frac{\mathrm{d}}{\mathrm{d}\theta}\boldsymbol{b}(\theta) - \frac{\mathrm{d}}{\mathrm{d}\theta}\boldsymbol{A}(\theta)\boldsymbol{x}(\theta)\right).$$

Proof. We use the product rule and the identity

$$\frac{\mathrm{d}}{\mathrm{d}\theta}\boldsymbol{A}^{-1}(\theta) = -\boldsymbol{A}^{-1}(\theta)\frac{\mathrm{d}}{\mathrm{d}\theta}\left\{\boldsymbol{A}(\theta)\right\}\boldsymbol{A}^{-1}(\theta)$$

to obtain

$$
\begin{aligned}
\frac{\mathrm{d}}{\mathrm{d}\theta}\boldsymbol{x}(\theta) &= \frac{\mathrm{d}}{\mathrm{d}\theta}\left\{\boldsymbol{A}^{-1}(\theta)\boldsymbol{b}(\theta)\right\} \\
&= \frac{\mathrm{d}}{\mathrm{d}\theta}\left\{\boldsymbol{A}^{-1}(\theta)\right\}\boldsymbol{b}(\theta) + \boldsymbol{A}^{-1}(\theta)\frac{\mathrm{d}}{\mathrm{d}\theta}\left\{\boldsymbol{b}(\theta)\right\} \\
&= -\boldsymbol{A}^{-1}(\theta)\frac{\mathrm{d}}{\mathrm{d}\theta}\left\{\boldsymbol{A}(\theta)\right\}\boldsymbol{A}^{-1}(\theta)\boldsymbol{b}(\theta) + \boldsymbol{A}^{-1}(\theta)\frac{\mathrm{d}}{\mathrm{d}\theta}\left\{\boldsymbol{b}(\theta)\right\} \\
&= \boldsymbol{A}^{-1}(\theta)\left(\frac{\mathrm{d}}{\mathrm{d}\theta}\left\{\boldsymbol{b}(\theta)\right\} - \frac{\mathrm{d}}{\mathrm{d}\theta}\left\{\boldsymbol{A}(\theta)\right\}\boldsymbol{A}^{-1}(\theta)\boldsymbol{b}(\theta)\right) \\
&= \boldsymbol{A}^{-1}(\theta)\left(\frac{\mathrm{d}}{\mathrm{d}\theta}\left\{\boldsymbol{b}(\theta)\right\} - \frac{\mathrm{d}}{\mathrm{d}\theta}\left\{\boldsymbol{A}(\theta)\right\}\boldsymbol{x}(\theta)\right).
\end{aligned}
$$

$\square$

In order to compute the derivative of kernel matrices with respect to a point $\xi_k \in X_n$, the following remark is useful to simplify the notation.

Remark 5.15. Let $H \in C^1(\Omega \times \Omega)$. Then

$$
\frac{\partial}{\partial x_k}H(x_i, x_j) = \begin{cases}
H^{(1,0)}(x_k, x_k) + H^{(0,1)}(x_k, x_k) & \text{for } i = k, j = k \\
H^{(1,0)}(x_k, x_j) & \text{for } i = k, j \neq k \\
H^{(0,1)}(x_i, x_k) & \text{for } i \neq k, j = k \\
0 & \text{for } i \neq k, j \neq k
\end{cases}.
$$

Thus, the matrices from $\mathbb{R}^{n \times n}$ can be written as

$$
\left(\frac{\partial}{\partial x_k}H(x_i, x_j)\right)_{i,j=1}^{n} = \left(H^{(0,1)}(x_i, x_k)\right)_{i=1}^{n} \cdot \boldsymbol{e}_k^{\mathsf{T}} + \boldsymbol{e}_k \cdot \left(\left(H^{(1,0)}(x_k, x_j)\right)_{j=1}^{n}\right)^{\mathsf{T}} \in \mathbb{R}^{n \times n},
$$

where $\boldsymbol{e}_k = (\delta_{i,k})_{i=1}^{n}$ denotes the k-th unit column vector.

Now we are prepared to compute the Jacobian of Ψ. To simplify the notation we define the following $n \times n$ matrices:

$$
\begin{aligned}
\boldsymbol{G}^{(0,1)} &:= K^{(0,1)}(\xi_i, \xi_k)_{i,k=1}^{n}, \quad \boldsymbol{G}^{(0,2)} := K^{(0,2)}(\xi_i, \xi_k)_{i,k=1}^{n} \\
\boldsymbol{G}^{(1,1)} &:= K^{(1,1)}(\xi_i, \xi_k)_{i,k=1}^{n}, \quad \boldsymbol{G}^{(1,2)} := K^{(1,2)}(\xi_i, \xi_k)_{i,k=1}^{n} \\
\boldsymbol{W}_0 &:= \mathrm{diag}(\check{\boldsymbol{w}}_0(X_n^{\mathbf{2}})), \qquad \boldsymbol{W}_1 := \mathrm{diag}(\check{\boldsymbol{w}}_1(X_n^{\mathbf{2}})),
\end{aligned}
$$

where

$$
\begin{aligned}
\check{\boldsymbol{w}}_0(X_n^{\mathbf{2}}) &= (\check{w}_{1,0}(X_n^{\mathbf{2}}), \ldots, \check{w}_{n,0}(X_n^{\mathbf{2}})), \\
\check{\boldsymbol{w}}_1(X_n^{\mathbf{2}}) &= (\check{w}_{1,1}(X_n^{\mathbf{2}}), \ldots, \check{w}_{n,1}(X_n^{\mathbf{2}}))
\end{aligned}
$$

are a partition of the vector of optimal weights $\check{\boldsymbol{w}}(X_n^{\mathbf{2}})) = \boldsymbol{G}^{-1}(X_n^{\mathbf{2}})\,\boldsymbol{b}(X_n^{\mathbf{2}})$.

Moreover, define

$$
\boldsymbol{H}'' := \mathrm{diag}(\check{r}''_{X_n^{\mathbf{2}}}(\xi_1), \ldots, \check{r}''_{X_n^{\mathbf{2}}}(\xi_k)) \in \mathbb{R}^{n \times n}
$$

to be the matrix with the second derivative of $\check{r}_{X_n^{\mathbf{2}}}$ evaluated at the points in X_n on the diagonal.

Theorem 5.16. *The Jacobian* $J_\Psi(\boldsymbol{x}) \in \mathbb{R}^{n \times n}$ *of* Ψ *is given by*

$$J_\Psi(X_n) = \underbrace{(\boldsymbol{0} \quad \boldsymbol{I}_n)}_{\in \mathbb{R}^{n \times 2n}} \boldsymbol{G}^{-1}(X_n^{\boldsymbol{2}}) \left(\begin{pmatrix} \boldsymbol{0} \\ \boldsymbol{H}'' \end{pmatrix} - \begin{pmatrix} \boldsymbol{G}^{(0,1)}\boldsymbol{W}_0 + \boldsymbol{G}^{(0,2)}\boldsymbol{W}_1 \\ \boldsymbol{G}^{(1,1)}\boldsymbol{W}_0 + \boldsymbol{G}^{(1,2)}\boldsymbol{W}_1 \end{pmatrix} \right) \tag{5.16}$$

Proof. First we define a block-partitioning of $\boldsymbol{G}(X_n^{\boldsymbol{2}})$, i.e.

$$\boldsymbol{G}(X_n^{\boldsymbol{2}}) = \begin{pmatrix} \boldsymbol{A}(X_n) & \boldsymbol{B}(X_n) \\ \boldsymbol{B}^T(X_n) & \boldsymbol{D}(X_n) \end{pmatrix} \in \mathbb{R}^{2n \times 2n},$$

where

$$\boldsymbol{A}(X_n) = (K(\xi_i, \xi_j))_{i,j=1}^n, \qquad \boldsymbol{B}(X_n) = \left(K^{(0,1)}(\xi_i, \xi_j) \right)_{i,j=1}^n$$

$$\boldsymbol{B}^\intercal(X_n) = \left(K^{(1,0)}(\xi_i, \xi_j) \right)_{i,j=1}^n, \qquad \boldsymbol{D}(X_n) = \left(K^{(1,1)}(\xi_i, \xi_j) \right)_{i,j=1}^n.$$

Having in mind Remark 5.15, we obtain

$$\frac{\partial}{\partial \xi_k} \boldsymbol{A}(X_n) = \left(K^{(0,1)}(\xi_i, \xi_k) \right)_{i=1}^n \cdot \boldsymbol{e}_k^\intercal + \boldsymbol{e}_k \cdot \left(\left(K^{(1,0)}(\xi_k, \xi_j) \right)_{j=1}^n \right)^\intercal$$

$$\frac{\partial}{\partial \xi_k} \boldsymbol{B}(X_n) = \left(K^{(0,2)}(\xi_i, \xi_k) \right)_{i=1}^n \cdot \boldsymbol{e}_k^\intercal + \boldsymbol{e}_k \cdot \left(\left(K^{(1,1)}(\xi_k, \xi_j) \right)_{j=1}^n \right)^\intercal$$

$$\frac{\partial}{\partial \xi_k} \boldsymbol{B}^\intercal(X_n) = \left(K^{(1,1)}(\xi_i, \xi_k) \right)_{i=1}^n \cdot \boldsymbol{e}_k^\intercal + \boldsymbol{e}_k \cdot \left(\left(K^{(2,0)}(\xi_k, \xi_j) \right)_{j=1}^n \right)^\intercal$$

$$\frac{\partial}{\partial \xi_k} \boldsymbol{D}(X_n) = \left(K^{(1,2)}(\xi_i, \xi_k) \right)_{i=1}^n \cdot \boldsymbol{e}_k^\intercal + \boldsymbol{e}_k \cdot \left(\left(K^{(2,1)}(\xi_k, \xi_j) \right)_{j=1}^n \right)^\intercal$$

Moreover, it holds for $\boldsymbol{b}(X_n^{\boldsymbol{2}}) = (\ell_\Omega(\xi_1), \ldots, \ell_\Omega(\xi_n), \ell'_\Omega(\xi_1), \ldots, \ell'_\Omega(\xi_n))$ that

$$\frac{\partial}{\partial \xi_k} \boldsymbol{b}(X_n^{\boldsymbol{2}}) = \begin{pmatrix} \boldsymbol{e}_k \ell'_\Omega(\xi_k) \\ \boldsymbol{e}_k \ell''_\Omega(\xi_k) \end{pmatrix} \in \mathbb{R}^{2n}. \tag{5.17}$$

Now we compute

$$\frac{\partial}{\partial \xi_k} \{\boldsymbol{G}(X_n^{\boldsymbol{2}})\} \check{\boldsymbol{w}}(X_n^{\boldsymbol{2}}) = \begin{pmatrix} \frac{\partial}{\partial \xi_k} \boldsymbol{A}(X_n) & \frac{\partial}{\partial \xi_k} \boldsymbol{B}(X_n) \\ \frac{\partial}{\partial \xi_k} \boldsymbol{B}^\intercal(X_n) & \frac{\partial}{\partial \xi_k} \boldsymbol{D}(X_n) \end{pmatrix} \begin{pmatrix} \check{\boldsymbol{w}}_0(X_n^{\boldsymbol{2}}) \\ \check{\boldsymbol{w}}_1(X_n^{\boldsymbol{2}}) \end{pmatrix}$$

$$= \begin{pmatrix} \left(K^{(0,1)}(\xi_i, \xi_k) \right)_{i=1}^n \cdot \boldsymbol{e}_k^\intercal & \left(K^{(0,2)}(\xi_i, \xi_k) \right)_{i=1}^n \cdot \boldsymbol{e}_k^\intercal \\ \left(K^{(1,1)}(\xi_i, \xi_k) \right)_{i=1}^n \cdot \boldsymbol{e}_k^\intercal & \left(K^{(1,2)}(\xi_i, \xi_k) \right)_{i=1}^n \cdot \boldsymbol{e}_k^\intercal \end{pmatrix} \begin{pmatrix} \check{\boldsymbol{w}}_0(X_n^{\boldsymbol{2}}) \\ \check{\boldsymbol{w}}_1(X_n^{\boldsymbol{2}}) \end{pmatrix}$$

$$+ \begin{pmatrix} \boldsymbol{e}_k \cdot \left(\left(K^{(1,0)}(\xi_k, \xi_j) \right)_{j=1}^n \right)^\intercal & \boldsymbol{e}_k \cdot \left(\left(K^{(1,1)}(\xi_k, \xi_j) \right)_{j=1}^n \right)^\intercal \\ \boldsymbol{e}_k \cdot \left(\left(K^{(2,0)}(\xi_k, \xi_j) \right)_{j=1}^n \right)^\intercal & \boldsymbol{e}_k \cdot \left(\left(K^{(2,1)}(\xi_k, \xi_j) \right)_{j=1}^n \right)^\intercal \end{pmatrix} \begin{pmatrix} \check{\boldsymbol{w}}_0(X_n^{\boldsymbol{2}}) \\ \check{\boldsymbol{w}}_1(X_n^{\boldsymbol{2}}) \end{pmatrix}$$

$$= \begin{pmatrix} \widecheck{w}_{k,0}(X_n^{\mathbf{2}}) \left(K^{(0,1)}(\xi_i,\xi_k) \right)_{i=1}^n + \widecheck{w}_{k,1}(X_n^{\mathbf{2}}) \left(K^{(0,2)}(\xi_i,\xi_k) \right)_{i=1}^n \\ \widecheck{w}_{k,0}(X_n^{\mathbf{2}}) \left(K^{(1,1)}(\xi_i,\xi_k) \right)_{i=1}^n + \widecheck{w}_{k,1}(X_n^{\mathbf{2}}) \left(K^{(1,2)}(\xi_i,\xi_k) \right)_{i=1}^n \end{pmatrix}$$
$$+ \begin{pmatrix} \boldsymbol{e}_k \left(\sum_{i=1}^n \sum_{j=0}^1 \widecheck{w}_{i,j}(X_n^{\mathbf{2}}) K^{(1,j)}(\xi_i,\xi_k) \right) \\ \boldsymbol{e}_k \left(\sum_{i=1}^n \sum_{j=0}^1 \widecheck{w}_{i,j}(X_n^{\mathbf{2}}) K^{(2,j)}(\xi_i,\xi_k) \right) \end{pmatrix}.$$

Therefore, having in mind (5.17), it holds that

$$\frac{\partial}{\partial \xi_k} \boldsymbol{b}(X_n^{\mathbf{2}}) - \frac{\partial}{\partial \xi_k} \left\{ \boldsymbol{G}(X_n^{\mathbf{2}}) \right\} \widecheck{\boldsymbol{w}}(X_n^{\mathbf{2}})$$
$$= \begin{pmatrix} \boldsymbol{e}_k r'_{X_n^{\mathbf{2}}}(\xi_k) \\ \boldsymbol{e}_k r''_{X_n^{\mathbf{2}}}(\xi_k) \end{pmatrix} - \begin{pmatrix} \widecheck{w}_{k,0}(X_n^{\mathbf{2}}) \left(K^{(0,1)}(\xi_i,\xi_k) \right)_{i=1}^n + \widecheck{w}_{k,1}(X_n^{\mathbf{2}}) \left(K^{(0,2)}(\xi_i,\xi_k) \right)_{i=1}^n \\ \widecheck{w}_{k,0}(X_n^{\mathbf{2}}) \left(K^{(1,1)}(\xi_i,\xi_k) \right)_{i=1}^n + \widecheck{w}_{k,1}(X_n^{\mathbf{2}}) \left(K^{(1,2)}(\xi_i,\xi_k) \right)_{i=1}^n \end{pmatrix}$$
$$= \begin{pmatrix} \boldsymbol{0} \\ \boldsymbol{e}_k r''_{X_n^{\mathbf{2}}}(\xi_k) \end{pmatrix} - \begin{pmatrix} \widecheck{w}_{k,0}(X_n^{\mathbf{2}}) \left(K^{(0,1)}(\xi_i,\xi_k) \right)_{i=1}^n + \widecheck{w}_{k,1}(X_n^{\mathbf{2}}) \left(K^{(0,2)}(\xi_i,\xi_k) \right)_{i=1}^n \\ \widecheck{w}_{k,0}(X_n^{\mathbf{2}}) \left(K^{(1,1)}(\xi_i,\xi_k) \right)_{i=1}^n + \widecheck{w}_{k,1}(X_n^{\mathbf{2}}) \left(K^{(1,2)}(\xi_i,\xi_k) \right)_{i=1}^n \end{pmatrix}$$
$$=: \boldsymbol{c}(X_n,k).$$

Now, the matrix $\boldsymbol{C}(X_n) = (\boldsymbol{c}(X_n,1),\ldots,\boldsymbol{c}(X_n,n))$ whose columns are given by the vectors $\boldsymbol{c}(X_n,k), k = 1,\ldots,n$, can be written as

$$\boldsymbol{C}(X_n) = \begin{pmatrix} \boldsymbol{0} \\ \boldsymbol{H}'' \end{pmatrix} - \begin{pmatrix} \boldsymbol{G}^{(0,1)}\boldsymbol{W}_0 + \boldsymbol{G}^{(0,2)}\boldsymbol{W}_1 \\ \boldsymbol{G}^{(1,1)}\boldsymbol{W}_0 + \boldsymbol{G}^{(1,2)}\boldsymbol{W}_1 \end{pmatrix}.$$

Finally, because of Lemma 5.14 we obtain

$$\frac{\partial}{\partial \xi_k} \widecheck{\boldsymbol{w}}(X_n^{\mathbf{2}}) = \frac{\partial}{\partial \xi_k} \left\{ \boldsymbol{G}^{-1}(X_n^{\mathbf{2}})\boldsymbol{b}(X_n^{\mathbf{2}}) \right\} = \boldsymbol{G}^{-1}(X_n^{\mathbf{2}})\boldsymbol{c}(X_n,k) =: \boldsymbol{h}(X_n,k) \in \mathbb{R}^{2n}$$

and the derivative with respect to the point ξ_k of Ψ consists of the $(n+1),\ldots,(2n)$ components of $\boldsymbol{h}(X_n,k)$, i.e.

$$\frac{\partial}{\partial \xi_k} \Psi(X_n) = (\boldsymbol{h}_{n+1}(X_n,k),\ldots,\boldsymbol{h}_{2n}(X_n,k)) \in \mathbb{R}^n,$$

which equals (5.16).

$\square$

5.2.3 Obtaining starting points for Newton's method

Newton's method is a well-established approach for the solution of nonlinear systems of equations. If provided with a starting point sufficiently close to the solution, it converges quadratically [48, 121]. However, if the starting point is too far away, it does not necessarily converge at all. Therefore, we propose the following approach to generate good starting points.

Let $\widecheck{X}_n \subset (a,b) = \Omega$ be a set of n ordered optimal points, i.e.

$$a < \widecheck{\xi}_1 < \ldots, < \widecheck{\xi}_n < b.$$

Algorithm 2: Computation of optimal quadrature points in $\mathcal{H}_K$.

Input:

- extended totally positive kernel function $K : \Omega \times \Omega \to \mathbb{R}$.

- Riesz-representer $\ell_\Omega : \Omega \to \mathbb{R}$ of L_Ω.

- derivatives of K and ℓ_Ω up to order 2.

Initialize: $k := 0$, $X_0 = \emptyset$.
repeat

    1. $k := k + 1$

    2. Define starting points $\bar{\xi}_1, \ldots, \bar{\xi}_k$ according to (5.18) or (5.19).

    3. Assemble and initialize the closed-form Jacobian (5.16).

    4. Solve the nonlinear equation (5.15) by Newton's method.

    5. Store the solution X_k as well as the associated optimal weights $\check{\boldsymbol{w}}(X_k)$.

until $k = n$;
Output: Optimal quadrature points X_k and optimal weights $\check{\boldsymbol{w}}(X_k)$ for $k = 1, \ldots, n$.

We construct starting values $\bar{\xi}_1, \ldots, \bar{\xi}_{n+1}$ for the problem of computing a set of $n + 1$ optimal points by

$$
\begin{aligned}
\bar{\xi}_1 &:= \frac{\check{\xi}_1 + a}{2} \\
\bar{\xi}_i &:= \frac{\check{\xi}_{i+1} + \check{\xi}_i}{2} \quad \text{for } i = 2, \ldots, n \\
\bar{\xi}_{n+1} &:= \frac{b + \check{\xi}_n}{2}.
\end{aligned} \tag{5.18}
$$

On unbounded domains like e.g. $\Omega = (-\infty, \infty)$ we proceed similarly, i.e.

$$
\begin{aligned}
\bar{\xi}_1 &:= \check{\xi}_1 - \frac{\check{\xi}_2 - \check{\xi}_1}{2} \\
\bar{\xi}_i &:= \frac{\check{\xi}_{i+1} + \check{\xi}_i}{2} \quad \text{for } i = 2, \ldots, n \\
\bar{\xi}_{n+1} &:= \check{\xi}_n + \frac{\check{\xi}_n - \check{\xi}_{n-1}}{2}.
\end{aligned} \tag{5.19}
$$

Now we are prepared to compute optimal quadrature points and weights in univariate reproducing kernel Hilbert spaces $\mathcal{H}_K$, where K is extended totally positive. The nonlinear system of equations (5.15), i.e. $\Psi(X_n) = \boldsymbol{0}$ can be solved by Newton's method, cf. [48, 114], which is implemented in many numerical analysis libraries. We used the implementation from [126]. If the kernel K has partial derivatives up to order 2, we can use the closed-form solution of the

Jacobian of Ψ given in (5.16). After a set of k optimal quadrature points has been computed, it is utilized to construct the starting points for the search for $n+1$ points. The overall procedure is summarized in Algorithm 2. We remark that for the case of kernels that are less than two times differentiable, one can still use the direct minimization approach, cf. Section 5.2.1.

5.2.4 Exploiting the symmetry of certain RKHS

Let us assume that $\Omega = (-\alpha, \alpha)$ and the reproducing kernel $K : \Omega \times \Omega \to \mathbb{R}$ of $\mathcal{H}_K$ fulfills the condition

$$K(x, -y) = K(-x, y). \tag{5.20}$$

Moreover, we assume that it holds

$$\omega(x) = \omega(-x) \quad \text{for all } x \in \Omega. \tag{5.21}$$

All kernels of the form $K(x, y) = g(xy)$ or $K(x, y) = g(|x - y|)$ are examples that fulfill (5.20). We will see that this kind of symmetry allows to construct optimal point sets with cardinality $2n$ or $2n + 1$ by constructing an optimal set of n points for the modified kernel

$$\tilde{K}(x, y) := K(x, y) + K(x, -y). \tag{5.22}$$

We remark that (5.20) can be generalized to $K(x, a - y) = K(a - x, y)$ for some $a \in \Omega$, but in order to keep the notation simple we will stick to the case $a = 0$.

In the following, we will show that optimal weights and points for the approximation of

$$L_{(-\alpha,\alpha)}(f) = \int_{-\alpha}^{\alpha} f(x)\,\omega(x)\,\mathrm{d}x$$

in the Hilbert space $\mathcal{H}_K$ can be obtained by optimal weights and points for the approximation of

$$L_{(0,\alpha)}(f) = \int_0^{\alpha} f(x)\omega(x)\,\mathrm{d}x$$

in the Hilbert space $\mathcal{H}_{\tilde{K}}$, where $\tilde{K}$ is given by (5.22).

Before we proceed, we need a simple Lemma.

Lemma 5.17. *Let K fulfill* (5.20). *Then it holds*

1. *$\ell_\Omega(x) = \ell_\Omega(-x)$.*
2. *$K^{(1,0)}(x, -y) = -K^{(1,0)}(-x, y)$.*
3. *$\ell'_\Omega(x) = -\ell'_\Omega(x)$.*
4. *$K^{(1,0)}(0, y) + K^{(1,0)}(0, -y) = 0$.*
5. *$K^{(1,0)}(0, 0) = 0$.*

Proof. Claim 1. follows from the symmetry of ω, i.e. (5.21). The claims 2.-5. follow by differentiating both sides of (5.20) with respect to x. $\qquad \square$

Proposition 5.18. *Let* $X_n = (\xi_1, \ldots, \xi_n) \in (0, \alpha)^n$ *and* $\check{w}(X_n, \tilde{K})$ *the associated optimal quadrature weights for the approximation of* $L_{(0,\alpha)}$ *in* $\mathcal{H}_{\tilde{K}}$.
With $X_{2n} := (-\xi_n, \ldots, -\xi_1, \xi_1, \ldots, \xi_n)$ *it holds*

$$\check{w}(X_{2n}, K) = (\check{w}_n(X_n, \tilde{K}), \ldots, \check{w}_1(X_n, \tilde{K}), \check{w}_1(X_n, \tilde{K}), \ldots, \check{w}_n(X_n, \tilde{K})),$$

i.e. the 2n optimal weights for the approximation of $L_{(-\alpha,\alpha)}$ *using the symmetric point set* X_{2n} *in* $\mathcal{H}_K$ *can be obtained by computing n optimal weights for* $L_{(0,\alpha)}$ *in* $\mathcal{H}_{\tilde{K}}$.

Proof. Let $\boldsymbol{v} := (\check{w}_n(X_n, \tilde{K}), \ldots, \check{w}_1(X_n, \tilde{K}), \check{w}_1(X_n, \tilde{K}), \ldots, \check{w}_n(X_n, \tilde{K}))$. We have to show that $\boldsymbol{v} = \check{w}(X_{2n}, K)$. To this end, note that the Riesz-representer of the error functional $R_{X_{2n}, \boldsymbol{v}}(f) = L_{(-\alpha,\alpha)}(f) - Q_{X_{2n}, \boldsymbol{v}}(f)$ is

$$r_{X_{2n}, \boldsymbol{v}}(x) = \ell_{(-\alpha,\alpha)}(x) - \sum_{i=1}^n \check{w}_i(X_n, \tilde{K})(K(x, \xi_i) + K(x, -\xi_i)). \tag{5.23}$$

We will prove the two equalities

$$\begin{aligned}
\check{r}_{X_n}(x) &= r_{X_{2n}, \boldsymbol{v}}(x) \quad \text{for all } x \in (0, \alpha) \\
r_{X_{2n}, \boldsymbol{v}}(x) &= r_{X_{2n}, \boldsymbol{v}}(-x) \quad \text{for all } x \in \Omega = (-\alpha, \alpha).
\end{aligned} \tag{5.24}$$

Because of $\check{r}_{X_n}(\xi_i) = 0$ for $i = 1, \ldots, n$, the identities (5.24) imply that $r_{X_{2n}, \boldsymbol{v}}(\pm \xi_i) = 0$ and hence the optimality of $\boldsymbol{v}$.

Regarding the first equality, we note that it holds for $x \in (0, \alpha)$ that

$$\ell_{(0,\alpha)}(x) = \ell_{(-\alpha,\alpha)}(x)$$

because of

$$\int_0^\alpha \tilde{K}(x, y)\, \omega(y)\, \mathrm{d}y = \int_0^\alpha K(x, y)\, \omega(y)\, \mathrm{d}y + \int_0^\alpha K(x, -y)\, \omega(y)\, \mathrm{d}y = \int_{-\alpha}^\alpha K(x, y)\, \omega(y)\, \mathrm{d}y.$$

Then, having in mind (5.23), we can compute for $x \in (0, \alpha)$

$$\begin{aligned}
\check{r}_{X_n}(x) &= \ell_{(0,\alpha)}(x) - \sum_{i=1}^n \check{w}_i(X_n, \tilde{K}) \tilde{K}(x, \xi_i) \\
&= \ell_{(-\alpha,\alpha)}(x) - \sum_{i=1}^n \check{w}_i(X_n, \tilde{K}) \left(K(x, \xi_i) + K(x, -\xi_i) \right) \\
&= r_{X_{2n}, \boldsymbol{v}}(x).
\end{aligned}$$

Regarding the second equality in (5.24), we use the identities $\ell_{(-\alpha,\alpha)}(-x) = \ell_{(-\alpha,\alpha)}(x)$ and

$K(-x, y) = K(x, -y)$ to compute

$$r_{X_{2n}, \boldsymbol{v}}(-x) = \ell_{(-\alpha, \alpha)}(-x) - \sum_{i=1}^{n} \check{w}_i(X_n, K) \left(K(-x, \xi_i) + K(-x, -\xi_i) \right)$$

$$= \ell_{(-\alpha, \alpha)}(-x) - \sum_{i=1}^{n} \check{w}_i(X_n, K) \left(K(x, -\xi_i) + K(x, \xi_i) \right)$$

$$= r_{X_{2n}, \boldsymbol{v}}(x).$$

$\square$

An immediate consequence is the following theorem, which allows to obtain optimal quadrature rules with $2n$ points at reduced costs.

Theorem 5.19. *Let $\check{X}_n = (\check{\xi}_1, \ldots, \check{\xi}_n) \in (0, \alpha)^n$ be a vector of optimal points for the approximation of $L_{(0, \alpha)}(f)$ in $\mathcal{H}_{\tilde{K}}$. Moreover, let $\check{\boldsymbol{w}}(\check{X}_n, \tilde{K}) = (\check{w}_1(\check{X}_n, \tilde{K}), \ldots, \check{w}_n(\check{X}_n, \tilde{K})) \in \mathbb{R}^n$ be the optimal weights for $\check{X}_n$ in $\mathcal{H}_{\tilde{K}}$. Then it holds that*

(i) The points

$$X_{2n} := (-\check{\xi}_n, \ldots, -\check{\xi}_1, \check{\xi}_1, \ldots, \check{\xi}_n) \in (-\alpha, \alpha)^{2n}$$

are optimal for approximating $L_{(-\alpha, \alpha)}(f)$ in the Hilbert space $\mathcal{H}_K$.

(ii) The associated optimal weights for X_{2n} in $\mathcal{H}_K$ are given by

$$\boldsymbol{w}(X_{2n}, K) = (\check{w}_n(\check{X}_n, \tilde{K}), \ldots, \check{w}_1(\check{X}_n, \tilde{K}), \check{w}_1(\check{X}_n, \tilde{K}), \ldots, \check{w}_n(\check{X}_n, \tilde{K})) \in \mathbb{R}^{2n}.$$

Proof. Since X_{2n} is symmetric, the optimality of the weights (ii) follows by Proposition 5.18. For the optimality of the points we have to show that

$$\check{r}'_{X_{2n}}(\pm\check{\xi}_i) = 0 \quad \text{for } i = 1, \ldots, n.$$

This follows from the symmetry (5.24) in the proof of Proposition 5.18 and the optimality of $\check{\xi}$, i.e.

$$\check{r}'_{X_{2n}}(\check{\xi}_i) = 0 \quad \text{for } i = 1, \ldots, n.$$

$\square$

This allows to compute optimal quadrature formulas with $2n$ points in $\mathcal{H}_K$ by solving the associated problem in $\mathcal{H}_{\tilde{K}}$ for n points. In order to deal with the case of $2n+1$ nodes, we define the kernels

$$K_0(x, y) = K(x, y) - \frac{K(x, 0)K(0, y)}{K(0, 0)}$$

and

$$\tilde{K}_0(x, y) := \tilde{K}(x, y) - \frac{\tilde{K}(x, 0)\tilde{K}(0, y)}{\tilde{K}(0, 0)} = K_0(x, y) + K_0(x, -y).$$

Theorem 5.20. *Let $\check{X}_n = (\check{\xi}_1, \ldots, \check{\xi}_n) \in (0, \alpha)^n$ be a vector of optimal points for the approximation of $L_{(0, \alpha)}(f)$ in the Hilbert space $\mathcal{H}_{\tilde{K}_0}$. Let $\check{\boldsymbol{w}}(\check{X}_n, \tilde{K}) = (\check{w}_1(\check{X}_n, \tilde{K}_0), \ldots, \check{w}_n(\check{X}_n, \tilde{K}_0)) \in \mathbb{R}^n$ denote the associated optimal weights for $\check{X}_n$ in $\mathcal{H}_{\tilde{K}_0}$.*

Then, it holds that

(i) *The points*
$$X_{2n+1} := (-\check{\xi}_n, \ldots, -\check{\xi}_1, 0, \check{\xi}_1, \ldots, \check{\xi}_n) \in (-\alpha, \alpha)^{2n+1}$$
are optimal for approximating $L_{(-\alpha,\alpha)}(f) = \int_{-\alpha}^{\alpha} f(x)\omega(x)\,\mathrm{d}x$ *in the Hilbert space* $\mathcal{H}_K$.

(ii) *With the definition*
$$w_0(\check{X}_n) := \frac{1}{K(0,0)} \left(\ell_\Omega(0) - \sum_{i=1}^{n} \check{w}_i(\check{X}_n, \tilde{K}_0) \left(K(0, \check{\xi}_i) + K(0, -\check{\xi}_i) \right) \right)$$

the weights
$$\boldsymbol{v} := (\check{w}_n(\check{X}_n, \tilde{K}_0), \ldots, \check{w}_1(\check{X}_n, \tilde{K}_0), w_0(\check{X}_n), \check{w}_1(\check{X}_n, \tilde{K}_0), \ldots, \check{w}_n(\check{X}_n, \tilde{K}_0)) \in \mathbb{R}^{2n+1}$$

are optimal for X_{2n+1} *in* $\mathcal{H}_K$, *i.e.* $\check{\boldsymbol{w}}(X_{2n+1}) = \boldsymbol{v}$.

Proof. We first note that the optimality of the points $\check{X}_n$ for $L_{(0,\alpha)}$ in $\mathcal{H}_{\tilde{K}_0}$ implies the optimality of $(-\check{\xi}_n, \ldots, -\check{\xi}_1, \check{\xi}_1, \ldots, \check{\xi}_n)$ for $L_{(-\alpha,\alpha)}$ in $\mathcal{H}_{K_0}$. Therefore, the error representer of the associated optimal quadrature formula in $\mathcal{H}_{K_0}$ is

$$\check{r}_{X_{2n}}(x) = L_{(-\alpha,\alpha)}^{(y)} K_0(x, y) - \sum_{i=1}^{n} \check{w}_i(\check{X}_n) \left(K_0(x, -\check{\xi}_i) + K_0(x, \check{\xi}_i) \right),$$

and fulfills $\check{r}'_{X_{2n}}(\pm\xi_i) = \check{r}'_{X_{2n}}(\pm\xi_i) = 0$. Therefore, in the spirit of the proofs for Proposition 5.18 and Theorem 5.19, it remains to show that

$$r_{X_{2n+1},\boldsymbol{v}}(x) = \check{r}_{X_{2n}}(x) \quad \text{for all } x \in \Omega.$$

To this end, noting that

$$r_{X_{2n+1},\boldsymbol{v}}(x) = \ell_{(-\alpha,\alpha)}(x) - \sum_{i=1}^{n} \check{w}_i(\check{X}_{2n}) \left(K(x, -\check{\xi}_i) + K(x, \check{\xi}_i) \right) - w_0(\check{X}_n)K(x, 0)$$

we can compute

$$\begin{aligned}
\check{r}_{X_{2n}}(x) &= L_{(-\alpha,\alpha)}^{(y)} K_0(x, y) - \sum_{i=1}^{n} \check{w}_i(\check{X}_n) \left(K_0(x, -\check{\xi}_i) + K_0(x, \check{\xi}_i) \right) \\
&= \ell_{(-\alpha,\alpha)}(x) - \frac{K(x,0)\ell_{(-\alpha,\alpha)}(0)}{K(0,0)} \\
&\quad - \sum_{i=1}^{n} \check{w}_i(\check{X}_n) \left(K(x, -\check{\xi}_i) + K(x, \check{\xi}_i) - \frac{K(x,0)}{K(0,0)} (K(0, \check{\xi}_i) + K(0, -\check{\xi}_i)) \right) \\
&= \ell_{(-\alpha,\alpha)}(x) - \sum_{i=1}^{n} \check{w}_i(\check{X}_{2n}) \left(K(x, -\check{\xi}_i) + K(x, \check{\xi}_i) \right) - w_0(\check{X}_n)K(x, 0).
\end{aligned}$$

It remains to show that $\check{r}_{X_{2n+1}}(0) = \check{r}'_{X_{2n+1}}(0) = 0$, which follows by inserting $x = 0$ and using Lemma 5.17. $\qquad\square$

5.3 Greedy construction of nested point sets using matching pursuit

In the preceding section we dealt with the problem of computing optimal quadrature points without any additional constraints, i.e. all the n points and n weights were considered as degrees of freedom and could be varied to minimize the worst-case error. The resulting optimal quadrature points are pairwise distinct and strictly contained in the interval of integration $\Omega = (a, b)$, i.e. $a < \check{\xi}_1 < \check{\xi}_2 < \ldots < \check{\xi}_n < b$. However, numerical experiments suggest that the optimal point sets $\check{X}_n$ are not contained in $\check{X}_m$ for $m > n$, except for the midpoint of the interval if certain symmetry conditions of K are fulfilled. Therefore, the optimal quadrature points are *not nested*. But in many practical applications nestedness is a big advantage because, for example, one can increase the accuracy of the numerical approximation from n to $m = n + k$ function values without evaluating the integrand at all the m points. Instead, one can re-use the first n values requiring only an additional k function evaluations. Moreover, for the construction of *sparse tensor product* cubature rules, cf. Section 2.4.2 and Chapter 7, nestedness of the underlying univariate quadrature rule is advantageous. Therefore, we will spend this section on the construction of *nested quadrature rules*, keeping the following points in mind:

1. The nested quadrature rules should use optimal weights for a given RKHS. This is important with regard to the construction of optimal tensor product cubature-rules in Chapter 7.

2. The nested quadrature rules should have a small worst-case error, preferably comparable to the n-th minimal worst-case error of the non-nested optimal quadrature rule discussed in Section 5.1.

3. The nested quadrature rules should be stable, i.e. the ℓ_1-norm of the vector of optimal weights $\check{\boldsymbol{w}}(X_n)$ should not grow with n.

There are several approaches to construct nested quadrature rules that directly minimize the worst-case error by a greedy approach, cf. [89, 136]. Then, however, it is not guaranteed that the resulting points are well-separated. In fact, already for the univariate Hardy space $\mathbb{H}_2$ stability problems occur. Therefore, we will go for a different approach that is well-established in the field of nonlinear approximation and yields well-separated point sets which lead to stable quadrature rules.

5.3.1 Orthogonal matching pursuit and nonlinear approximation

In the following, we will discuss the application of orthogonal matching pursuit to the construction of optimally weighted quadrature rules. To this end, let us first recall the setting of best n-term approximation.

Nonlinear approximation

The following generalization of a basis in a Hilbert space will be essential.

Definition 5.21. (Dictionary)
Let $\mathcal{H}$ be a Hilbert space with inner product $\langle \cdot, \cdot \rangle_{\mathcal{H}}$. A dictionary $\mathcal{D} \subset \mathcal{H}$ for $\mathcal{H}$ is a set of functions that fulfills the following two conditions:

(i) For each dictionary element $\phi \in \mathcal{D}$ it holds $\|\phi\|_{\mathcal{H}} = \sqrt{\langle \phi, \phi \rangle_H} = 1$.

(ii) The closure of the span of $\mathcal{D}$ equals $\mathcal{H}$, i.e.

$$\mathcal{H} = \overline{\text{span } \mathcal{D}}.$$

A dictionary is not necessarily a basis because it can be *redundant*.

For a given dictionary $\mathcal{D} \subset \mathcal{H}$ one can now ask the question how well a given function $f \in \mathcal{H}$ can be approximated by elements from this dictionary. This is formalized by the *best n-term approximation error*, i.e.

$$\inf_{\phi_1, \ldots, \phi_n \in \mathcal{D}} \inf_{w_1, \ldots, w_n \in \mathbb{R}} \left\| f - \sum_{i=1}^{n} w_i \phi_i \right\|_{\mathcal{H}}. \tag{5.25}$$

If a set of n dictionary elements $\phi_1, \ldots, \phi_n \in \mathcal{D}$ is fixed, the second inf in (5.25) is a classical best-approximation problem which due to the Hilbert space structure breaks down to the solution of the linear system

$$\sum_{i=1}^{n} w_i \langle \phi_i, \phi_j \rangle_{\mathcal{H}} = \langle \phi_j, f \rangle_{\mathcal{H}} \quad \text{for all } j = 1, \ldots, n.$$

However, due to the first inf over all possible combinations of n dictionary elements $\phi_1, \ldots, \phi_n \in \mathcal{D}$ this problem is referred to as *nonlinear approximation problem*.

Greedy approach to best n-term approximation

A popular greedy approach to solve the problem (5.25) is well-known by the name *Orthogonal Matching Pursuit* (OMP) [45, 123, 155] or *Orthogonal Greedy Algorithm* (OGA) [151]. For a given dictionary $\mathcal{D} \subset \mathcal{H}$ and an element $f \in \mathcal{H}$ it works as follows: First, we need a so-called selection function $\kappa : \mathcal{H} \to \mathcal{D}$

$$\kappa(g) := \arg\max_{\phi \in \mathcal{D}} |\langle g, \phi \rangle_{\mathcal{H}}|, \quad g \in \mathcal{H} \tag{5.26}$$

which selects the dictionary element that maximizes the absolute value of the inner product between its argument g and all the elements from the dictionary. Moreover, for a given finite-dimensional subspace $H_0 \subset \mathcal{H}$, we need the orthogonal projection $P_{H_0} : \mathcal{H} \to H_0$.

Then, step-by-step an approximation space H_n is constructed by the greedy procedure outlined in Algorithm 3.

In order to illustrate the behaviour of OMP, we consider the following example.

Example 5.22. Assume the dictionary consists of an orthonormal basis of $\mathcal{H}$, i.e. $\langle \varphi, \psi \rangle_H = 0$ for $\varphi \neq \psi$ and $\varphi, \psi \in \mathcal{D}$. Then, each function $f \in \mathcal{H}$ can be written as

$$f(\boldsymbol{x}) = \sum_{\phi \in \mathcal{D}} \langle f, \phi \rangle_{\mathcal{H}} \, \phi(\boldsymbol{x})$$

Algorithm 3: Orthogonal matching pursuit

Initialize: $k := 0$, $r_0 := f$, $H_0 := \{0\}$.

repeat

      1. $k := k + 1$

      2. $\varphi_k := \kappa(r_{k-1})$ (compute the next dictionary element)

      3. $H_k := \operatorname{span}(H_{k-1} \cup \{\varphi_k\})$ (update the subspace)

      4. $r_k := f - P_{H_k}(f)$ (compute projection on subspace and associated residual)

until $k = n$;

Output: The projection $P_{H_n}f$ of f onto H_n is an approximation to f in the H-norm.

---

and after k steps the OMP algorithm has automatically selected the k largest coefficients $\langle f, \phi \rangle_{\mathcal{H}}$ of f. In this case, the OMP approximation equals the best n-term approximation in (5.25) because

$$\|f - P_{H_n}f\|_{\mathcal{H}}^2 = \sum_{\phi \notin H_n} \langle f, \phi \rangle_{\mathcal{H}}^2.$$

However, in general, the dictionary is not orthogonal.

Now, we are going to apply this generic approach to the approximation of functionals in RKHS.

5.3.2 Greedy approach to quadrature in RKHS

As discussed before, the approximation of a linear functional $L_\Omega : \mathcal{H}_K \to \mathbb{R}$ using point-evaluation functionals $\delta_\xi, \xi \in \Omega$ is dual to the problem of approximating $\ell_\Omega \in \mathcal{H}_K$ using $K(\cdot, \xi), \xi \in \Omega$, where $K(\cdot, \xi)$ is the Riesz-representer of δ_ξ.

Recalling that

$$\|K(\cdot, \xi)\|_{\mathcal{H}_K} = \sqrt{\langle K(\cdot, \xi), K(\cdot, \xi) \rangle_{\mathcal{H}_K}} = \sqrt{K(\xi, \xi)}$$

and that $\mathcal{H}_K = \overline{\operatorname{span}\{K(\cdot, x) | x \in \Omega\}}$, we note that the set of normalized point-evaluation representers

$$\mathcal{D}_\Omega(K) := \left\{ \frac{K(\cdot, \xi)}{\sqrt{K(\xi, \xi)}} \Big| \xi \in \Omega \right\},$$

is a dictionary for $\mathcal{H}_K$ in the sense of Definition 5.21. The idea to use orthogonal matching pursuit in this setting appeared for example in [150, 151].

Next, we need to compute the projections onto the subspaces spanned by $\{K(\cdot, \xi_i), i = 1, \dots n\}$. To this end, let $H_m = \operatorname{span}\{K(\cdot, \xi_1), \dots, K(\cdot, \xi_m)\}$ be a subspace spanned by m kernel functions. The orthogonal projection $P_{H_m} : \mathcal{H}_k \to H_m$ is explicitly given by the spline algorithm, cf. Section 3.3, i.e.

$$P_{H_m}f(x) := \sum_{i=1}^{m} \sum_{j=1}^{m} G_{i,j}^{-1}(X_m) K(x, \xi_j) f(\xi_i).$$

Algorithm 4: OMP greedy approach to compute nested quadrature rules in RKHS

Input: kernel function $K : \Omega \times \Omega \to \mathbb{R}$, representer $\ell_\Omega : \Omega \to \mathbb{R}$.

Initialize: $k := 0$, $X_0 = \emptyset$, $\check{r}_{X_0} = \ell_\Omega$.

repeat

    1. $k := k + 1$

    2. $\xi_k := \arg\max_{x \in \Omega} |\check{r}_{X_{k-1}}(x)|^2 / K(x,x)$ (solve global optimization problem)

    3. $X_k := X_{k-1} \cup \{\xi_k\}$ (add new point)

    4. $\check{\boldsymbol{w}}(X_k) = \boldsymbol{G}^{-1}(X_k, K)\boldsymbol{b}(X_k, K)$ (compute optimal weights)

    5. $\check{r}_{X_k} := \ell_\Omega(x) - \sum_{i=1}^{k} \check{w}_i(X_k) K(x, \xi_i)$ (update error representer)

until $k = n$;

Output: Quadrature points X_n and optimal weights $\check{\boldsymbol{w}}(X_k)$ for all $k = 1, \dots, n$.

Moreover, for the special case of $f = \ell_\Omega$, the projection of f on the subspace H_m is given by $P_m \ell_\Omega(x) = \sum_{i=1}^{m} \check{w}_i(X_m) K(x, \xi_i)$ and the residual $f - P_{H_m} f$ is just the Riesz-representer of the quadrature rule that uses the points $X_m = (\xi_1, \dots, \xi_m)$, i.e.

$$\ell_\Omega - P_{H_m} \ell_\Omega = \check{r}_{X_m}.$$

Finally, we need the selection-function $\kappa : \mathcal{H}_K \to \mathcal{D}_\Omega(K)$, cf. (5.26). To this end, we observe that to each point $x \in \Omega$ there corresponds a dictionary element $\phi \in \mathcal{D}_\Omega(K)$. Therefore, for a given function $g \in \mathcal{H}_K$, we can write the selection function $\kappa : \mathcal{H}_K \to \mathcal{D}_\Omega(K)$ as

$$\kappa(g) := \arg\max_{\phi \in \mathcal{D}_\Omega(K)} |\langle g, \phi \rangle_{\mathcal{H}_K}| = \arg\max_{x \in \Omega} |\langle g, K(\cdot, x) / \sqrt{K(x,x)} \rangle_{\mathcal{H}_K}|$$

$$= \arg\max_{x \in \Omega} |g(x) / \sqrt{K(x,x)}| = \arg\max_{x \in \Omega} |g(x)|^2 / K(x,x).$$

Here, we used that $K(\cdot, x)$ represents point-evaluation and that the maximizer of a positive function is invariant with respect to taking the square.

We see that with our particular choice of the dictionary $\mathcal{D}_\Omega(K)$, the orthogonal matching pursuit algorithm can easily be realized for RKHS by solving a global optimization problem for the smooth function $|g|^2 / K(x,x)$.

We summarize the final procedure in Algorithm 4. Note that the only input required by this approach is the kernel function $K : \Omega \times \Omega \to \mathbb{R}$ and the Riesz-representer of L_Ω in $\mathcal{H}_K$ that is given by $\ell_\Omega(x) = \int_\Omega K(x,y)\omega(y)\,\mathrm{d}y$.

We visualized the sequence of maximization problems in Figure 5.4. Note the similarity to the construction of Leja points in Section 2.3.4, where also repeated maximization problems have to be solved in order to obtain nested point sets.

This approach is applicable for $d \geq 2$ as well, but unfortunately global optimization problems quickly become intractable when the dimensionality increases. However, for $d = 1$ it can be
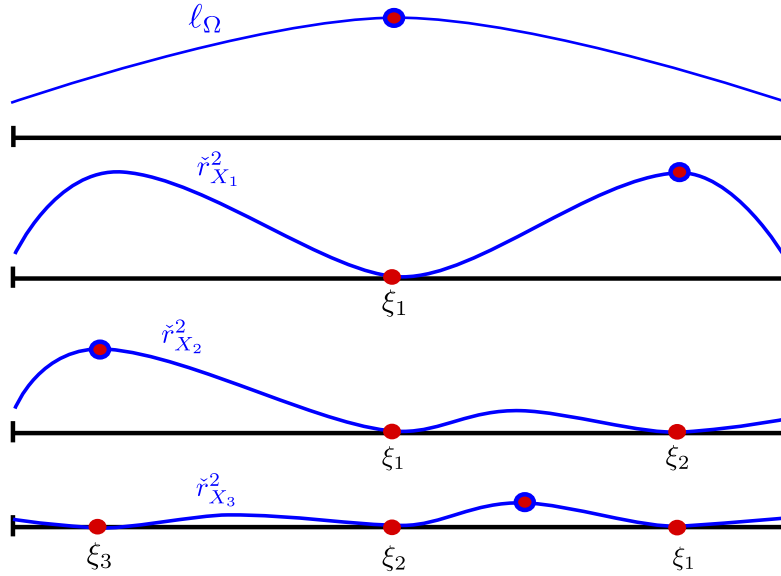
Figure 5.4: Orthogonal matching pursuit for approximation of ℓ_Ω with $K(x,x) = 1$.

solved by splitting Ω into $k+1$ sub-intervals

$$\Omega = (a,b) = (a,\xi_1] \cup (\xi_1,\xi_2] \cup \ldots \cup (\xi_{k-1},\xi_k] \cup (\xi_k,b] = \bigcup_{i=1}^{k+1} \Omega_i.$$

Since $\check{r}_{X_k}(\xi_k) = 0$, we know by Rolle's theorem that there exists a local maximum of $\check{r}_{X_k}^2$ in every Ω_i. Therefore, in the k-th step we solve $(k+1)$ local optimization problems and obtain the global solution by the largest of all the local ones.

5.3.3 Symmetric point sets

Sometimes it is advantageous to have nested point sets that are symmetric. One reason is that symmetric points, which also lead to symmetric weights by Proposition 5.18, integrate all odd functions exactly. Therefore, we will modify Algorithm 4 such that it produces points that are symmetric by following the ideas from Section 5.2.4.

In particular, we assume that the integration domain is zero-centered, i.e. $\Omega = (-\alpha, \alpha)$ and the weight function is even, i.e. $\omega(x) = \omega(-x)$ for all $x \in \Omega$. Moreover, for all $x, y \in \Omega$ it shall hold $K(x,-y) = K(-x,y)$. Then, we set the first quadrature point $\xi_1 = 0$ and apply Algorithm 4 to the kernel $\tilde{K}(x,y) = K(x,y) + K(x,-y)$.

Each point ξ_k that is computed in the k-th iteration of the algorithm is then mirrored at zero and the final set of points after n iterations has the form

$$X_{2n+1}^s = (0, \xi_1, -\xi_1, \xi_2, -\xi_2, \ldots, \xi_n, -\xi_n)$$

and a cardinality of $2n+1$. The procedure is outlined in Algorithm 5.

Algorithm 5: OMP greedy approach for symmetric nested quadrature rules on $\Omega = (-\alpha, \alpha)$.

Input: kernel function $K : \Omega \times \Omega \to \mathbb{R}$, representer $\ell_\Omega : \Omega \to \mathbb{R}$.

Initialize: $k := 1$, $X_1 = X_1^s = \{0\}$, $\check{r}_{X_1} = \ell_\Omega(x) - \tilde{K}(x,0)\ell_\Omega(0)/\tilde{K}(0,0)$. **repeat**

  1. $k := k + 1$

  2. $\xi_k := \arg\max_{x \in (0,\alpha)} |\check{r}_{X_{k-1}}(x)|^2/\tilde{K}(x,x)$ (solve global optimization problem)

  3. $X_k := X_{k-1} \cup \{\xi_k\}$ and $X_{2k+1}^s := X_{2k-1} \cup \{-\xi_k, \xi_k\}$ (add new point)

  4. $\check{\boldsymbol{w}}(X_k) = \boldsymbol{G}^{-1}(X_k, \tilde{K})\boldsymbol{b}(X_k, \tilde{K})$ (compute optimal weights in $\mathcal{H}_{\tilde{K}}$)

  5. $\check{r}_{X_k} := \ell_\Omega(x) - \sum_{i=1}^{k} \check{w}_i(X_k)\tilde{K}(x, \xi_i)$ (update symmetrized error representer)

until $k = n$;

Output: Symmetric set of nested quadrature points X_{2n+1}^s.

5.3.4 Extension to unbounded domains and singular function spaces

A possible extension of the classical orthogonal matching pursuit introduces a certain prior on the dictionary which moderates how much certain dictionary elements are preferred over others. This can be realized by some function $\eta : \mathcal{D} \to \mathbb{R}_+$ which modifies the selection function κ to

$$\kappa_\eta(g) := \arg\max_{\phi \in \mathcal{D}} |\langle g, \phi \rangle_\mathcal{H}|\, \eta(\phi).$$

In our setting, where we use the dictionary $\mathcal{D}_\Omega(K)$ and each element corresponds to a point $x \in \Omega$, the prior on the dictionary elements can be realized as weight function $\nu : \Omega \to \mathbb{R}_{\geq 0}$.

Inspired by weighted Leja sequences, we choose $\nu(x) = \sqrt{\omega(x)}$ for integration with respect to non-constant weight functions ω. This is especially important when dealing with integration on unbounded domains like $\Omega = \mathbb{R}$. Moreover, it turned out to be beneficial to use the Chebyshev weight function $\nu(x) = \sqrt{(1 - x^2)}$ for integration on $(-1, 1)$ when the function $x \mapsto K(x, x)$ or its derivative is unbounded as $x \to \pm 1$, like e.g. in $\mathbb{H}_1$ or $\mathcal{T}_{\mathrm{Li}_2}$.

The weighted OMP greedy algorithm for the construction of nested quadrature rules is outlined in Algorithm 6 and visualized for $K(x, x) = 1$ in Figure 5.5.

Finally, we remark that it is of course possible to combine the weighted greedy approach in Algorithm 6 with the symmetric greedy approach in Algorithm 5.
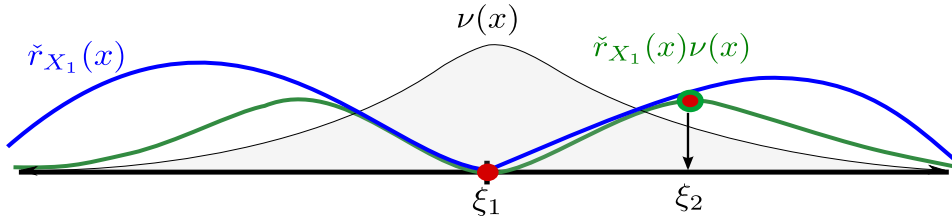
Figure 5.5: Weighted orthogonal matching pursuit with weight function $\nu : \Omega \to \mathbb{R}_+$.

Algorithm 6: Weighted OMP greedy approach to compute nested quadrature rules in RKHS

Input: kernel function $K : \Omega \times \Omega \to \mathbb{R}$, representer $\ell_\Omega : \Omega \to \mathbb{R}$, weight function $\nu : \Omega \to \mathbb{R}_+$.

Initialize: $k := 0$, $X_0 = \emptyset$, $\check{r}_{X_0} = \ell_\Omega$

repeat

1. $k := k + 1$

2. $\xi_k := \arg\max_{x \in \Omega} |\check{r}_{X_{k-1}}(x)\nu(x)|^2 / K(x, x)$ (solve weighted optimization problem)

3. $X_k := X_{k-1} \cup \{\xi_k\}$.   (add new point)

4. $\check{\boldsymbol{w}}(X_k) = \boldsymbol{G}^{-1}(X_k, K)\boldsymbol{b}(X_k, K)$ (compute optimal weights)

5. $\check{r}_{X_k} := \ell_\Omega(x) - \sum_{i=1}^{k} \check{w}_i(X_k)K(x, \xi_i)$ (update error representer)

until $k = n$;

Output: Quadrature points X_n and optimal weights $\check{\boldsymbol{w}}(X_k)$ for all $k = 1, \ldots, n$.

---

6 Application to optimal quadrature in certain RKHS from scientific computing

In Chapter 5 we have introduced two algorithms for the construction of both, optimal and nested univariate quadrature, rules that approximate

$$L_\Omega(f) = \int_\Omega f(x)\,\omega(x)\,\mathrm{d}x$$

in a univariate reproducing kernel Hilbert space $\mathcal{H}_K$ with kernel $K : \Omega \times \Omega \to \mathbb{R}$. Here, $\Omega \subset \mathbb{R}$ is a one dimensional domain and $\omega : \Omega \to \mathbb{R}_+$ a positive weight function.

This chapter is concerned with the validation of these quadrature rules in a variety of reproducing kernel Hilbert spaces that are relevant in applications from numerical analysis, scientific computing and engineering. In order to apply the algorithms from Chapter 5 to the construction of quadrature formulas in specific spaces $\mathcal{H}_K$ efficiently, we have to derive closed-form representations of

$$\|L_\Omega\|^2_{\mathcal{H}_K^\star} = L_\Omega^{(x)} L_\Omega^{(y)} K(x,y) \quad \text{and} \quad \ell_\Omega(x) = L_\Omega^{(y)} K(x,y), \tag{6.1}$$

which are the squared norm and the Riesz-representer of L_Ω in $\mathcal{H}_K$, respectively. Moreover, we need certain derivatives of the kernel K and the function ℓ_Ω, but since differentiation in general is a simple task the main problem is the derivation of (6.1).

After the desired optimal and nested quadrature rules have been computed we will compare them not only with each other but also to Gaussian, Clenshaw-Curtis and Leja quadrature. Even though the optimal quadrature points will not be used in Chapters 7 and 8, they will serve as a benchmark for the performance of other quadrature rules in the respective setting. To this end, we define

$$\mathbf{w\check{c}e}_n(\mathcal{H}_K) = \mathbf{w\check{c}e}(\check{Q}_{\check{X}_n}) \tag{6.2}$$

to be the worst-case error of a quadrature rule with n optimal points $\check{X}_n$ and associated optimal weights $\check{\boldsymbol{w}}(\check{X}_n)$. Here we note that our numerical experiments suggest that in all the investigated settings the optimal quadrature points obtained by Algorithm 2 are unique. However, this has been proven only for translation invariant kernels of the form $K(x,y) = g(x-y)$ for integration with respect to the uniform density $\omega \equiv 1$, cf. [27]. If in fact the uniqueness would hold true for all of the kernels considered in this thesis, the quantity (6.2) would equal the n-th minimal worst-case error in $\mathcal{H}_K$, cf. (2.5) in Section 2.1.2.

Our main observation regarding the performance of the OMP greedy approach is the following:

- If $\mathbf{w\check{c}e}_n(\mathcal{H}_K)$ decays *algebraically* with order $\mathcal{O}(n^{-s}), s \in \mathbb{N}$, the OMP greedy quadrature also exhibits a convergence rate of $\mathcal{O}(n^{-s})$, albeit with a slightly worse constant than the optimal algorithm.

- If $\mathbf{w\check{c}e}_n(\mathcal{H}_K)$ decays exponentially with order $\mathcal{O}(e^{-\alpha n}), \alpha > 0$, the OMP greedy quadrature achieves a convergence rate of $\mathcal{O}(e^{-\frac{\alpha}{2}n})$.

- If $\mathbf{w\check{c}e}_n(\mathcal{H}_K)$ decays sub-exponentially with order $\mathcal{O}(e^{-\alpha\sqrt{n}}), \alpha > 0$, the OMP greedy quadrature achieves a convergence rate of $\mathcal{O}(e^{-\beta\sqrt{n}})$, where the precise relationship between α and β is not clear. However, in the considered cases we have $\beta > \alpha/2$.

Beside the relationship between optimal points and the OMP greedy points with respect to their worst-case errors we also consider further properties, like the distribution of both, optimal and OMP greedy points, or the stability of the resulting optimal quadrature weights. Regarding the latter, we note that the stability of optimal quadrature rules follows from the positivity of their weights, cf. Theorem 5.9. The stability of the OMP greedy points will be investigated numerically. It turns out that they behave similar to Leja points, i.e. the associated optimal weights are not all positive, but the quantity $\sum_{i=1}^{n} |\check{w}_i(X_n)|$ seems to be uniformly bounded for all $n \in \mathbb{N}$.

Moreover, we investigate the distribution of the OMP greedy points, relative to the respective optimal points. Here we observe that in many settings the OMP greedy points are distributed in the same way as the optimal point sets. This is a similarity to Gaussian and Leja quadrature, where the respective point sets also lead to the same distribution.

Finally, we compare the performance of our new quadrature rules with respect to the worst-case error to other, well-known quadrature rules from the literature. Therefore, in the upcoming plots we give the worst-case errors of the following quadrature rules.

Optimal: Optimal quadrature points and weights, cf. Section 5.2.

OMP Greedy: The points are selected by the approach from Section 5.3, which is based on orthogonal matching pursuit. The weights are computed to be optimal in $\mathcal{H}_K$.

Weighted Greedy: The points are selected by the approach from Section 5.3, but an additional weight is employed.

Gaussian-quadrature: Classical Gaussian quadrature rule that achieves the maximal polynomial degree of exactness which is $2n - 1$. Depending on the setting we use either Gauss-Legendre for integration on bounded intervals like $[-1, 1]$ or $[0, 1]$, or Gauss-Hermite for integration on $(-\infty, \infty)$.

Clenshaw-Curtis: Common quadrature rule that is nested for $n = 2^k - 1, k \in \mathbb{N}$. It is exact for polynomials up to degree $n - 1$. Their construction is explained e.g. in [38, 159].

Leja: The points are maximally nested with polynomial degree of exactness of $n - 1$. Their construction for integration on $[-1, 1]$ is explained in Section 2.3.4 and for integration on $(-\infty, \infty)$ in Section 2.3.4.

All computations were carried out with arbitrary precision floating points arithmetic [62], where it was necessary to use an accuracy of ε^2 to compute worst-case errors of the magnitude ε, cf. the discussion at the end of Section 4.1.1.
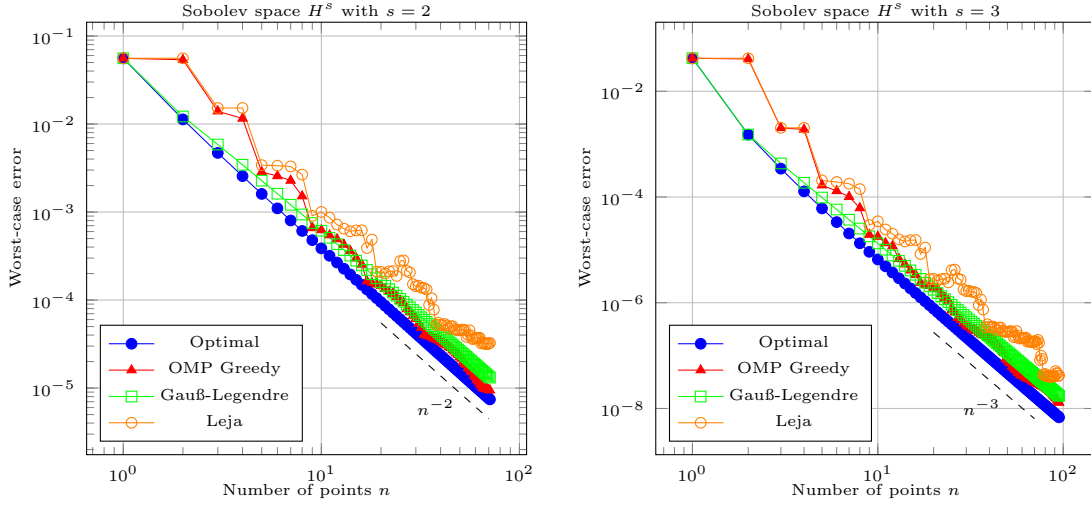
Figure 6.1: Log-log plot of the worst-case errors in H^s on $[0,1]$ for $s \in \{2,3\}$.

6.1 Sobolev spaces

Our first examples are Sobolev spaces with smoothness $s \in \mathbb{N}$. The non-periodic Sobolev space H^s on $[0,1]$ as well as its reproducing kernel

$$K_s(x,y) = 1 + \frac{(-1)^{s+1}}{(2s)!} B_{2s}(|x-y|) + \sum_{j=1}^{s} \frac{B_j(x)B_j(y)}{(j!)^2}$$

was already discussed in Section 3.6.1. Moreover, the reproducing kernel of the periodic Sobolev space $\tilde{H}^s$ is

$$\tilde{K}_s(x,y) = \sum_{k \in \mathbb{Z}} \rho(k)^{-2s} \exp\left(2\pi \mathrm{i}k(x-y)\right) = 1 + \frac{(-1)^{s+1}}{(2s)!} B_{2s}(|x-y|).$$

In order to apply the algorithms from Chapter 5, we need to compute the Riesz-representer of $L_\Omega f = \int_0^1 f(x)\,\mathrm{d}x$ in both spaces. Due to the representation as Bernoulli polynomials, which fulfill $L_\Omega B_k = 0$, we obtain

$$\ell_\Omega(x) = 1 \quad \text{and therefore} \quad \|L_\Omega\|_{(H^s)^\star} = \|L_\Omega\|_{(\tilde{H}^s)^\star} = 1.$$

It is well-known that for both, periodic and non-periodic Sobolev spaces, it is possible to achieve the best possible convergence rate of the worst-case error, i.e. n^{-s} by using equidistant points, cf. [28, 109, 116]. Also, classical Gaussian quadrature with its $2n-1$ polynomial degree of exactness exhibits this rate of convergence, which is a consequence of polynomial best approximation results in Sobolev spaces [109].

Therefore, it is not surprising that the improvement by choosing optimal point sets is neglectable. However, it is still interesting to note that even the greedy algorithm achieves the
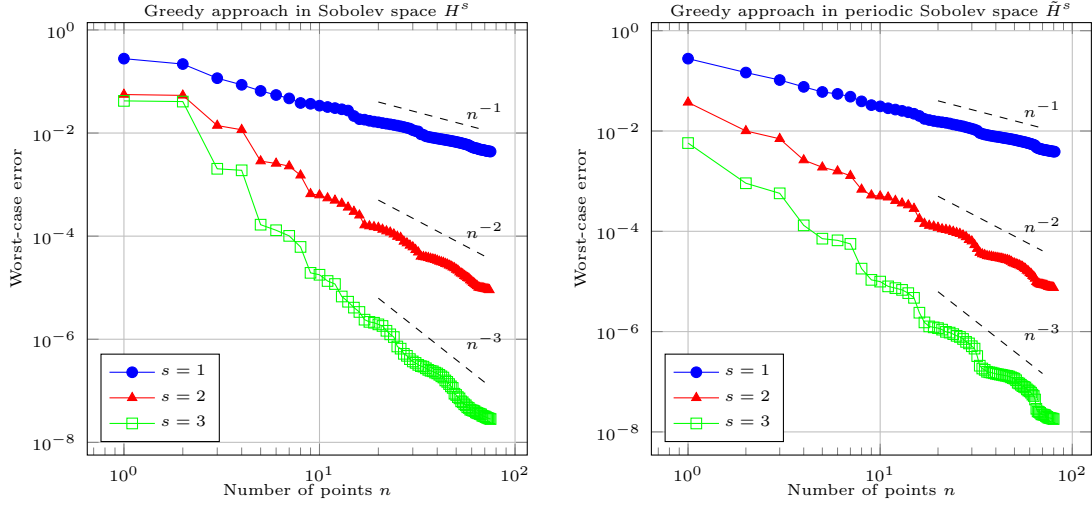
Figure 6.2: Log-log plot of worst-case error of the OMP greedy quadrature in both, periodic and non-periodic Sobolev spaces on $[0,1]$.

best possible rate n^{-s}, albeit with a slightly worse constant.

To be more precise, in Figure 6.1 we compare worst-case errors of optimal points to greedy points as well as to Gaussian quadrature and Leja quadrature in the non-periodic Sobolev spaces H^s for $s \in \{2,3\}$. The data is plotted in a log-log-scale. Clearly, all the considered methods achieve a convergence rate of n^{-s}. The decay of the Leja quadrature, however, is not as smooth and straight as the rates of the other methods.

In Figure 6.2 the worst-case errors of the OMP greedy points for both, the periodic Sobolev space $\tilde{H}^s$ and the non-periodic Sobolev space H^s on $[0,1]$ are given. Here, we considered smoothness parameters $s \in \{1,2,3\}$. Clearly, the OMP greedy method achieves the best possible rate of n^{-s} in both spaces for all the considered smoothness settings.

Moreover, we comment on the stability of the OMP greedy points. We computed the quantities

$$\sigma(n) := \sum_{i=1}^{n} |\breve{w}_i(X_n)| \tag{6.3}$$

for X_n being the nested point sets obtained by the OMP greedy algorithm. For both spaces, $\tilde{H}^s$ and H^s and all smoothness parameters $s \in \{1,2,3\}$ we found that $\sigma(n) \leq 1.1$. Therefore, we claim that the OMP greedy quadrature rules are stable.

Finally, we consider the distribution of optimal and OMP greedy points. To this end, in Figure 6.3 their cumulative distribution functions are given on the left-hand side. Both point sets are distributed uniformly over the domain $\Omega = [0,1]$. This is consistent with the right-hand side picture, where the convergence of the largest optimal quadrature point to the interval's boundary is plotted in a log-log scale. Since the largest optimal point is always located *within* $(0,1)$, it can only approach $x = \pm 1$ but never actually hits the boundary. The observed convergence is of order n^{-1}, which is consistent with a uniform or equidistant distribution.
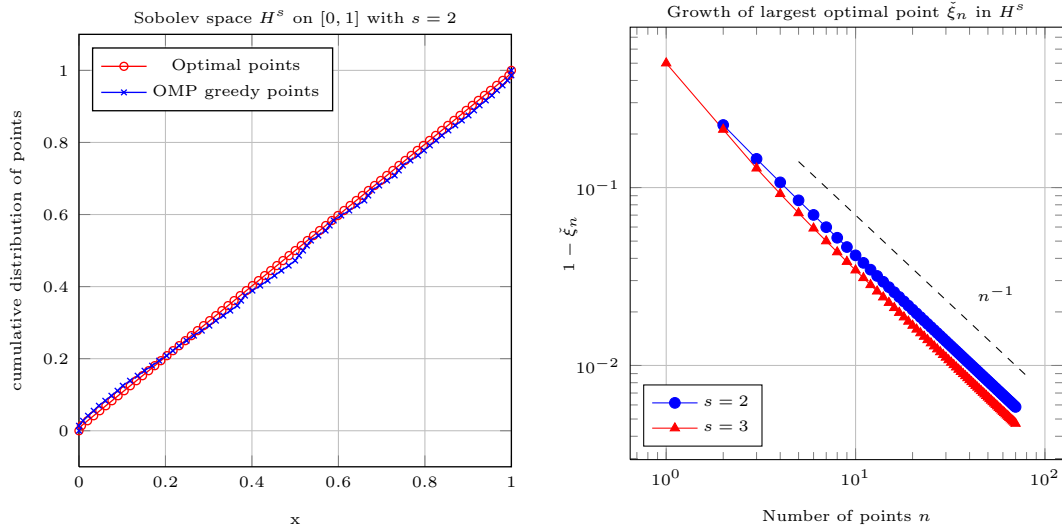
Figure 6.3: Distribution of optimal and greedy points for non-periodic Sobolev spaces on $[0, 1]$.

6.2 Hardy spaces on open discs

The next example are Hardy spaces $\mathbb{H}_r$ which consist of functions that are analytic in the open disc $\mathbb{D}_r = \{z \in \mathbb{C} : |z| < r\}$ and are square integrable on its boundary. Its reproducing kernel was given in Section 3.6.2, i.e.

$$K_r(x, y) = \frac{r^2}{r^2 - xy} = \sum_{k=0}^{\infty} r^{-2k} x^k y^k.$$

We consider integration on $\Omega = (-1, 1)$ with respect to the uniform measure, i.e.

$$L_\Omega(f) = \int_{-1}^{1} f(x) \, \mathrm{d}x. \tag{6.4}$$

The extended total positivity of K_r is an immediate consequence of Theorem 5.3 with $u(x) = x$ and $\lambda_k = r^{-2k}$.

In order to apply the results from Chapter 5, we need a closed formula for both, the Riesz-representer ℓ_Ω and the norm $\|L_\Omega\|_{\mathbb{H}_r^\star}$ of L_Ω.

Proposition 6.1.

(i) *The Riesz-representer of $L_\Omega(f)$ given in* (6.4) *is*

$$\ell_\Omega(x) = \frac{2r^2}{x} \tanh^{-1}\left(\frac{x}{r^2}\right).$$

(ii) The operator norm of L_Ω in $\mathbb{H}_r$ is given by

$$\|L_\Omega\|^2_{\mathbb{H}_r^\star} = 2r^2 \left(\mathrm{Li}_2 \left(\frac{1}{r^2} \right) - \mathrm{Li}_2 \left(-\frac{1}{r^2} \right) \right),$$

where $\mathrm{Li}_2(x) = \sum_{k=1}^\infty \frac{x^k}{k^2}$ denotes the di-logarithm, cf. [165] and the references therein for an overview of the properties of the Li_2-function.

Proof. Regarding (i) we use the identity

$$\tanh^{-1}(x) = \sum_{k=0}^\infty \frac{x^{2k+1}}{2k+1}$$

and compute

$$\ell_\Omega(x) = L_\Omega^{(y)} K_r(x, y) = \sum_{k \in \mathbb{N}_0} r^{-2k} x^k \int_{-1}^1 y^k \, \mathrm{d}y = \sum_{k \in \mathbb{N}_0} r^{-2k} x^k \frac{1 + (-1)^k}{k+1}$$

$$= \sum_{k \in \mathbb{N}_0} r^{-4k} x^{2k} \frac{2}{2k+1} = \frac{2r^2}{x} \sum_{k \in \mathbb{N}_0} \left(\frac{x}{r^2} \right)^{2k+1} \frac{1}{2k+1}$$

$$= \frac{2r^2}{x} \tanh^{-1} \left(\frac{x}{r^2} \right).$$

The norm of L_Ω is computed by

$$\|L_\Omega\|^2_{\mathbb{H}_r^\star} = L_\Omega^{(x)} L_\Omega^{(y)} K_r(x, y)$$

$$= \sum_{k \in \mathbb{N}_0} r^{-2k} \left(\int_{-1}^1 x^k \, \mathrm{d}x \right)^2 = \sum_{k \in \mathbb{N}_0} r^{-2k} \frac{(1 + (-1)^k)^2}{(k+1)^2}$$

$$= \sum_{k \in \mathbb{N}_0} r^{-2k} \frac{2}{(k+1)^2} \left(1 + (-1)^k \right) = 2r^2 \sum_{k \in \mathbb{N}_0} r^{-2(k+1)} \frac{1}{(k+1)^2} \left(1 + (-1)^k \right)$$

$$= 2r^2 \sum_{k=1}^\infty r^{-2k} \frac{1}{k^2} \left(1 + (-1)^{k-1} \right) = 2r^2 \left(\sum_{k=1}^\infty \frac{(r^{-2})^k}{k^2} - \sum_{k=1}^\infty \frac{(-r^{-2})^k}{k^2} \right)$$

$$= 2r^2 \left(\mathrm{Li}_2(r^{-2}) - \mathrm{Li}_2(-r^{-2}) \right)$$

$\square$

Now we are prepared to apply the results from Chapter 5 to compute both, optimal and nested quadrature rules for $\mathbb{H}_r$. These are then compared to several other quadrature rules on $(-1, 1)$ in $\mathbb{H}_r$ for different $r > 1$ in Figures 6.4 and 6.5. The data is plotted in a semi-logarithmic scale, i.e. the respective worst-case errors on the y-axis are logarithmically scaled. Clearly, a large radius of analyticity r allows for a faster rate of convergence.

It is known that optimal quadrature points for $\mathbb{H}_r$ converge to the Gauss-Legendre points as $r \to \infty$, cf. [103]. Therefore, for large r the benefit of using optimal quadrature points
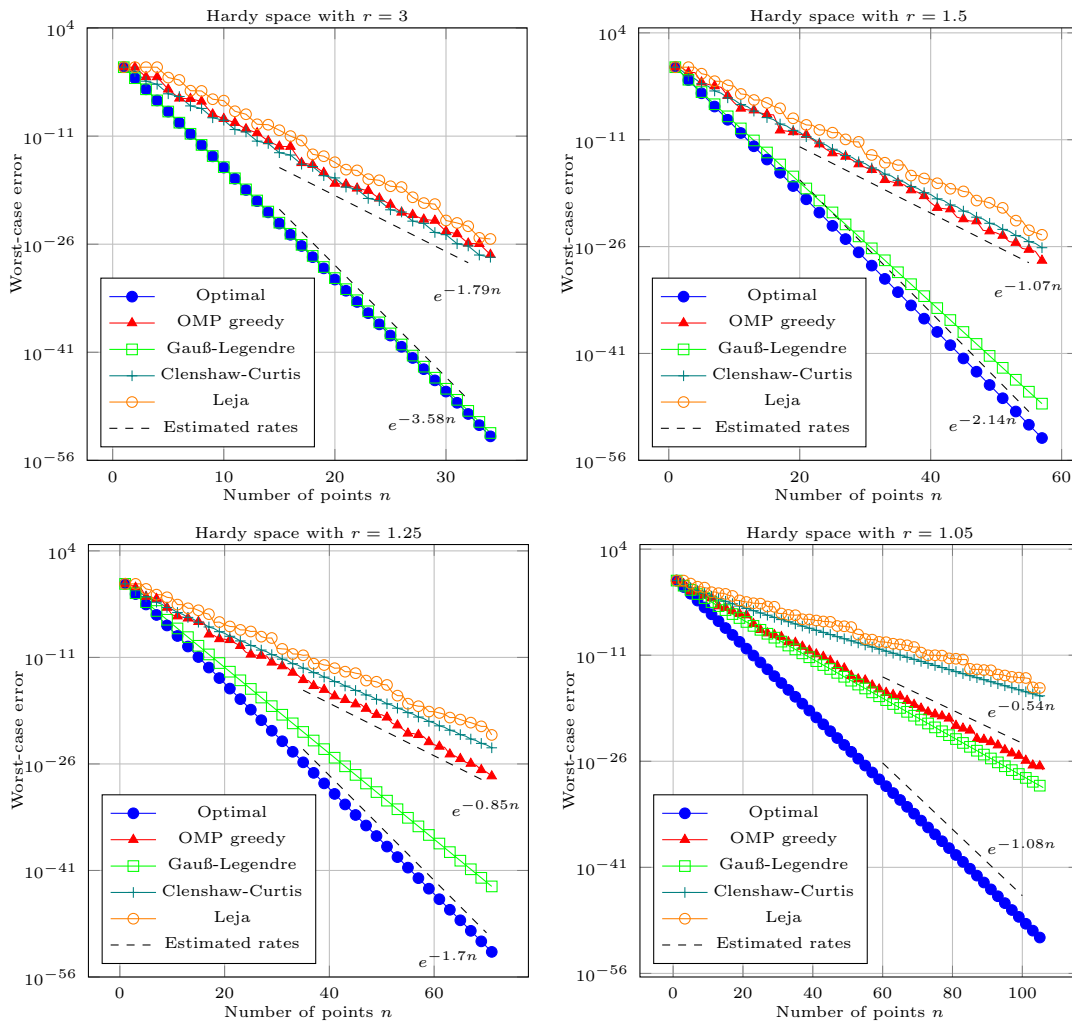
Figure 6.4: Semi-logarithmic plots of the worst-case errors in the Hardy space $\mathbb{H}_r$ with relatively large radii $r \in \{3, 1.5, 1.25, 1.05\}$.

over classical Gaussian quadrature is neglectable, cf. Figure 6.4. Both, Gauss-Legendre and optimal points exhibit the almost same exponentially decaying worst-case error. The Clenshaw-Curtis and Leja quadrature exhibit about half of the exponential convergence rate. This is not surprising because they integrate polynomials up to degree $n-1$ exactly, which is about half of the degree the Gaussian approach can achieve.

The same holds for the OMP greedy method which achieves a worst-case error that is not much better than the one of the nested polynomial based approaches.

However, as r tends to 1 the situation changes. Even though for $r > 1$ all the considered methods achieve an exponential rate of convergence [80, Thm 5.7], the optimal quadrature rule clearly outperforms the Gaussian approach if $r < 1.25$. For the limiting case $r = 1$ it is known that the rate of convergence of Gauss-Legendre quadrature drops to $\mathcal{O}(n^{-2})$, cf. [99].
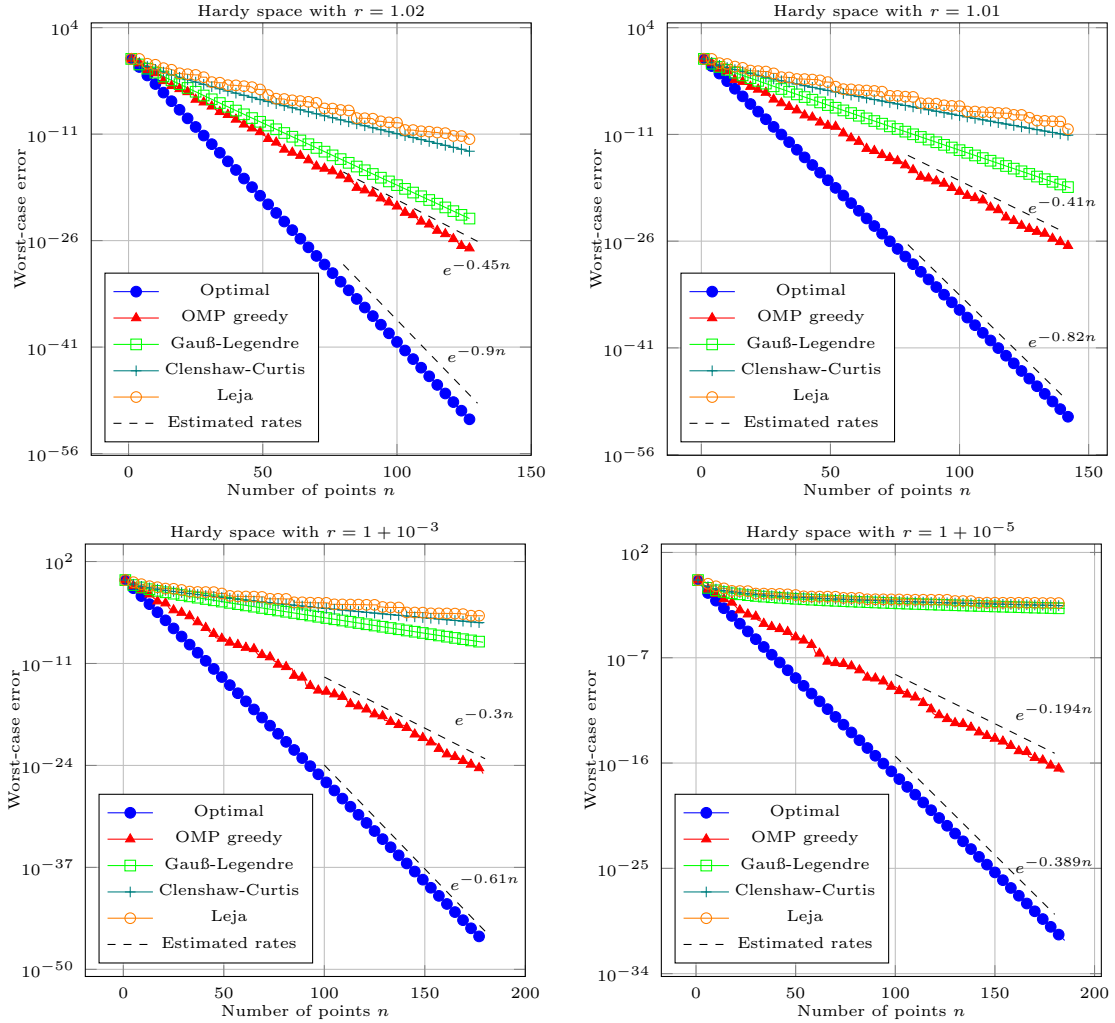
Figure 6.5: Semi-logarithmic plot of the worst-case errors in the Hardy space $\mathbb{H}_r$ for small radii $r \in \{1.02, 1.01, 1.001, 1.00001\}$.

However, it was shown in [3] that the optimal algorithm with optimal points for quadrature in $\mathbb{H}_1$ converges at a rate of

$$\mathbf{w\check{c}e}(\check{X}_n, \mathbb{H}_1) \asymp n^{1/4} \exp\left(-\frac{\pi}{\sqrt{2}}\sqrt{n}\right). \tag{6.5}$$

In Figure 6.6 we observe that the optimal quadrature rule computed by the approach from Section 5.2 attains this best possible rate, while the quadrature rules based on a polynomial degree of exactness converge algebraically only.

Let us discuss the performance of the *nested quadrature rules* obtained by the OMP greedy procedure from Section 5.3 in more detail. We have estimated both, the optimal rate and the greedy rate using a least-squares approach. Clearly, the estimated rates match the ones that
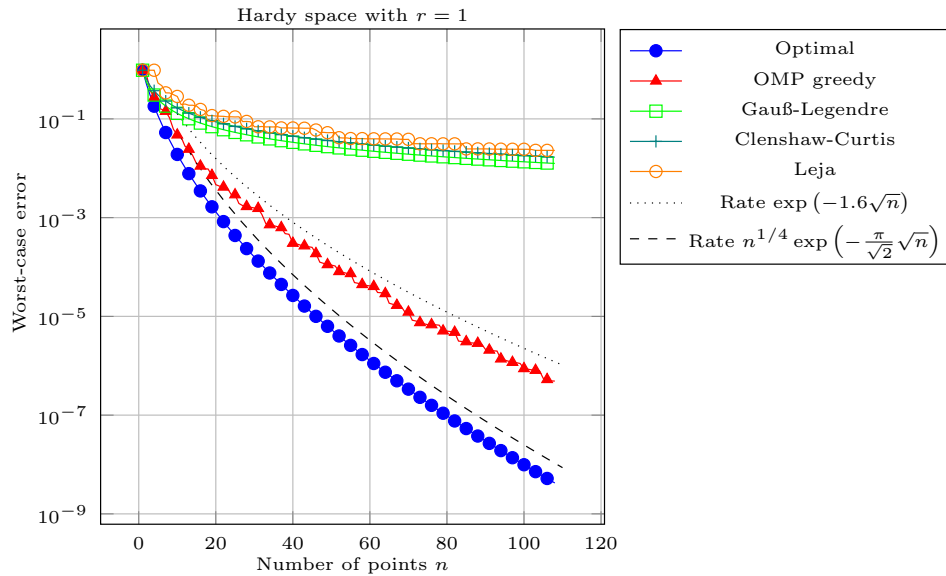
Figure 6.6: Semi-logarithmic worst-case error plot for $\mathbb{H}_r$ with $r = 1$.

can be observed in Figures 6.4 and 6.5. Here, it sticks out that for $r > 1$ the greedy rate is always about half of the rate that the optimal points achieve. For $r < 1.01$, the greedy rate is even better than Gauss-Legendre quadrature and hence offers a real benefit in settings where the integrand is analytic in just a small neighborhood of the integration domain.

Even more interesting is the limiting case $r = 1$. Now, the optimal rate is sub-exponential, cf. (6.5), and we estimate $\exp(-1.6\sqrt{n})$ for the OMP greedy rate, where the weight function $\nu(x) = \sqrt{1 - x^2}$ was employed, cf. Section 5.3.

A very pleasant observation is the stability of weights associated to the OMP greedy quadrature points X_n in $\mathbb{H}_r$. We computed

$$\sigma(n) := \sum_{i=1}^{n} |\check{w}_i(X_n)|$$

with various radii $r \in \{1, 1 + 10^{-5}, 1 + 10^{-3}, 1.01, 1.02, 1.05, 1.25, 1.5, 3\}$. In all these cases, the value of $\sigma(n)$ never exceeded 3.2. Therefore, we claim that the OMP greedy quadrature rules for $\mathbb{H}_r$ are stable.

Finally, Figure 6.8 studies the distribution of the optimal quadrature points in $\mathbb{H}_r$: It is well-known that Gauss-Legendre points are more concentrated close to the boundary than in the inner part of the interval. In fact, the largest node ξ_n^G of an n-point Gauss-Legendre quadrature rule converges to 1 at a rate of about n^{-2}, cf. [147], i.e. it holds

$$1 - \xi_n^G \preceq n^{-2}.$$

For the $\mathbb{H}_r$-optimal quadrature points we see a similar behaviour if $r \gg 1$. For smaller r, however, we observe that for small n the points tend much faster, i.e. at sub-exponential speed, to the boundary. But when n gets larger their algebraic asymptotic behaviour becomes apparent.
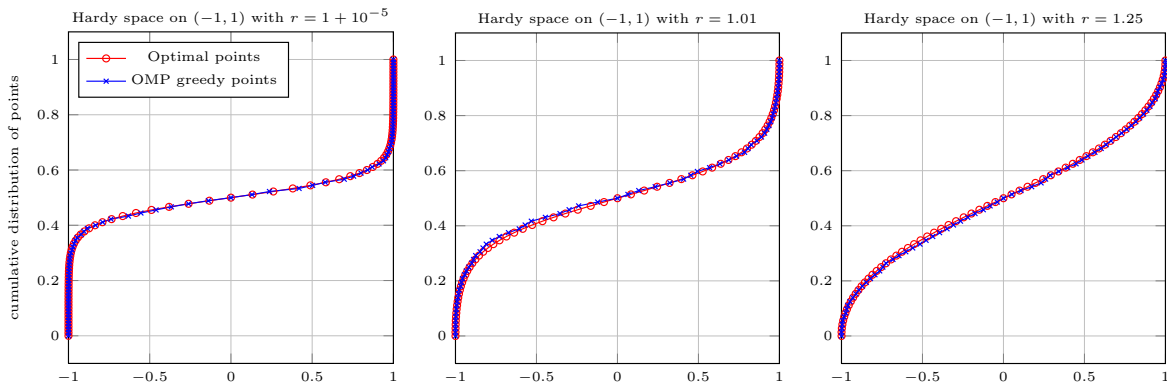
Figure 6.7: Distribution of optimal and greedy points for Hardy spaces on $(-1, 1)$.

In the limiting case $r = 1$, there certainly is a super-algebraic convergence of the largest optimal quadrature point towards the boundary.

Moreover, in Figure 6.7 the cumulative distribution functions of both, optimal points and OMP greedy points are depicted for $r \in \{1 + 10^{-5}, 1.01, 1.25\}$. In all cases the greedy construction yields a point distribution that exactly matches the one of the respective optimal points. However, for small r the distribution is substantially more concentrated at the boundary, which is consistent with the observations regarding the growth of the largest optimal node. Again, we remark the similarity to the relationship between Leja points on $[-1, 1]$ and Gauss-Legendre quadrature, which also distribute in the same way, cf. Figure 2.2.
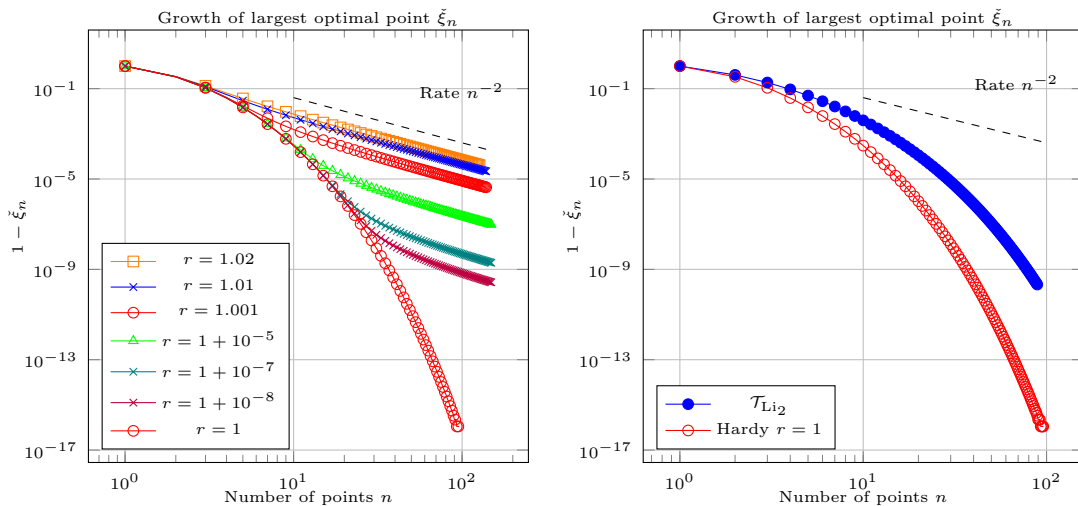
Figure 6.8: Convergence of optimal quadrature points to the boundary in the Hardy space $\mathbb{H}_r$ and the Taylor space generated by the di-logarithm $\mathcal{T}_{\mathrm{Li}_2}$.

6.3 Taylor space generated by the di-logarithm

The Taylor space $\mathcal{T}_{\mathrm{Li}_2}$ that is generated by the di-logarithm Li_2 was introduced in Section 3.6.3. It consists of functions that are analytic in the open unit disc and have quadratically decaying power-series coefficients. Its kernel is given by

$$K(x, y) = 1 + \mathrm{Li}_2(xy) = 1 + \sum_{k=1}^{\infty} \frac{x^k y^k}{k^2}.$$

Again, we consider integration on $\Omega = (-1, 1)$ with respect to the uniform measure, i.e.

$$L_\Omega(f) = \int_{-1}^{1} f(x) \, \mathrm{d}x.$$

The extended total positivity also follows from Theorem 5.3 with $u(x) = x$ and $\lambda_k = k^{-2}$.

In order to apply the results from Chapter 5 we need a closed formula for both, the Riesz-representer ℓ_Ω and the norm $\|L_\Omega\|_{\mathcal{T}_{\mathrm{Li}_2}^\star}$ of L_Ω.

Proposition 6.2. *(i) The Riesz-representer of $L_\Omega(f) = \int_{-1}^{1} f(x) \, \mathrm{d}x$ in $\mathcal{T}_{\mathrm{Li}_2}$ is given by*

$$\ell_\Omega(x) = \frac{2 \tanh^{-1}(x)}{x} + \log(1 - x^2) + \frac{1}{2}\mathrm{Li}_2(x^2).$$

(ii) The operator norm of L in $\mathcal{T}_{\mathrm{Li}_2}$ is

$$\|L_\Omega\|_{\mathcal{T}_{\mathrm{Li}_2}^\star}^2 = 8(\log(2) - 1) + \frac{2}{3}\pi^2.$$

Proof. Regarding (i) we use $\log(1 - x) = -\sum_{k=1}^{\infty} \frac{x^k}{k}$, the definition of Li_2 and the identity $\frac{1}{k^2(k+1)} = \frac{1}{k^2} - \frac{1}{k} + \frac{1}{k+1}$ to compute

$$
\begin{aligned}
\ell(x) &= \int_{-1}^{1} K(x, y) \, \mathrm{d}y = \int_{-1}^{1} 1 + \mathrm{Li}_2(xy) \, \mathrm{d}y \\
&= 2 + \sum_{k=1}^{\infty} \frac{x^k}{k^2} \frac{(1 + (-1)^k)}{k+1} \\
&= 2 + \sum_{k=1}^{\infty} \left(x^k + (-x)^k \right) \left(\frac{1}{k^2} - \frac{1}{k} + \frac{1}{k+1} \right) \\
&= 2 + \sum_{k=1}^{\infty} \frac{x^k + (-x)^k}{k^2} - \sum_{k=1}^{\infty} \frac{x^k}{k} - \sum_{k=1}^{\infty} \frac{(-x)^k}{k} + \sum_{k=1}^{\infty} \frac{x^k + (-x)^k}{k+1} \\
&= 2 + \sum_{k=1}^{\infty} \frac{2x^{2k}}{4k^2} + \log(1 - x) + \log(1 + x) + \sum_{k=1}^{\infty} \frac{x^k + (-x)^k}{k+1} \\
&= 2 + \frac{\mathrm{Li}_2(x^2)}{2} + \log(1 - x^2) + \sum_{k=1}^{\infty} \frac{x^k + (-x)^k}{k+1}
\end{aligned}
$$

$$= 2 + \frac{\mathrm{Li}_2(x^2)}{2} + \log(1 - x^2) + \frac{2}{x} \sum_{k=1}^{\infty} \frac{x^{2k+1}}{2k+1}$$

$$= 2 + \frac{\mathrm{Li}_2(x^2)}{2} + \log(1 - x^2) + \frac{2}{x} \left(\tanh^{-1}(x) - x \right)$$

$$= \frac{\mathrm{Li}_2(x^2)}{2} + \log(1 - x^2) + \frac{2 \tanh^{-1}(x)}{x}.$$

For (ii) we first note that it holds

$$\sum_{k=1}^{\infty} \frac{1}{1 + 2k} - \frac{1}{2k} = \log(2) - 1$$

because

$$\sum_{k=1}^{\infty} \frac{1}{1 + 2k} - \frac{1}{2k} = \lim_{n \to \infty} \sum_{k=1}^{n} \frac{1}{1 + 2k} - \frac{1}{2k} = \lim_{n \to \infty} \sum_{k=1}^{n} \frac{1}{1 + 2k} + \frac{1}{2k} - \frac{1}{k}$$

$$= \lim_{n \to \infty} -1 + \sum_{k=1}^{2n} \frac{1}{k} - \sum_{k=1}^{n} \frac{1}{k} = \lim_{n \to \infty} -1 + h(2n) - h(n),$$

where $h(n)$ denotes the harmonic series. It behaves like $h(n) = \log(n) + \gamma + o(1)$, where $\gamma \approx 0.5772$ denotes the Euler-Mascheroni constant. Hence we can conclude that

$$\sum_{k=1}^{\infty} \frac{1}{1 + 2k} - \frac{1}{2k} = \lim_{n \to \infty} -1 + h(2n) - h(n) = \lim_{n \to \infty} -1 + \log(2n) - \log(n) + o(1)$$

$$= -1 + \log(2).$$

Moreover, it holds that

$$\sum_{k=1}^{\infty} \frac{2}{(1 + 2k)^2} = \frac{\pi^2 - 8}{4}$$

because

$$\sum_{k=1}^{\infty} \frac{1}{(1 + 2k)^2} = \sum_{k=1}^{\infty} \frac{1}{k^2} - 1 - \sum_{k=1}^{\infty} \frac{1}{(2k)^2} = \frac{\pi^2}{6} - 1 - \frac{\pi^2}{24} = \frac{\pi^2}{8} - 1.$$

Now we are in the position to prove (ii) by computing

$$\|L\|_{\mathcal{T}_{\mathrm{Li}_2}^*}^2 = L^{(x)} L^{(y)} K(x, y) = \int_{-1}^{1} \int_{-1}^{1} 1 + \mathrm{Li}_2(xy) \, \mathrm{d}x \, \mathrm{d}y$$

$$= 4 + \sum_{k=1}^{\infty} k^{-2} \left(\int_{-1}^{1} x^k \, \mathrm{d}x \right)^2 = 4 + \sum_{k=1}^{\infty} k^{-2} \frac{\left(1 + (-1)^k \right)^2}{(k + 1)^2}$$

$$= 4 + \sum_{k=1}^{\infty} \left(2(1 + (-1)^k) \right) \left(\frac{1}{k^2} - \frac{2}{k} + \frac{1}{(1 + k)^2} + \frac{2}{(1 + k)} \right)$$
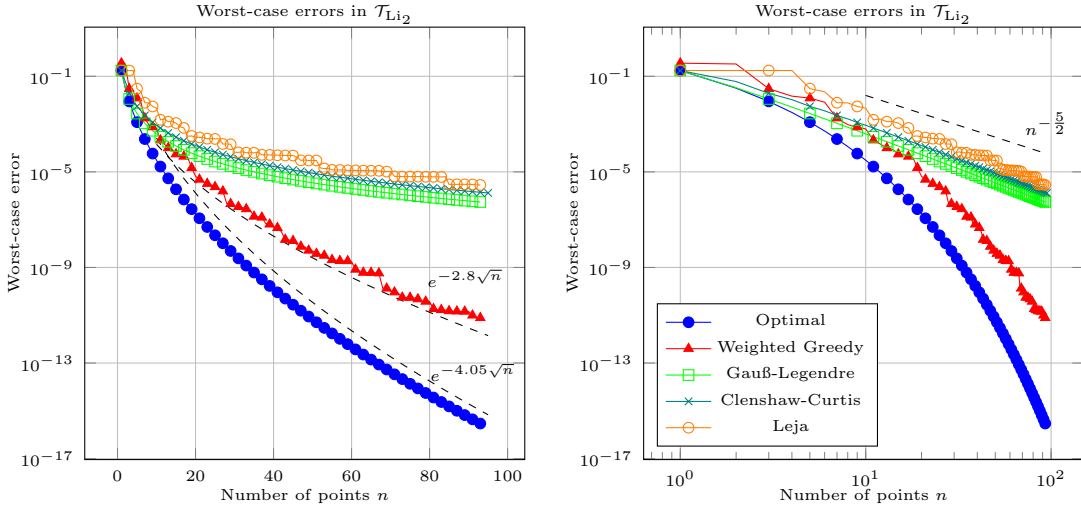
Figure 6.9: Semi-logarithmic and double-logarithmic plots for the worst-case error in the Taylor space $\mathcal{T}_{\mathrm{Li}_2}$.

$$= 4 + 2\left(\sum_{k=1}^{\infty}\frac{1+(-1)^k}{k^2} + \sum_{k=1}^{\infty}\frac{1+(-1)^k}{(1+k)^2} + \sum_{k=1}^{\infty}\frac{2(1+(-1)^k)}{(1+k)} - \frac{2(1+(-1)^k)}{k}\right)$$

$$= 4 + 2\left(\frac{1}{2}\sum_{k=1}^{\infty}\frac{1}{k^2} + \sum_{k=1}^{\infty}\frac{2}{(1+2k)^2} + 4\sum_{k=1}^{\infty}\frac{1}{1+2k} - \frac{1}{2k}\right)$$

$$= 4 + 2\left(\frac{\mathrm{Li}_2(1)}{2} + \frac{\pi^2-8}{4} + 4(\log(2)-1)\right)$$

$$= 4 + \frac{\pi^2}{6} + \frac{\pi^2-8}{2} + 8(\log(2)-1)$$

$$= \frac{2\pi^2}{3} + 8(\log(2)-1).$$

$\square$

In Figure 6.9, the worst-case error of both, the optimal and the weighted OMP greedy quadrature with $\nu(x) = \sqrt{1-x^2}$ are given. Here, the left-hand picture is a semi-logarithmic plot while the right hand picture contains the same data, but as a log-log plot. Clearly, the optimal quadrature rule converges sub-exponentially at a rate estimated by a least-squares approach to be $\exp(-4.05\sqrt{n})$. The OMP greedy method exhibits a rate of approximately $\exp(-2.8\sqrt{n})$.

In order to discuss the performance of the polynomial based approaches Gauss-Legendre, Clenshaw Curtis and Leja, the log-log-plot is more informative. Here, we see that all the polynomial based quadrature rules achieve an algebraic convergence rate of about $n^{-5/2}$. This is a clear advice to use optimal quadrature rules instead of classical ones if the integrand has singular derivatives. We will make use of this in Chapter 8 when we deal with certain integrals from econometrics.

Moreover, we computed the stability $\sigma(n)$, cf. (6.3), for the OMP greedy quadrature points in $\mathcal{T}_{\mathrm{Li}_2}$. Here, it turned out that $\sigma(n) \leq 2.4$ for all $n = 1, \ldots, 120$. We conclude that the nested quadrature rules for $\mathcal{T}_{\mathrm{Li}_2}$ obtained by the OMP greedy procedure are stable.

Finally, we also considered the distribution of optimal points in $\mathcal{T}_{\mathrm{Li}_2}$ in Figure 6.8. Similar to the Hardy space with $r = 1$ the points tend super algebraically to the boundary, albeit at a slower rate than the optimal points for the Hardy space.

6.4 The Hermite space

The univariate Hermite space $\mathcal{M}_\tau$ was introduced in Section 3.6.4 and consists of functions whose Hermite coefficients are square summable with respect to the weight τ^{-k}. Its kernel is given by the Mehler kernel, i.e.

$$K(x,y) = \frac{1}{\sqrt{1-\tau^2}} \exp\left(\frac{1}{\tau^{-1}+1}xy - \frac{1}{2(\tau^{-2}-1)}(x-y)^2\right) = \sum_{k=0}^{\infty} \tau^{-k} H_k(x) H_k(y). \quad (6.6)$$

In order to apply the results from Chapter 5 we have to make sure that K is extended totally positive. To this end, we use Theorem 5.4 with

$$\tilde{K}(x,y) = \frac{1}{\sqrt{1-\tau^2}} \exp\left(\left(\frac{1}{\tau^{-1}+1} + \frac{1}{\tau^{-2}-1}\right)xy\right) \quad \text{and} \quad v(x) = \exp\left(-\frac{1}{2(\tau^{-2}-1)}x^2\right).$$

Now, the extended total positivity of $K(x,y) = \tilde{K}(x,y)v(x)v(y)$ follows from the extended total positivity of the function $\exp(c\,xy), c > 0$, cf. [94].

We consider integration on $\mathbb{R} = (-\infty, \infty)$ with respect to the Gaussian measure, i.e.

$$L_\Omega(f) = \int_{\mathbb{R}} f(x) \frac{1}{\sqrt{2\pi}} e^{-\frac{x^2}{2}} \, \mathrm{d}x.$$

We note that the Riesz-representer ℓ_Ω and the norm $\|L_\Omega\|_{\mathcal{T}_{\mathrm{Li}_2}^\star}$ of L_Ω are given by

$$\ell_\Omega(x) = 1 \quad \text{and} \quad \|L_\Omega\|_{\mathcal{M}_\tau^\star} = 1,$$

which is a direct consequence of the series representation (6.6) and $L_\Omega(H_k) = 0$ for all Hermite polynomials H_k with $k \geq 1$.

Now we can use the algorithms from Chapter 5 to construct optimal points on the one hand and nested quadrature points on the other. For the latter, we will employ the OGA greedy method in both variants, unweighted and weighted.

For small values of $\tau \in (0, 1)$, e.g. $\tau = 0.25$, the Gauss-Hermite and the optimal quadrature rule achieve almost the same error, cf. Figure 6.10. This is not surprising because the Gaussian approach integrates the first $2n - 1$ summands of the Hermite expansion exactly and the remaining part is very small due to the strong decay of the Hermite coefficients. If on the other hand τ is close to one, there is a substantial difference between optimal quadrature and Gauss-Hermite quadrature, albeit both of them achieve an exponential convergence rate.
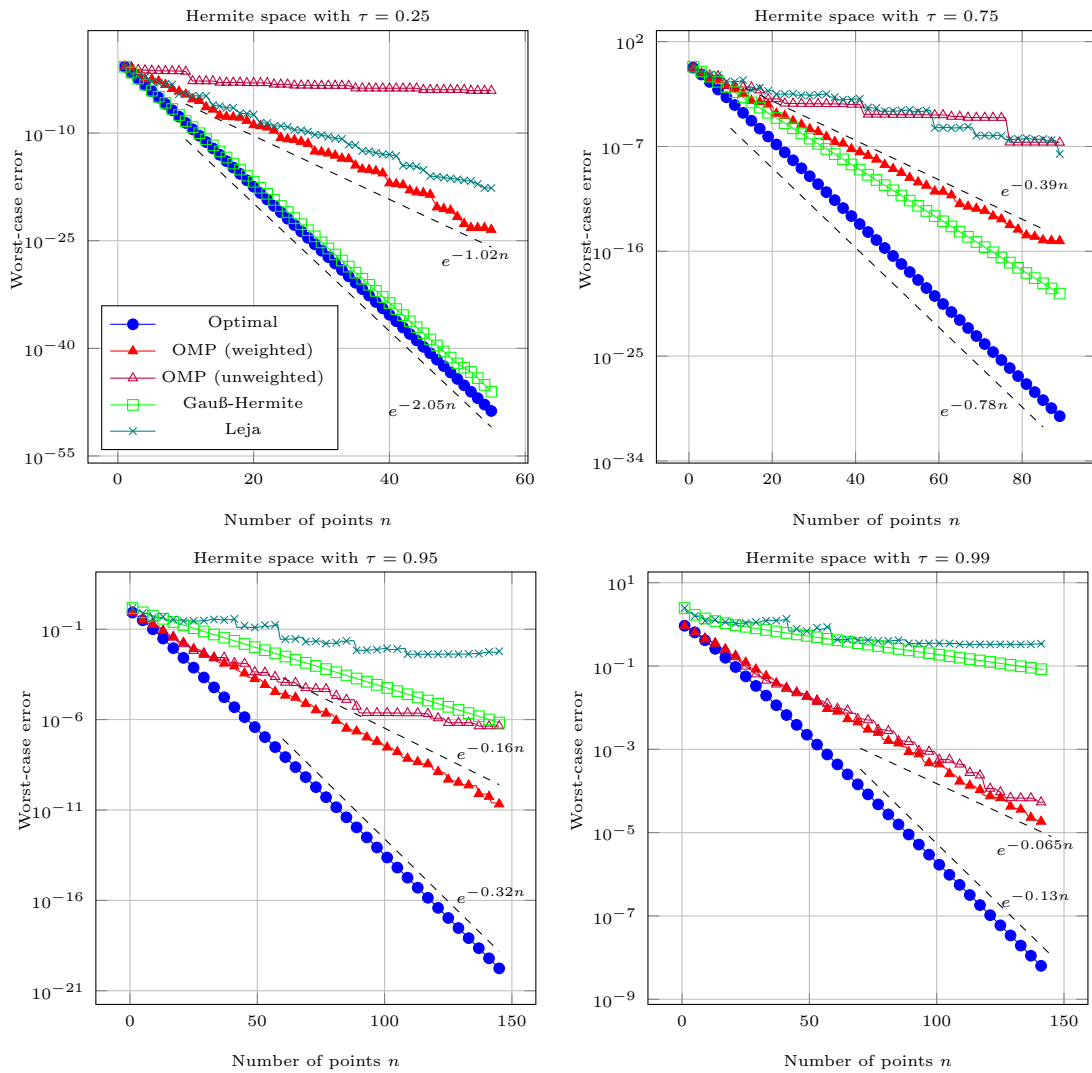
Figure 6.10: Semi-logarithmic worst-case error plots for the Hermite space $\mathcal{M}_\tau$.

Regarding the OMP greedy algorithm, we note that for small τ there is a substantial difference between the weighted and the unweighted variant. While the weighted greedy points achieve approximately half of the geometric convergence rate as the optimal points, the unweighted greedy points fail completely, especially for small τ. However, for larger τ the difference between weighted and unweighted OMP greedy points is not that prominent, albeit still clearly visible.

Finally, we also computed worst-case error for the weighted Leja sequence from Section 2.3.4. Similar to the Gauss-Hermite quadrature rule it is very competitive for small τ and almost achieves the error level as the weighted OMP greedy points. But for larger τ the convergence rate of the Leja points deteriorates until almost no convergence is visible anymore.

We also computed the values $\sigma(n)$, cf. (6.3) to study the stability of the OMP greedy quadrature points X_n for integration in $\mathcal{M}_\tau$. In all the considered settings, i.e. $\tau \in \{0.25, 0.75, 0.95, 0.99\}$
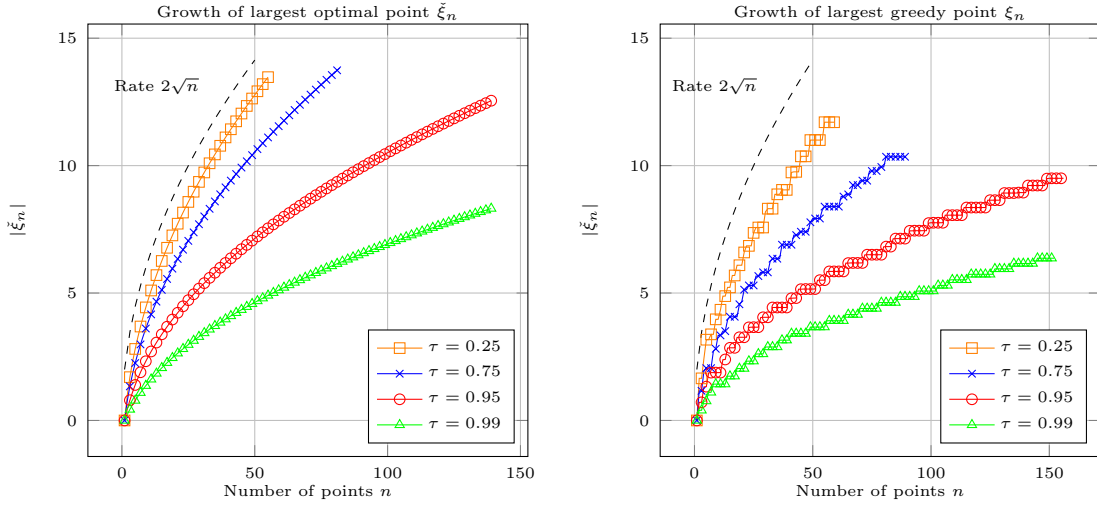
Figure 6.11: Growth of the largest optimal node and the largest greedy note for $\tau \in \{0.25, 0.75, 0.95, 0.99\}$.

the value of $\sigma(n)$ never exceeded 1.4. Therefore, we claim that the OMP greedy quadrature rules for $\mathcal{M}_\tau$ are stable.

Finally we investigated the distribution of optimal and weighted greedy points in $\mathcal{M}_\tau$. But here the greedy points do not just distribute differently, they also exhibit a different growth behaviour, as can be observed in Figure 6.11. Here, the largest optimal points grows at a sub-linear rate in all the considered settings. Even though the largest greedy point also grows sub-linearly, this happens at a substantially slower rate. We do not have an explanation for this behaviour at this point.

6.5 The Gaussian space

Our final example consists in the RKHS in which the Gaussian kernel

$$K(x,y) = \exp\left(-\gamma^2(x-y)^2\right)$$

is reproducing, cf. Section 3.6.5. Its extended total positivity is well-known and was proven in e.g. [94].

In order to apply our results from Chapter 5, we need the Riesz-representer ℓ_Ω and the norm $\|L_\Omega\|$ for $\mathcal{H}_K$ of the functional $L_\Omega(x) = \int_{-1}^1 f(x)\,\mathrm{d}x$ in closed-form. To this end, we use the change of variable $z = \gamma(x-y)$ to obtain

$$\ell_\Omega(x) = \int_{-1}^1 K(x,y)\,\mathrm{d}y = \int_{-1}^1 \exp\left(-\gamma^2(x-y)^2\right)\,\mathrm{d}y = \frac{1}{\gamma}\int_{\gamma(x-1)}^{\gamma(x+1)} e^{-z^2}\,\mathrm{d}z,$$
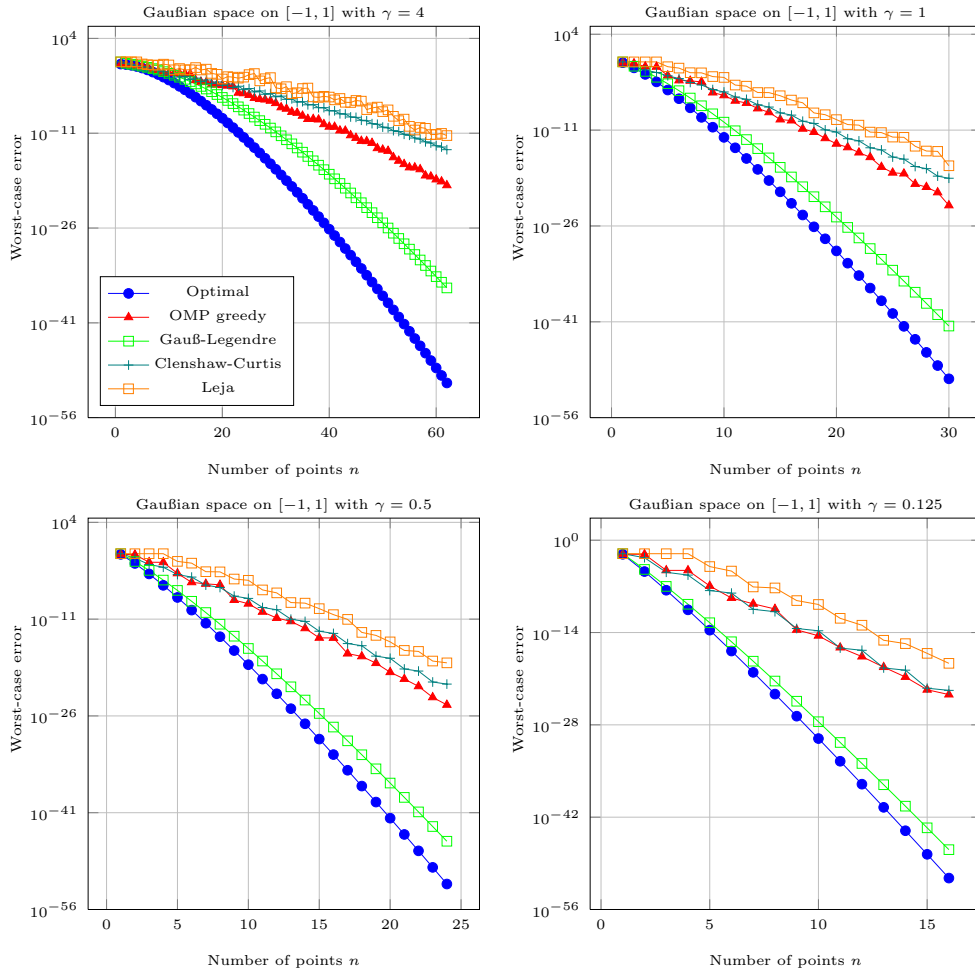
Figure 6.12: Semi-logarithmic worst-case error plots for the Gaussian space.

and by the definition of the error function $\operatorname{erf}(x) = \frac{2}{\sqrt{\pi}} \int_0^x e^{-t^2} \, \mathrm{d}t$ it holds

$$\ell_\Omega(x) = \frac{\sqrt{\pi}}{2\gamma} \left(\operatorname{erf}(\gamma(1+x)) + \operatorname{erf}(\gamma(1-x)) \right).$$

Moreover, the antiderivative of $\operatorname{erf}(x)$ is $x \operatorname{erf}(x) - e^{-x^2}/\sqrt{\pi}$. Therefore, a change of variable leads to

$$\begin{aligned}
\|L_\Omega\|_{\mathcal{H}_K^\star}^2 &= \int_{-1}^1 \int_{-1}^1 K(x,y) \, \mathrm{d}x \, \mathrm{d}y = \int_{-1}^1 \int_{-1}^1 \exp\left(\gamma^2(x-y)^2 \right) \, \mathrm{d}x \, \mathrm{d}y \\
&= \frac{\sqrt{\pi}}{2\gamma} \left(\int_{-1}^1 \operatorname{erf}(\gamma(1+x)) \, \mathrm{d}x + \int_{-1}^1 \operatorname{erf}(\gamma(1-x)) \, \mathrm{d}x \right) \\
&= \frac{2\sqrt{\pi}\gamma \operatorname{erf}(2\gamma) + e^{-4\gamma^2} - 1}{\gamma^2}.
\end{aligned}$$
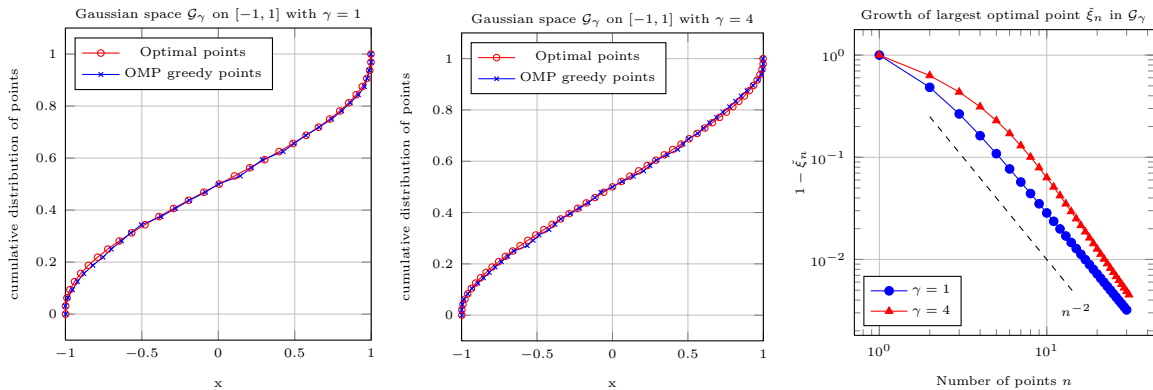
Figure 6.13: Distribution of optimal and greedy points for Gaussian spaces on $(-1, 1)$.

Now we can construct both, optimal and OMP greedy points for the Gaussian space. In Figure 6.12, we compare their worst-case errors to Clenshaw-Curtis, Leja and Gauss-Legendre quadrature for shape parameters $\gamma \in \{1/8, 1/2, 1, 4\}$. We computed worst-case errors up to 10^{-55} using arbitrary precision arithmetic [62]. Clearly, the integration problem becomes more simple if γ decreases. Moreover, we observe that the worst-case error decays super-exponentially. The results from [131] imply that it is of order $\mathcal{O}(e^{-\alpha n \log(n)})$, where $\alpha > 0$.

Regarding the stability of the OMP greedy quadrature points X_n, we computed $\sigma(n)$, cf. (6.3). In all the considered settings, i.e. $\gamma \in \{0.125, 0.5, 1, 4\}$ the value of $\sigma(n)$ never exceeded 3.2. Therefore, we claim that the OMP greedy quadrature rules for the Gaussian space are stable. However, especially for small values of γ one has to use arbitrary precision arithmetic with a sufficient accuracy to compute the weights. Here, the accuracy needs to be at least the value of the worst-case error squared. Therefore, in the given examples we used floating point arithmetic with a precision of about 800 binary digits.

Finally, Figure 6.13 compares the distribution of optimal points and OMP greedy points for $\gamma \in \{1, 4\}$. Clearly, both point construction have the same distribution, as it was also observed for the Hardy and Sobolev spaces before. Moreover, we observe a quadratic convergence of the largest optimal point to the boundary, which seems to be typical for analytic function spaces on a bounded domain.

7 Quasi–optimal tensor product integration in RKHS

This chapter is concerned with the construction of multivariate integration algorithms based on tensor products of the optimally weighted nested quadrature rules we constructed in Chapter 5.

We first deal with the properties of generalized sparse grid cubature that use univariate quadrature rules with optimal weights. In this setting, the sparse grid construction yields a multivariate cubature rule that is also optimal with respect to the weights. Therefore, the worst-case error enjoys a simplified representation and an optimal index set can be constructed without any knowledge about a priori error bounds by employing the dimension-adaptive sparse grid technique [70] to a specific function from the Hilbert space. Then, every index set which is optimal for this particular function is also optimal with respect to the worst-case error for the whole space. In combination with the greedy procedure that was proposed in Section 5.3, we therefore obtain a true black-box algorithm that only needs the univariate reproducing kernel as an input and automatically produces stable and effective integration algorithms for the multivariate problem.

Moreover, for (sub-)exponential error bounds on the univariate quadrature rules, we provide novel error bounds for the associated quasi-optimal sparse grid algorithm. These generalize the results we obtained previously in [80].

Finally, we validate both, our automatic index set construction and the theoretical upper bounds in various tensor product spaces.

7.1 Worst-case error of tensor product quadrature formulae

In this section, we deal with the problem of optimal integration in tensor products of RKHS. Here, we will follow the sparse grid paradigm from Section 2.4.2 with the additional assumption that the underlying univariate quadrature rules are nested and use optimal weights. Then, the multivariate sparse grid cubature rule inherits the property of being optimally weighted. This was already studied in [161, 162] in a more general setting. We losely follow their presentation, albeit provide different proofs for some of the results.

Let $\mathcal{H}_{K_1}, \ldots, \mathcal{H}_{K_d}$ be RKHS of functions on $\Omega_1, \ldots, \Omega_d$, respectively. Moreover, let

$$L_{\Omega_j}(f) := \int_{\Omega_j} f(x)\,\omega_j(x)\,\mathrm{d}x, \quad j = 1, \ldots, d$$

be linear functionals on $\mathcal{H}_j$. Their Riesz-representers will be denoted by

$$\ell_{\Omega_j}(x) = \int_{\Omega_j} K(x, y)\, \omega_j(y)\, \mathrm{d}y.$$

In the following we assume product structure of the integration domain $\Omega_{(d)} := \Omega_1 \times \ldots \times \Omega_d$, as well as of the weight function $\omega_{(d)}(\boldsymbol{x}) = \prod_{j=1}^d \omega_j(x_j)$. We want to approximate the functional

$$L_{\Omega_{(d)}}(f) = L_{\Omega_1} \otimes \cdots \otimes L_{\Omega_d} = \int_{\Omega_{(d)}} f(\boldsymbol{x})\, \omega_{(d)}(\boldsymbol{x})\, \mathrm{d}\boldsymbol{x}$$

using cubature algorithms of the form

$$Q_{\mathcal{A}}(f) := \sum_{\boldsymbol{k} \in \mathcal{A}} \left(\bigotimes_{j=1}^d \Delta_{k_j}^{(j)} \right) f, \tag{7.1}$$

where $\mathcal{A} \subset \mathbb{N}_0^d$ is a downward-closed set of multi-indices and $\Delta_k^{(j)} : \mathcal{H}_{K_j} \to \mathbb{R}$ is a hierarchical quadrature rule for $\mathcal{H}_{K_j}$ that can be written as linear combination of n_k function evaluations at points from nested sets $X_{n_k} \subset X_{n_{k+1}}$, i.e

$$\Delta_k^{(j)}(f) = \sum_{i=1}^{n_k} v_{i,k}^{(j)} f(\xi_i^{(j)}), \quad v_{i,k}^{(j)} \in \mathbb{R}. \tag{7.2}$$

The sequence $(n_k)_{k=0}^\infty$ is assumed to be non-decreasing and positive. In most cases, the choice $n_0 = 1$ is reasonable because the total number of function-values needed by $Q_{\mathcal{A}}$ is given by

$$N = N(Q_{\mathcal{A}}) = \sum_{\boldsymbol{k} \in \mathcal{A}} \prod_{j=1}^d (n_{k_j} - n_{k_j-1}),$$

where we define $n_{-1} = 0$ for technical reasons. In the special case $n_{k_j} - n_{k_j-1} = 1$ it holds $N = |\mathcal{A}|$.

For the construction of the $\Delta_k^{(j)} : \mathcal{H}_{K_j} \to \mathbb{R}$, $j = 1, \ldots, d$, we start from a sequence of univariate *nested quadrature rules*

$$Q_k^{(j)}(f) = \sum_{i=1}^{n_k} w_{i,k}^{(j)} f(\xi_i^{(j)}), \quad \text{for } k = 0, 1, 2, \ldots, \tag{7.3}$$

with the convention $Q_{-1}^{(j)}(f) = 0$. Note that due to the nestedness of the sets $X_k^{(j)} = (\xi_1^{(j)}, \ldots, \xi_{n_k}^{(j)})$ the labeling of the points $\xi_i^{(j)}$ in (7.3) does not depend on the level k. Moreover, we assume that the univariate quadrature rules are convergent, i.e.

$$\lim_{k \to \infty} Q_k^{(j)}(f) = L_{\Omega_j}(f), \quad \text{for all } f \in \mathcal{H}_{K_j} \text{ and } j = 1, \ldots, d. \tag{7.4}$$

Now, the aforementioned hierarchical quadrature rules associated to $Q_k^{(j)}$ can be defined by

$$
\begin{aligned}
\Delta_k^{(j)}(f) &= Q_k^{(j)}(f) - Q_{k-1}^{(j)}(f) \\
&= \sum_{i=1}^{n_k} w_{i,k}^{(j)} f(\xi_i^{(j)}) - \sum_{i=1}^{n_{k-1}} w_{i,k-1}^{(j)} f(\xi_i^{(j)}) \\
&= \sum_{i=n_{k-1}+1}^{n_k} w_{i,k}^{(j)} f(\xi_i^{(j)}) + \sum_{i=1}^{n_{k-1}} \left(w_{i,k}^{(j)} - w_{i,k-1}^{(j)} \right) f(\xi_i^{(j)}) \\
&=: \sum_{i=1}^{n_k} v_{i,k}^{(j)} f(\xi_i^{(j)}).
\end{aligned}
\tag{7.5}
$$

This definition implies by (7.4) that

$$
L_{\Omega_j}(f) = \sum_{k=1}^{\infty} \Delta_k^{(j)}(f), \quad \text{for all } j = 1, \ldots, d
$$

and hence

$$
L_{\Omega_{(d)}}(f) = L_{\Omega_1} \otimes \cdots \otimes L_{\Omega_d}(f) = \sum_{\boldsymbol{k} \in \mathbb{N}_0^d} \Delta_{\boldsymbol{k}}(f),
$$

where

$$
\Delta_{\boldsymbol{k}} f := \left(\bigotimes_{j=1}^d \Delta_{k_j}^{(j)} \right) f.
$$

In order to derive a simplified worst-case error representation for arbitrary tensor product formulas of the form (7.1), we require the following lemma.

Lemma 7.1. *Let $f(\boldsymbol{x}) := \prod_{j=1}^d f_j(x_j)$ be the product of univariate functions $f_j \in \mathcal{H}_{K_j}$. Then it holds for $Q_{\mathcal{A}}$ of the form (7.1) that*

$$
Q_{\mathcal{A}}(f) = \sum_{\boldsymbol{k} \in \mathcal{A}} \prod_{j=1}^d \left(\Delta_{k_j}^{(j)}(f_j) \right).
$$

Proof. Using the product structure of f and (7.2) we obtain

$$
\begin{aligned}
\left(\bigotimes_{j=1}^d \Delta_{k_j}^{(j)} \right) f &= \sum_{i_1=1}^{n_{k_1}} \cdots \sum_{i_d=1}^{n_{k_d}} \left(\prod_{j=1}^d v_{i_j,k_j}^{(j)} \right) \left(\prod_{j=1}^d f_j(\xi_{i_j}^{(j)}) \right) \\
&= \prod_{j=1}^d \left(\sum_{i_j=1}^{n_{k_j}} v_{i_j,k_j}^{(j)} f_j(\xi_{i_j}^{(j)}) \right) = \prod_{j=1}^d \Delta_{k_j}^{(j)}(f_j).
\end{aligned}
$$

$\square$

Now we are in the position to compute the worst-case error of $Q_{\mathcal{A}}$ with a complexity of approximately $|\mathcal{A}|^2$ instead of N^2.

Proposition 7.2. *Let $\Delta_k^{(j)}$ for $j = 1, \ldots, d$ and $k \in \mathbb{N}$ be defined as in (7.5). For any downward-closed index set $\mathcal{A} \subset \mathbb{N}_0^d$ the worst-case error of the cubature rule (7.1) is given by*

$$\|L_{\Omega_{(d)}} - Q_{\mathcal{A}}\|_{\mathcal{H}_{K_{(d)}}^\star}^2 = \prod_{j=1}^d \|L_{\Omega_j}\|_{\mathcal{H}_{K_j}^\star}^2 - 2\sum_{\boldsymbol{k} \in \mathcal{A}} \prod_{j=1}^d \Delta_{k_j}^{(j)}(\ell_{\Omega_j}) + \sum_{\boldsymbol{k} \in \mathcal{A}} \sum_{\boldsymbol{v} \in \mathcal{A}} \prod_{j=1}^d (\Delta_{k_j}^{(j)})^{(x)} (\Delta_{v_j}^{(j)})^{(y)} K_j(x,y).$$

Proof. The proof follows directly from the worst-case error formula (3.14) in Corollary 3.6, Lemma 7.1 and the product structure of both, $\ell_{\Omega_{(d)}}$ and $K_{(d)}$. $\qquad\square$

From now on, besides the nestedness of the univariate quadrature rules $Q_k^{(j)}$, we will additionally assume that the univariate quadrature rules use optimal weights $\check{\boldsymbol{w}}(X_k^{(j)})$, i.e. have the form

$$\check{Q}_k^{(j)}(f) = \sum_{i=1}^{n_k} \check{w}_{i,k}^{(j)}(X_k^{(j)}) f(\xi_i^{(j)}). \tag{7.6}$$

Here,
$$X_k^{(j)} := (\xi_1^{(j)}, \ldots, \xi_{n_k}^{(j)})$$

is a set of integration points that fulfills $X_k^{(j)} \subset X_{k+1}^{(j)}$ and

$$\check{\boldsymbol{w}}_k^{(j)}(X_k^{(j)}) = (\check{w}_{1,k}^{(j)}(X_k^{(j)}), \ldots, \check{w}_{n_k,k}^{(j)}(X_k^{(j)})) \in \mathbb{R}^{n_k}, \quad j = 1, \ldots, d \text{ and } k \in \mathbb{N}_0$$

is the vector of optimal weights that can be computed by

$$\check{\boldsymbol{w}}_k^{(j)}(X_k^{(j)}) = \boldsymbol{G}^{-1}(X_k^{(j)}, K_j)\, \boldsymbol{b}(X_k^{(j)}, K_j).$$

Consequently, we will denote the hierarchical quadrature rules that are built from the optimal quadrature rules $\check{Q}_k^{(j)}$ by

$$\check{\Delta}_k^{(j)}(f) = \check{Q}_k^{(j)}(f) - \check{Q}_{k-1}^{(j)}(f), \tag{7.7}$$

which enjoy the following orthogonality properties.

Proposition 7.3. *Let $\check{r}_{X_k^{(j)}}$ denote the Riesz-representer of $\check{R}_{X_k^{(j)}} = L_{\Omega_j} - \check{Q}_k^{(j)}$. Then it holds for $k, l \in \mathbb{N}_0$ that*

$$\langle \check{\Delta}_k^{(j)}, \check{\Delta}_l^{(j)} \rangle_{\mathcal{H}_{K_j}^\star} = \begin{cases} \|\check{R}_{X_{k-1}^{(j)}}\|_{\mathcal{H}_{K_j}^\star}^2 - \|\check{R}_{X_k^{(j)}}\|_{\mathcal{H}_{K_j}^\star}^2 & \text{for } k = l \\ 0 & \text{for } k \neq l \end{cases}. \tag{7.8}$$

In particular, we have for $k \in \mathbb{N}_0$

$$\|\check{\Delta}_k\|_{\mathcal{H}_{K_j}^\star} = \sqrt{\|\check{R}_{X_{k-1}^{(j)}}\|_{\mathcal{H}_{K_j}^\star}^2 - \|\check{R}_{X_k^{(j)}}\|_{\mathcal{H}_{K_j}^\star}^2} = \sqrt{\check{\Delta}_k(\ell_{\Omega_j})}. \tag{7.9}$$

Note here that for $k = 0$, it holds $\|\check{R}_{X_{k-1}^{(j)}}\|_{\mathcal{H}_{K_j}^\star} = \|L_{\Omega_j}\|_{\mathcal{H}_{K_j}^\star}$.

Proof. For the sake of readability, we will drop the dependence on the dimension j. We note that it holds $\check{Q}_s(\check{r}_{X_t}) = 0$ for all $s \leq t$ because $\check{r}_{X_t}(\xi_i) = 0$, $i = 1, \ldots, n_t$.

Without loss of generality assume $l \leq k$, which implies $X_l \subset X_k$. Let us treat the second case of (7.8) first. Then we have $k \geq l - 1$ and using $\check{r}_{X_{k-1}}(\xi_i) = 0, i = 1, \ldots, n_{k-1}$ we compute

$$
\begin{aligned}
\langle \check{\Delta}_k, \check{\Delta}_l \rangle_{\mathcal{H}_K^\star} &= \langle \check{Q}_k - \check{Q}_{k-1}, \check{Q}_l - \check{Q}_{l-1} \rangle_{\mathcal{H}_K^\star} \\
&= \langle L_\Omega - \check{Q}_{k-1} - (L_\Omega - \check{Q}_k), \check{Q}_l - \check{Q}_{l-1} \rangle_{\mathcal{H}_K^\star} \\
&= \langle \check{R}_{X_{k-1}} - \check{R}_{X_k}, \check{Q}_l - \check{Q}_{l-1} \rangle_{\mathcal{H}_K^\star} \\
&= \check{Q}_l(\check{r}_{X_{k-1}}) - \check{Q}_l(\check{r}_{X_k}) - \check{Q}_{l-1}(\check{r}_{X_{k-1}}) + \check{Q}_{l-1}(\check{r}_{X_k}) \\
&= 0 - 0 - 0 + 0 = 0.
\end{aligned}
$$

Regarding the first case $k = l$ we have

$$
\begin{aligned}
\langle \check{\Delta}_k, \check{\Delta}_k \rangle_{\mathcal{H}_K^\star} = \langle \check{Q}_k - \check{Q}_{k-1}, \check{Q}_k - \check{Q}_{k-1} \rangle_{\mathcal{H}_K^\star} &= \langle \check{R}_{X_{k-1}} - \check{R}_{X_k}, \check{R}_{X_{k-1}} - \check{R}_{X_k} \rangle_{\mathcal{H}_K^\star} \\
&= \|\check{R}_{X_{k-1}}\|^2_{\mathcal{H}_K^\star} + \|\check{R}_{X_k}\|^2_{\mathcal{H}_K^\star} - 2\langle \check{R}_{X_k}, \check{R}_{X_{k-1}} \rangle_{\mathcal{H}_K^\star}.
\end{aligned}
$$

Now, the first claim follows by

$$
\langle \check{R}_{X_k}, \check{R}_{X_{k-1}} \rangle_{\mathcal{H}_K^\star} = L_\Omega(\check{r}_{X_k}) - \check{Q}_{X_{k-1}}(\check{r}_{X_k}) = L_\Omega(\check{r}_{X_k}) = \|\check{R}_{X_k}\|^2_{\mathcal{H}_K},
$$

cf. (3.14) in Corollary 3.6.

The second equality in (7.9) is a direct consequence of $\|\check{R}_{X_k}\|^2_{\mathcal{H}_k^\star} = \check{R}_{X_k}(\ell_\Omega)$. $\qquad \square$

As a consequence of the univariate orthogonality property, we obtain for the tensor products

$$
\check{\Delta}_{\boldsymbol{k}} = \bigotimes_{j=1}^d \check{\Delta}_{k_j}^{(j)} \tag{7.10}
$$

the analogue result

$$
\langle \check{\Delta}_{\boldsymbol{k}}, \check{\Delta}_{\boldsymbol{l}} \rangle_{\mathcal{H}_{K_{(d)}}^\star} = 0 \quad \text{for } \boldsymbol{k} \neq \boldsymbol{l}
$$

and

$$
\langle \check{\Delta}_{\boldsymbol{k}}, \check{\Delta}_{\boldsymbol{k}} \rangle_{\mathcal{H}_{K_{(d)}}^\star} = \|\check{\Delta}_{\boldsymbol{k}}\|^2_{\mathcal{H}_{K_{(d)}}^\star} = \prod_{j=1}^d \left(\|\check{R}_{X_{k-1}^{(j)}}\|^2_{\mathcal{H}_{K_j}^\star} - \|\check{R}_{X_k^{(j)}}\|^2_{\mathcal{H}_{K_j}^\star} \right) = \check{\Delta}_{\boldsymbol{k}}(\ell_{\Omega_{(d)}}).
$$

Let $\check{\Delta}_{\boldsymbol{k}} : \mathcal{H}_{K_{(d)}} \to \mathbb{R}$ be the tensor product of the $\check{\Delta}_k^{(j)}$ given in (7.7), which are differences of optimal univariate quadrature rules $\check{Q}_k^{(j)}$ in (7.6). Then, the sparse tensor product algorithm

$$
\check{Q}_{\mathcal{A}}(f) := \sum_{\boldsymbol{k} \in \mathcal{A}} \check{\Delta}_{\boldsymbol{k}}(f) \tag{7.11}
$$

uses the information given by the function values at the set

$$
\boldsymbol{X}_{\mathcal{A}} := \bigcup_{\boldsymbol{k} \in \mathcal{A}} X_{n_{k_1}}^1 \times \ldots \times X_{n_{k_d}}^d.
$$

Theorem 7.4. *Among all algorithms that use function values at $\boldsymbol{\xi} \in \boldsymbol{X}_{\mathcal{A}}$, the algorithm $\check{Q}_{\mathcal{A}}$ in (7.11) minimizes the worst-case error.*

Proof. We recall from Section 3.2 that a linear cubature algorithm that uses function values from the set $\boldsymbol{X}_{\mathcal{A}}$ is optimal in $\mathcal{H}_{K_{(d)}}$, if and only if it integrates exactly all functions

$$\left\{ K_{(d)}(\cdot, \boldsymbol{\xi}), \boldsymbol{\xi} \in \boldsymbol{X}_{\mathcal{A}} \right\}, \quad \text{where } K_{(d)}(\cdot, \boldsymbol{\xi}) = \prod_{j=1}^{d} K_j(\cdot, \xi_j) \tag{7.12}$$

i.e. the Riesz-representers of the point evaluation functionals that it uses.

To see that this is the case, we note that for $j = 1, \ldots, d$ the univariate quadrature rules $\check{Q}_k^{(j)}$ use the points from $X_{n_{k_j}}^{(j)}$ and, due to the choice of the optimal weights, are exact on the nested sequence of spaces

$$V_k^{(j)} := \operatorname{span} \left\{ K_j(\cdot, \xi_i^{(j)}), i = 1, \ldots, n_k \right\}.$$

Now, Theorem 2.5 yields the desired exactness on (7.12). $\square$

The following corollary summarizes the results from this section.

Corollary 7.5. *Let $\check{\Delta}_{\boldsymbol{k}} : \mathcal{H}_{K_{(d)}} \to \mathbb{R}$ be as defined in (7.10), i.e. the tensor product of $\check{\Delta}_k^{(j)}$ given by (7.7), which are differences of the optimal quadrature rules $\check{Q}_k^{(j)}$ in (7.6).*

Then, the sparse tensor product algorithm

$$\check{Q}_{\mathcal{A}}(f) := \sum_{\boldsymbol{k} \in \mathcal{A}} \check{\Delta}_{\boldsymbol{k}}(f)$$

is optimal among all algorithms that use the same function values at the set

$$\boldsymbol{X}_{\mathcal{A}} := \bigcup_{\boldsymbol{k} \in \mathcal{A}} X_{n_{k_1}}^1 \times \ldots \times X_{n_{k_d}}^d.$$

Moreover, because of the orthogonality of the hierarchical tensor product rules $\check{\Delta}_{\boldsymbol{k}}$, the squared worst-case error of $\check{Q}_{\mathcal{A}}$ can be represented as either an infinite sum, i.e.

$$\left\| L_{\Omega_{(d)}} - \check{Q}_{\mathcal{A}} \right\|_{\mathcal{H}_{K_{(d)}}^\star}^2 = \sum_{\boldsymbol{k} \in \mathbb{N}_0^d \setminus \mathcal{A}} \| \check{\Delta}_{\boldsymbol{k}} \|_{\mathcal{H}_{K_{(d)}}^\star}^2$$

$$= \sum_{\boldsymbol{k} \in \mathbb{N}_0^d \setminus \mathcal{A}} \prod_{j=1}^{d} \left(\| \check{R}_{X_{k_j-1}^{(j)}} \|_{\mathcal{H}_{K_j}^\star}^2 - \| \check{R}_{X_{k_j}^{(j)}} \|_{\mathcal{H}_{K_j}^\star}^2 \right) \tag{7.13}$$

$$\leq \sum_{\boldsymbol{k} \in \mathbb{N}_0^d \setminus \mathcal{A}} \prod_{j=1}^{d} \| \check{R}_{X_{k_j-1}^{(j)}} \|_{\mathcal{H}_{K_j}^\star}^2 \tag{7.14}$$

or a finite sum which equals the error of $Q_\mathcal{A}$ for integration of $\ell_{\Omega_{(d)}}$, i.e.

$$
\begin{aligned}
\left\| L_{\Omega_{(d)}} - \check{Q}_\mathcal{A} \right\|_{\mathcal{H}_{K_{(d)}}^\star}^2 &= L_{\Omega_{(d)}}(\ell_{\Omega_{(d)}}) - \check{Q}_\mathcal{A}(\ell_{\Omega_{(d)}}) = \| L_{\Omega_{(d)}} \|_{\mathcal{H}_{K_{(d)}}^\star}^2 - \sum_{\boldsymbol{k} \in \mathbb{N}_0^d \setminus \mathcal{A}} \| \check{\Delta}_{\boldsymbol{k}} \|_{\mathcal{H}_{K_{(d)}}^\star}^2 \\
&= \prod_{j=1}^d \| L_{\Omega_j} \|_{\mathcal{H}_{K_j}^\star}^2 - \sum_{\boldsymbol{k} \in \mathcal{A}} \prod_{j=1}^d \left(\| \check{R}_{X_{k_j-1}^{(j)}} \|_{\mathcal{H}_{K_j}^\star}^2 - \| \check{R}_{X_{k_j}^{(j)}} \|_{\mathcal{H}_{K_j}^\star}^2 \right).
\end{aligned}
\tag{7.15}
$$

Using (7.15), it is possible to compute the worst-case error for any index set $\mathcal{A} \subset \mathbb{N}_0^d$ by simply computing the worst-case errors of the univariate quadrature rules $\check{Q}_k^{(j)}$. Therefore, the cost is only linear in the cardinality $|\mathcal{A}|$ of $\mathcal{A}$. Moreover, because the worst-case error of $Q_\mathcal{A}$ *equals* the integration error of $Q_\mathcal{A}$ applied to the function $\ell_{\Omega_{(d)}} \in \mathcal{H}_{K_{(d)}}$, the construction of quasi–optimal index sets can be done automatically by means of the classical dimension-adaptive sparse grid Algorithm 1 from Section 2.4.2.

For theoretical considerations however, when a priori information on the asymptotic behaviour of the univariate worst-case errors $\| \check{R}_{X_k^{(j)}} \|_{\mathcal{H}_{K_j}^\star}$ is available, the infinite sums (7.13) and (7.14) are more convenient to obtain bounds on the worst-case error of $Q_\mathcal{A}$.

Before we proceed with an a priori error analysis for analytic functions, we discuss both, a greedy technique to obtain index sets where no a priori information on $\| \Delta_{\boldsymbol{k}} \|$ is available and the choice of quasi-optimal index sets based on given bounds for $\| \Delta_{\boldsymbol{k}} \|$.

To this end, we will assume from now on, that $n_k - n_{k-1} = 1$, i.e. the point sets $X_k^{(j)}$ are maximally nested, and therefore $\Delta_k^{(j)}$ uses exactly one additional function evaluation. Actually one could also assume that $n_k - n_{k-1} = c$, where c is independent of the level k. Then, all the results would remain valid, but for the sake of readability we stick to this more simple case for now.

7.2 Adaptive construction of the index set

The choice of good index sets $\mathcal{A}$ aims to make the worst-case error (7.15) of $\check{Q}_\mathcal{A}$ as small as possible. Therefore, it is natural to define the index set such that it contains those indices $\boldsymbol{k} \in \mathbb{N}_0^d$ with the highest contribution $\| \check{\Delta}_{\boldsymbol{k}} \|$. However, there are infinitely many $\| \check{\Delta}_{\boldsymbol{k}} \|$ to compute. Besides, the downward-closedness of $\mathcal{A}$ has to be satisfied at all times. Therefore, and because of $\| \check{\Delta}_{\boldsymbol{k}} \|^2 = \check{\Delta}_{\boldsymbol{k}}(\ell_{\Omega_{(d)}})$, we propose the use of Algorithm 1 applied to the specific function $f(\boldsymbol{x}) = \ell_{\Omega_{(d)}}(\boldsymbol{x})$. The procedure is outlined in Algorithm 7. Here, step-by-step the index set $\mathcal{A}$ is constructed by searching in its direct neighbourhood for suitable candidates that promise the highest error contribution. After a suitable index $\boldsymbol{k}^*$ is found, the associated point $(\xi_{k_1^*}^{(1)}, \ldots, \xi_{k_d^*}^{(d)})$ is added to the set $\boldsymbol{X}$ and the new weight $w_{\boldsymbol{k}^*}$ is computed from the weights of the hierarchical quadrature rule $\check{\Delta}_{\boldsymbol{k}^*}$. Moreover, the weights associated to the points that are already in $\boldsymbol{X}$ also have to be updated. This leads to a total cost complexity of $\mathcal{O}(N^2)$ floating point operations, where $N = |\mathcal{A}| = |\boldsymbol{X}|$ denotes the total number of cubature points that are constructed by the algorithm. This is a substantial reduction over the naive construction of optimal weights for unstructured point sets which has a complexity of $\mathcal{O}(N^3)$ due to the inversion of a dense $N \times N$ matrix.

Algorithm 7: Dimension-adaptive construction of optimally weighted cubature rule $Q_{\mathcal{A}}$.

Input:

1. Representer $\ell_{\Omega_{(d)}} = \prod_{j=1}^{d} \ell_{\Omega_j}$ of $L_{\Omega_{(d)}}$ in $\mathcal{H}_{K_{(d)}}$.

2. Optimally weighted nested quadrature-rules $\check{Q}_{X_k}^{(j)}$ with $|X_k| = k + 1$ for $j = 1, \ldots, d$.

3. Desired accuracy $\varepsilon > 0$.

Initialize:

1. Compute the hierarchical weights of $\check{\Delta}_k^{(j)}(f) = \sum_{i=1}^{k+1} v_{i,k}^{(j)} f(\xi_i^{(j)})$.

2. Set of active indices: $\mathcal{A} = \{\mathbf{0}\}$.

3. Set of cubature points: $\boldsymbol{X} = \{(\xi_1^{(1)}, \ldots, \xi_1^{(d)})\}$.

4. Squared worst-case error: $W = \prod_{j=1}^{d} \|L_{\Omega_j}\|_{\mathcal{H}_{K_j}}^2 - \Delta_{\mathbf{0}}(\ell_{\Omega_{(d)}})$.

repeat

1. Determine admissible neighbours $\mathcal{B} = \{\mathcal{A} + \boldsymbol{e}_j : j = 1, \ldots, d\}$.

2. For all $\boldsymbol{k} \in \mathcal{B}$ compute $\|\check{\Delta}_{\boldsymbol{k}}\|_{\mathcal{H}_{K_{(d)}}^{\star}}^2$.

3. Determine (some) $\boldsymbol{k}^* = \arg\max_{\boldsymbol{k} \in \mathcal{B}} \|\check{\Delta}_{\boldsymbol{k}}\|_{\mathcal{H}_{K_{(d)}}^{\star}}^2$.

4. Add $\boldsymbol{k}^*$ and deal with hanging nodes:
   foreach $\boldsymbol{k} \leq \boldsymbol{k}^* : \boldsymbol{k} \notin \mathcal{A}$ **do**

       a) Add the index $\boldsymbol{k}$ to $\mathcal{A}$.

       b) Update worst-case error: $W := W - \|\check{\Delta}_{\boldsymbol{k}}\|_{\mathcal{H}_{K_{(d)}}^{\star}}^2$.

       c) Add the point $(\xi_{k_1+1}^{(1)}, \ldots, \xi_{k_d+1}^{(d)})$ to $\boldsymbol{X}$.

       d) Update the weights: $w_{\boldsymbol{k}} = \prod_{j=1}^{d} v_{k_j+1,k_j}^{(j)}$.
           foreach $\boldsymbol{l} < \boldsymbol{k}$ **do**
               $w_{\boldsymbol{l}} = w_{\boldsymbol{l}} + \prod_{j=1}^{d} v_{l_j+1,k_j}^{(j)}$.

           end

   end

until $\sqrt{W} < \varepsilon$;

Output:

- Cubature rule $Q_{\mathcal{A}} f = \sum_{\boldsymbol{k} \in \mathcal{A}} w_{\boldsymbol{k}} f(\xi_{k_1}^{(1)}, \ldots, \xi_{k_d}^{(d)})$ that uses $N = |\mathcal{A}|$ points.

- Worst-case error $\|L_{\Omega_{(d)}} - Q_{\mathcal{A}}\|_{\mathcal{H}_{K_{(d)}}} = \sqrt{W}$.

7.3 Quasi-optimal index sets

The choice of good index sets $\mathcal{A}$ aims to make the worst-case error (7.15) of $\check{Q}_{\mathcal{A}}$, i.e.

$$\left\| L_{\Omega_{(d)}} - \check{Q}_{\mathcal{A}} \right\|^2_{\mathcal{H}^\star_{K_{(d)}}} = \sum_{\boldsymbol{k} \in \mathbb{N}_0^d \setminus \mathcal{A}} \|\check{\Delta}_{\boldsymbol{k}}\|^2_{\mathcal{H}^\star_{K_{(d)}}},$$

as small as possible. To this end, we will assume in the following the existence of functions $\rho_j : \mathbb{N}_0 \to \mathbb{R}_+$ that fulfill

$$\rho_j(k_j) \asymp \left\| \check{\Delta}^{(j)}_{k_j} \right\|^2_{\mathcal{H}^\star_{K_j}}$$

and are monotonically decreasing. Then, the function

$$\rho(\boldsymbol{k}) := \prod_{j=1}^d \rho_j(k_j) \asymp_{d,\rho} \left\| \check{\Delta}_{\boldsymbol{k}} \right\|^2_{\mathcal{H}^\star_{K_{(d)}}}$$

is also monotonically decreasing with respect to each component $k_j, j = 1, \ldots, d$.

Hence, for a given cardinality $m \in \mathbb{N}$ a quasi–optimal index set $\mathcal{A}$ contains the m multi-indices with the highest value of $\rho(\boldsymbol{k})$. Here, the downward-closedness of $\mathcal{A}$ follows from the monotonicity of ρ.

Therefore, every downward-closed index set $\mathcal{A}$ that fulfills

$$\boldsymbol{k} \in \mathcal{A} \quad \Rightarrow \quad \rho(\boldsymbol{k}) > \rho(\boldsymbol{l}) \quad \text{for all } \boldsymbol{l} \in \mathbb{N}_0^d \setminus \mathcal{A}$$

is quasi-optimal. Consequently,

$$\mathcal{A}_\rho(\varepsilon) := \left\{ \boldsymbol{k} \in \mathbb{N}_0^d : \rho(\boldsymbol{k}) \geq \varepsilon \right\}$$

is a quasi-optimal index set. Since we are interested in analytic functions that allow for exponential or sub-exponential convergence rates, we define the family of index sets

$$\mathcal{A}_\rho(T) := \left\{ \boldsymbol{k} \in \mathbb{N}_0^d : \rho(\boldsymbol{k}) \geq e^{-T} \right\}.$$

The worst-case error of $Q_{\mathcal{A}_\rho(T)}$ can be bounded by

$$\|L_{\Omega_{(d)}} - Q_{\mathcal{A}}\|_{\mathcal{H}_{K_{(d)}}} \leq \left(\sum_{\boldsymbol{k} \in \mathbb{N}_0^d \setminus \mathcal{A}_\rho(T)} \rho(\boldsymbol{k}) \right)^{1/2}. \tag{7.16}$$

In order to derive a bound for (7.16) in terms of the total number of points $N = |\mathcal{A}_\rho(T)|$, the following two problems have to be solved.

Error bound: Bound (7.16) in terms of the parameter T by some function $G : \mathbb{R}_{\geq 0} \to \mathbb{R}_+$, i.e.

$$\sum_{\boldsymbol{k} \in \mathbb{N}_0^d \setminus \mathcal{A}_\rho(T)} \rho(\boldsymbol{k}) \asymp G(T). \tag{7.17}$$

Cost bound: Bound the cardinality of the index set $\mathcal{A}_\rho(T)$ in terms of the parameter T by some function $\eta : \mathbb{R}_{\geq 0} \to \mathbb{R}_{\geq 0}$, i.e.

$$N := |\mathcal{A}_\rho(T)| = \sum_{\boldsymbol{k} \in \mathcal{A}_\rho(T)} 1 \asymp \eta(T).$$

We will relate the discrete problem (7.17) to a continuous integral. To this end, we need the auxiliary set

$$\mathcal{E}_\rho(T) := \left\{ \boldsymbol{x} \in \mathbb{R}_{\geq 0}^d : \rho(\boldsymbol{x}) \geq e^{-T} \right\},$$

which fulfills

$$\mathcal{A}_\rho(T) = \mathcal{E}_\rho(T) \cap \mathbb{N}_0^d.$$

Moreover, let

$$\mathcal{A}_\rho^\square(T) := \bigcup_{\boldsymbol{k} \in \mathcal{A}_\rho(T)} \bigotimes_{j=1}^d [k_j, k_j + 1) \quad \subset \mathbb{R}_{\geq 0}^d.$$

Then, it holds

$$\mathcal{A}_\rho(T) \quad \subset \quad \mathcal{E}_\rho(T) \quad \subset \quad \mathcal{A}_\rho^\square(T).$$

For the treatment of (7.17) the following Lemma will be useful.

Lemma 7.6. *Let $\rho_j : \mathbb{R}_{\geq 0} \to \mathbb{R}_+$ be monotonically decreasing and fulfill*

$$\sup_{x \in \mathbb{R}_+} \frac{\rho_j(x-1)}{\rho_j(x)} < \infty \quad \text{for } j = 1, \dots, d.$$

Then it holds

$$\sum_{\boldsymbol{k} \in \mathbb{N}_0^d \setminus \mathcal{A}_\rho(T)} \rho(\boldsymbol{k}) \quad \preceq_{d,\rho} \quad \int_{\mathbb{R}_{\geq 0}^d \setminus \mathcal{E}_\rho(T)} \rho(\boldsymbol{x}) \, \mathrm{d}\boldsymbol{x}.$$

Proof.

$$\sum_{\boldsymbol{k} \in \mathbb{N}_0^d \setminus \mathcal{A}_\rho(T)} \rho(\boldsymbol{k}) = \int_{\mathbb{R}_{\geq 0}^d \setminus \mathcal{A}_\rho^\square(T)} \rho(\lfloor \boldsymbol{x} \rfloor) \, \mathrm{d}\boldsymbol{x}$$

$$= \int_{\mathbb{R}_{\geq 0}^d \setminus \mathcal{A}_\rho^\square(T)} \frac{\rho(\lfloor \boldsymbol{x} \rfloor)}{\rho(\boldsymbol{x})} \rho(\boldsymbol{x}) \, \mathrm{d}\boldsymbol{x}$$

$$\leq \sup_{\boldsymbol{z} \in \mathbb{R}_{\geq 0}^d \setminus \mathcal{A}_\rho^\square(T)} \frac{\rho(\lfloor \boldsymbol{z} \rfloor)}{\rho(\boldsymbol{z})} \int_{\mathbb{R}_{\geq 0}^d \setminus \mathcal{A}_\rho^\square(T)} \rho(\boldsymbol{x}) \, \mathrm{d}\boldsymbol{x}.$$

Now, using $(\mathbb{R}_{\geq 0}^d \setminus \mathcal{A}_\rho^\square(T)) \subset (\mathbb{R}_{\geq 0}^d \setminus \mathcal{E}_\rho(T))$, the claim follows by

$$\int_{\mathbb{R}_{\geq 0}^d \setminus \mathcal{A}_\rho^\square(T)} \rho(\boldsymbol{x}) \, \mathrm{d}\boldsymbol{x} \leq \int_{\mathbb{R}_{\geq 0}^d \setminus \mathcal{E}_\rho(T)} \rho(\boldsymbol{x}) \, \mathrm{d}\boldsymbol{x}$$

and

$$\frac{\rho(\lfloor \boldsymbol{z} \rfloor)}{\rho(\boldsymbol{z})} \leq \frac{\rho(\boldsymbol{z} - \boldsymbol{1})}{\rho(\boldsymbol{z})}.$$

$\square$

Remark 7.7. The conditions for Lemma 7.6 are easy to verify. For example, assume that $\rho_j(k) \asymp e^{-ak^p}$ and hence

$$\frac{e^{-a(k-1)^p}}{e^{-ak^p}} = \exp(a(k^p - (k-1)^p)), \tag{7.18}$$

which is constant for $p = 1$. Moreover, for $p \in (0, 1)$ the concavity of $k \mapsto k^p$ yields that (7.18) is monotonically decreasing, yet bounded from below by zero. Therefore, Lemma 7.6 is applicable. However, for $p > 1$, the convexity of $k \mapsto k^p$ implies that (7.18) is monotonically increasing and therefore unbounded, which implies that Lemma 7.6 is not applicable in this case.

Now, we can apply this approach to the setting of (sub-)exponentially decaying ρ, which appears e.g. in the treatment of analytic function spaces [80, 153].

7.4 Error bounds for (sub-)exponential decay

In this section, we extend the approach of [80] to the more general setting

$$\rho(\boldsymbol{k}) = \exp\left(-\sum_{j=1}^d a_j k_j^p\right), \quad p \in (0, 1] \text{ and } \boldsymbol{a} \in \mathbb{R}_+^d. \tag{7.19}$$

We will relate the discrete summation problem to a continuous integration problem. To this end, we define the sets

$$\mathcal{A}_{\boldsymbol{a},p}(T) = \left\{ \boldsymbol{k} \in \mathbb{N}_0^d : \sum_{j=1}^d a_j k_j^p \leq T \right\} \quad \subset \mathbb{N}_0^d$$

and

$$\mathcal{E}_{\boldsymbol{a},p}(T) = \left\{ \boldsymbol{x} \in \mathbb{R}_{\geq 0}^d : \sum_{j=1}^d a_j x_j^p \leq T \right\} \quad \subset \mathbb{R}_{\geq 0}^d.$$

Clearly, the quasi-optimal index set $\mathcal{A}_\rho(T) = \{\boldsymbol{k} \in \mathbb{N}_0^d : \rho(\boldsymbol{k}) \geq e^{-T}\}$ related to (7.19) is given by $\mathcal{A}_{\boldsymbol{a},p}(T)$.

The next Lemma links our problem to the incomplete Gamma function.

Lemma 7.8. *For $p \in (0, \infty)$ and $\boldsymbol{a} \in \mathbb{R}_+^d$ it holds that*

$$
\int\limits_{\mathbb{R}_+^d \setminus \mathcal{E}_{\boldsymbol{a},p}(T)} \exp\left(-\sum_{j=1}^d a_j x_j^p\right) \mathrm{d}\boldsymbol{x} = p^{-d} \left(\prod_{j=1}^d a_j^{-\frac{1}{p}}\right) \int\limits_{\mathbb{R}_+^d \setminus \mathcal{E}_{\boldsymbol{1},1}(T)} \exp\left(-\sum_{j=1}^d y_j\right) \left(\prod_{j=1}^d y_j^{\frac{1}{p}-1}\right) \mathrm{d}\boldsymbol{y}.
$$

Proof. The equality follows by the change of variable $y_j = a_j x_j^p$. $\qquad\square$

Next, we set $\beta := 1/p$ and concentrate on the integral

$$
\int\limits_{\mathbb{R}_+^d \setminus \mathcal{E}_{\boldsymbol{1},1}(T)} \exp\left(-\sum_{j=1}^d y_j\right) \left(\prod_{j=1}^d y_j^{\beta-1}\right) \mathrm{d}\boldsymbol{y},
$$

which for $d = 1$ equals the upper incomplete Gamma function.

$$
\int\limits_{T}^{\infty} \exp\left(-y_1\right) y_1^{\beta-1} \, \mathrm{d}y_1 = \Gamma(\beta, T).
$$

Before we proceed, we briefly discuss the incomplete Gamma function.

Remark 7.9. (Comments on the incomplete Gamma function Γ)

1. If $S \in \mathbb{R}_{\geq 0}$ is fixed, $\Gamma(\beta, S)$ is strictly increasing in β. If on the other hand $\beta \in \mathbb{N}$ is fixed, $\Gamma(\beta, S)$ is a strictly decreasing function in S. This can easily be seen from the integral representation

$$
\Gamma(\beta, S) = \int_S^\infty t^{\beta-1} e^{-t} \, \mathrm{d}t.
$$

2. For $S = 0$, it holds

$$
\int_0^\infty e^{-t} t^{\beta-1} \, \mathrm{d}t = \Gamma(\beta, 0) = \Gamma(\beta), \tag{7.20}
$$

which for $\beta \in \mathbb{N}$ equals $(\beta - 1)!$. This implies

$$
\int_0^S \exp\left(-t\right) t^{\beta-1} \, \mathrm{d}t = \Gamma(\beta) - \Gamma(\beta, S). \tag{7.21}
$$

3. For $\beta \in \mathbb{N}$, we have the equality, cf. [1]

$$
\frac{\Gamma(\beta, S)}{\Gamma(\beta)} = e^{-S} \sum_{k=0}^{\beta-1} \frac{S^k}{k!}. \tag{7.22}
$$

The following bounds for $\Gamma(\beta, S)$ will be useful.

Lemma 7.10. *For $\beta \in \mathbb{N}$ and $S \in \mathbb{R}_{\geq 0}$, it holds that*

$$e^{-S} S^{\beta-1} \leq \Gamma(\beta, S).$$

Moreover, for $B > 1$ and $S \geq B(\beta - 1)$, it holds that

$$\Gamma(\beta, S) \leq \frac{B}{B-1} e^{-S} S^{\beta-1}.$$

In particular, we have for $S \geq \beta$

$$e^{-S} S^{\beta-1} \leq \Gamma(\beta, S) \leq \beta \, e^{-S} S^{\beta-1}.$$

Proof. The lower bound follows from (7.22), while the upper bound is proven in [25]. $\qquad \square$

Moreover, we will need the following lemma.

Lemma 7.11. *For $n, k \in \mathbb{N}_0$, it holds that*

$$\int_0^S (S - x)^k x^n \, \mathrm{d}x = S^{k+n+1} \frac{k! \, n!}{(k+n+1)!}.$$

Proof. The change of variable $z = 1 - S^{-1} x$ yields

$$\int_0^S (S - x)^k x^n \, \mathrm{d}x = S^{k+n+1} \int_0^1 z^k (1 - z)^n \, \mathrm{d}z. \tag{7.23}$$

Now we use n times integration by parts to obtain

$$
\begin{aligned}
\int_0^1 z^k (1 - z)^n \, \mathrm{d}z &= \left[\frac{z^{k+1}}{k+1} (1 - z)^n \right]_0^1 - \frac{n}{k+1} \int_0^1 z^{k+1} (-1)(1 - z)^{n-1} \, \mathrm{d}z \\
&= \frac{n}{k+1} \int_0^1 z^{k+1} (1 - z)^{n-1} \, \mathrm{d}z \\
&= \frac{n(n-1)}{(k+1)(k+2)} \int_0^1 z^{k+2} (1 - z)^{n-2} \, \mathrm{d}z \\
&= \ldots \\
&= \frac{n(n-1)(n-2)\ldots(n-(n-1))}{(k+1)(k+2)(k+3)\ldots(k+(n-1)+1)} \\
&\quad \cdot \int_0^1 z^{k+(n-1)+1} (1 - z)^{n-(n-1)-1} \, \mathrm{d}z \\
&= \frac{n! k!}{(k+n)!} \int_0^1 z^{k+n} \, \mathrm{d}z \\
&= \frac{n! k!}{(k+n)!} \frac{1}{k+n+1} = \frac{n! k!}{(k+n+1)!},
\end{aligned}
$$

which in combination with (7.23) proves the claim. $\qquad \square$

Proposition 7.12. *For $S \in \mathbb{R}_{\geq 0}$, $\beta \in \mathbb{N}$ and $d \in \mathbb{N}$ we have*

$$\int_{\{\sum_{j=1}^{d} y_j \leq S\}} \exp\left(-\sum_{j=1}^{d} y_j\right) \prod_{j=1}^{d} y_j^{\beta-1} \, \mathrm{d}\boldsymbol{y} = \Gamma(\beta)^d - \Gamma(\beta)^d \frac{\Gamma(\beta d, S)}{\Gamma(\beta d)}. \tag{7.24}$$

Proof. We use mathematical induction in d. To this end, we note that (7.24) holds true for $d = 1$, cf. (7.21). Let us assume that it holds for $d \in \mathbb{N}$. Then we can compute for $d + 1$

$$\int_{\{\sum_{j=1}^{d+1} y_j \leq S\}} \exp\left(-\sum_{j=1}^{d+1} y_j\right) \prod_{j=1}^{d+1} y_j^{\beta-1} \, \mathrm{d}\boldsymbol{y}$$

$$= \int_0^S e^{-y_1} y_1^{\beta-1} \int_{\{\sum_{j=2}^{d+1} y_j \leq S-y_1\}} \exp\left(-\sum_{j=2}^{d+1} y_j\right) \prod_{j=2}^{d+1} y_j^{\beta-1} \, \mathrm{d}\boldsymbol{y}$$

$$= \int_0^S e^{-y_1} y_1^{\beta-1} \left(\Gamma(\beta)^d - \Gamma(\beta)^d \frac{\Gamma(\beta d, S-y_1)}{\Gamma(\beta d)} \right) \, \mathrm{d}y_1 \tag{7.25}$$

$$= (\Gamma(\beta) - \Gamma(\beta, S)) \Gamma(\beta)^d - \frac{\Gamma(\beta)^d}{\Gamma(\beta d)} \int_0^S e^{-y_1} y_1^{\beta-1} \Gamma(\beta d, S-y_1) \, \mathrm{d}y_1.$$

Concentrating on the integral, we continue by using (7.22) and Lemma 7.11 to compute

$$\int_0^S e^{-y_1} y_1^{\beta-1} \Gamma(\beta d, S-y_1) \, \mathrm{d}y_1 = \int_0^S e^{-y_1} y_1^{\beta-1} \Gamma(\beta d) e^{-(S-y_1)} \sum_{k=0}^{\beta d-1} \frac{(S-y_1)^k}{k!} \, \mathrm{d}y_1$$

$$= \Gamma(\beta d) e^{-S} \sum_{k=0}^{\beta d-1} \int_0^S \frac{(S-y_1)^k y_1^{\beta-1}}{k!} \, \mathrm{d}y_1 \tag{7.26}$$

$$= \Gamma(\beta d) e^{-S} \sum_{k=0}^{\beta d-1} \frac{S^{k+\beta}(\beta-1)!}{(k+\beta)!}$$

$$= \Gamma(\beta d) e^{-S} \Gamma(\beta) \sum_{k=0}^{\beta d-1} \frac{S^{k+\beta}}{(k+\beta)!}.$$

Combining (7.25) with (7.26) and using (7.22) twice, we obtain

$$\int_{\{\sum_{j=1}^{d+1} y_j \leq S\}} \exp\left(-\sum_{j=1}^{d+1} y_j\right) \prod_{j=1}^{d+1} y_j^{\beta-1} \, \mathrm{d}\boldsymbol{y}$$

$$= (\Gamma(\beta) - \Gamma(\beta, S)) \, \Gamma(\beta)^d - \frac{\Gamma(\beta)^d}{\Gamma(\beta d)} \int\limits_0^S e^{y_1} y_1^{\beta-1} \Gamma\left(\beta d, S - y_1\right) \, \mathrm{d}y_1$$

$$= \Gamma(\beta)^{d+1} - \Gamma(\beta)^d \Gamma(\beta) e^{-S} \sum_{k=0}^{\beta-1} \frac{S^k}{k!} - \frac{\Gamma(\beta)^d}{\Gamma(\beta d)} \Gamma(\beta d) e^{-S} \Gamma(\beta) \sum_{k=0}^{\beta d-1} \frac{S^{k+\beta}}{(k+\beta)!}$$

$$= \Gamma(\beta)^{d+1} - \Gamma(\beta)^{d+1} e^{-S} \left(\sum_{k=0}^{\beta-1} \frac{S^k}{k!} + \sum_{k=0}^{\beta d-1} \frac{S^{k+\beta}}{(k+\beta)!} \right)$$

$$= \Gamma(\beta)^{d+1} - \Gamma(\beta)^{d+1} e^{-S} \sum_{k=0}^{\beta(d+1)-1} \frac{S^k}{k!}$$

$$= \Gamma(\beta)^{d+1} - \Gamma(\beta)^{d+1} \frac{\Gamma(\beta(d+1), S)}{\Gamma(\beta(d+1))}.$$

$\square$

Proposition 7.12 in combination with (7.20) yields the following equality.

Corollary 7.13. *For $d \in \mathbb{N}$, $p \in (0,1]$, $1/p \in \mathbb{N}$ and $T \in \mathbb{R}_{\geq 0}$ we have*

$$\int\limits_{\mathbb{R}_+^d \setminus \mathcal{E}_{\mathbf{1},1}(T)} \exp\left(-\sum_{j=1}^d y_j \right) \left(\prod_{j=1}^d y_j^{\frac{1}{p}-1} \right) \, \mathrm{d}\boldsymbol{y} = \Gamma(1/p)^d \frac{\Gamma(d/p, S)}{\Gamma(d/p)}.$$

Moreover, using Lemma 7.8 and 7.6, we arrive at the following result.

Theorem 7.14. *Let $\boldsymbol{a} \in \mathbb{R}_+^d$ and $p \in (0,1]$ such that $1/p \in \mathbb{N}$. Then it holds for $T \geq 0$*

$$\sum_{\boldsymbol{k} \in \mathbb{N}_0^d \setminus \mathcal{A}_{\boldsymbol{a},p}(T)} \exp\left(-\sum_{j=1}^d a_j k_j^p \right) \preceq_{d,\boldsymbol{a},p} \Gamma(1/p)^d \frac{\Gamma(d/p, T)}{\Gamma(d/p)} \preceq_{d,\boldsymbol{a},p} \Gamma(d/p, T).$$

To get a complete picture, we still need to derive an estimate for the cost of $\check{Q}_{\mathcal{A}_{\boldsymbol{a},p}(T)}$, i.e. we need to derive bounds for the cardinality $|\mathcal{A}_{\boldsymbol{a},p}(T)|$. We generalize the result in [14] for $p = 1$ to arbitrary $p \in (0,1]$. To this end, we note that it holds

$$|\mathcal{A}_{\boldsymbol{a},p}(T)| = \operatorname{vol} \mathcal{A}_{\boldsymbol{a},p}^{\square}(T), \quad \text{where } \mathcal{A}_{\boldsymbol{a},p}^{\square}(T) = \bigcup_{\boldsymbol{k} \in \mathcal{A}_{\boldsymbol{a},p}(T)} [\boldsymbol{k}, \boldsymbol{k}+1). \tag{7.27}$$

The following Lemma relates (7.27) to the volume of $\mathcal{E}_{\boldsymbol{a},p}(T)$.

Lemma 7.15. *For $p \in (0,1]$ and $\boldsymbol{a} \in \mathbb{R}_+^d$ it holds that*

$$\operatorname{vol} \mathcal{E}_{\boldsymbol{a},p}(T) \quad \leq \quad |\mathcal{A}_{\boldsymbol{a},p}(T)| \quad \leq \quad \operatorname{vol} \mathcal{E}_{\boldsymbol{a},p}\left(T + \sum_{j=1}^d a_j \right).$$

Proof. The claim follows by the inclusions

$$
\mathcal{E}_{\boldsymbol{a},p}(T) \quad \subseteq \quad \mathcal{A}^{\square}_{\boldsymbol{a},p}(T) \quad \subseteq \quad \mathcal{E}_{\boldsymbol{a},p}\left(T + \sum_{j=1}^{d} a_j\right),
$$

of which the first one is obvious. The second one follows from $a_j(k_j + 1)^p \leq a_j k_j^p + a_j$ if $p \in (0,1]$. $\qquad\square$

Next, we note that it holds for all $\boldsymbol{a} \in \mathbb{R}^d_+$ and $p \in (0,\infty)$, cf. [160, Sec. 3], that

$$
\operatorname{vol} \mathcal{E}_{\boldsymbol{a},p}(T) = \left(\prod_{j=1}^{d} a_j^{-1/p}\right) T^{\frac{d}{p}} \frac{\Gamma(1 + 1/p)^d}{\Gamma(1 + d/p)},
$$

which for the special case $1/p \in \mathbb{N}$ reads

$$
\operatorname{vol} \mathcal{E}_{\boldsymbol{a},p}(T) = \left(\prod_{j=1}^{d} a_j^{-1/p}\right) T^{\frac{d}{p}} \frac{((1/p)!)^d}{(d/p)!}. \tag{7.28}
$$

Combining (7.28) with Lemma 7.15 we have arrived at the following theorem, which generalizes the result in [14].

Theorem 7.16. *For $p \in (0,1]$ with $1/p \in \mathbb{N}$ and $\boldsymbol{a} \in \mathbb{R}^d_+$, the cardinality $|\mathcal{A}_{\boldsymbol{a},p}(T)|$ can be bounded from below and above by*

$$
\left(\prod_{j=1}^{d} a_j^{-1/p}\right) T^{\frac{d}{p}} \frac{((1/p)!)^d}{(d/p)!} \quad \leq \quad |\mathcal{A}_{\boldsymbol{a},p}(T)| \quad \leq \quad \left(\prod_{j=1}^{d} a_j^{-1/p}\right) \left(T + \sum_{j=1}^{d} a_j\right)^{\frac{d}{p}} \frac{((1/p)!)^d}{(d/p)!}.
$$

Setting $N = |\mathcal{A}_{\boldsymbol{a},p}(T)|$ and defining

$$
\operatorname{gm}(\boldsymbol{a}) = \left(\prod_{j=1}^{d} a_j\right)^{1/d} \quad \text{and} \quad \kappa(x) := (x!)^{1/x}
$$

we can deduce from Theorem 7.16 that it holds

$$
T \leq N^{\frac{p}{d}} \left(\prod_{j=1}^{d} a_j^{1/p}\right)^{p/d} \left(\frac{(d/p)!}{((1/p)!)^d}\right)^{p/d} = \frac{\kappa(d/p)}{\kappa(1/p)} \operatorname{gm}(\boldsymbol{a}) N^{\frac{p}{d}}
$$

$$
T \geq N^{\frac{p}{d}} \left(\prod_{j=1}^{d} a_j^{1/p}\right)^{p/d} \left(\frac{(d/p)!}{((1/p)!)^d}\right)^{p/d} - \sum_{j=1}^{d} a_j = \frac{\kappa(d/p)}{\kappa(1/p)} \operatorname{gm}(\boldsymbol{a}) N^{\frac{p}{d}} - \sum_{j=1}^{d} a_j. \tag{7.29}
$$

Now we are prepared to prove the main result of this section.

Theorem 7.17. *For $p \in (0,1]$ with $1/p \in \mathbb{N}$ and $\boldsymbol{a} \in \mathbb{R}_+^d$, it holds that*

$$\sum_{\boldsymbol{k} \in \mathbb{N}_0^d \setminus \mathcal{A}_{\boldsymbol{a},p}(T)} \exp\left(-\sum_{j=1}^d a_j k_j^p\right) \preceq_{d,\boldsymbol{a},p} \exp\left(-\frac{\kappa(d/p)}{\kappa(1/p)} \mathrm{gm}(\boldsymbol{a}) N^{\frac{p}{d}}\right) \cdot N^{1-\frac{p}{d}}.$$

Proof. Using Theorem 7.14, the monotonicity of $\Gamma(d/p, \cdot)$ in combination with (7.29) and Lemma 7.10, we can compute for $T > d/p$

$$\sum_{\boldsymbol{k} \in \mathbb{N}_0^d \setminus \mathcal{A}_{\boldsymbol{a},p}(T)} e^{-\sum_{j=1}^d a_j k_j^p} \preceq_{d,\boldsymbol{a},p} \Gamma(d/p, T)$$

$$\leq \Gamma\left(\frac{d}{p}, \frac{\kappa(d/p)}{\kappa(1/p)} \mathrm{gm}(\boldsymbol{a}) N^{\frac{p}{d}} - \sum_{j=1}^d a_j\right)$$

$$\preceq_{d,\boldsymbol{a},p} \exp\left(-\frac{\kappa(d/p)}{\kappa(1/p)} \mathrm{gm}(\boldsymbol{a}) N^{\frac{p}{d}} + \sum_{j=1}^d a_j\right)$$

$$\cdot \left(\frac{\kappa(d/p)}{\kappa(1/p)} \mathrm{gm}(\boldsymbol{a}) N^{\frac{p}{d}} - \sum_{j=1}^d a_j\right)^{\frac{d}{p}-1}$$

$$\preceq_{d,\boldsymbol{a},p} \exp\left(-\frac{\kappa(d/p)}{\kappa(1/p)} \mathrm{gm}(\boldsymbol{a}) N^{\frac{p}{d}}\right) \cdot \left(\frac{\kappa(d/p)}{\kappa(1/p)} \mathrm{gm}(\boldsymbol{a}) N^{\frac{p}{d}}\right)^{\frac{d}{p}-1}$$

$$\preceq_{d,\boldsymbol{a},p} \exp\left(-\frac{\kappa(d/p)}{\kappa(1/p)} \mathrm{gm}(\boldsymbol{a}) N^{\frac{p}{d}}\right) \cdot N^{1-\frac{p}{d}}.$$

$\square$

In order to obtain a more simple upper bound, we use Stirling's approximation to bound

$$\frac{\kappa(d/p)}{\kappa(1/p)} > \frac{(2\pi)^{\frac{1}{2(d/p)}} (d/p)^{1+\frac{1}{2(d/p)}} e^{-1}}{e^p (1/p)^{1+p/2} e^{-1}} > \frac{(d/p) e^{-1}}{e^p (1/p)^{1+p/2} e^{-1}} = d e^{-p} p^{p/2}, \quad (7.30)$$

which implies the following Corollary, because $e^{-ax^p} x^b \preceq_{a,p,b} e^{-(a-\varepsilon)x^p}$ for all $\varepsilon > 0$.

Corollary 7.18. *Under the assumptions of Theorem 7.17, it holds*

$$\sum_{\boldsymbol{k} \in \mathbb{N}_0^d \setminus \mathcal{A}_{\boldsymbol{a},p}(T)} \exp\left(-\sum_{j=1}^d a_j k_j^p\right) \preceq_{d,\boldsymbol{a},p} \exp\left(-d\, e^{-p} p^{p/2} \mathrm{gm}(\boldsymbol{a}) N^{\frac{p}{d}}\right).$$

Remark 7.19. Note at this point that for $p = 1$ both, Theorem 7.17 and Corollary 7.18 recover the exact result from [80].

Finally, we are in the position to derive the desired upper bound for the worst-case error. To this end, we recall (7.16). Inserting the results from this section, we arrive at the following theorem.

Theorem 7.20. *Let $\boldsymbol{a} \in \mathbb{R}_+^d$ and $p \in (0,1]$ such that $1/p \in \mathbb{N}$. Assume that for each $j = 1, \ldots, d$ a sequence of optimally weighted nested quadrature rules $\check{Q}_{X_k^{(j)}}^{(j)}$ is given and the associated hierarchical quadrature rules fulfill $\|\check{\Delta}_k^{(j)}\|_{\mathcal{H}_{K_j}^\star} \asymp \exp(-a_j k^p)$.*

Then, a quasi–optimal index set for the sparse tensor product algorithm (7.1) is given by $\mathcal{A}_{\boldsymbol{a},p}(T) = \left\{ \sum_{j=1}^d a_j k_j^p \leq T \right\}$ and the worst-case error of $\check{Q}_{\mathcal{A}_{\boldsymbol{a},p}(T)}$ in $\mathcal{H}_{K_{(d)}} = \bigotimes_{j=1}^d \mathcal{H}_{K_j}$ can be bounded by

$$\left\| L_{\Omega_{(d)}} - \check{Q}_{\mathcal{A}_{\boldsymbol{a},p}(T)} \right\|_{\mathcal{H}_{K_{(d)}}^\star} \preceq_{\boldsymbol{a},d,p} \exp\left(-\frac{\kappa(d/p)}{\kappa(1/p)} \mathrm{gm}(\boldsymbol{a}) N^{\frac{p}{d}} \right) \cdot N^{\frac{1}{2} - \frac{p}{2d}}$$

$$\preceq_{\boldsymbol{a},d,p} \exp\left(-d\, e^{-p} p^{p/2} \mathrm{gm}(\boldsymbol{a}) N^{\frac{p}{d}} \right). \tag{7.31}$$

Using Theorem 7.17 and (7.16) we compute

Proof.

$$\left\| L_{\Omega_{(d)}} - \check{Q}_{\mathcal{A}_{\boldsymbol{a},p}(T)} \right\|_{\mathcal{H}_{K_{(d)}}^\star} = \left(\sum_{\boldsymbol{k} \in \mathbb{N}_0^d \setminus \mathcal{A}_{\boldsymbol{a},p}(T)} \|\Delta_{\boldsymbol{k}}\|_{\mathcal{H}_{K_{(d)}}}^2 \right)^{1/2}$$

$$\preceq_{\boldsymbol{a},d,p} \left(\sum_{\boldsymbol{k} \in \mathbb{N}_0^d \setminus \mathcal{A}_{\boldsymbol{a},p}(T)} \exp\left(-\sum_{j=1}^d 2 a_j k_j^p \right) \right)^{1/2}$$

$$\preceq_{\boldsymbol{a},d,p} \left(\exp\left(-\frac{\kappa(d/p)}{\kappa(1/p)} \mathrm{gm}(2\boldsymbol{a}) N^{\frac{p}{d}} \right) \cdot N^{1 - \frac{p}{d}} \right)^{1/2}$$

$$= \exp\left(-\frac{\kappa(d/p)}{\kappa(1/p)} \mathrm{gm}(\boldsymbol{a}) N^{\frac{p}{d}} \right) \cdot N^{\frac{1}{2} - \frac{p}{2d}}.$$

The inequality (7.31) follows from (7.30), cf. Corollary 7.18.   □

7.5   Numerical experiments

This section is devoted to the validation of the algorithm proposed in Section 7.2 on the one hand and the theoretical results from Section 7.4 on the other. To this end, we compute optimal index sets $\mathcal{A}$ by means of Algorithm 7 and compute the worst-case error associated to $\check{Q}_{\mathcal{A}}$ using the worst-case error formula (7.15). As underlying univariate quadrature rules for approximation of L_{Ω_j} in $\mathcal{H}_{K_j}$, we will employ the optimally weighted nested quadrature rules obtained by the OMP greedy approach from Section 5.3.

The numerical results are then compared to the worst-case error predicted by Theorem 7.20, i.e.

$$\mathbf{wce}(\check{Q}_{\mathcal{A}_{\boldsymbol{a},p}(T)}, \mathcal{H}_{K_{(d)}}) \preceq_{\boldsymbol{a},d,p} \exp\left(-\frac{\kappa(d/p)}{\kappa(1/p)} \mathrm{gm}(\boldsymbol{a}) N^{\frac{p}{d}} \right) \cdot N^{\frac{1}{2} - \frac{p}{2d}}, \tag{‡}$$

where the values of $\boldsymbol{a}$ and p stem from (sub-)exponential upper bounds on the hierarchical

quadrature rules of the form

$$\|\check{\Delta}_k^{(j)}\|_{\mathcal{H}_{K_j}^\star} \le c \exp(-a_j k_j^p), \quad j = 1, \dots, d.$$

To this end, we need a bound for $\|\Delta_k^{(j)}\|_{\mathcal{H}_{K_j}^\star}$. Here, Proposition 7.3 implies the bound

$$\|\check{\Delta}_k^{(j)}\|_{\mathcal{H}_{K_j}^\star} = \sqrt{\|\check{R}_{X_{k-1}^{(j)}}\|_{\mathcal{H}_{K_j}^\star}^2 - \|\check{R}_{X_k^{(j)}}\|_{\mathcal{H}_{K_j}^\star}^2} \le \|\check{R}_{X_{k-1}^{(j)}}\|_{\mathcal{H}_{K_j}^\star}, \tag{7.32}$$

where, throughout this section, $\|\check{R}_{X_{k-1}^{(j)}}\|_{\mathcal{H}_{K_j}^\star}$ is the worst-case error of the optimally weighted univariate quadrature rule using the points $X_k^{(j)} = (\xi_1^{(j)}, \dots, \xi_{k+1}^{(j)})$ that are constructed by the OMP greedy method from Section 5.3.

We compare the optimally weighted sparse grid algorithm with classical sparse grids that are based on non-optimal univariate quadrature rules. Then, however, it is not possible to automatically construct optimal index sets that minimize the worst-case error, because the worst-case error formula does not offer a suitable simplification.

7.5.1 Hardy space

The d-fold tensor product of Hardy spaces

$$\mathbb{H}_{\boldsymbol{r}} = \mathbb{H}_{r_1} \otimes \cdots \otimes \mathbb{H}_{r_d}$$

consists of functions that are analytic in polydiscs

$$\mathbb{D}_{\boldsymbol{r}} = \{\boldsymbol{z} \in \mathbb{C}^d : |z_j| < r_j\}$$

with radii $r_1, \dots, r_d \in [1, \infty)$.

The performance of the OMP greedy method in univariate $\mathbb{H}_r$ has been studied in Section 6.2. Our first example consists of a d-fold tensor product of $\mathbb{H}_r$ with either $r = 1.01$ or $r = 1.25$. As these are isotropic examples, we will omit the parameter j in the following.

From Figure 6.4 in combination with (7.32), we obtain the bounds

$$\|\Delta_k\|_{\mathbb{H}_{1.01}^\star} \preceq \exp(-0.41k) \quad \text{and} \quad \|\Delta_k\|_{\mathbb{H}_{1.25}^\star} \preceq \exp(-0.85k),$$

respectively. These values are inserted for a_j into (‡) with $p = 1$ and plotted as dashed lines in the upper row of Figure 7.1. Clearly, the observed worst-case errors of $Q_{\mathcal{A}}$, where $\mathcal{A}$ is constructed automatically by Algorithm 7, match the predicted rate of a sparse grid method with quasi–optimal index set in $\mathbb{H}_{\boldsymbol{r}}$.

Moreover, in both cases the optimally weighted tensor product method clearly outperforms the sparse grid based on Clenshaw-Curtis quadrature and the classical Smolyak index set. However, for $r = 1.25$ the difference is less prominent than for $r = 1.01$. For a larger radius r the error of both methods improves substantially.
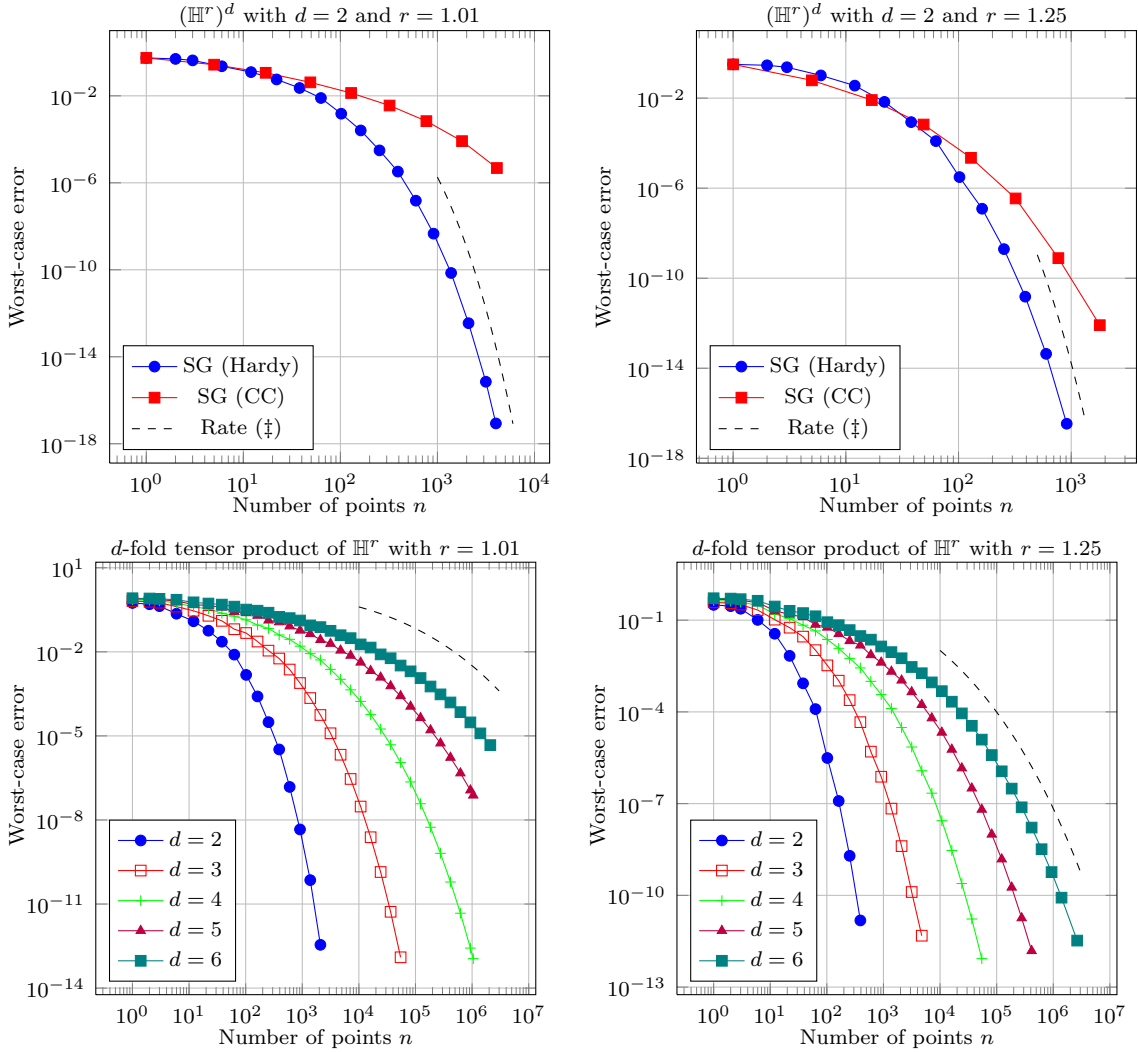
Figure 7.1: Worst-case errors in tensor products of Hardy spaces $\mathbb{H}_{1.01}$ and $\mathbb{H}_{1.25}$.

In the lower row of Figure 7.1, the worst-case errors of $Q_{\mathcal{A}}$ for dimensionalities $d = 2, \ldots, 6$ are given. We can see the deterioration of the convergence rate as the dimensionality d of the tensor product space increases. However, the super-algebraic rate is clearly visible in all the considered cases.

As before, the dashed line represents the bound ($\ddagger$). Here, it is only given for $d = 6$ where it matches the observed worst-case error quite well.

Finally, in Figure 7.2 an index set derived by Algorithm 7 for the bivariate tensor product Hardy space $\mathbb{H}_{1.25} \otimes \mathbb{H}_{1.25}$ is depicted. It basically has the expected structure $\{k_1 + k_2 \leq T\}$, i.e. a simplex. The point set associated to this particular index set is given on the right-hand side.
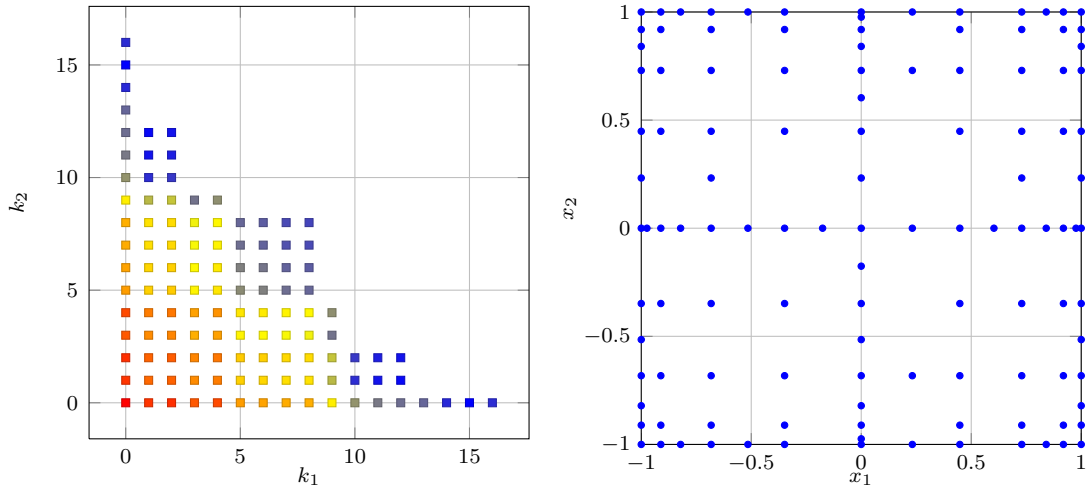
Figure 7.2: Optimal index set with associated $N = 116$ points for integration in the Hardy space $\mathbb{H}^2_{1.25}$. The colors encode the magnitude of $\|\check{\Delta}_{\boldsymbol{k}}\|$.

7.5.2 Taylor space generated by the di-logarithm

The d-fold tensor product of the Taylor space $\mathcal{T}_{\text{Li}_2}$ is denoted by $\mathcal{T}^d_{\text{Li}_2}$ and contains functions on $[-1, 1]^d$ whose mixed partial derivatives of order one are in $\mathbb{H}_{\mathbf{1}} = \bigotimes^d_{j=1} \mathbb{H}_1$, i.e.

$$\frac{\partial^{|\mathbf{u}|}}{\prod_{j\in\mathbf{u}} \partial x_j} f(\boldsymbol{x}) \in \mathbb{H}_{\mathbf{1}} \quad \text{for all } |\mathbf{u}|_\infty \leq 1.$$

The performance of the OMP greedy method in univariate $\mathcal{T}_{\text{Li}_2}$ has been studied in Section 6.3. From Figure 6.9 in combination with (7.32) we obtain the bound

$$\|\Delta_k\|_{\mathcal{T}^\star_{\text{Li}_2}} \preceq \exp(-2.8\sqrt{k}).$$

This is inserted for a_j into (‡) with $p = 1/2$ and plotted as dashed lines in Figure 7.3. Clearly, the observed worst-case errors of $Q_{\mathcal{A}}$, where $\mathcal{A}$ is constructed automatically by Algorithm 7 based on the univariate OMP greedy point set for $\mathcal{T}_{\text{Li}_2}$, match the predicted rate.

Moreover, we get for the Clenshaw-Curtis method in the univariate $\mathcal{T}_{\text{Li}_2}$ the algebraic convergence rate n^{-s} with $s = 5/2$ from Figure 6.9. Inserting this into the standard sparse grid error bound $N^{-s} \log(N)^{(d-1)(s+1/2)}$, cf. [140], yields the observed rate of the Clenshaw Curtis sparse grid. The sub-exponential rate obtained by the optimal cubature rule offers a clear advantage over the algebraic rate of the conventional Clenshaw-Curtis sparse grid.

Moreover, in Figure 7.4 an index set generated by Algorithm 7 for the bivariate Taylor space $\mathcal{T}^2_{\text{Li}_2}$ is depicted. It has approximately the expected structure $\{k_1^{1/2} + k_2^{1/2} \leq T\}$, i.e. a ball with respect to the $\ell_{1/2}$ quasi norm. The associated point set is given on the right-hand side. It appears that the points get denser around the boundary of $[-1, 1]^2$ than it is the case for the Hardy example from before.
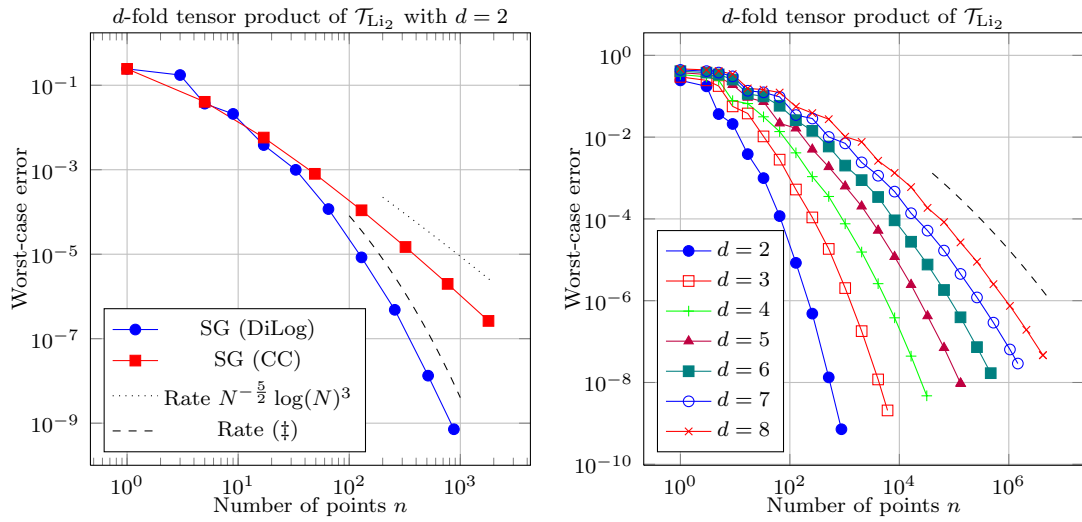
Figure 7.3: Worst-case error in the Taylor space $\mathcal{T}_{\mathrm{Li}_2}$ generated by the di-logarithm.
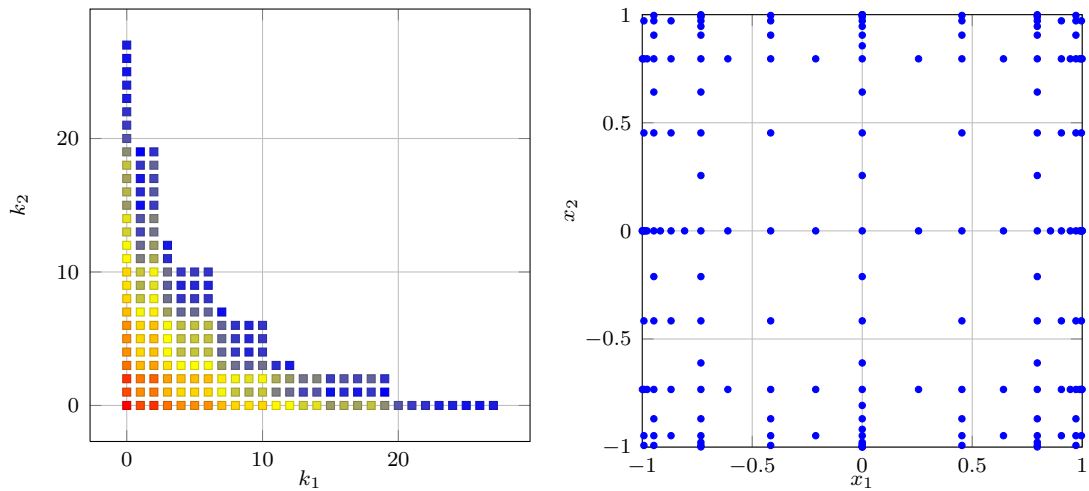
Figure 7.4: Optimal index set with associated $N = 180$ points for integration in the bivariate Taylor space $\mathcal{T}_{\mathrm{Li}_2}^2$.
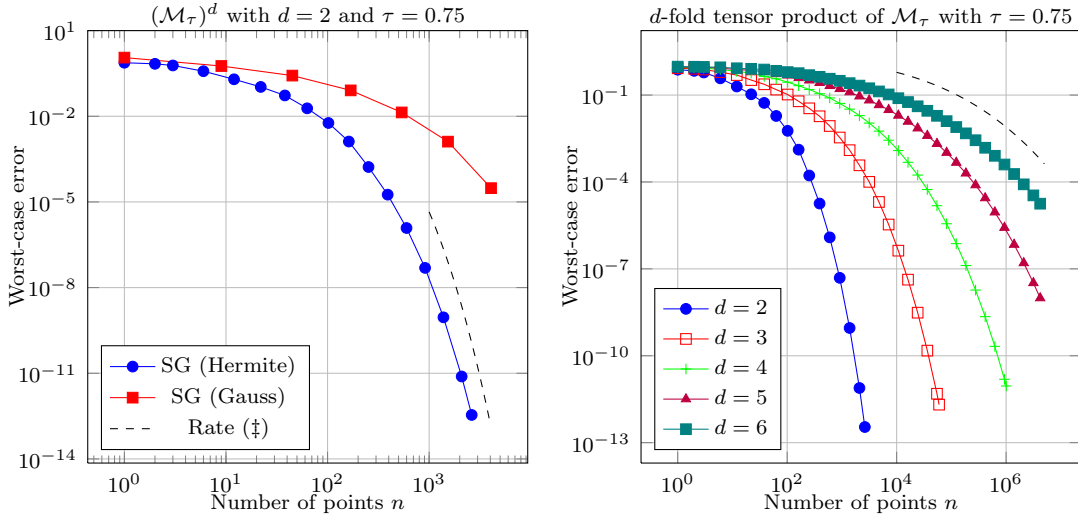
Figure 7.5: Worst-case errors in the Hermite space $\mathcal{M}_{3/4}$.

7.5.3 Hermite space

The d-fold tensor product of the Hermite space $\mathcal{M}_\tau$ is denoted by $\mathcal{M}_{\boldsymbol{\tau}}^d$ and contains functions on $\mathbb{R}^d$ whose Hermite coefficients

$$\hat{f}_{\boldsymbol{k}} = \frac{1}{(2\pi)^{d/2}} \int_{\mathbb{R}^d} f(\boldsymbol{x}) \left(\prod_{j=1}^{d} H_{k_j}(x_j) \right) e^{-\frac{\boldsymbol{x}^{\mathsf{T}}\boldsymbol{x}}{2}} \, \mathrm{d}\boldsymbol{x}$$

are summable with respect to the weight induced by $\boldsymbol{\tau} = (\tau_1, \ldots, \tau_d) \in (0,1)^d$, i.e.

$$\sum_{\boldsymbol{k} \in \mathbb{N}_0^d} \hat{f}_{\boldsymbol{k}}^2 \prod_{j=1}^{d} \tau_j^{-k_j}.$$

The performance of the OMP greedy method in the univariate $\mathcal{M}_\tau$ has been studied in Section 6.4.

From Figure 6.10 in combination with (7.32) we obtain for the asymptotics of the univariate quadrature rules the estimate

$$\|\Delta_k\|_{\mathcal{M}_{0.75}^\star} \preceq \exp(-0.39k).$$

This is inserted for a_j into (‡) with $p = 1$ and plotted as dashed lines in 7.5. Clearly, the observed worst-case errors of $Q_{\mathcal{A}}$, where $\mathcal{A}$ is constructed automatically by Algorithm 7 based on the univariate OMP greedy point set for $\mathcal{M}_{0.75}$, match the predicted rate of a sparse grid method with quasi–optimal index set in $\mathcal{M}_{0.75}^\star$. Moreover, we compare the optimally weighted tensor product method with classical sparse grids based on Gauss-Hermite quadrature, which is not nested. Even though the Gauss-Hermite based sparse grid exhibits super algebraic convergence
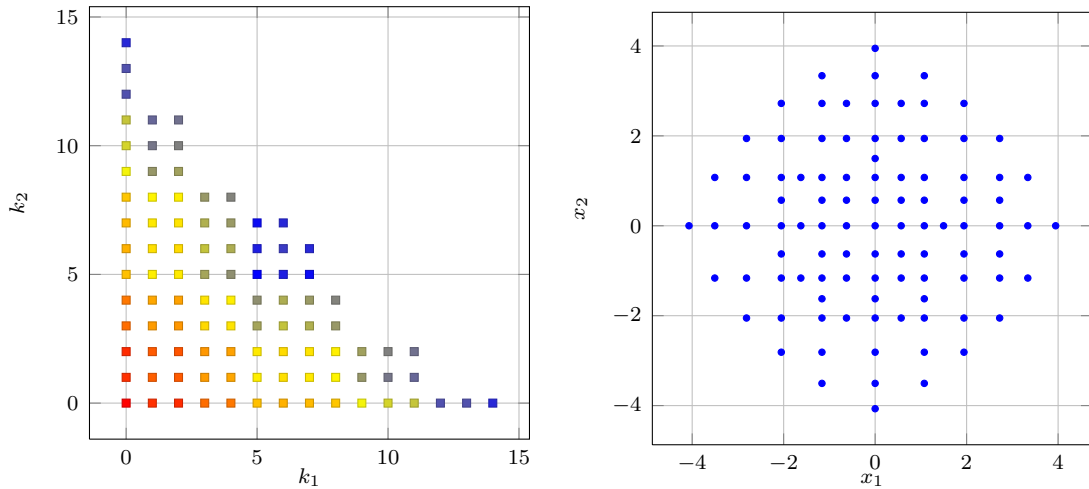
Figure 7.6: Optimal index set with associated $N = 97$ points for integration in the bivariate Hermite space $\mathcal{M}^2_{3/4}$. The colors encode the magnitude of $\|\check{\Delta}_{\boldsymbol{k}}\|$.

it is clearly dominated by the approach that is specifically tailored to the Hermite space by using optimal weights and the OMP greedy points.

As the dimension d gets larger the isotropic problem gets considerably harder, as it can be observed on the right-hand side plot of Figure 7.5. Here, the worst-case errors of the optimally weighted tensor product rules are given for dimensionalities $d = 2, \ldots, 6$. Clearly, for both, $d = 2$ and $d = 6$, our predicted convergence rate matches the one that is computed by Algorithm 7.

Finally, in Figure 7.6 an automatically generated index set and the associated point set are given. Here, similarly to the Hardy example, the index set has the expected structure of a regular simplex, i.e. $\{k_1 + k_2 \leq T\}$. The points are distributed regularly within the region where the Gaussian measure exhibits its biggest mass, i.e. they are centered around zero and get less dense in regions with large distance from the origin.

7.5.4 An anisotropic example

Finally, we will deal with an anisotropic example, i.e. tensor products of different function spaces. Here, we consider

$$H^1 \otimes \underbrace{\mathbb{H}_{1.25} \otimes \cdots \otimes \mathbb{H}_{1.25}}_{(d-1) \text{ times}},$$

i.e. the tensor product of a Sobolev space with the $(d-1)$-fold tensor product of analytic Hardy spaces.

In Figure 7.7, the worst-case errors associated to this setting are plotted. We considered dimensions $d = 1, \ldots, 6$. For $d = 1$, the Hardy space is not present at all and we observe the rate N^{-1}, which can be expected for the univariate Sobolev space. Now, when the dimension d is increased, the convergence rate basically stays the same and the dimensionality of the Hardy space only influences the preasymptotic regime. For the setting of linear information, this kind of behaviour was predicted e.g. in [42].
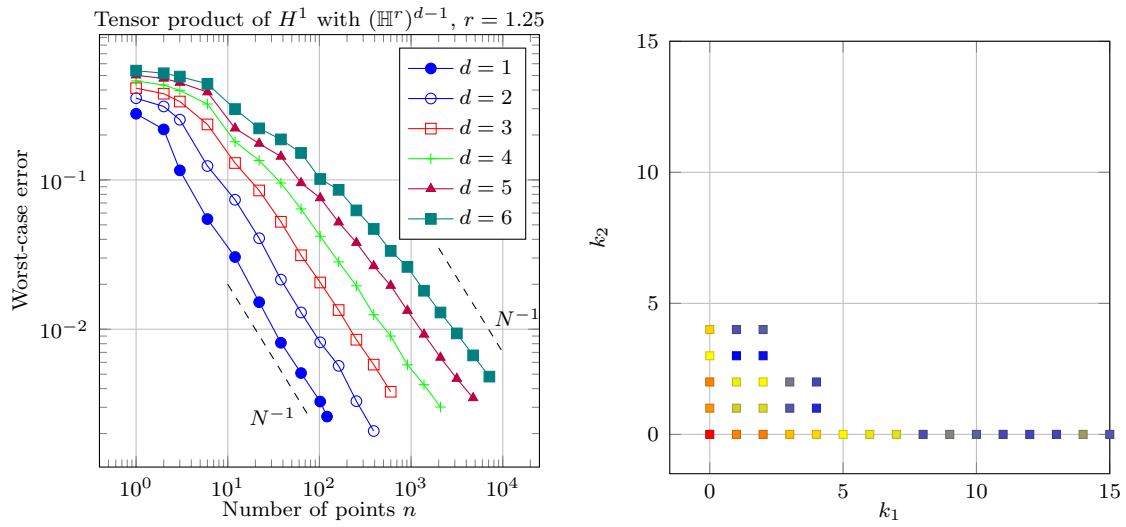
Figure 7.7: Left: Worst-case error in mixed-Sobolev-Hardy space. Right: An index set typical for this constellation.

On the right-hand side of Figure 7.7, an index set for the bivariate case $H^1 \otimes \mathbb{H}_{1.25}$ is depicted. Clearly, the greedy approach from Algorithm 7 correctly identifies the structure of this space and pays more emphasis in the directions associated to the Sobolev space. This is not surprising because substantially more points are required in the Sobolev direction than in the Hardy directions in order to balance all the error contributions.

8 Applications

This chapter is concerned with the application of this thesis' results to practical integration problems. To this end, we first deal with some simple test functions that fit into the different settings considered so far.

Then, we deal with an integration problem from econometrics, where researchers often face smooth and moderate-dimensional integrals, which are ideal to be treated with sparse grid techniques [87]. Here, we consider discrete choice models which aim at explaining and predicting the behaviour of individuals that are facing the choice between two or more discrete alternatives. Examples are the decision which car to buy or whether to invest savings into risky or more conservative asset classes. We concentrate on the multivariate probit model whose estimation requires the computation of multivariate normal probabilities. To this end, we use the so-called Genz algorithm [66] in combination with optimal tensor products of the quadrature rules for the Taylor space generated by the di-logarithm, i.e. $\mathcal{T}_{\mathrm{Li}_2}$.

Our second application is related to differential equations which often depend on parameters that are not always known precisely. Therefore, practitioners are interested in the uncertainty of the solution, given the uncertainty of the input. Here, we concentrate on an elliptic differential equation whose diffusion coefficient is parameterized on d patches of the spatial domain. The computation of the mean of the solution as well as the mean of other quantities of interest derived from particular solutions requires the solution of high-dimensional integrals as well.

In both, the econometric model problem and also the parametric differential equation, we identify scenarios where the approach developed in this thesis offers a substantial reduction of computational cost over conventional methods. However, there are also settings where our approach is not better, but not worse either.

8.1 Synthetic test functions

To validate our construction we start with simple test functions that have a certain multiplicative structure. We compare dimension-adaptive sparse grids, cf. Section 2.4.3, that are based on our new optimally weighted and nested quadrature rules with other state-of-the-art cubature algorithms. Here, we consider dimension-adaptive sparse grids based on Clenshaw-Curtis and Leja points as well as plain Monte Carlo and quasi–Monte Carlo based on the Sobol sequence. Our first test function is

$$f_d(\boldsymbol{x}) = \prod_{j=1}^{d} 1 + \frac{((1 - x_j)(1 + x_j))^{7/8}}{8}, \tag{8.1}$$

which is bounded in $[-1, 1]$ but has a singular first derivative. Therefore, it fits into the setting of $\mathcal{T}_{\mathrm{Li}_2}$, i.e. the Taylor space of bounded analytic function with derivative in the Hardy space
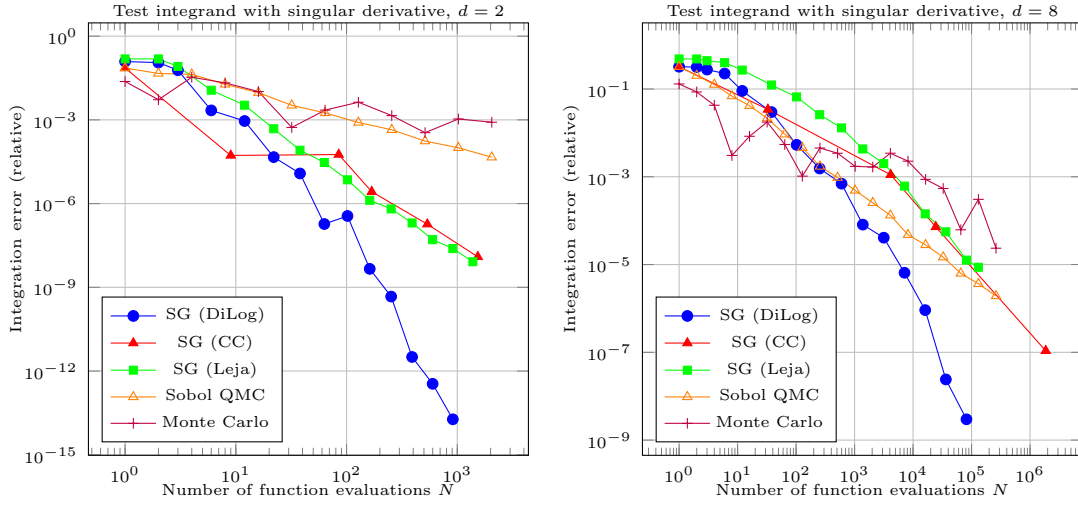
Figure 8.1: Test function (8.1) associated to $\mathcal{T}_{\mathrm{Li}_2}$.

$\mathbb{H}_1$. Since this space is generated by the di-logarithm Li_2, we use the sparse grid that is based on the OMP greedy quadrature rule obtained by Algorithm 6 with weight $\nu(x) = \sqrt{1 - x^2}$. It is denoted by SG(DiLog). Moreover, we consider SG(CC) and SG(Leja) which are dimension-adaptive sparse grids based on Clenshaw-Curtis and Leja quadrature, respectively.

The results for dimension $d = 2$ and $d = 8$ are given in Figure 8.1. The new approach clearly offers an advantage over the conventional methods, which only converge algebraically. However, the SG(DiLog) approach exhibits a super-algebraic rate as it is predicted by the results in Chapter 7.

The next example is related to the Hardy space $\mathbb{H}_r$ with $r > 1$. Since we are on a bounded domain and all derivatives of functions in $\mathbb{H}_r$ are bounded in $[-1, 1]$, we can use the unweighted OMP greedy quadrature obtained by Algorithm 4 as building block for the dimension-adaptive sparse grid denoted by SG (Hardy).

We consider the test function

$$f_d(\boldsymbol{x}) = \prod_{j=1}^{d} \left(1 + \frac{1}{2^j(1.02 - x_j)(1.02 + x_j)} \right), \tag{8.2}$$

which clearly fulfills $f_d \in \mathbb{H}_{1.02}$.

The results are given in Figure 8.2 for dimensions $d = 2$ and $d = 8$. Even though the Leja-based sparse grid is pre-asymptotically inferior to all the other considered methods, in the long run it achieves the same asymptotic convergence rate as the sparse grid that is specifically tailored to the Hardy space $\mathbb{H}_{1.02}$. However, in $d = 8$ the preasymptotic problems of the Leja approach gets so bad that it converges even worse than Monte Carlo, at least in the regime up to 10^5 points. However, SG (Hardy) reaches a relative error of 10^{-6} with less than 3×10^4 function values, whereas the Clenshaw-Curtis based adaptive sparse grid SG (CC) needs more than 10^6 points for the same accuracy.
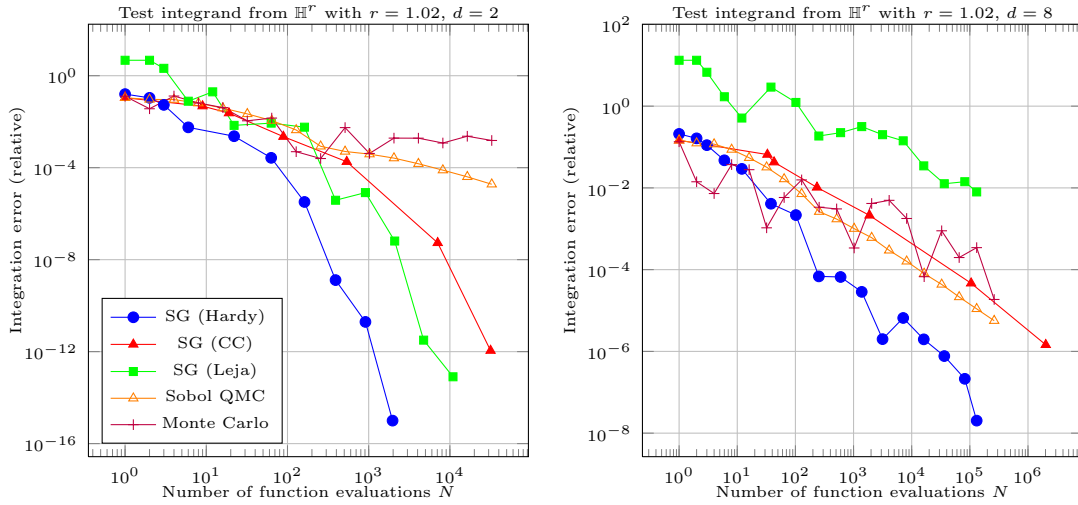
Figure 8.2: Test function (8.2) for the Hardy space setting.

Our final example is related to the Hermite space and deals with integration on $\mathbb{R}$ with respect to the Gaussian probability density function, i.e.

$$\int_{-\infty}^{\infty} f(x) \frac{e^{-\frac{x^2}{2}}}{\sqrt{2\pi}} \, \mathrm{d}x. \tag{8.3}$$

The test function is

$$f_d(\boldsymbol{x}) = \prod_{j=1}^{d} \exp\left(-\frac{t^2}{2(1-t^2)} x_j^2 + x_j\right), \tag{8.4}$$

where we choose $t = 0.9$ to fit into the $\mathcal{M}_{0.9}$ setting.

We compare the performance of the dimension-adaptive sparse grids based on the optimal quadrature rule obtained by Algorithm 6 with $\nu(x) = \sqrt{\exp(-x^2/2)}$, i.e. SG (optimal). We compare this with Monte Carlo that is based on random function values drawn according to the standard normal distribution on $\mathbb{R}^d$. Moreover, we consider sparse grids based on the Leja sequence from Section 2.3.4, which is suited for the integration problem (8.3). Finally, we consider sparse grids based on Gauss-Hermite, which, however, are not nested.

In Figure 8.3, the relative integration errors for $d = 2$ and $d = 6$ are given. For small dimensionalities the polynomial based approaches SG (Leja) and SG (Hermite) achieve exponential convergence, albeit at a slower rate than the optimally weighted sparse grid SG (optimal). However, as the dimension increases the polynomial based approaches get difficulties because on their first level they are exact for constant functions. The function in (8.4), however, is far away from being constant. Instead, for large dimensions it behaves like a Dirac function which is difficult to approximate with polynomials.
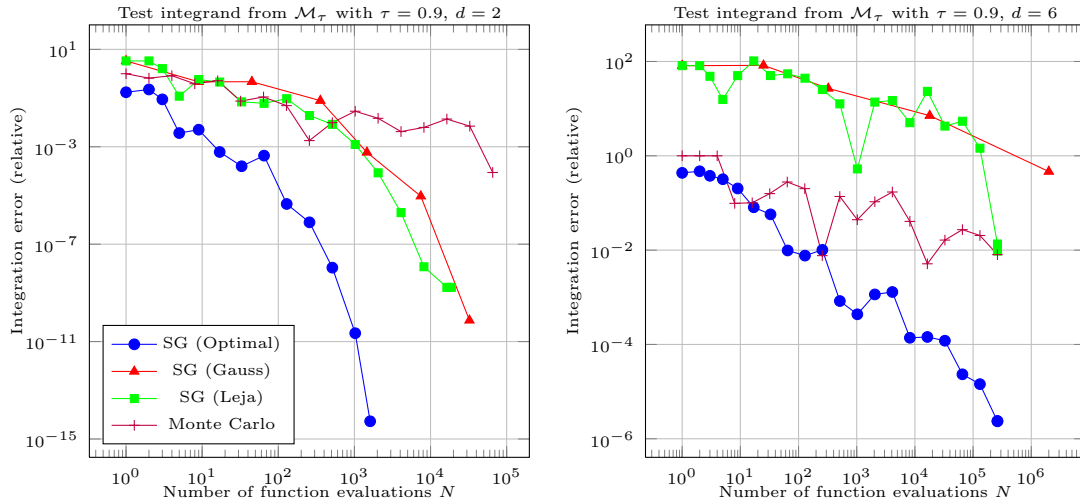
Figure 8.3: Test function Hermite space given in (8.4).

8.2 Computing multivariate normal probabilities in econometrics

Econometrics is a discipline from economics that is concerned with the extraction of economic phenomena from real-world data based on the concurrent development of theory and observation. Many models that aim to explain real world phenomena involve variables or parameters that cannot be directly observed. An example are so-called *discrete choice models* which aim to explain, and predict choices between two or more discrete alternatives. Here, the choice of a certain alternative depends on the utility it provides for an individual, which of course chooses the alternative with highest utility. However, the utility is usually not observable and has to be estimated by means of other quantities that are observable and linked to utility by an economic model.

8.2.1 Discrete choice models

The utility of alternative $j = 1, \ldots, J$ for individual $m = 1, \ldots, M$, say $U_{m,j}$, is not observable. Instead, a large class of econometric models [152] assumes that there holds a relationship of the form

$$U_{m,j} = \sum_{l=1}^{q} \beta_l z_l^{(m,j)} + \epsilon_{m,j} = \boldsymbol{\beta}^\mathsf{T} \boldsymbol{z}^{(m,j)} + \epsilon_{m,j}, \qquad (8.5)$$

where the vector $\boldsymbol{z}^{(m,j)} = (z_1^{(m,j)}, \ldots, z_q^{(m,j)}) \in \mathbb{R}^q$ contains observable properties of the alternatives and the individuals. The error terms $\boldsymbol{\epsilon}_m = (\epsilon_{m,1}, \ldots, \epsilon_{m,J}), m = 1, \ldots, M$ represent unobserved characteristics of the alternatives and the individuals that are modelled by independent and identically distributed random variables. After a distribution for $\boldsymbol{\epsilon}_m$ has been fixed, the unknown parameters $\boldsymbol{\beta} = (\beta_1, \ldots, \beta_q)$ can be estimated from observed data, i.e. each individual $m = 1, \ldots, M$ chooses an alternative $j(m) \in \{1, \ldots, J\}$ if his utility $U_{m,j(m)}$ for $j(m)$ is larger than the utility of the alternatives $U_{m,k}, k \neq j(m)$.

The conditional probability of this observed choice is

$$
\begin{aligned}
P_m(\boldsymbol{\beta}) &= \mathbb{P}[U_{m,j(m)} \geq U_{m,k} \text{ for all } k = 1, \ldots, J | \boldsymbol{z}^{(m,1)}, \ldots, \boldsymbol{z}^{(m,J)}] \\
&= \mathbb{P}[\boldsymbol{\beta}^{\mathsf{T}} \boldsymbol{z}^{(m,j(m))} + \epsilon_{m,j(m)} \geq \boldsymbol{\beta}^{\mathsf{T}} \boldsymbol{z}^{(m,k)} + \epsilon_{m,k} \text{ for all } k = 1, \ldots, J | \boldsymbol{z}^{(m,1)}, \ldots, \boldsymbol{z}^{(m,J)}] \\
&= \mathbb{P}[\epsilon_{m,k} - \epsilon_{m,j(m)} \leq \boldsymbol{\beta}^{\mathsf{T}}(\boldsymbol{z}^{(m,j(m))} - \boldsymbol{z}^{(m,k)}) \text{ for all } k = 1, \ldots, J | \boldsymbol{z}^{(m,1)}, \ldots, \boldsymbol{z}^{(m,J)}] \\
&=: \mathbb{P}[\boldsymbol{x} \leq \boldsymbol{b}^{(m)}(\boldsymbol{\beta})],
\end{aligned}
\tag{8.6}
$$

where $\boldsymbol{x} = (x_1, \ldots, x_{J-1})$ is distributed like the $(J-1)$ nontrivial differences of the error terms $\epsilon_{m,k} - \epsilon_{m,j(m)}$ and $\boldsymbol{b}_m(\boldsymbol{\beta}) \in \mathbb{R}^{J-1}$ is given by $b_k(\boldsymbol{\beta}) = \boldsymbol{\beta}^{\mathsf{T}}(\boldsymbol{z}^{(m,j(m))} - \boldsymbol{z}^{(m,k)})$ for $k \neq j(m)$. Assume that the distribution of $\boldsymbol{x}$ is absolutely continuous with respect to the Lebesgue measure, i.e. there exists a probability density function φ such that $\mathbb{P}[\boldsymbol{x} \in A] = \int_{\mathbb{R}^d} \chi_A(\boldsymbol{x}) \varphi(\boldsymbol{x}) \, \mathrm{d}\boldsymbol{x}$. Each conditional choice probability $P_m(\boldsymbol{\beta}), m = 1, \ldots, M$ then can be written as

$$
P_m(\boldsymbol{\beta}) = \mathbb{P}[\boldsymbol{x} \leq \boldsymbol{b}_m(\boldsymbol{\beta})] = \int_{-\infty}^{b_1^{(m)}(\boldsymbol{\beta})} \cdots \int_{-\infty}^{b_{J-1}^{(m)}(\boldsymbol{\beta})} \varphi(\boldsymbol{x}) \, \mathrm{d}\boldsymbol{x}.
\tag{8.7}
$$

For now assume that (8.7) is known and can be evaluated. Then, the likelihood of the observed choices equals

$$
\prod_{m=1}^{M} P_m(\boldsymbol{\beta}).
\tag{8.8}
$$

Maximizing (8.8) with respect to the unknown parameters $\boldsymbol{\beta}$ is the so-called *maximum likelihood estimator*. We denote $\boldsymbol{\beta}^* = \arg\min \mathcal{L}(\boldsymbol{\beta})$ as the set of parameters that explains the observed data best. Moreover, maximizing (8.8) is equivalent to maximizing the log-likelihood function

$$
\mathcal{L}(\boldsymbol{\beta}) := \frac{1}{M} \log \left(\prod_{m=1}^{M} P_m(\boldsymbol{\beta}) \right) = \frac{1}{M} \sum_{m=1}^{M} \log P_m(\boldsymbol{\beta}).
\tag{8.9}
$$

This is usually done by standard approaches from numerical optimization, e.g. Newton-Raphson type algorithms [114]. However, if the integral in (8.7) does not have a closed-form solution, the log-likelihood function has to be approximated by numerical cubature methods. Here, each summand in (8.9) requires the solution of a multivariate integral.

To this end, assume that $\tilde{P}_m(\boldsymbol{\beta}) \approx P_m(\boldsymbol{\beta})$, $m = 1, \ldots, M$ are approximations to (8.7) obtained by numerical cubature. The approximated log-likelihood function then reads

$$
\tilde{\mathcal{L}}(\boldsymbol{\beta}) = \sum_{m=1}^{M} \log(\tilde{P}_m(\boldsymbol{\beta})).
$$

The error of this approximation in a monotone norm $\| \cdot \|$ can then be bounded by

$$
\left\| \tilde{\mathcal{L}}(\boldsymbol{\beta}) - \mathcal{L}(\boldsymbol{\beta}) \right\| = \frac{1}{M} \left\| \sum_{m=1}^{M} \log(\tilde{P}_m(\boldsymbol{\beta})) - \log(P_m(\boldsymbol{\beta})) \right\|
$$

$$= \frac{1}{M} \Big\| \sum_{m=1}^{M} \log \left(\frac{\tilde{P}_m(\boldsymbol{\beta}))}{P_m(\boldsymbol{\beta})} \right) \Big\|$$

$$= \frac{1}{M} \Big\| \sum_{m=1}^{M} \log \left(1 + \frac{\tilde{P}_m(\boldsymbol{\beta})) - P_m(\boldsymbol{\beta})}{P_m(\boldsymbol{\beta})} \right) \Big\|$$

$$\leq \frac{1}{M} \sum_{m=1}^{M} \Big\| \frac{\tilde{P}_m(\boldsymbol{\beta}) - P_m(\boldsymbol{\beta})}{\min(P_m(\boldsymbol{\beta}), \tilde{P}_m(\boldsymbol{\beta}))} \Big\|,$$

where the last inequality follows from $\log(1 + x) \leq x$ and the triangle inequality.

Therefore, the approximation error of the log-likelihood function basically depends on the relative integration error of (8.7).

8.2.2 Multinomial probit and Genz algorithm

The *multinomial probit model* [152] assumes that the error terms in (8.5) are jointly normal distributed. The $(J-1)$ differences of the error terms are therefore also jointly normal distributed. Denote the covariance matrix of this joint distribution by $\Sigma \in \mathbb{R}^{(J-1)\times(J-1)}$. For every evaluation of $\mathcal{L}(\boldsymbol{\beta})$ there have to be computed M integrals of the form

$$P_m(\boldsymbol{\beta}) = \frac{1}{\sqrt{\det(\Sigma)(2\pi)^d}} \int_{-\infty}^{b_1^{(m)}(\boldsymbol{\beta})} \cdots \int_{-\infty}^{b_{J-1}^{(m)}(\boldsymbol{\beta})} \exp\left(-\frac{1}{2} \boldsymbol{x}^{\mathsf{T}} \Sigma^{-1} \boldsymbol{x} \right) d\boldsymbol{x}. \qquad (8.10)$$

There are several approaches to tackle this problem, e.g. using spherical coordinate transformations [47], locally adaptive schemes [137] or the partially analytic simulator [146].

However, the most efficient approach turned out to be the GHK simulator which is equivalent to the Genz-Algorithm, which relies on a sequence of variable transformations to obtain an integration problem that is defined on the open unit cube. This approach was independently developed by Genz [66], Geweke and Hajivassiliou [24, 71] and Keane [97]. In statistics, this method is often referred to as Genz-algorithm, while in econometrics it is called GHK-simulator. In this setting, regular sparse grids based on the Gauss-Legendre quadrature were firstly utilized in [86]. In the following, we will demonstrate that the sparse grid approach can benefit from our new univariate quadrature formulas. We remark that this approach can also be applied to the computation of other probabilities, e.g. the t-distribution [67].

8.3 Application to the Genz algorithm

The Genz algorithm consists in a reformulation of the $(J-1)$-dimensional integral (8.10) on an unbounded domain as a $(J-2)$-dimensional integral on the unit cube $(0,1)^{J-2}$. For the sake of a consistent notation we now set $d := J - 2$ and recall that the evaluation of the likelihood function for multinomial probit models boils down to the computation of

$$F(\boldsymbol{b}) := \frac{1}{\sqrt{\det(\Sigma)(2\pi)^d}} \int_{-\infty}^{b_1} \cdots \int_{-\infty}^{b_{d+1}} \exp\left(-\frac{1}{2} \boldsymbol{x}^t \Sigma^{-1} \boldsymbol{x} \right) d\boldsymbol{x}, \qquad (8.11)$$

where $\Sigma \in \mathbb{R}^{(d+1) \times (d+1)}$ is a covariance matrix which depends on the joint probability distribution of the differences of the error terms in (8.6). $F(\boldsymbol{b})$ has to be evaluated for many different $\boldsymbol{b} \in \mathbb{R}^{d+1}$, already for a single evaluation of (8.9).

The Genz-algorithm [66] consists of several transformations and finally leads to the integral

$$F(\boldsymbol{b}) = \hat{b}_1 \int_{(0,1)^d} \prod_{i=2}^{d+1} \hat{b}_i(x_1, \ldots, x_{i-1}) \; \mathrm{d}\boldsymbol{w}, \tag{8.12}$$

where the $\hat{b}_i$ are recursively defined by

$$\hat{b}_i(x_1, \ldots, x_{i-1}) = \Phi \left(C_{i,i}^{-1} \cdot \left(b_i - \sum_{j=1}^{i-1} C_{i,j} \cdot \Phi^{-1}(x_j \cdot \hat{b}_j(x_1, \ldots, x_{j-1})) \right) \right). \tag{8.13}$$

Here, the matrix $\boldsymbol{C} \in \mathbb{R}^{(d+1) \times (d+1)}$ denotes a Cholesky factor[1] of the covariance-matrix, i.e. $\boldsymbol{C}\boldsymbol{C}^T = \Sigma$, and $\Phi : \mathbb{R} \to (0, 1)$ is the cumulative Gaussian distribution function.

The main advantage of the Genz-algorithm in a dimension-adaptive sparse grid setting, cf. [79], stems from the fact that it enforces a priority ordering onto the variables $x_1, \ldots, x_{d-1}$, where x_1 contributes the most and x_d contributes the fewest to the value of $F(\boldsymbol{b})$. This is because x_d appears in only one factor of (8.12), while x_1 appears in all of them. Furthermore, the dimensionality of the original integration problem is reduced by one from $d + 1$ to d. A disadvantage is of course the increased cost for the evaluation of the transformed integrand in formula (8.12). Moreover, while the original integrand was analytic in the whole complex plane, the new integrand is only analytic within the open disc $\{z \in \mathbb{C} : |z - \frac{1}{2}| < \frac{1}{2}\}$. This is due to the inverse cumulative distribution function Φ^{-1} that introduces a singularity at the origin and in some dimensions a fast growth of the integrand for arguments close to one.

Taking a close look at (8.12), we note that each factor of the integrand (8.13) is $[0, 1]$-valued. In particular, it is bounded. Computing the partial derivatives of (8.13) explicitly for $d > 2$ is a complicated task because of the recursive nature of $\hat{b}_i$. However, for $d = 1$ a simple application of the chain rule reveals that the first derivative can be singular because of the boundary singularities of Φ^{-1}.

This motivates using our multivariate cubature rules that are constructed for integration in the Taylor space $\mathcal{T}_{\mathrm{Li}_2}$ which contains functions that are bounded on the unit disc and have derivatives in the Hardy space $\mathbb{H}_1$. Since $\mathbb{H}_1$ contains singular analytic functions like e.g. $x \mapsto x^{-p}, p \in (0, 1/2)$ or $x \mapsto \log(x)^q, q \in \mathbb{N}$, we believe that this is a sensible choice.

In our numerical experiments we compare the dimension-adaptive sparse grid approach, cf. Section 2.4.3, based on the symmetric OMP greedy points tailored to the space $\mathcal{T}_{\mathrm{Li}_2}$, denoted by *SG (DiLog)* with dimension-adaptive sparse grids based on Clenshaw Curtis quadrature, denoted by *SG (CC)* and *Sobol QMC* as well as plain *Monte Carlo*. Note that Leja-based sparse grids are not applicable here because the Genz integrand cannot be evaluated at ± 1. This is due to the singularity of the inverse cumulative distribution function Φ^{-1}.

We consider a special covariance structure for which the integral in (8.11) has a closed form solution [53, 66]. Namely, we assume that the covariance matrix Σ has constant variance $\Sigma_{i,i} = 1$

---

[1]Cholesky factorization is here only unique modulo row and column permutation.
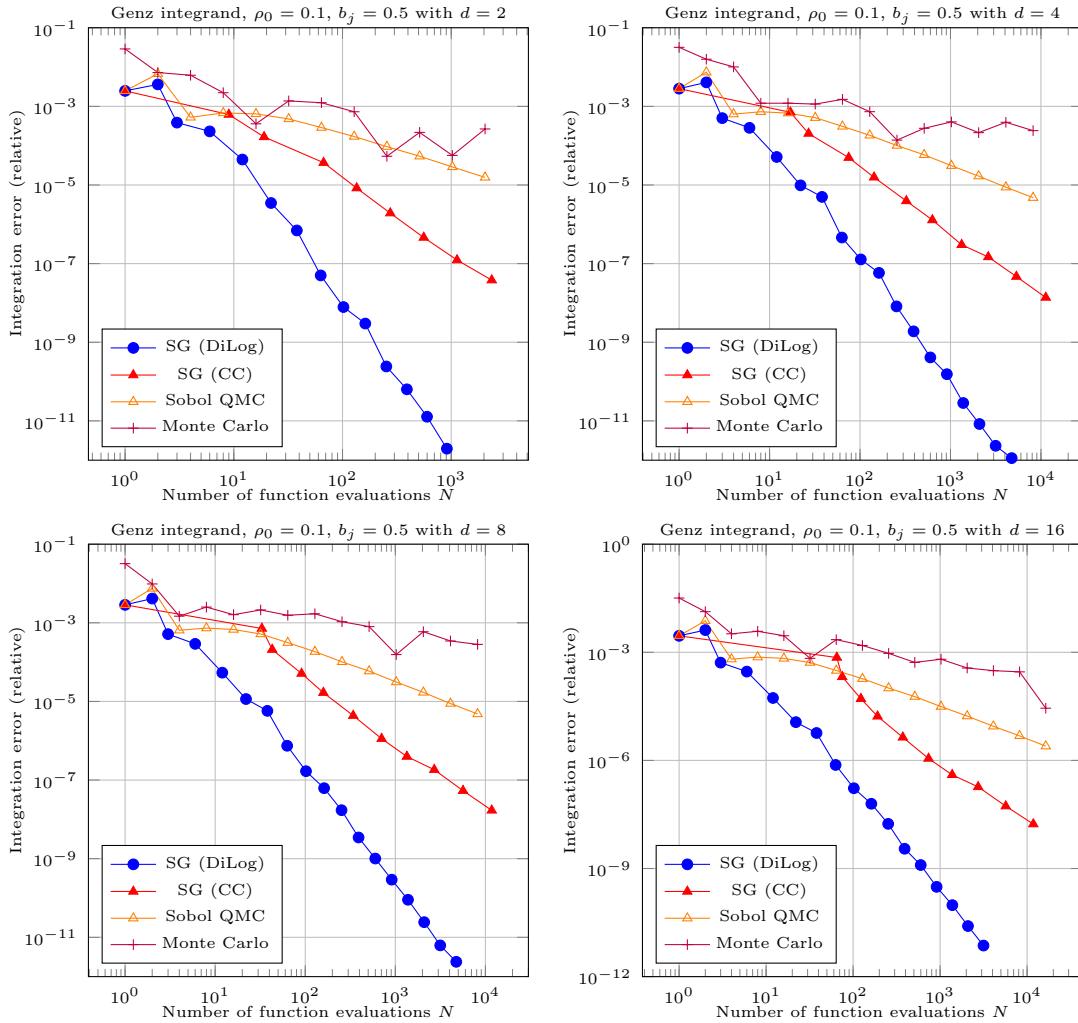
Figure 8.4: Computing multivariate normal probabilities with constant boundary vector $\boldsymbol{b}$.

and covariance $\Sigma_{i,j} = v_i \cdot v_j$ for $i \neq j$, where $v_i \in (-1, 1), i = 1, \ldots, d + 1$. We remark that the normalization of the variance to one is not a restriction because it is always possible to shift the variance via a diagonal transformation to the boundaries of integration $b_1, \ldots, b_{d+1}$.

In our first example, we choose a constant correlation $\Sigma_{j,k} = \rho_0 = 0.1$ and all $b_j = \frac{1}{2}$. In Figure 8.4, it can be observed that the dimension-adaptive sparse grid approach is superior to (Q)MC for small values of d. Especially if it is based on the new generalized optimally weighted nested quadrature rules tailored to the $\mathcal{T}_{\mathrm{Li}_2}$-space, it performs very well and super-algebraic convergence is clearly visible. As the dimensionality increases, the integration problem gets harder, but the relatively low correlation of this example leads to a fast decay of the importance of higher order interactions between the dimensions. The dimension-adaptive sparse grids correctly detect which directions are important and exploits the low effective dimensionality. Therefore, the convergence rate for the $d = 16$ dimensional problem is not much worse than for the 8-dimensional one.
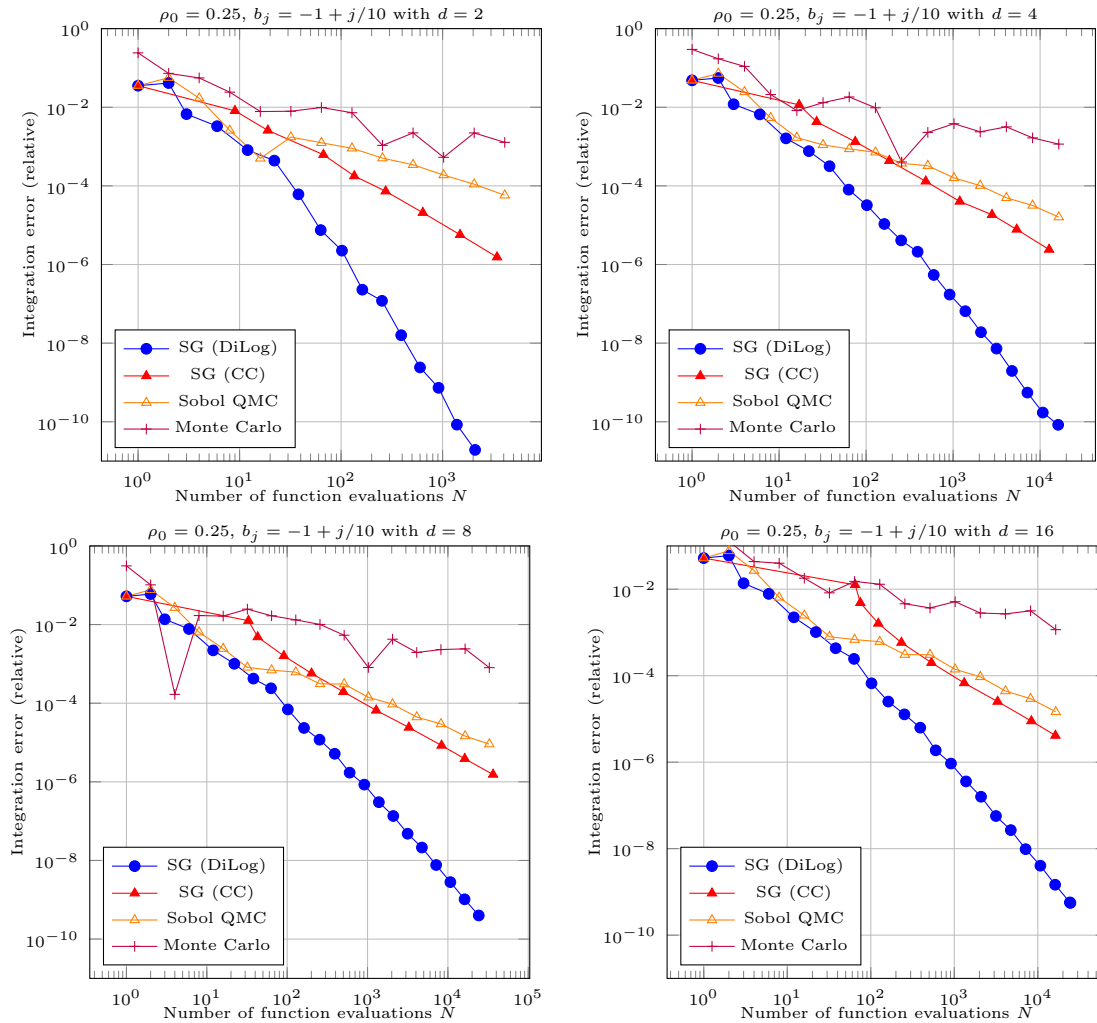
Figure 8.5: Computing multivariate normal probabilities with varying boundary vector **b**.

In our second example, we use different values for the boundaries, namely $b_j = -1 + \frac{j}{10}$ and a bigger correlation $\Sigma_{j,k} = \rho_0 = 0.25$. The convergence behaviour is similar to the first example, as can be seen from Figure 8.5. This demonstrates that our new approach indeed allows to deal with varying boundary values as it is needed in practical applications.

8.4 Parametric PDEs with analytic regularity

The rapid growth in compute power as well as the development of advanced numerical simulation techniques allows to use computer simulations to produce reliable and accurate results when the input data is known exactly. However, in many applications there is a relatively large amount of uncertainty in the input data such as model coefficients, forcing terms, boundary conditions and geometry [6]. This can be due to measurement errors, but some quantities cannot even be

observed at all and are only given as probabilistic description. Then it is desirable to quantify the uncertainty of the simulation's output, given the uncertainty of the input data which usually propagates through the model. Therefore, also the quantities derived from the simulation are random variables, whose expectation and (co-)variance are of great interest.

In this thesis, we consider a well-established model problem [6, 41, 83, 110, 112] for uncertainty quantification of PDEs, namely a parameterized elliptic diffusion problem. Assume that D is a convex Lipschitz domain and $(\Omega, \mathcal{F}, \mu)$ a complete probability space on a domain $\Omega \subset \mathbb{R}^d$ with σ-algebra $\mathcal{F} \subset 2^\Omega$ of events and probability measure $\mu : \mathcal{F} \to [0, 1]$. We assume that μ is absolutely continuous with respect to the Lebesgue measure which implies that $\mathrm{d}\mu(\boldsymbol{x}) = \omega(\boldsymbol{x})\, \mathrm{d}\boldsymbol{x}$, for a probability density function $\omega : \Omega \to \mathbb{R}_+$.

The random elliptic diffusion problem consists in finding a solution $u : D \times \Omega \to \mathbb{R}$ which μ-almost surely satisfies

$$
\begin{aligned}
-\mathrm{div}_{\boldsymbol{y}}\left(a(\boldsymbol{y}, \boldsymbol{x})\nabla_{\boldsymbol{y}}u(\boldsymbol{y}, \boldsymbol{x})\right) &= g(\boldsymbol{y}) && \text{for all } \boldsymbol{y} \in D \text{ and } \boldsymbol{x} \in \Omega \\
u(\boldsymbol{y}, \boldsymbol{x}) &= 0 && \text{for all } \boldsymbol{y} \in \partial D \text{ and } \boldsymbol{x} \in \Omega.
\end{aligned}
\tag{8.14}
$$

Here, $\mathrm{div}_{\boldsymbol{y}}$ and $\nabla_{\boldsymbol{y}}$ act on the spatial variable $\boldsymbol{y} \in D \subset \mathbb{R}^s, s \in \{1, 2, 3\}$ only. The loading $g \in L_2(D)$ is assumed to be deterministic. But the diffusion coefficient $a(\boldsymbol{y}, \boldsymbol{x})$ depends, beside on $\boldsymbol{y}$, also on the parametric variable $\boldsymbol{x} \in \Omega \subset \mathbb{R}^d, d \in \mathbb{N}$. Therefore, the solution u of (8.14) depends on the parametric variable $\boldsymbol{x}$ as well.

In order to guarantee the existence of a solution for almost all $\boldsymbol{x} \in \Omega$, we assume, cf. [6, 40], the *uniform ellipticity* of the problem, i.e. there exists $0 < a_{\min} < a_{\max} < \infty$ such that

$$
a_{\min} \le a(\boldsymbol{y}, \boldsymbol{x}) \le a_{\max} \quad \text{for all } (\boldsymbol{y}, \boldsymbol{x}) \in D \times \Omega.
$$

Defining $V := H_0^1(D)$ and its dual $V^\star = H^{-1}(D)$, cf. [26], the Lax-Milgram Lemma then implies the existence of a weak solution $u(\cdot, \boldsymbol{x})$ to (8.14), i.e. for almost all $\boldsymbol{x} \in \Omega$ it holds

$$
\int_D a(\boldsymbol{y}, \boldsymbol{x})\nabla_{\boldsymbol{y}}u(\boldsymbol{y}, \boldsymbol{x}) \cdot \nabla v(\boldsymbol{y})\, \mathrm{d}\boldsymbol{y} = \int_D \nabla f(\boldsymbol{y}) \cdot \nabla v(\boldsymbol{y})\, \mathrm{d}\boldsymbol{y} \quad \text{for all } v \in V.
\tag{8.15}
$$

This solution satisfies the estimate

$$
\|u(\cdot, \boldsymbol{x})\|_V \le \frac{\|f\|_{V^\star}}{a_{\min}}.
$$

Often, engineers are interested in a so-called *quantity of interest* (QoI) $Q : V \to \mathbb{R}$ that is derived from the solution $u(\cdot, \boldsymbol{x})$. Since the solution depends on $\boldsymbol{x}$ also the QoI depends on $\boldsymbol{x}$ and induces a mapping $f : \Omega \to \mathbb{R}$ given by

$$
f(\boldsymbol{x}) = Q(u(\cdot, \boldsymbol{x})).
$$

Frequently, it is assumed that Q is a linear functional on V. Examples are the mean of $u(\cdot, \boldsymbol{x})$ over some domain $\tilde{D} \subseteq D$, i.e.

$$
f(\boldsymbol{x}) = \int_{\tilde{D}} u(\boldsymbol{y}, \boldsymbol{x})\, \mathrm{d}\boldsymbol{y}
$$

or the evaluation of $u(\cdot, \boldsymbol{x})$ or its gradient at a point $\tau \in D$, i.e.

$$f(\boldsymbol{x}) = u(\tau, \boldsymbol{x}) \quad \text{or} \quad f(\boldsymbol{x}) = \nabla_{\boldsymbol{y}} u(\boldsymbol{y}, \boldsymbol{x})_{|\boldsymbol{y}=\tau}.$$

The QoI can either be reconstructed as a function, or its expectation and also higher order moments, can be computed. Since we deal with multivariate integration, we will approximate the expectation of f, i.e. we will aim for the computation of

$$\int_{\Omega} f(\boldsymbol{x}) \, \omega(\boldsymbol{x}) \, \mathrm{d}\boldsymbol{x}.$$

Note that each evaluation of f now requires the solution of (8.14) with parameters $\boldsymbol{x} \in \Omega$ and the subsequent evaluation of the functional Q.

8.5 Application to affine linear diffusion coefficients

A special case of the parametric diffusion coefficient $a(\boldsymbol{y}, \boldsymbol{x})$ is of the form

$$a(\boldsymbol{y}, \boldsymbol{x}) = \bar{a}(\boldsymbol{y}) + \sum_{k=1}^{d} x_j \psi_j(\boldsymbol{y}),$$

which is referred to as *affine linear diffusion coefficient*, cf. [41, 153]. Now, assume that $a(\boldsymbol{y}, \cdot)$ can be continued holomorphically to $\mathbb{C}^d$ and $a(\cdot, \boldsymbol{z}) \in L^\infty(D)$ for all $\boldsymbol{z} \in \mathbb{C}^d$. Defining the poly disc

$$\mathbb{D}_{\boldsymbol{r}} := \left\{ \boldsymbol{z} \in \mathbb{C}^d : |z_j| < r_j, j = 1, \ldots, d \right\}$$

assume that there exists a positive $\delta < a_{\min}$ and $\boldsymbol{r} = (r_1, \ldots, r_d) > \boldsymbol{1}$ such that it holds for all $\boldsymbol{z} \in \mathbb{D}_{\boldsymbol{r}}$ and all $\boldsymbol{y} \in D$ that

$$\Re\, a(\boldsymbol{y}, \boldsymbol{z}) \geq \delta.$$

Then, we say that $a : D \times \Omega \to \mathbb{R}$ satisfies the $(\delta, \boldsymbol{r})$-*polydisc uniform ellipticity assumption* DUE$(\delta, \boldsymbol{r})$.

By Theorem 1 in [153], the solution map

$$\boldsymbol{x} \mapsto u(\cdot, \boldsymbol{x})$$

can be continued holomorphically to $\mathbb{D}_{\boldsymbol{r}}$ if a satisfies the DUE$(\delta, \boldsymbol{r})$, cf. also [41]. This holds for the QoI $f(\boldsymbol{x}) = Q(u(\cdot, \boldsymbol{x}))$ as well [81]. This motivates using our optimally weighted cubature rules that are tailored to the Hardy space

$$\mathbb{H}_{\boldsymbol{r}} = \bigotimes_{j=1}^{d} \mathbb{H}_{r_j}$$

of functions that are analytic in polydiscs $\mathbb{D}_{\boldsymbol{r}}$.

In order to avoid the discussion about the additional error that is introduced by the numerical approximation of $u(\cdot, \boldsymbol{x})$ by e.g. finite element discretization, we consider a simple model prob-

lem whose solution cannot be determined in closed-form, but can be computed exactly using piecewise quadratic finite elements.

8.5.1 Model problem

As a model problem we consider Example 2.2 from [7], see also [41].

Let $(D_j)_{j=1}^d$ be a partition of a bounded Lipschitz domain $D \subset \mathbb{R}^s, s \in \{1, 2, 3\}$, i.e.

$$D = \bigcup_{j=1}^d D_j$$

and

$$a(\boldsymbol{y}, \boldsymbol{x}) := 1 + \sum_{j=1}^d x_j \psi_j(\boldsymbol{y}), \tag{8.16}$$

where

$$\psi_j(\boldsymbol{y}) = \frac{1}{r_j} \chi_{D_j}(\boldsymbol{y})$$

is the characteristic function of D_j, scaled with the factor r_j^{-1}.

For $\Omega_{(d)} = [-1, 1]^d$, we note that the problem (8.14) is elliptic if $r_j > 1, j = 1, \ldots, d$ and therefore has a unique solution $u(\cdot, \boldsymbol{x})$ for all $\boldsymbol{x} \in [-1, 1]^d$. Moreover, (8.16) satisfies $\mathrm{DUE}(\delta, \boldsymbol{r})$, which implies the analyticity in $\mathbb{D}_{\boldsymbol{r}}$ of the solution map.

Now assume that the spatial dimension is one, i.e. $s = 1$ in (8.14) and $D = [0, 1]$. The problem (8.14) then reads

$$-\frac{\mathrm{d}}{\mathrm{d}y}\left(a(y, \boldsymbol{x})\frac{\mathrm{d}}{\mathrm{d}y}u(y, \boldsymbol{x})\right) = g(y) \qquad \text{for all } y \in D \text{ and } \boldsymbol{x} \in \Omega_{(d)}$$
$$u(0, \boldsymbol{x}) = u(1, \boldsymbol{x}) = 0 \qquad\qquad \text{for all } \boldsymbol{x} \in \Omega_{(d)}. \tag{8.17}$$

This is equivalent to

$$-\left(1 + \frac{x_j}{r_j}\right)\frac{\mathrm{d}^2}{\mathrm{d}y^2}u(y, \boldsymbol{x}) = g(y) \quad \text{for all } y \in D_j \text{ and } \boldsymbol{x} \in \Omega_{(d)}. \tag{8.18}$$

Now, let $G(y)$ be a second antiderivative of g, i.e. $G''(y) = g(y)$. Then, the solution to (8.17) is a piecewise function and on each D_j it holds

$$u(\cdot, \boldsymbol{x})_{|D_j} \in \mathrm{span}\,\{\chi_{D_j}(y)1,\ \chi_{D_j}(y)y,\ \chi_{D_j}(y)G(y)\},$$

which amounts to $3d$ degrees of freedom of the *exact solution* to the equation (8.18) for fixed $\boldsymbol{x}$. Because the solution $u(\cdot, \boldsymbol{x})$ has to be continuous on D and fulfill the boundary condition $u(0, \boldsymbol{x}) = u(1, \boldsymbol{x}) = 0$, there are $3d - 2 - (d-1) = 2d - 1$ remaining degrees of freedom of the exact solution to (8.17).

Moreover, if we set $g(y) \equiv 1$, the problem reads

$$-\left(1 + \frac{x_j}{r_j}\right) \frac{\mathrm{d}^2}{\mathrm{d}y^2} u(y, \boldsymbol{x}) = 1 \quad \text{for all } y \in D_j \text{ and } \boldsymbol{x} \in \Omega_{(d)} \tag{8.19}$$

and for every $\boldsymbol{y} \in \Omega_{(d)}$, the solution $u(\cdot, \boldsymbol{y})$ can now be computed exactly by piecewise quadratic finite elements on $[0, 1]$ because now $G(y) = \frac{1}{2}y^2$. Assuming that each patch D_j is of the form

$$D_j = \left[\frac{j-1}{d}, \frac{j}{d}\right],$$

the basis functions are chosen to be the quadratic Lagrange polynomials on each D_j defined by their values at $(j-1)/d$, $\frac{2j-1}{d}$ and $\frac{j}{d}$. The weak formulation (8.15) then leads to a sparse system of linear equations, whose solution yields the values $u_k = u(y_k, \boldsymbol{x})$ of $u(\cdot, \boldsymbol{x})$ at $y_k = k/(2d)$, $k = 1, \ldots, 2d - 1$.

8.5.2 Numerical results

In this section, we will compare the performance of dimension-adaptive sparse grids based on the optimally weighted nested quadrature rules computed by Algorithm 4 to the performance of classical integration methods like plain Monte Carlo or Sobol quasi–Monte Carlo, which in the following plots is denoted by *Sobol QMC*. Moreover, we use the dimension-adaptive approach based on Clenshaw-Curtis, which is denoted by *SG (CC)* and Leja points as discussed in Section 2.3.4, denoted by *SG (Leja)*. These represents the current state-of-the-art for the integration of smooth multivariate functions [13, 37, 108, 111, 112, 153]. Since the integrands are analytic in a region strictly larger than the domain of integration $[-1, 1]^d$, the sparse grids based on Leja points, as well as on Clenshaw-Curtis, and the respective optimal quadrature rules are expected to yield super-algebraic convergence rates.

To this end, we first consider an isotropic example with relatively large radius of analyticity in every dimension. The quantity of interest Q is chosen to be the area below the solution $u(\cdot, \boldsymbol{x})$, i.e. the integral with respect to the spatial variable y over $D = [0, 1]$

$$f(\boldsymbol{x}) = Q(u(\cdot, \boldsymbol{x})) = \int_{[0,1]} u(y, \boldsymbol{x}) \, \mathrm{d}y, \tag{8.20}$$

where $u(\cdot, \boldsymbol{x})$ is a solution to (8.19).

In Figure 8.6 the relative integration errors are given as log-log-plot for dimension $d \in \{2, 4, 6, 8\}$. As the experiments in Section 6.2 suggest, there is not much of a difference in using classical polynomial based methods compared to the optimal approach in Hardy spaces $\mathbb{H}_r$ with large radius of analyticity r. We can see that for small point numbers N the Leja points perform worse than Clenshaw-Curtis quadrature. We believe that this is because on the first level the Leja sequence uses the point $\boldsymbol{1}$, while the Clenshaw-Curtis method and also the Sobol method have their first point equal to $\boldsymbol{0}$. Asymptotically the Leja based sparse grid can benefit from its finer granularity, i.e. the points do not increase exponentially on each level. However, the effect that is already visible in $d = 2$ becomes even more prominent in $d = 6$ and $d = 8$, where it takes about 10^5 points for the SG (Leja) method to overtake SG (CC). Still, both methods
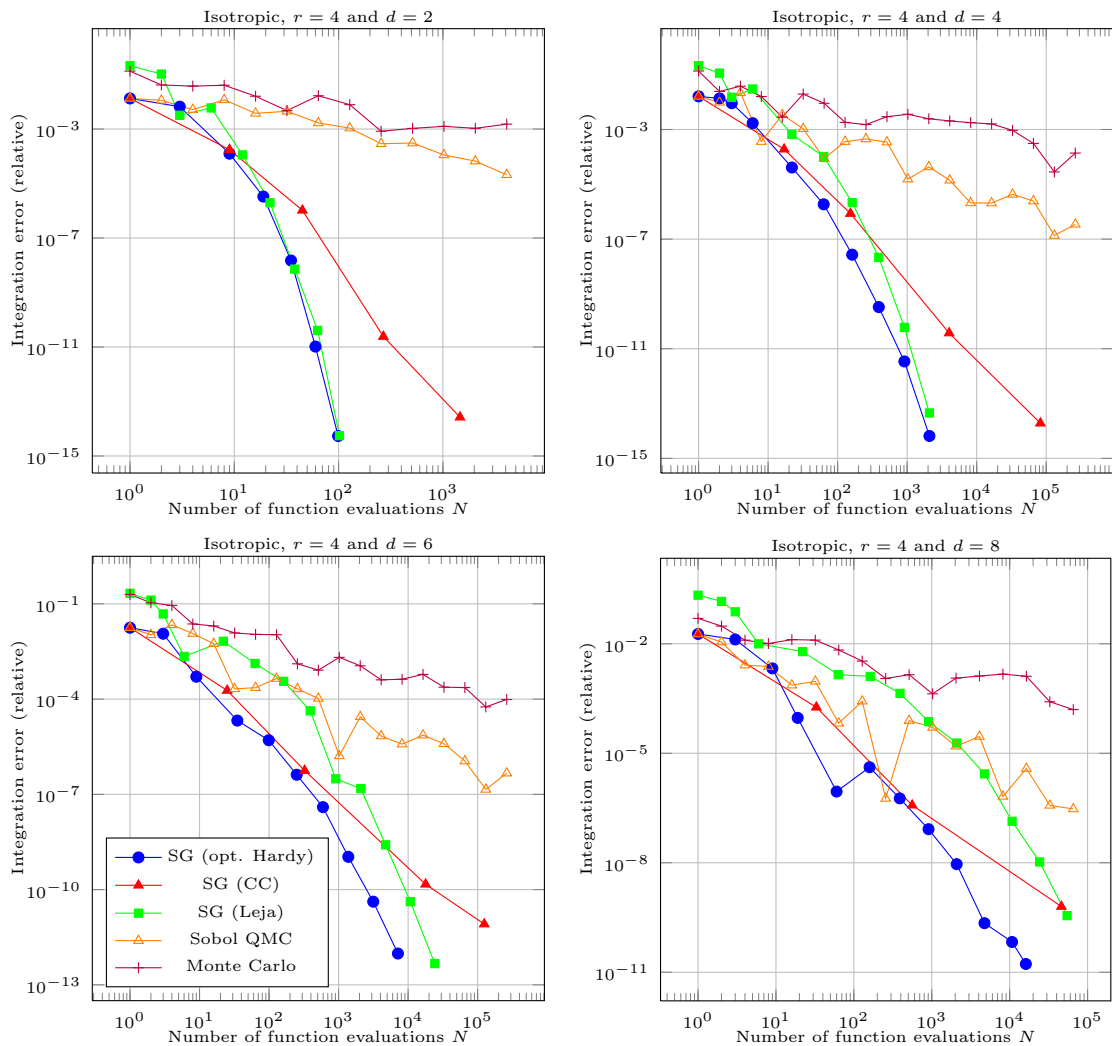
Figure 8.6: Isotropic example with large domain of analyticity with QoI given by (8.20).

exhibit a convergence rate that decays faster than any algebraic rate N^{-s}, which is due to the analyticity of the integrand.

Moreover, we note that the dimension-adaptive sparse grid based on the optimally weighted nested quadrature rules for the Hardy space with radius $r = 4$ outperforms all the other methods. However, in $d = 2$ the benefit over Leja points is rather small.

The picture changes when decreasing the radius of analyticity. To this end, in Figure 8.7 we consider the same setup as in Figure 8.6 albeit with $r = 1.1$, which is substantially smaller than before. Now, the bad preasymptotic behaviour of the Leja based adaptive sparse grid is even more prominent, especially when the dimension gets large. For $d = 8$, it is even less effective than the plain Monte Carlo approach.

However, the sparse grid based on the nested optimally weighted quadrature for the Hardy space $\mathbb{H}_r$ with $r = 1.1$ is the method of choice for all the considered dimensionalities $d = 2, 4, 6, 8$. For
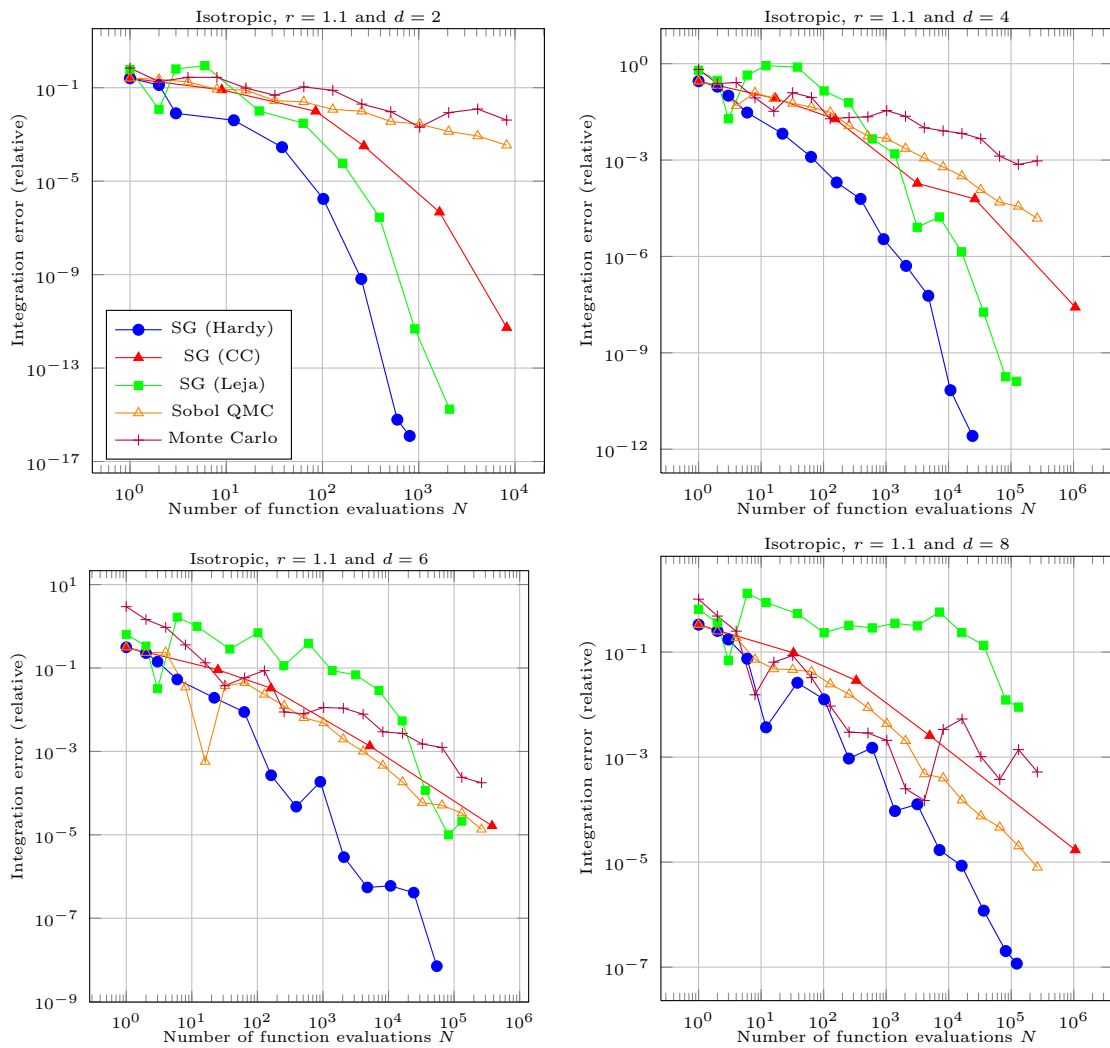
Figure 8.7: Isotropic example with moderate radius of analyticity with QoI given by (8.20).

the eight-dimensional example it achieves a relative error of 10^{-5} with about $N = 10^4$ points, while the Sobol quasi–Monte Carlo method needs about $N = 3 \cdot 10^5$ points. Therefore, using the approach proposed in this thesis saves more than 95% of the compute power over conventional approaches.

In Figure 8.8 the results for $r = 1.01$ are given. The effects that became visible in Figure 8.7 are now even more prominent. The Leja points suffer substantially from their bad pre-asymptotic behaviour that even leads to an increasing error for $N \leq 20$ in $d = 2$. For $d = 8$, convergence is not even visible at all. Therefore, it seems sensible to start the Leja sequence at the point 0 and not at 1. This is plausible because functions in $\mathbb{H}_{1.01}$ contain functions with much faster growth close to the boundary than functions in $\mathbb{H}_{1.1}$ or $\mathbb{H}_4$.

The picture for the other considered cubature rules basically remains the same as before. Clenshaw-Curtis based adaptive sparse grids still exhibit super-algebraic convergence, yet it is
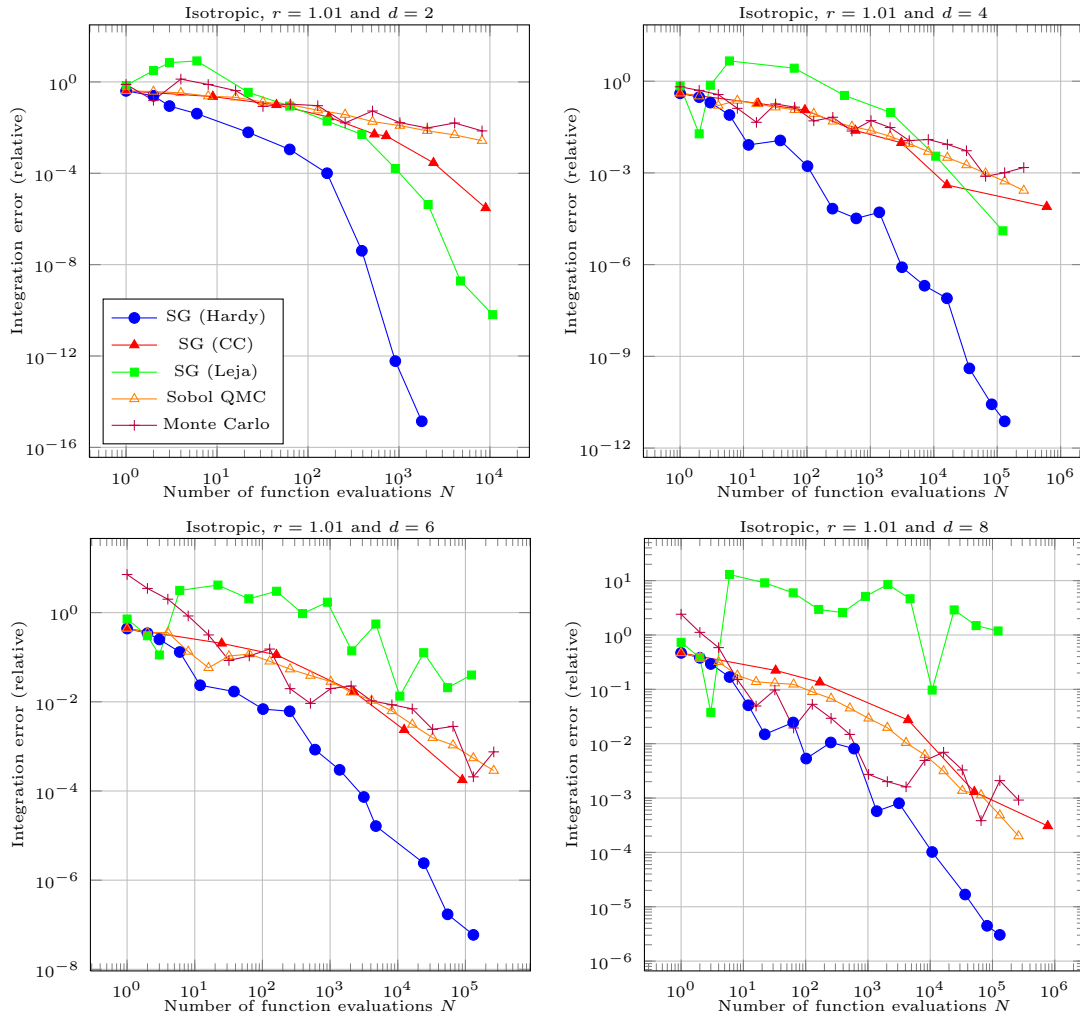
Figure 8.8: Isotropic example for small radius of analyticity with QoI given by (8.20).

not competitive with the sparse grid approach based on the nested optimally weighted quadrature rules tailored to $\mathbb{H}_r$ with $r = 1.01$.

Up to now all the considered examples dealt with a setup where all the $r_j, j = 1, \ldots, d$ coincide. Next, we consider an anisotropic example. To this end, we assume that $r_j = 1 + \frac{2^j}{100}$, i.e. the radii of the polydiscs increase with the dimensionality. In Figure 8.9 the relative integration errors are given as log-log-plots for dimensions $d \in \{2, 4, 8, 16\}$. Since we start with rather small radii, it is not surprising that already in $d = 2$ the optimally weighted adaptive sparse grids yield a substantial improvement over the other considered approaches, saving more than 90% of the evaluations. As the dimensionality increases, the integration problem becomes harder and more evaluations are needed to achieve a high accuracy for the relative integration error. However, from $d = 8$ to $d = 16$ the picture basically does not change. This is because the higher dimensions are so smooth that they hardly contribute to the integral at all. For $d = 32$, which is not depicted here, there is also no difference visible.
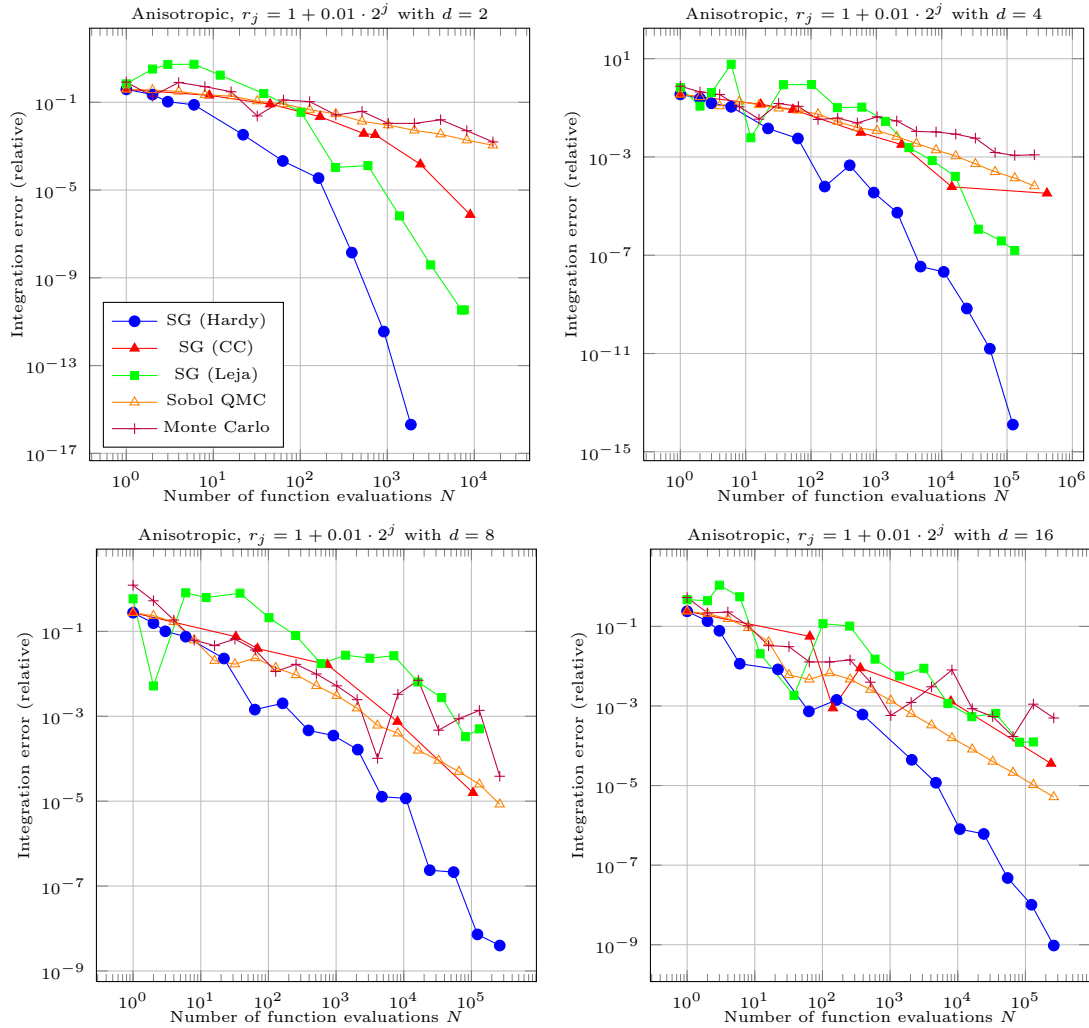
Figure 8.9: Anisotropic example for dimensions $d \in \{2, 4, 8, 16\}$ with QoI given by (8.20).

We observe a substantial benefit when employing the optimally weighted quadrature rules for the Hardy space within the dimension-adaptive sparse grids. However, we respected the anisotropy of the problem in the construction of the optimally weighted quadrature rules. This means that for each coordinate direction a different quadrature rule was used, each tailored to the regularity of the respective dimension. This was not the case for the other methods, which, besides of the dimension-adaptive construction of the sparse grid, used the same underlying univariate quadrature rule for all the coordinate directions.

The next example has an anisotropic structure as well, albeit now the radii are given by $r_j = 1 + 0.08 \cdot 2^j$. In Figure 8.10, it can be seen that the difference between the sparse grid based on optimally weighted quadrature rules and the conventional sparse grids is now less prominent. This is explained by the fact that for larger radii the performance of optimal and polynomial quadrature rules in Hardy spaces basically is the same, cf. Section 6.2. Again, the
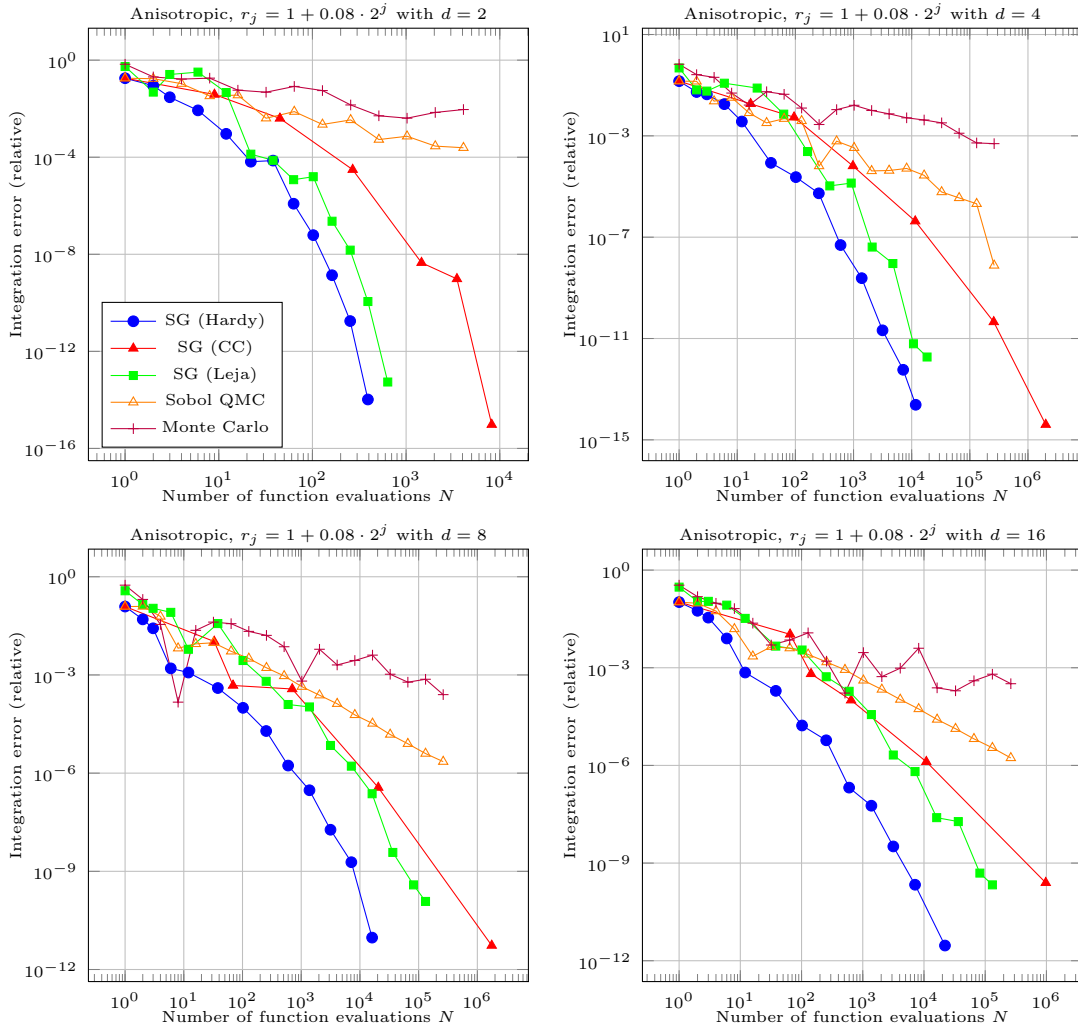
Figure 8.10: Anisotropic example for dimensions $d \in \{2, 4, 8, 16\}$ with QoI given by (8.20).

picture does not change much from $d = 8$ to $d = 16$, which is due to the exponentially increasing radii of analyticity.

Until now we concentrated on the functional (8.20) that represents the spatial expectation of the solution as quantity of interest. Finally, we consider a different QoI, namely the functional

$$Q(u(\cdot, \boldsymbol{x}) = \delta_{1/2}(u(\cdot, \boldsymbol{x})) = u(0.5, \boldsymbol{x}), \tag{8.21}$$

which represents the evaluation of the solution in the middle of its domain, i.e. at $y = 0.5$

We observe in Figure 8.11 that the choice of the functional does not influence the performance of the different algorithms. As before, for small dimensionality, e.g. $d = 4$, the new approach based on optimally weighted quadrature rules that are tailored to the respective Hardy space leads to a reasonable advantage over the conventional schemes. In larger dimensions, the difference becomes even more prominent. For example, in $d = 16$ dimensions, the Clenshaw-Curtis based
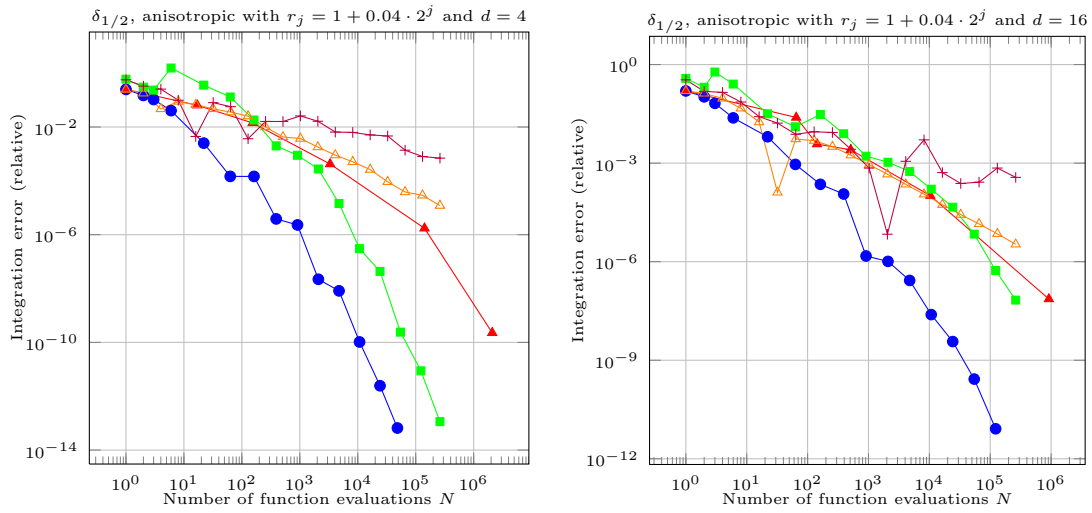
Figure 8.11: Anisotropic examples with the QoI defined in (8.21).

sparse grid needs about 100 times more evaluations of the integrand than the new approach to obtain a relative accuracy of 10^{-7}. Given that each evaluation requires the solution of a differential equation, this factor needs to be multiplied with the cost of the finite element or finite differences approximation of this solution.

Therefore, choosing an appropriate cubature rule for the problem at hand can make the difference between a computation that can be done on a laptop or an expensive parallel cluster.

9 Conclusion

In this final chapter we summarize the results of this thesis, discuss questions that have been left unanswered and give an outlook on future research.

9.1 Summary

This thesis dealt with the construction of algorithms for numerical integration of multivariate functions. We considered functions from tensor products of reproducing kernel Hilbert spaces (RKHS) and concentrated on algorithms that use optimal weights with respect to the worst-case error.

After giving a brief overview on numerical integration and its relationship to information-based complexity in Chapter 2, we recalled the theory of RKHS in Chapter 3. Here, we derived the well-known worst-case error formula in a general setting as well as some results on algorithms with optimal weights. This was the functional theoretic foundation for the remainder of this thesis. Finally, we gave several examples for RKHS that are important in numerical analysis and scientific computing. Here, we also discussed the Taylor space $\mathcal{T}_{\mathrm{Li}_2}$ which is generated by the di-logarithm and contains bounded analytic functions with derivatives in the Hardy space $\mathbb{H}_1$. To our best knowledge, this space has not appeared anywhere in the literature before, although it proved to be very useful for certain applications from econometrics.

The first main contribution of this thesis was Chapter 4, where we investigated to which extent optimal weights can improve the performance of Monte Carlo and Halton cubature in function spaces with dominating mixed smoothness H^s_{mix}. Conventional Monte Carlo and Halton cubature only achieve convergence rates of $N^{-1/2}$ and $N^{-1+\varepsilon}, \varepsilon > 0$, respectively, which is independent of the smoothness parameter $s \geq 1$. Here, we observed that both methods can achieve a worst-case error of $N^{-s+\varepsilon}, \varepsilon > 0$ if optimal weights are employed. The second goal of Chapter 4 was the development of a theoretical framework that can predict the aforementioned numerical results. Here, we used a recently developed oversampling approach [39, 106] to construct stable auxiliary cubature rules whose properties imply the convergence of the optimal worst-case error with the asymptotical rate $N^{-s+1/2} \log(N)^{ds-1/2}$.

However, this approach is not suited for spaces of analytic functions. Moreover, the complexity of constructing optimal cubature weights for unstructured point sets is $\mathcal{O}(N^3)$, which is problematic for practical applications that often require large point numbers N. Therefore, point sets are desirable, which have a structure that can be exploited to compute optimal cubature weights at reduced cost complexity. Here, we used the sparse grid technique which relies on combinations of well-chosen tensor products of univariate quadrature rules. Moreover, if the univariate quadrature rule uses optimal weights, the associated sparse grid cubature is also optimally weighted and can be assembled at cost $\mathcal{O}(N^2)$.

Therefore, we studied optimally weighted univariate quadrature rules in Chapters 5 and 6. Here, we first dealt with the problem of choosing optimal quadrature points, whose associated optimal weights are all positive. Even though the computation of optimal points is an ill-conditioned problem, it turned out that in one dimension it can be reformulated as a certain nonlinear system of equations which is stable and can be solved by Newton's method. This approach was validated in a number of relevant kernel Hilbert spaces and proved to be superior to all the other considered state-of-the-art approaches like Gaussian quadrature, Clenshaw-Curtis or Leja points. Moreover, we discussed the construction of optimally weighted nested quadrature rules. To this end, we proposed a weighted variant of orthogonal matching pursuit (OMP) to construct maximally nested quadrature points with a greedy procedure. Compared to their optimal counter parts, these points achieve almost the same convergence rate. In certain settings they perform even better than the non-nested Gaussian quadrature rules. Moreover, it turned out that the resulting quadrature weights are stable in the sense that their ℓ_1-norm is uniformly bounded. This is analogous to Leja points, which share this stability property, even though there is no theoretical explanation for it yet. Another interesting property is that in certain settings the empirical distribution of the OMP greedy points converges to the distribution of the optimal point sets. This is another similarity to Leja points, which distribute asymptotically like Gauss-Legendre points on $[-1, 1]$.

Chapter 7 was built onto the aforementioned results for the univariate setting, since a sparse grid that is based on optimally weighted nested quadrature rules is also optimal with respect to the weights. This property implied a simplified worst-case error representation that allowed to construct quasi–optimal index sets with a well-established greedy approach known as dimension-adaptivity. In combination with the greedy construction of the univariate nested quadrature rules, we thus have constructed a true black-box approach to numerical integration in RKHS, which only requires the univariate kernels as input.

The second part of Chapter 7 was devoted to a priori error bounds for quasi-optimal sparse grids that use (sub-)exponentially convergent quadrature rules. Here, we extended the results from [80] and improved on [13, 153]. These theoretical results, as well as our greedy construction of quasi-optimal index sets, were validated in several function spaces.

Finally, in Chapter 8 we demonstrated the practical relevance of cubature rules that are tailored to specific RKHS. First, we considered the computation of multivariate normal probabilities by the Genz-algorithm, which is the main bottleneck in the estimation of probit models. The most common approach leads here to integrands that are bounded and analytic but have singular derivatives. Therefore, classical quadrature rules with polynomial degree of exactness deteriorate to an algebraic rate of convergence. Our new approach, however, converges super-algebraically, even in higher dimensions.

Moreover, we dealt with parametric differential equations. It was proven in [41, 81, 153] that for affine linear diffusion coefficients the parametric solution belongs to certain tensor products of Hardy spaces. Here, we could demonstrate that an optimally weighted sparse grid technique which respects the structure of the multivariate Hardy space can substantially outperform classical approaches based on Leja points or Clenshaw-Curtis.

9.2 Outlook

There are several directions in which this thesis could be expanded or complemented. We will comment on some of them in the following.

First of all, it would be desirable to prove an upper bound for optimally weighted Monte Carlo cubature in Sobolev spaces with mixed smoothness H^s_{mix} that has the observed N^{-s} main rate. We are convinced that the approach from Section 4.2 is able to close the currently existing gap in the main rate, if it is properly refined, cf. Remark 4.6. Besides, we also observed that classical quasi–Monte Carlo points, like the Halton sequence, can benefit from using optimal weights. An adaption of the proof for random points to the QMC setting is already work in progress. Moreover, instead of aiming for weights with minimal ℓ_2-norm, one could go for the ℓ_1-norm. The induced sparsity of the solution could improve the powers of the log-terms, cf. Remark 4.7.

Regarding optimal quadrature points, we observed that in the Hardy space $\mathbb{H}_r, r > 1$ exponential convergence rates beyond the theoretical predicted r^{-2n} are possible, especially when r is close to one. Here, one could try to extend the results in [3], where matching upper and lower bounds for optimal quadrature points in the case $r = 1$ were proven.

Moreover, it is remarkable that the OMP greedy construction yields the optimal convergence rate in Sobolev spaces and half of the optimal convergence rate in analytic function spaces. This behaviour resembles the relationship between Kolmogorov width and the error of empirical interpolation, cf. [50]. However, a direct transfer of the proof technique was not possible so far.

In Chapter 6 we obtained evidence that the OMP greedy points have the same empirical distribution as the associated optimal points. This property is shared by Leja and Gaussian points, which also distribute in the same way. This is proven using logarithmic potential theory [108, 132]. An alteration of this technique that is applicable to kernel functions instead of polynomials, would certainly be an interesting, yet very challenging problem.

Instead of applying the OMP greedy approach to the univariate quadrature problem and using tensor products for multivariate problems, a direct application in the multivariate setting is also possible. But then we recur to the setting of $\mathcal{O}(N^3)$ complexity for the construction of the optimal weights. However, if the kernel has certain symmetry properties, the approach from Section 5.2.4 can be extended to the multivariate case es well, allowing to reduce the computation of certain symmetric point sets with $2^d N$ points to the case of N points. The total reduction in complexity could therefore amount to a factor of $(2^d)^3 = 8^d$.

This approach could also lead to interesting applications in machine learning, where numerical integration schemes were recently utilized to construct low dimensional feature spaces, called random Fourier features [35, 127].

Finally, we remark that we only considered affine linear diffusion coefficients for the parametric differential equation in Section 8.4. The case of log-normal distributed random fields is also important. However, a suitable RKHS that contains the parametric solution has to be determined first.

Bibliography

[1] M. Abramowitz and I. Stegun. *Handbook of Mathematical Functions: With Formulas, Graphs, and Mathematical Tables*. Applied Mathematics Series. Dover Publications, 1964.

[2] H. Amann and J. Escher. *Analysis I*. Birkhäuser, 2002.

[3] J.-E. Andersson and B. Bojanov. A note on the optimal quadrature in H^p. *Numerische Mathematik*, 44(2):301–308, 1984.

[4] N. Aronszajn. Theory of reproducing kernels. *Transactions of the American Mathematical Society*, 68(3):337–404, 1950.

[5] K. Babenko. On the approximation of periodic functions of several variables by trigonometric polynomials. *Nauk SSSR*, 132:247–250, 1960.

[6] I. Babuška, F. Nobile, and R. Tempone. A stochastic collocation method for elliptic partial differential equations with random input data. *SIAM J. on Numerical Analysis*, 52(2):317–355, 2007.

[7] M. Bachmayr and A. Cohen. Kolmogorov widths and low-rank approximations of parametric elliptic PDEs. *Mathematics of Computation*, 86:701–724, 2017.

[8] N. Bakhvalov. On the optimality of linear methods for operator approximation in convex classes of functions. *USSR Computational Mathematics and Mathematical Physics*, 11(4):244–249, 1971.

[9] R. Barrar and H. Loeb. Multiple zeros and applications to optimal linear functionals. *Numerische Mathematik*, 25(3):251–262, 1975.

[10] R. Barrar and H. Loeb. On a nonlinear characterization problem for monosplines. *Journal of Approximation Theory*, 18(3):220–240, 1976.

[11] R. Barrar, H. Loeb, and H. Werner. On the existence of optimal integration formulas for analytic functions. *Numerische Mathematik*, 23(2):105–117, 1974.

[12] D. Barrow. On multiple node Gaussian quadrature formulae. *Mathematics of Computation*, 32(142):431–439, 1978.

[13] J. Beck, F. Nobile, L. Tamellini, and R. Tempone. Convergence of quasi-optimal stochastic Galerkin methods for a class of PDEs with random coefficients. *Computers and Mathematics with Applications*, 67(4):732–751, 2014.

[14] A. Beged-Dov. Lower and upper bounds for the number of lattice points in a simplex. *SIAM J. on Applied Mathematics*, 22(1):106–108, 1972.

[15] R. Bellmann. *Adaptive Control Processes: A Guided Tour*. Princeton University Press, 1961.

[16] A. Berlinet and C. Thomas-Agnan. *Reproducing Kernel Hilbert Spaces in Probability and Statistics*. Springer, 2004.

[17] K. Binder and D. Heermann. *Monte Carlo Simulation in Statistical Physics: An Introduction.* Springer-Verlag Berlin Heidelberg, 2010.

[18] B. Bohn. *Error analysis of regularized and unregularized least-squares regression on discretized function spaces.* Dissertation, Institut für Numerische Simulation, Universität Bonn, 2016.

[19] B. Bohn and M. Griebel. An adaptive sparse grid approach for time series predictions. In J. Garcke and M. Griebel, editors, *Sparse grids and Applications*, volume 88 of *Lecture Notes in Computational Science and Engineering*, pages 1–30. Springer, 2012.

[20] B. Bojanov. Existence of extended monosplines of least deviation. *Serdica*, 3:261–272, 1977.

[21] B. Bojanov. On the existence of optimal quadrature formulae for smooth functions. *Calcolo*, 16(1), 1979.

[22] B. Bojanov. Uniqueness of the optimal nodes of quadrature formulae. *Math. Comput.*, 36(154):525–546, 1981.

[23] B. Bojanov, D. Braess, and N. Dyn. Generalized Gaussian quadrature formulas. *Journal of Approximation Theory*, 48(4):335–353, 1986.

[24] A. Borsch-Supan and V. Hajivassiliou. Smooth unbiased multivariate probability simulators for maximum likelihood estimation of limited dependent variable models. *Journal of Econometrics*, 58(3):347–368, 1993.

[25] J. Borwein and O. Chan. Inequalities for the incomplete Gamma function. *Math. Inequaities and Applications*, 12(1):115–121, 2009.

[26] D. Braess. *Finite Elements: Theory, Fast Solvers, and Applications in Solid Mechanics.* Cambridge University Press, 2007.

[27] D. Braess and N. Dyn. On the uniqueness of monosplines and perfect splines of least L_1-and L_2-norm. *Journal d'Analyse Mathématique*, 41(1):217–233, 1982.

[28] S. Brenner and R. Scott. *The Mathematical Theory of Finite Element Methods.* Springer-Verlag New York, 2008.

[29] F.-X. Briol, C. Oates, M. Girolami, M. Osborne, and D. Sejdinovic. Probabilistic integration: A role for statisticians in numerical analysis?, 2015. Preprint, arXiv:1512.00933.

[30] R. Brombeer. Über optimale Quadraturformeln mit freien Knoten zu Hilberträumen periodischer Funktionen. *Numerische Mathematik*, 30(2):149–164, 1978.

[31] H.-J. Bungartz and M. Griebel. A note on the complexity of solving Poisson's equation for spaces of bounded mixed derivatives. *Jornal of Complexity*, 15(2):167–199, 1999.

[32] H.-J. Bungartz and M. Griebel. Sparse grids. *Acta Numerica*, 13:147–269, 2004.

[33] J. Burbea. Total positivity of certain reproducing kernels. *Pacific Journal of Mathematics*, 67(1):101–130, 1976.

[34] J. Calvi and P. Van-Manh. Lagrange interpolation at real projections of Leja sequences for the unit disk. *Proc. Amer. Math. Soc.*, 140(12):4271–4284, 2012.

[35] R. Chitta, R. Jin, and A. Jain. Efficient kernel clustering using random fourier features. In *Proceedings of the 2012 IEEE 12th International Conference on Data Mining*, ICDM '12, pages 161–170, Washington, DC, USA, 2012. IEEE Computer Society.

[36] A. Chkifa. On the Lebesgue constant of Leja sequences for the complex unit disk and of their real projection. *J. of Approximation Theory*, 166:176–200, 2013.

[37] A. Chkifa, A. Cohen, and C. Schwab. High-dimensional adaptive sparse polynomial interpolation and applications to parametric PDEs. *Foundations of Computational Mathematics*, 14(4):601–633, 2013.

[38] C. Clenshaw and A. Curtis. A method for numerical integration on an automatic computer. *Numerische Mathematik*, 2(1):197–205, 1960.

[39] A. Cohen, M. Davenport, and D. Leviatan. On the stability and accuracy of least squares approximations. *Foundations of Computational Mathematics*, 13(5):819–834, 2013.

[40] A. Cohen, R. DeVore, and C. Schwab. Convergence rates of best n-term Galerkin approximations for a class of elliptic sPDEs. *Foundations of Computational Mathematics*, 10(6):615–646, 2010.

[41] A. Cohen, R. DeVore, and C. Schwab. Analytic regularity and polynomial approximation of parametric and stochastic elliptic PDEs. *Analysis and Applications*, 9(01):11–47, 2011.

[42] D. Dũng and M. Griebel. Hyperbolic cross approximation in infinite dimensions. *Journal of Complexity*, 33:55–88, 2016. Also available as INS Preprint No. 1501.

[43] D. Dũng, V. Temlyakov, and T. Ullrich. Hyperbolic Cross Approximation. *ArXiv e-prints*, 2015. arXiv:1601.03978.

[44] D. Dũng and T. Ullrich. Lower bounds for the integration error for multivariate functions with mixed smoothness and optimal Fibonacci cubature for functions on the square. *to appear in Math. Nachrichten*, 2014. arXiv 1311.1563.

[45] G. Davis, S. Mallat, and Z. Zhang. Adaptive time-frequency decompositions with matching pursuits. *Optical Engineering*, 33(7):2183–2191, 1994.

[46] P. Davis and P. Rabinowitz. *Methods of Numerical Integration*. Academic Press, 1984.

[47] I. Deák. Three digit accurate multiple normal probabilities. *Numerische Mathematik*, 35(4):369–380, 1980.

[48] P. Deuflhard and A. Hohmann. *Numerische Mathematik: Eine algorithmisch orientierte Einführung*, volume 1. De Gruyter, Berlin, 2008.

[49] R. DeVore. Nonlinear approximation. *Acta Numerica*, 7:51–150, 1998.

[50] R. DeVore, G. Petrova, and P. Wojtaszczyk. Greedy Algorithms for Reduced Bases in Banach Spaces. *Constructive Approximation*, 37(3):455–466, 2013.

[51] J. Dick. A Taylor space for multivariate integration. *Monte Carlo Methods Appl.*, 12:99–112, 2006.

[52] J. Dick and F. Pillichshammer. *Digital nets and sequences. Discrepancy theory and quasi-Monte Carlo integration.* Cambridge University Press, Cambridge, 2010.

[53] C. Dunnett and M. Sobel. Approximations to the probability integral and certain percentage points of a multivariate analogue of Student's t-distribution. *Biometrika*, 42(112):258–260, 1955.

[54] P. Duren. *Theory of H_p spaces.* Dover books on mathematics. Courier Corporation, 2000.

[55] N. Dyn. Generalized monosplines and optimal approximation. *Constructive Approximation*, 1(1):137–154, 1985.

[56] U. Eckhardt. Einige Eigenschaften Wilfscher Quadraturformeln. *Numerische Mathematik*, 12(1):1–7, 1968.

[57] H. Engels. Über allgemeine Gaußsche Quadraturen. *Computing*, 10(1-2):83–95, 1972.

[58] M. Galassi et al. *GNU Scientific Library Reference Manual (3rd Ed.)*. 2016.

[59] G. Fasshauer and M. McCourt. *Kernel-based Approximation Methods using MATLAB*. World Scientific Publishing Co. Pte. Ltd., 2015.

[60] C. Feuersänger and M. Griebel. Principal manifold learning by sparse grids. *Computing*, 85(4):85–267, 2009.

[61] S. Foucart and H. Rauhut. *A Mathematical Introduction to Compressive Sensing*. Applied and Numerical Harmonic Analysis. Birkhäuser, 2013.

[62] L. Fousse, G. Hanrot, V. Lefèvre, P. Pélissier, and P. Zimmermann. Mpfr: A multiple-precision binary floating-point library with correct rounding. *ACM Trans. Math. Softw.*, 33(2), 2007.

[63] K. Frolov. Upper bounds on the error of quadrature formulas on classes of functions. *Dokl. Akad. Nauk SSSR*, 231:818–821, 1976. English transl. in Soviet Math. Dokl., 17 (1976).

[64] J. Garcke, T. Gerstner, and M. Griebel. Intraday foreign exchange rate forecasting using sparse grids. In J. Garcke and M. Griebel, editors, *Sparse Grids and Applications*, volume 88 of *Lecture Notes in Computational Science and Engineering*, pages 81–106, 2012.

[65] J. Garcke, M. Griebel, and M. Thess. Data mining with sparse grids. *Computing*, 67(3):225–253, 2001.

[66] A. Genz. Numerical computation of multivariate normal probabilities. *Journal of Computational and Graphical Statistics*, 1(2):141–149, 1992.

[67] A. Genz and F. Bretz. *Computation of Multivariate Normal and t Probabilities*. Springer, 2009.

[68] T. Gerstner. Sparse grid quadrature methods for computational finance. Habilitation, Institut für Numerische Simulation, University of Bonn, 2007.

[69] T. Gerstner and M. Griebel. Numerical integration using sparse grids. *Numerical Algorithms*, 18:209–232, 1998.

[70] T. Gerstner and M. Griebel. Dimension–adaptive tensor–product quadrature. *Computing*, 71(1):65–87, 2003.

[71] J. Geweke. Bayesian inference in econometric models using Monte Carlo integration. *Econometrica*, 57(6):1317–1339, 1989.

[72] A. Ghizzetti and A. Ossicini. Sull esistenza e unicitat delle formule di quadrature Gaussiane. *Rend. Mat.*, 8:1–15, 1975.

[73] P. Glasserman. *Monte Carlo Methods in Financial Engineering*. Springer, 2003.

[74] T. Goda, K. Suzuki, and T. Yoshiki. An explicit construction of optimal order quasi-Monte Carlo rules for smooth integrands. 2016. Preprint, arXiv: 1601.06501 [math.NA].

[75] C. Gouriéroux and A. Monfort. *Simulation-Based Econometric Methods*. Oxford University Press, 1997.

[76] M. Griebel and M. Hegland. A finite element method for density estimation with Gaussian priors. *SIAM Num ANAL*, 47(6):4759–4792, 2010.

[77] M. Griebel and M. Holtz. Dimension-wise integration of high-dimensional functions with applications to finance. *Journal of Complexity*, 26(5):455–489, 2010.

[78] M. Griebel and S. Knapek. Optimized tensor-product approximation spaces. *Constructive Approximation*, 16(4):525–540, 2000.

[79] M. Griebel and J. Oettershagen. Dimension-adaptive sparse grid quadrature for integrals with boundary singularities. In *Sparse grids and Applications*, volume 97 of *Lecture Notes in Computational Science and Engineering*, pages 109–136. Springer, 2014. Also available as INS Preprint no 1310.

[80] M. Griebel and J. Oettershagen. On tensor product approximation of analytic functions. *Journal of Approximation Theory*, 207:348–379, 2016. Also available as INS Preprint No. 1512.

[81] M. Griebel and C. Rieger. Reproducing kernel Hilbert spaces for parametric partial differential equations. 2015. submitted. Also available as INS preprint no. 1511.

[82] J. H. Halton. Algorithm 247: Radical-inverse quasi-random point sequence. *Commun. ACM*, 7(12):701–702, 1964.

[83] H. Harbrecht, M. Peters, and M. Siebenmorgen. Combination technique based k-th moment analysis of elliptic problems with random diffusion. *Journal of Computational Physics*, 252:128–141, 2013.

[84] M. Hegland. Adaptive sparse grids. In K. Burrage and R. B. Sidje, editors, *Proceedings of CTAC, Brisbane, 2001*, pages 335–353, 2001.

[85] S. Heinrich, E. Novak, G. Wasilkowski, and H. Wozniakowski. The inverse of the star-discrepancy depends linearly on the dimension. *Acta Arithmetica*, 96:279–302, 2001.

[86] F. Heiss. The panel probit model: Adaptive integration on sparse grids. *Advances in Econometrics*, 26:41pp, 2010.

[87] F. Heiss and V. Winschel. Likelihood approximation by numerical integration on sparse grids. *Journal of Econometrics*, 144(1):62–80, 2008.

[88] A. Hinrichs and J. Oettershagen. Optimal point sets for quasi-Monte Carlo integration of bivariate periodic functions with bounded mixed derivatives. In Ronald Cools and Dirk Nuyens, editors, *Monte Carlo and Quasi-Monte Carlo Methods: MCQMC, Leuven, Belgium, April 2014*, pages 385–405. Springer International Publishing, 2016.

[89] F. Huszár and D. Duvenaud. Optimally-weighted herding is bayesian quadrature. In *Proceedings of the Twenty-Eighth Conference on Uncertainty in Artificial Intelligence*, UAI'12, pages 377–386, Arlington, Virginia, United States, 2012. AUAI Press.

[90] D. Huybrechs. Stable high-order quadrature rules with equidistant points. *J. Comput. Appl. Math.*, 231(2):933–947, 2009.

[91] C. Irrgeher and G. Leobacher. High-dimensional integration on weighted Hermite spaces, and orthogonal transforms. *Journal of Complexity*, 31(2):174–205, 2015.

[92] P. Jantsch, C. Webster, and G. Zhang. On the Lebesgue constant of weighted Leja points for Lagrange interpolation on unbounded domains, 2016. arXiv Preprint 1606.07093.

[93] M. Kalos and P. Whitlock. *Monte Carlo Methods.* John Wiley & Sons, 1986.

[94] S. Karlin. *Total positivity, vol I.* Stanford University Press, 1968.

[95] S. Karlin. On a class of best nonlinear approximation problems. *Bull. Amer. Math. Soc*, 78(1):43–49, 1972.

[96] S. Karlin and W. Studden. *Tchebycheff systems: With applications in analysis and statistics (pure and applied mathematics).* Interscience Publishers, 1966.

[97] M. Keane. A computationally practical simulation estimator for panel data. *Econometrica*, 62(1):95–116, 1994.

[98] N. Korobov. The approximate computation of multiple integrals. *Dokl. Akad. Nauk SSSR*, 124:1207–1210, 1959.

[99] M. Kowalski, A. Werschulz, and H. Woźniakowski. Is Gauß quadrature optimal for analytic functions? *Numerische Mathematik*, 47(1):89–98, 1985.

[100] M. Krein. The ideas of P. L. Chebyshev and A. A. Markov in the theory of limiting values of integrals and their further development. *Uspekhi Mat. Nauk*, 6:3–120, 1951. In Russian. Translated in Amer. Math. Soc. Transl. Ser. 2, 12 (1951), pages 1–122.

[101] F. Kuo, I. Sloan, G. Wasilkowski, and H. Woźniakowski. On decompositions of multivariate functions. *Mathematics of Computation*, 79(270):953–966, 2010.

[102] F. Kuo, I. Sloan, and H. Woźniakowski. Multivariate integration for analytic functions with Gaussian kernels. *Mathematics of Computation*, 86(304):829–853, 2017.

[103] F. Larkin. Optimal approximation in Hilbert spaces with reproducing kernel functions. *Math. Comp*, 24(112):911–921, 1970.

[104] J. Ma, V. Rokhlin, and S. Wandzurra. Generalized Gaussian quadrature rules for systems of arbitrary functions. *SIAM Journal on Numerical Analysis*, 33(3):971–996, 1996.

[105] B. Merschen. Minimal quadrature formulae for the spaces H_2^R and L_2^R. A unified interpolatory approach. *Computing*, 34(2):169–177, 1985.

[106] G. Migliorati, F. Nobile, E. von Schwerin, and R. Tempone. Analysis of discrete L^2 projection on polynomial spaces with random evaluations. *Foundations of Computational Mathematics*, 14(3):419–456, 2014.

[107] T. Nahm. Error estimation and index refinement for dimension adaptive sparse grid quadrature with applications to the computation of path integrals. Master's thesis, Institut für Numerische Simulation, Universität Bonn, 2005.

[108] A. Narayan and J. Jakeman. Adaptive Leja sparse grid constructions for stochastic collocation and high-dimensional approximation. *SIAM J. on Scientific Computing*, 36(6):A2952–A2983, 2014.

[109] F. Narcowich, J. Ward, and H. Wendland. Sobolev bounds on functions with scattered zeros, with applications to radial basis function surface fitting. *Mathematics of Computation*, 74(250):743–764, 2005.

[110] F. Nobile, L. Tamellini, and R. Tempone. Convergence of quasi-optimal sparse grid approximation of Hilbert-valued functions: application to random elliptic PDEs. MATH-ICSE Technical Report Nr. 12.2014, 2014.

[111] F. Nobile, L. Tamellini, and R. Tempone. *Comparison of Clenshaw–Curtis and Leja Quasi-Optimal Sparse Grids for the Approximation of Random PDEs*, pages 475–482. Springer International Publishing, Cham, 2015.

[112] F. Nobile, R. Tempone, and C. Webster. An anisotropic sparse grid stochastic collocation method for partial differential equations with random input data. *SIAM J. on Numerical Analysis*, 46(5):2411–2442, 2008.

[113] F. Nobile, R. Tempone, and C. Webster. A sparse grid stochastic collocation method for partial differential equations with random input data. *SIAM Journal on Numerical Analysis*, 46(5):2309–2345, 2008.

[114] J. Nocedal and S. Wright. *Numerical Optimization*. Springer Series in Operations Research and Financial Engineering. Springer Publishing, New York, 2006.

[115] E. Novak. Zur unteren Fehlergrenze von Quadraturverfahren. Dissertation, University of Erlangen-Nürnberg, 1983.

[116] E. Novak. *Deterministic and Stochastic Error Bounds in Numerical Analysis*, volume 1349 of *Lecture Notes in Mathematics*. Springer-Verlag Berlin Heidelberg, 1988.

[117] E. Novak and K. Ritter. High dimensional integration of smooth functions over cubes. *Numerische Mathematik*, 75(1):79–97, 1996.

[118] E. Novak and H. Woźniakowski. *Tractability of Multivariate Problems: Volume I: Linear Information*, volume 6 of *EMS Tracts in Mathematics*. European Mathematical Society (EMS), 2009.

[119] E. Novak and H. Woźniakowski. *Tractability of Multivariate Problems: Volume II: Standard Information for Functionals*, volume 12 of *EMS Tracts in Mathematics*. European Mathematical Society (EMS), 2010.

[120] A. O'Hagan. Bayes-Hermite quadrature. *Journal of Statistical Planning and Inference*, 29(3):245–260, 1991.

[121] J. Ortega. The Newton-Kantorovich theorem. *The American Mathematical Monthly*, 75(6):658–660, 1968.

[122] A. Owen. Halton sequences avoid the origin. *SIAM Review*, 48(3):487–503, 2006.

[123] Y. Pati, R. Rezaiifar, and P. Krishnaprasad. Orthogonal matching pursuit: Recursive function approximation with applications to wavelet decomposition. In *Conference Record of The Twenty-Seventh Asilomar Conference on Signals, Systems and Computers*, pages 1–3, 1993.

[124] A. Paulik. Zur Existenz optimaler Quadraturformeln mit freien Knoten bei Integration analytischer Funktionen. *Numerische Mathematik*, 27(4):395–405, 1976.

[125] R. Platte, L. Trefethen, and A. Kuijlaars. Impossibility of fast stable approximation of analytic functions from equispaced samples. *SIAM Review*, 53(2):308–318, 2011.

[126] W. Press, S. Teukolsky, W. Vetterling, and B. Flannery. *Numerical Recipes 3rd Edition: The Art of Scientific Computing*. Cambridge University Press, New York, 2007.

[127] A. Rahimi and B. Recht. Random features for large-scale kernel machines. In J. C. Platt, D. Koller, Y. Singer, and S. T. Roweis, editors, *Advances in Neural Information Processing Systems 20*, pages 1177–1184. Curran Associates, Inc., 2008.

[128] C. Rasmussen and Z. Ghahramani. Bayesian Monte Carlo. In *Advances in Neural Information Processing Systems 15*, pages 489–496. MIT Press, 2003.

[129] N. Richter-Dyn. Properties of minimal integration rules I. *SIAM Journal on Numerical Analysis*, 7(1):67–78, 1970.

[130] N. Richter-Dyn. Properties of minimal integration rules II. *SIAM Journal on Numerical Analysis*, 8(3):497–508, 1971.

[131] C. Rieger and B. Zwicknagl. Sampling inequalities for infinitely smooth functions, with applications to interpolation and machine learning. *Advances in Computational Mathematics*, 32(1):103–129, 2010.

[132] E. Saff and V. Totik. *Logarithmic Potentials with External Fields*. Springer, Berlin, 1997.

[133] R. Schaback. Optimal nodes for interpolation in Hardy spaces. *Mathematische Zeitschrift*, 179(2):169–178, 1982.

[134] R. Schaback. Limit problems for interpolation by analytic radial basis functions. *Journal of Computational and Applied Mathematics*, 212(2):127–149, 2008.

[135] R. Schaback. Approximationsverfahren II: Lecture Notes on Kernel Methods. University Lecture, 2011.

[136] R. Schaback. Greedy sparse linear approximations of functionals from nodal data. *Numerical Algorithms*, 67(3):531–547, 2014.

[137] M. Schervish. Algorithm AS 195: Multivariate normal probabilities with error bound. *Journal of the Royal Statistical Society. Series C (Applied Statistics)*, 33(1):81–94, 1984.

[138] C. Schillings and C. Schwab. Sparse, adaptive Smolyak quadratures for Bayesian inverse problems. *Inverse Problems*, 29(6):065011, 2013.

[139] B. Schölkopf and A. Smola. *Learning with Kernels: Support Vector Machines, Regularization, Optimization, and Beyond*. MIT Press, Cambridge, MA, USA, 2001.

[140] W. Sickel and T. Ullrich. The Smolyak algorithm, sampling on sparse grids and function spaces of dominating mixed smoothness. *East J. on Approximations*, 13(4):387–425, 2007.

[141] I. Sloan and S. Joe. *Lattice Methods for Multiple Integration*. Oxford University Press, New York, 1994.

[142] S. Smolyak. Quadrature and interpolation formulas for tensor products of certain classes of functions. *Dokl. Akad. Nauk SSSR*, 4:240–243, 1963.

[143] I. Sobol. On the distribution of points in a cube and the approximate evaluation of integrals. *J. Comp. Mathematics and Math. Physics*, 7:86–112, 1967.

[144] I. Steinwart, D. Hush, and C. Scovel. An explicit description of the reproducing kernel Hilbert spaces of Gaussian RBF kernels. *Information Theory, IEEE*, 52(10):4635–4643, 2006.

[145] F. Stenger. Optimal convergence of minimum norm approximations in H^p. *Numerische Mathematik*, 29(4):345–362, 1978.

[146] S. Stern. A method for smoothing simulated moments of discrete probabilities in multinomial probit models. *Econometrica*, 60(4):943–952, 1992.

[147] G. Szegö. Inequalities for the zeros of Legendre polynomials and related functions. *Transactions of the American Mathematical Society*, 39(1):1–17, 1936.

[148] G. Szegö. *Orthogonal polynomials.* American Mathematical Society, 1975.

[149] R. Taylor and V. Totik. Lebesgue constants for Leja points. *IMA J. of Numerical Analysis*, 30(2):462–486, 2010.

[150] V. Temlyakov. Cubature formulas, discrepancy, and nonlinear approximation. *Journal of Complexity*, 19(3):352–391, 2003.

[151] V. Temlyakov. Greedy approximation. *Acta Numerica*, 17:235–409, 2008.

[152] K. Train. *Discrete Choice Methods with Simulation.* Cambridge University Press, 2003.

[153] H. Tran, C. Webster, and G. Zhang. Analysis of quasi-optimal polynomial approximations for parameterized PDEs with deterministic and stochastic coefficients. *ORNL report no. ORNL/TM-2014/468*, 2014. submitted.

[154] J. Traub, H. Woźniakowski, and G. Wasilkowski. *Information-Based Complexity.* Academic Press, 1988.

[155] J. Tropp and A. Gilbert. Signal recovery from random measurements via orthogonal matching pursuit. *IEEE Trans. Inf. Theor.*, 53(12):4655–4666, 2007.

[156] M. Ullrich and T. Ullrich. The role of Frolov's cubature formula for functions with bounded mixed derivative. *SIAM Journ. on Numerical Analysis*, 54, No. 2:969–993, 2016.

[157] G. Wahba. Smoothing noisy data with spline functions. *Numer. Math.*, 24(5):383–393, 1975.

[158] G. Wahba. *Spline Models for Observational Data.* SIAM, Philadelphia, 1990.

[159] J. Waldvogel. Fast Construction of the Fejér and Clenshaw–Curtis quadrature rules. *BIT Numerical Mathematics*, 46(1):195–202, 2006.

[160] X. Wang. Volumes of generalized unit balls. *Mathematics Magazine*, 78(5):390–395, 2005.

[161] G. Wasilkowski and H. Wozniakowski. Explicit cost bounds of algorithms for multivariate tensor product problems. *J. of Complexity*, 11(1):1–56, 1995.

[162] G. Wasilkowski and H. Woźniakowski. Weighted tensor product algorithms for linear multivariate problems. *J. Complexity*, 15:402–447, 1999.

[163] H. Wendland. *Scattered Data Approximation.* Cambridge University Press, 2004.

[164] H. Wilf. Exactness conditions in numerical quadrature. *Numerische Mathematik*, 6(1):315–319, 1964.

[165] D. Zagier. The dilogarithm function. In P. Cartier, P. Moussa, B. Julia, and P. Vanhove, editors, *Frontiers in Number Theory, Physics, and Geometry II: On Conformal Field Theories, Discrete Groups and Renormalization.* Springer Berlin Heidelberg, 2007.

[166] C. Zenger. Sparse grids. In W. Hackbusch, editor, *Parallel Algorithms for Partial Differential Equations*, volume 31 of *Notes on Numerical Fluid Mechanics*, pages 241–251. Vieweg, 1991.

[167] A. Zhensykbaev. Monosplines of minimal norm and the best quadrature formulae. *Russian Mathematical Surveys*, 36(4):121pp, 1981.

[168] B. Zwicknagl and R. Schaback. Interpolation and approximation in Taylor spaces. *J. of Approximation Theory*, 171:65–83, 2013.